Vector Fields During Cosmic Inflation: Stability Analysis and Phenomenological Signatures

A DISSERTATION
SUBMITTED TO THE FACULTY OF THE GRADUATE SCHOOL
OF THE UNIVERSITY OF MINNESOTA
BY

Burak Himmetoglu

IN PARTIAL FULFILLMENT OF THE REQUIREMENTS
FOR THE DEGREE OF
Doctor Of Philosophy

June, 2010

Acknowledgements

I would like to thank my colleagues Jose Cembranos, Emir Gumrukcuoglu and Serkay Olmez for valuable scientfic discussions. I would especially like to thank my adviser Marco Peloso for his support and guidance throughout my graduate studies.

Abstract

This thesis is based on the study of vector fields during cosmic inflation. Cosmic inflation has proven to be an accurate description of the very early universe, not only because of its success in resolving the classical problems of big bang cosmology, but also for introducing a natural mechanism for the generation of primordial fluctuations which give rise to the structure (galaxies and cluster of galaxies) in the universe. For simplicity, most inflationary scenarios assume that the expansion is driven by a scalar field. However, due to the fact that the underlying particle physics model of inflation is unknown, and due to some features emerged in some studies of the cosmic microwave background data, there have recently been considerable interest in vector field driven models of inflation. In this thesis, I present a complete stability analysis of some of the compelling models where vector fields are assumed to play an important role during inflation. The stability analysis is performed by studying all possible fluctuations around the background solution of these models. It is explicitly proven that for models where the gauge invariance of the vector field is broken, the background solution is unstable. The proof is performed both (1) by studying the quadratic action for the fluctuations, and showing that ghost instabilities are present in the model and (2) by studying the linearized Einstein equations and showing that the solutions diverge close to horizon crossing. For models that are free of instabilities, relevant power spectra are computed and the resulting phenomenology is discussed.

Contents

Acknowledgements **i**

Abstract **ii**

List of Tables **vi**

List of Figures **vii**

1 Introduction **1**

2 The Inflationary Universe **13**

2.1 Problems with Big-Bang Cosmology 14

2.2 The Physics of Inflation 17

2.3 Quantum Fields in a Cosmological Background 22

2.4 Quantum fluctuations of metric and scalar field during inflation 33

2.4.1 Scalar Perturbations 37

2.4.2 Tensor Perturbations 41

3 The Cosmic Microwave Background **45**

3.1 Formation of CMB anisotropies 46

3.2 CMB Observations and Inflation 56

4 The Ackerman-Carroll-Wise Model and its Stability **64**

4.1 The ACW model 67

4.2 Instability from a simplified computation 68

4.3 Instability from the full linearized equations 72

4.3.1 Classification of the perturbations 73
4.3.2 Solutions to the linearized equations for the perturbations 76
4.4 Ghost from the quadratic equation 80
4.4.1 Ghost instabilities in some other models 84

5 Models with vector fields non-minimally coupled to the curvature 88
5.1 General discussion of ghost instabilities 89
5.2 Review of some models with a RA^2 term 92
5.3 Identification of ghosts, and their associated instability 96
5.4 Ghost instability for $\langle A_\mu \rangle = 0$ 97
5.5 Ghost instability for $\langle A_\mu \rangle \neq 0$ 102
5.5.1 One vector plus a cosmological constant 103
5.5.2 One vector plus a scalar inflaton 115
5.5.3 Vector inflation 120
5.6 Discussion 131

6 Models with vector fields kinetically coupled to a scalar field 136
6.1 Anisotropic inflationary expansion due to coupled vector and scalar fields 137
6.1.1 Single Scalar Field Inflationary Background 139
6.1.2 Two Scalar Field Inflationary Background 143
6.2 Perturbations 146
6.2.1 General Properties of Coupled System of Perturbations 147
6.2.2 2d Vector Perturbations 150
6.3 Power Spectrum 154
6.4 Linearized Stability 158

7 General Two Point Correlators from Anisotropic Inflation 163
7.1 Perturbations and Power Spectra 164
7.1.1 Two point correlation functions 168
7.1.2 Evolution of the perturbations and initial conditions 169
7.1.3 Power spectra after isotropization 171
7.2 Discussion 174

8 Conclusions **178**

References **181**

Appendix A. Explicit expressions for the study of the ACW model **189**

Appendix B. Details of computations of subsection 5.5.1 **198**

Appendix C. Early time canonical action and initial conditions **215**

Appendix D. Details of calculations for $2d$ scalar perturbations **218**

Appendix E. Detailes of calculations for chapter 7 **224**

Appendix F. Comparison with isotropic case relevant for chapter 7 **227**

List of Tables

3.1 WMAP 7-year constraints for n_s, r and $dn_s/d\ln k$ 58

List of Figures

1.1 The horizon problem . . . 3
1.2 Anisotropic scale factors . . . 7
2.1 Phase plot for chaotic inflation . . . 21
2.2 Evolution in the Bunch-Davies vacuum . . . 29
2.3 Production of perturbations . . . 32
2.4 Power spectra in chaotic inflation . . . 44
3.1 World line of CMB photons . . . 47
3.2 Measurement of CMB photon energies . . . 48
3.3 C_l's from inflation . . . 56
3.4 WMAP constraints for single field inflation . . . 57
3.5 Alignment of lowest multipoles . . . 61
4.1 Instability arising in a simplified calculation . . . 72
4.2 Instability arising in the full calculation . . . 80
5.1 Evolution of the longitudinal mode α and α_0 . . . 102
5.2 Evolution of perturbations in the vicinity of the instability . . . 111
5.3 Evolution of eigenvalues . . . 114
5.4 Evolution of the kinetic determinant . . . 116
5.5 Numerical evolution of the background and the kinetic determinant . . . 120
5.6 Numerical evolution of eigenvalues . . . 121
5.7 Numerical evolution of eigenvalues . . . 129
5.8 Evolution of eigenvalues (close to the moment when $\lambda_3 = 0$) . . . 130
5.9 Evolution of eigenvalues and M^2 . . . 131
6.1 Background evolution in the model with vector hair . . . 142
6.2 Evolution of H and h and the phase space evolution . . . 143

6.3 Evolution of H and h 145
6.4 Phase space evolution 145
6.5 Spectra for fixed ξ's 155
6.6 The contour plot of the full spectrum 156
6.7 Fitted and numerical spectra 157
6.8 Spectrum at small scales 157
6.9 Vector mode stability at large and small scales 159
6.10 Scalar mode stability at large and small scales 161
6.11 Vector mode stability 162
7.1 Evolution of power for $c - 1 = 10^{-5}$ 173
7.2 Various correlation functions for $c - 1 = 10^{-5}$ 176
7.3 Angular dependence of g_* 177

Chapter 1

Introduction

Inflation has become a cornerstone of modern cosmology, which is the most compelling framework that describes the evolution of the very early universe. Inflation is an era of rapid accelerated expansion, during which the physical length scales grew much faster than the horizon which sets the length scale of casual processes. This behavior of the physical and casual length scales are crucial in solving the classical problems of big bang cosmology [1], which was the original motivation for inflation. The degree of homogeneity and flatness of the current observable horizon could only be explained by very fine tuned initial conditions within the big bang cosmology, which assumes that the universe is only dominated by radiation at very early times and that the temperature was infinitely high at the initial singularity (More precisely, big-bang cosmology makes sense until a temperature that is of the order of Planck Mass (M_p), where an unknown quantum theory of gravity is assumed to replace the known quantum field theory). For instance, the observable horizon today corresponds to about 10^6 regions that were casually disconnected at the time of Cosmic Microwave Background (CMB) formation in big bang cosmology. Therefore, one would naturally expect that the CMB to be very inhomogeneous, since each 10^6 disconnected patches would have evolved on their own. This is shown schematically in Figure 1.1. On the other hand, observations showed that the universe at the time of formation of the CMB was homogeneous up to a part in 10^5. Without inflation, a very finely tuned set of initial conditions over length scales which were physically disconnected at early times must be set in order to explain the current homogeneity of the observable horizon. Inflation resolves this puzzle, since physical

scales are stretched in the fast expansion, while the horizon scale changes very little at early times. As a consequence, during inflation, a single homogeneous region grew much more than in the following big-bang era, and covered all the universe we see today.

Inflation also addresses the flatness problem. Unless the universe has exactly flat geometry, the observed smallness of curvature today can only be explained with very special initial conditions. The curvature contribution to the energy density of the universe must be $\lesssim 1\%$ of the total today (For instance, the energy density of the curvature needed to be $< 10^{-18}$ of the total energy at the big-bang nucleosynthesis, when the universe was 1 second old.). Inflation solves this puzzle, since during an accelerated expansion the energy density of curvature decreases. In addition, inflation also solves the problem of unwanted relics, that are predicted by particle physics models, like topological defects and gravitation. Such relics are either stable, so that they should have been detected at an observable abundance (like topological defects) or long-lived to alter the evolution of the universe in an unwanted manner (like gravitinos; their late decay could easily change the abundance of elements formed during big-bang nucleosynthesis). One could possibly conclude that these particle physics models are invalid since we have not observed these relics. Inflation saves these models by diluting the number density of the relics to an unobservable amount (Notice that one needs to require that such relics are not re-produced after inflation. This puts constraints on the possible decays of the inflaton into matter).

Besides solving problems within big bang cosmology, inflation also provides a mechanism for generation of density perturbations that seed the structure we observe today. Although the universe is homogeneous and isotropic at large scales, the existence of structure and temperature fluctuations in the CMB has to be accounted for in a complete description. Observations suggest that the fluctuations in the CMB, which is of the 10^{-5} level, have almost scale invariant power spectrum. This observation has already ruled out some of the mechanisms of generation of structure, for example structure formed from cosmic strings. On the other hand, inflation offers a mechanism of generation of nearly scale invariant spectrum of perturbations. More precisely, during inflation quantum fluctuation are generated with a power spectrum proportional to the square of the expansion rate H. This expansion rate is almost constant, providing the

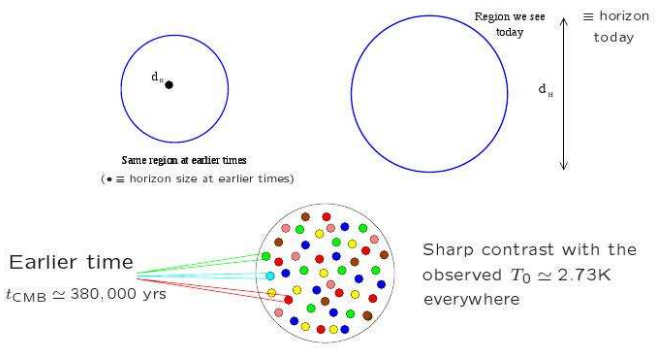

Figure 1.1: The horizon problem is shown schematically. Within big-bang cosmology, one expects a much more inhomogeneous temperature distribution in the CMB within the horizon today and at early times (left panel). Since the horizon grows faster than physical scales in a radiation/matter dominated universe, the physical region that we observe today (our horizon) contained several disconnected regions in the past.

nearly scale-invariance property of the spectrum. The deviation from the scale invariance depends on the rate of change of the expansion rate H. For example, in models where inflation is driven by a single scalar field, the deviation from scale invariance depends on the slope of the potential. The generated quantum fluctuations are stretched to scales larger then the horizon scale, where they stay frozen until they re-enter at a later time after inflation is over. The re-entered fluctuations then form potential wells, which seed the observed structure. Moreover, the CMB photons scattered from the potential wells result in the anisotropies in the temperature profile. This picture is in impressive agreement with CMB experiments [2, 3].

Although inflation provides the basic framework for the solution of cosmological puzzles and for the formation of structure in the universe, the underlying particle physics model is still unknown. Currently, observations can only detect a subset of fluctuations that could have been generated during inflation, which are the density fluctuations. This information is not enough for the determination of the energy scale at which inflation took place. However, from a possible detection of inflationary gravity waves, it is possible to directly measure this unknown energy scale [4]. Then, gravity waves from

inflation would lead to a probe into physics at very high energy scales, which cannot be reached in an earth-bound experiment. The ignorance of the energy scale of inflation has contributed to the variety of models of inflation given in the literature. The simplest models of inflation assume that the expansion is driven by a scalar field. It is possible to study the fluctuations of this scalar field (inflaton) and its coupling with gravitational degrees of freedom and a power spectrum can be calculated [5]. The calculated power spectrum can then be compared with the data, which would provide information on the properties of the inflaton field [6]. Since the underlying particle physics mechanism of inflation is unknown, it is legitimate to consider the possibility that inflation might be driven by higher spin fields, rather than a scalar field. For this reason, inflation driven by spinors, vector fields and p-forms have recently been considered [7, 8, 9]. Although the generalization seems trivial, one faces a couple of difficulties when incorporating higher spin fields in an inflationary framework. For instance, in order for a vector field to drive inflation, it needs to have a non-vanishing vacuum expectation value (vev) so that it dominates the energy density of the universe. A non-vanishing vev for a vector field faces two important obstacles. The first obstacle is the fact that the existence of a vev of a vector field breaks the rotational invariance of space and therefore the expansion of space proceeds anisotropically. This problem can be alleviated by considering a large number N of vector fields with random orientations. In this case, there would be an order $\mathrm{O}(1/\sqrt{N})$ anisotropy. Moreover, since a vector field has more degrees of freedom than a scalar field, the behavior of fluctuations would be different. These consequences have been exploited in order to address some nonstandard (and controversial) features emerged in some studies of the CMB data, which we will discuss briefly. The second obstacle is the fact that vector fields have different coupling to gravity than scalar fields, and it can be shown that minimally coupled vector fields (only through the kinetic term $g^{\mu\nu}\, g^{\alpha\beta}\, F_{\mu\alpha}\, F_{\nu\beta}$) can not support an inflationary expansion. This problem can be overcome, for example, by introducing a mass term for the vector field. If the mass term satisfies certain criteria, then the model admits inflationary background solutions. However, it also turns out that, when these criteria are met, these models are actually unstable. It is also possible to consider a mixed situation where inflationary expansion takes place with both vector fields and scalar fields [11, 12]. In this case, the overall expansion is driven by a scalar inflaton, but the vector field introduces a

small controllable anisotropy. Such models are studied in order to address some of the features that have emerged in studies of the CMB data, as we discuss below. It is also possible to consider models of vector curvaton, where the isotropic expansion of the universe is driven by some unspecified field and the vector curvaton, which has a small vev and therefore negligible effect on the background, is only responsible for generation of quantum fluctuations [13] [1] .

The study of higher spin fields, especially vector fields during inflation, was also motivated in part by the unexplained features that emerged in some studies of the CMB data. As mentioned above, the CMB observations are in very good agreement with the inflationary picture. However, a number of studies of the data have obtained some features which seem to be anomalous within the standard inflationary picture. The most studied among these features are, the low power in the quadrupole moment [14, 15, 16, 17, 18], the alignment of the lowest multipoles and claims of statistical anisotropy [18, 19, 20, 21, 22, 23, 24], an asymmetry in power between the northern and southern hemispheres [25, 26, 27, 28, 29, 30, 31], a nongaussian deviation in the southern hemisphere, known as the 'cold-spot' [32, 33, 34, 35, 36, 37]. Although the statistical significance of these effects is highly debated, no explanation in the lines of a systematic or a foreground effect has been given for all of them. This has led some authors to consider the possibility that such effects might have a cosmological origin. As discussed in the previous paragraph, existence of a vector field vev results in the presence of a preferred direction, which leads to a breakage of statistical isotropy, and possibly the alignment of multipoles. In order to test such claims, one has to perform a perturbative analysis of these models, not only for testing the stability and consistency of them, but also for making robust predictions for the power spectra. The main aim of this thesis is to perform this analysis for some of the compelling models that have appeared in the literature and discuss their phenomenological significance.

The possibility that an anisotropic expansion could be responsible for the alignment of the lowest multipoles and the breaking of statistical anisotropy was first discussed in [38, 39], and in [40, 41] and perturbations around an anisotropic Bianchi-I geometry

[1] A curvaton is a field responsible for the generation of the primordial perturbations, but which had negligible energy density during inflation. This can offer a richer phenomenology than normal minimal models in which a unique field - the inflaton - is responsible for both driving inflation and the generation of primordial perturbations.

were studied. A Bianchi-I geometry is a simple generalization of the flat FRW metric, where the three spatial directions can have different expansion rates and the metric is given by

$$ds^2 = -dt^2 + a^2(t)\,dx^2 + b^2(t)\,dy^2 + c^2(t)\,dz^2\,. \tag{1.1}$$

The Bianchi-I geometry is a subset of models that describe a class of spatially homogeneous (but not isotropic) geometries. In the above mentioned studies, the anisotropy is assumed to be given as an initial condition and no source is assumed to produce the anisotropy. The inflationary expansion is driven by a scalar field, and therefore the initial anisotropy vanishes rapidly. This is a reminiscent of Wald's theorem [10] that all Bianchi models (with a possible exception of the Bianchi-IX model) approach to a flat FRW universe in the presence of a cosmological constant Λ and of sources that satisfy strong and weak energy conditions. The isotropization takes place at a time scale $t_{\rm iso} \sim 1/\sqrt{\Lambda}$, so any pre-existing anisotropy decays exponentially with time.

In order that the anisotropic phase is observable, it must have occurred at a very fined tuned moment; it was shown that such anisotropic solutions originate from a singularity (that is of the Kasner type). In one Hubble time, the background solution goes from this initial singularity to an isotropic solution (with an exponentially decreasing anisotropy). The subsequent inflationary expansion can not be too long (or the modes sensitive to the non-standard expansion are inflated to too large scales to be visible) nor too short (or the strong anisotropic stage would leave a too strong imprint, incompatible with observations). Indeed one must require that this brief anisotropic period took place precisely 60 e-folds before the end of inflation, when the largest scales we observe today were at a comparable wavelength to the horizon. Therefore, one requires a considerable amount of fine tuning in this model in order that the largest observable scales are modified. Moreover, the regime close to the singularity is characterized by a large growth of some metric perturbations (which later become gravity waves; so this stage can potentially produce an observable gravity wave signal [42]). One can not start too close to the singularity, or perturbation theory breaks down. Therefore, there is a strong sensitivity on initial conditions, which can not be given in a predictive way from the model.

To avoid the tuning mentioned in the previous paragraph, it is possible to consider a prolonged anisotropic expansion by including a cosmological constant (or an inflaton)

plus ingredients that violate the premises of Wald's theorem [10]. This has been achieved by adding quadratic curvature invariants in the gravitational action [43], with the use of the Kalb-Ramond axion [44] and with vector fields [45]. Anisotropy can therefore persist during inflation, but its amount can be kept small if the energy of these extra fields are small (contrary to the case just discussed, in which the anisotropic phase is short, but the anisotropy necessarily originates at a time very close to a singularity). This situation is schematically shown in Figure 1.2. In this thesis, we will concentrate on the case of vector fields, as described in the previous paragraphs.

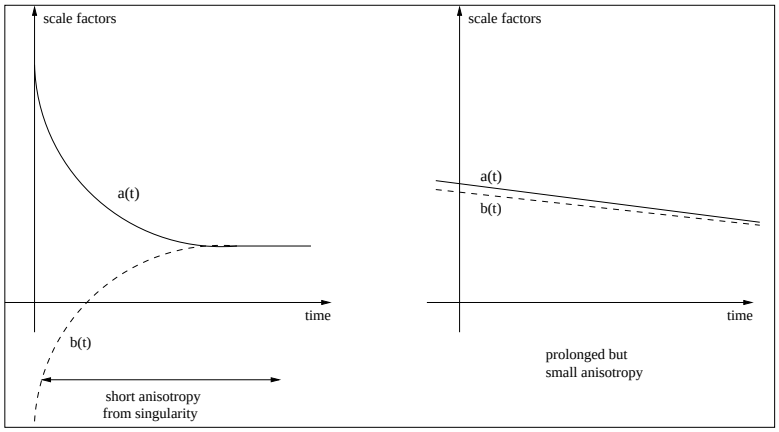

Figure 1.2: The evolution of scale factors in an anisotropic universe is schematically shown. The figure in the left shows the case when there is an initial singularity. The figure in right shows the case with vector field driven anisotropy. For simplicity, a $2d$ anisotropy ($b = c$ in 1.1) is considered.

As previously discussed, the unexplained features that emerged in the studies of the CMB data have motivated numerous studies on vector fields during inflation. The first one among these studies is the Ackerman-Carroll-Wise model [46], where the vector field is forced to have a fixed norm through a lagrange multiplier field λ which is coupled by the term $\lambda \left(A^\mu A_\mu - m^2 \right)$. The vector field has a non vanishing vev along a spatial direction and therefore the three dimensional rotational symmetry is broken down to a two dimensional one, so the resulting background metric is Bianchi-I with two distinct scale factors (let us denote them by $a(t)$ and $b(t)$). This type of fixed norm vector field avoids the premises of Wald's theorem, therefore in the existence of a cosmological constant, the background expands anisotropically with two constant Hubble rates, $H_a =$

$\dot{a}/a$ and $H_b = \dot{b}/b$. When the norm $m^2 \to 0$, the two scale factors become equal and the metric reduces to a de-Sitter space. This model has attracted considerable attention, since it has a simple background solution and a controllable anisotropy. Moreover, simply from the symmetries of the background, one can expect [46] that this model produces a power spectrum of the type

$$P(\vec{k}) = P_{\rm iso}(k)\,[1 + g_*\,(\hat{k}\cdot\hat{n})^2] \tag{1.2}$$

where $P_{\rm iso}$ is the standard isotropic power, $\hat{k}$ is the unit vector in the direction of the co-moving momentum $\vec{k}$, $\hat{n}$ is the unit vector along the preferred direction set by the vev of the vector field and g_* parameterizes the deviation from the standard spectrum. Although the method followed by the original reference in obtaining the power spectrum was incomplete and later this model was shown to be unstable (as we will also demonstrate in this thesis), the simple form of the power spectrum 1.2 was studied by many groups and comparison with the CMB data was made [47, 48]. The original reference has obtained the power spectrum by studying the quantum fluctuations of a test field $\delta\chi$ only around the anisotropic background solution. It was then assumed that the fluctuations of the test field are converted to density fluctuations after inflation during the reheating era through the mechanism described in [49] [2] . It was assumed that the perturbations of the coupled vector field-metric system are negligible compared to those of the test field $\delta\chi$. Later, a complete analysis including all the degrees of freedom in the system was done in references [50, 51] and it was incorrectly concluded that the system is stable, and the predictions of the original reference [46] was valid. However, these references only considered the very small ($k \gg H$) and very large scale limits ($k \ll H$) of the perturbations. In references [52, 53] it was shown that instabilities arise at intermediate scales when the perturbations cross the horizon scale ($k \sim H$), which is due to the fact that longitudinal vector polarization, which would not exist if the vector field was minimally coupled and $U(1)$ symmetry was restored, becomes a ghost at this moment. This was found both by studying the linearized Einstein equations for the perturbations and the quadratic action for them. We provide the details of these results in chapter 4.

[2] We briefly discuss this mechanism in chapter 2.

As mentioned previously, it is possible to obtain prolonged expansion by an appropriate choice for the mass term for the vector field. Reference [8] has considered a mass term of the form $(m^2 - \xi\, R)\, A^\mu\, A_\mu$, where R is the curvature scalar and ξ is a constant. When there are three mutually orthogonal vector fields and when $\xi = 1/6$, it was shown that the background evolution of the vector field resembles that of a minimally coupled scalar field. This analogy with a minimally coupled scalar inflaton with mass m was then exploited to construct a slowly rolling vector inflation. Then, as long as $m^2 \ll H$, where H is the expansion rate during inflation, the vector field supports slow roll inflation. In the case where there are N randomly oriented vector fields, one would have a spatially isotropic universe on average with $\mathrm{O}(1/\sqrt{N})$ level anisotropy. In a similar manner, reference [11] considered a single vector field with the same coupling and a small vev along with a scalar field that drives the overall isotropic expansion of the universe. The vector field serves to introduce a small anisotropy. Vector curvaton models was also considered in references [13], where the $1/6\, R\, A^\mu\, A_\mu$ coupling provide the scale invariance of the spectrum of perturbations resulting from the vector field. The deviation from scale invariance is proportional to m^2, and it is small as long as $m/H \ll 1$. Even without detailed calculations, it is possible to suspect that all these models are problematic [52]. This can be seen by checking the sign of the mass squared term $M_A^2 = (m^2 - \xi\, R)$, assuming that the background geometry can be approximated by a de-Sitter space where $R \propto H^2$. This is equivalent to assuming small anisotropy, so that the metric and vector field perturbations are decoupled and can be studied separately. When anisotropy is finite, metric and vector field perturbations are coupled and one has to study the full system. Then, the requirements of slow-roll for the case of vector inflation and scale invariance in the case of the vector curvaton requires $M_A^2 < 0$. In this case, the longitudinal vector polarization of the vector field, which would otherwise be absent when $M_A^2 = 0$ (i.e the $U(1)$ invariance would be restored and there would only be transverse modes), becomes a ghost which indicates the instability of the vacuum state of the theory. Unlike a scalar field, where a negative mass squared term indicating existence of tachyonic modes, for the vector field a negative mass squared term leads to a longitudinal mode which is a ghost. The reason is due to the fact that the kinetic term for the longitudinal mode is proportional to M_A^2 (which vanishes when $M_A^2 = 0$ and the longitudinal mode drops from the action) and when $M_A^2 < 0$, the kinetic energy

of the quantum excitations are unbounded from below. This leads to a UV-divergent rate of vacuum decay into ghost-nonghost pairs (which is energetically allowed now) and therefore the vacuum is unstable. Detailed discussions on the existence and effects of ghosts are given in chapters 4 and 5. This claim is also verified in reference [54], where all perturbations of the models [8, 11] were included, and no approximation was made.

The ghost instability is not the only problem associated with the models mentioned in the previous paragraph. We have argued that when $M_A^2 < 0$, the models are plagued by the instability of the vacuum. This instability does not necessarily show up in the classical equations of motions for the fields, and it could only be problem of the quantum theory of the modes. However, during the evolution of the modes after inflation, there is a moment when the terms m^2 and H^2 become comparable and the mass squared term vanishes. This leads to a divergent behavior in the solutions of the classical equations of motion, as will be demonstrated. When gravitational degrees of freedom are taken into account, the situation is more complicated. Initially, the spectrum does not have any ghosts, but the longitudinal vector polarization becomes a ghost close to horizon crossing, and as in the case of the ACW model, this leads to an instability in the solutions of the equations of motion for the perturbations. It is possible that these instabilities, including the one in the ACW model, arise only in the linearized theory and that the full nonlinear theory is regular. However, phenomenological predictions are based on linearized calculations, and therefore their validity is questionable. Another possibility is to assume that the models could be regularized above a certain scale where the quantum theory is cured, and the theory with the ghost is only an effective one. There are however stringent experimental constraints on an effective theory with ghosts, coming from the amount of observed gamma ray background and the cut-off scale satisfies $\Lambda_{\rm UV} \lesssim MeV$ when the ghost has only gravitational couplings to matter [97]. The limit is even more stringent when there are stronger couplings. Inflationary physics takes place at much higher energy scales than MeV, therefore the inflationary predictions based on such models are still questionable. Besides, the classical equations of motions for the perturbations can be shown to diverge at scales where the effective theory is valid; this happens when m^2 and H^2 are comparable after inflation. The detailed discussions on these issues are provided in chapter 5.

The non-minimal coupling to curvature scalar R, along with the lagrange multiplier terms were considered in the vector field action in order to obtain a prolonged expansion due to them. Wald's theorem was proven when the source of expansion is a cosmological constant. A natural question to ask is whether Wald's theorem can be invalid, when the cosmological constant is replaced with an inflaton field ϕ. Indeed, it was shown in reference [12] that when the vector field is coupled to the inflaton field kinetically through $f^2(\phi)\, F^{\mu\nu}\, F_{\mu\nu}$, then it is possible to obtain background solutions with small but growing anisotropy, even though the vector field obeys the required energy conditions of the Wald's theorem. This is achieved by an appropriate coupling function $f(\phi)$. Indeed such couplings are also considered for generating inflationary magnetic fields, since it breaks the conformal invariance of the vector field and induces particle production [55, 56]. Moreover, since the $U(1)$ symmetry of the vector field is intact in such a coupling, one does not expect any instabilities like the ones mentioned previously. Indeed this have been proven explicitly by studying the complete system of perturbations in reference [57]. Moreover, a preliminary study on the power spectra is also made and spectrum for one of the gravitational wave modes are computed. The details of this work are given in chapter 6. Later in reference [58], the full spectrum of perturbations are studied, and scalar-scalar, scalar-tensor and tensor-tensor correlators are calculated. The dependence for g_*, which was used originally in the ACW model for parameterizing the anisotropic spectrum is also calculated in this case. Moreover, the appearance of nonzero scalar-tensor correlators might be tested in the near feature through the CMB polarization experiments [4], through a possible detection of temperature-E mode correlation. The details of this work is given in section chapter 7.

This thesis is organized as follows: In chapter 2 we review the standard inflationary cosmology; we discuss the problems in big-bang cosmology and explain how inflation solves them. Then we discuss how inflation can be realized in a concrete model and review the formalism and computation of the spectrum of perturbations in an inflationary model. In chapter 3, we briefly discuss the physics of the formation of the CMB and then discuss comparison of CMB experiments with inflationary models. We give an up to date and brief review of the cosmological interpretation of the CMB data and its implications for inflation. We then discuss the features in the CMB that might be anomalous, which in part motivated the vector field studies. In chapter 4, we study the

background and perturbations of the ACW model and explicitly prove that it is plagued by instabilities. We also provide a brief stability analysis of the first vector inflation model by Ford [45], and prove that it is plagued by ghost instabilities. In chapter 5, we study models of vector inflation and vector curvaton explicitly and prove that they are also plagued by instabilities. In both chapters we consider all of the degrees of freedom in the models and study both the linearized Einstein equations and the quadratic action to reach our conclusions. In chapter 6 we discuss the model where the vector field is kinetically coupled to a scalar field and prove that the model is stable. We provide a partial study of gravity waves when there are multiple scalar fields along with a vector field in the model. Finally in chapter 7 we study the full spectrum of the same model (with a single scalar field) and compute scalar-scalar, scalar-tensor and tensor-tensor correlators. We also provide a discussion of our results and their phenomenological implications. We also provide extensive appendices that contain some of the extensive calculations done through out the thesis.

Chapter 2

The Inflationary Universe

The evolution of the universe is well described by the so called big-bang theory, where the universe started at a very hot and dense phase, and cooled down by expansion. The big-bang theory assumes that the energy density of the universe is dominated only by radiation and matter, and the temperature was infinitely high at the initial singularity (More precisely, up to $T \sim M_p$ is the moment one can discuss, given our ignorance of quantum gravity). This picture successfully explains the presence of the cosmic microwave background (CMB) radiation, which results from the decoupling of photons from protons and electrons, and the process of nucleosynthesis during when the light elements in the universe are formed. Despite its success, big bang cosmology has several shortcomings. These shortcomings are either related to a need of extreme fine tuning of initial conditions, or to the absence of some relics predicted by particle physics models. In addition to these shortcomings, big-bang theory is also incomplete since the mechanism that leads to the formation of structure is unexplained. Although the observed universe is homogeneous and isotropic at large scales, the inhomogeneity of the order 10^{-5} still exits and accounts for the structure we observe today. There is no successful and complete mechanism within the big-bang theory that can account for the formation of the observed structure. The inflationary paradigm, besides resolving the shortcomings of the big-bang theory, also introduces a natural mechanism of generation of quantum perturbations, which seed the structure in the universe. The inflationary mechanism of generation of fluctuations has robust predictions on the temperature anisotropy spectrum, which has proven to be in successful agreement with the

CMB experiments. These features of inflation has made it a widely accepted framework for the early universe.

In this chapter, we will briefly discuss the some of the basic results of big-bang cosmology. Then, we will discuss the flatness and horizon problems, all of which are related to the requirement of very special and fined tuned initial conditions. We will also comment on the problem of unwanted relics and explain how inflation solves all of these problems. Finally, we will briefly introduce the theory of cosmological perturbations during inflation, and discuss some of its basic predictions.

2.1 Problems with Big-Bang Cosmology

The evolution of the universe is described by the Friedmann-Robertson-Walker (FRW) metric, which is given by

$$ds^2 = -dt^2 + a^2(t)\,\left(\frac{dr^2}{1-kr^2} + r^2\,\left(d\theta^2 + \sin^2\theta\, d\phi^2\right)\right) \tag{2.1}$$

where $k = 0,\, -1,\, +1$ describes a spatially flat, open and closed geometries respectively. The solution of Einstein Equations in the presence of a perfect fluid source results in the Friedmann equations, namely

$$\begin{aligned} R_{\mu\nu} - \frac{1}{2}\, g_{\mu\nu}\, R &= \frac{1}{M_p^2}\, T_{\mu\nu} \quad , \quad T^{\mu}_{\nu} = \mathrm{diag}\,(-\rho,\, p,\, p,\, p) \\ H^2 + \frac{k}{a^2} &= \frac{\rho}{3M_p^2}, \quad \frac{\ddot{a}}{a} = -\frac{1}{6M_p^2}\,(\rho + 3p) \end{aligned} \tag{2.2}$$

where ρ is the energy density and p is the pressure of the perfect fluid source, $H \equiv \dot{a}/a$, M_p is the reduced Planck Mass and overdot denotes derivative with respect to cosmic time t. The fluid source obeys the conservation equation, which can be obtained either by the Bianchi identity $\nabla_\mu\, T^{\mu}_{\nu} = 0$, or by combining the Friedmann equations, which is

$$\dot{\rho} + 3\,H\,\,(\rho + p) = 0\,. \tag{2.3}$$

The first Friedmann equation can be written in slightly different way, by diving the both sides of the equation with the critical density $\rho_c \equiv 3\,M_p^2\,H^2$ which gives

$$\Omega - 1 = \frac{k}{a^2\,H^2} \quad , \quad \Omega \equiv \frac{\rho}{\rho_c}\,. \tag{2.4}$$

At the early hot and dense epochs of the universe, the energy density is determined by the relativistic degrees of freedom, therefore the universe is radiation dominated. The equation of state for the perfect fluid during radiation domination is given by $p = \rho/3$, and the solution to Friedmann equations gives ($\rho_R \propto a^{-4}$) and $H \propto a^{-2}$. This can be easily understood, since the energy density is diluted by the expansion of the universe which provides the volume factor a^{-3} and the extra factor of a^{-1} comes from the fact that the energy of radiation is further diluted by the redshift of wavelength. On the other hand, when the universe cools down, it becomes matter dominated ($p = 0$), and the Friedmann equations give $\rho_M \propto a^{-3}$ and $H \propto a^{-3/2}$, which only involves the volume dilution factor. Another key quantity is the total entropy, which is conserved when the universe expands adiabatically. The entropy density s is given by

$$s = \frac{\rho + p}{T} \tag{2.5}$$

where T is the temperature, determined by the relativistic degrees of freedom present in the universe. The entropy density can also be expressed more explicitly as a function of temperature as

$$s = \frac{2\pi^2}{45}\, g_*(T)\, T^3 \tag{2.6}$$

where g_* denotes the number of relativistic degrees of freedom. The total entropy is simply given by $S = s\, a^3$, so entropy conservation $dS = 0$ leads to the simple temperature dependence of the scale factor $a \propto T^{-1}$ obtained using equations (2.5) and (2.6).

The flatness problem can be understood by calculating the value of $|\Omega - 1|$ at very early epochs, for example close to Planck scale when the temperature of the universe was $T = T_{\rm Pl} \sim 10^{19}$GeV, using the observed value of today which lies in the interval $-0.0133 < \Omega_0 - 1 < 0.084$ [2]. Using equation (2.4), we get

$$\frac{|\Omega - 1|_{t_{\rm Pl}}}{|\Omega - 1|_{t_0}} = \frac{|\Omega - 1|_{t_{\rm Pl}}}{|\Omega - 1|_{t_{\rm eq}}}\, \frac{|\Omega - 1|_{t_{\rm eq}}}{|\Omega - 1|_{t_0}} \simeq \left(\frac{a(t_{\rm Pl})}{a(t_{\rm eq})}\right)^2 \frac{a(t_{\rm eq})}{a(t_0)} \tag{2.7}$$

where $t_{\rm eq}$ is the time of radiation matter equality. In writing the above expression we neglected the temperature dependence of g_*. The ratio $a(t_0)/a(t_{\rm eq}) = 1 + z_{\rm eq}$ defines the redshift at matter-radiation equality which is approximately at $z_{\rm eq} \simeq 10^4$. Using the fact that the temperature was $T_{\rm eq} \simeq eV$ at equality and it was $T_{\rm Pl} \simeq 10^{19} GeV$ during

the Planck epoch, the above equation gives

$$\frac{|\Omega - 1|_{t_{\rm Pl}}}{|\Omega - 1|_{t_0}} \simeq \left(\frac{T_{\rm eq}}{T_{\rm Pl}}\right)^2 (1 + z_{\rm eq})^{-1} \simeq 10^{-60} \,. \tag{2.8}$$

This result clearly shows that the value of $(\Omega - 1)$ must be fined tuned to a value which is very close to zero, but not exactly zero, in order to obtain the O(1) value today. Although this is possible in principle, the extreme fine tuning is hardly acceptable and unnatural. In principle, the observations are consistent with a flat geometry where $(\Omega - 1)$ is exactly zero. In this case, there is no flatness problem. The flatness problem is then associated with open or closed FRW geometries. However, theoretical models of a quantum generation of a universe predicts a closed geometry, because it has finite volume. In this case, extreme fine tuning is needed to generate a closed universe which is very close to being flat.

The horizon problem can also be formulated as to be a problem of fine tuning, since the degree of homogeneity and isotropy of the observable universe (the horizon scale today) can only be achieved under very special initial conditions. Any physical length scale λ grows with the scale factor $a(t)$, therefore the horizon scale today H_0^{-1} corresponds to a physical length scale $\lambda_H(t_{\rm ls})$ at the time of last scattering (when CMB radiation is formed), which is given by

$$\lambda_H(t_{\rm ls}) = H_0^{-1} \, \frac{a(t_{\rm ls})}{a(t_0)} = H_0^{-1} \, (1 + z_{\rm lss}) \tag{2.9}$$

where $z_{\rm lss} \simeq 1100$. On the other hand, the horizon scale at the last scattering surface is given by

$$R_H(t_{\rm lss}) = H_0^{-1} \, \left(\frac{a(t_{\rm lss})}{a(t_0)}\right)^{3/2} = H_0^{-1} \, (1 + z_{\rm lss})^{-3/2} \tag{2.10}$$

since the universe was matter dominated at the time of last scattering. From equations (2.9) and (2.10), we get

$$\left(\frac{\lambda_H(t_{\rm lss})}{R_H(t_{\rm lss})}\right)^3 = (1 + z_{\rm lss})^{3/2} \simeq 10^6 \,. \tag{2.11}$$

This result shows that our horizon corresponds to 10^6 casually disconnected regions at the time of last scattering. Since the horizon today is homogeneous to a high accuracy, this means that there are 10^6 physically disconnected regions that have the same temperature at the time of last scattering, which is unnatural.

The above mentioned problems with the standard big-bang cosmology can be resolved, if there is an epoch where the universe underwent a period of fast expansion such that the physical scales grew much faster than the horizon scale. Since any physical length scale grows as $\lambda \sim a$ and the horizon scale is given by $H^{-1} = a/\dot{a}$, the horizon problem can be resolved if

$$\left(\frac{\lambda}{H^{-1}}\right)_{t}^{-1} > \left(\frac{\lambda}{H^{-1}}\right)_{t_{\rm in}}^{-1} \tag{2.12}$$

where $t > t_{\rm in}$. This requires $\dot{a}(t) > \dot{a}(t_{\rm in})$, so $\ddot{a} > 0$. As a result, $a\,H$ grows during inflation and as a result of equation (2.4), the universe flattens. Therefore, if this period is long enough, the curvature problem is also resolved (Notice that it is possible to have a tiny amount of inflation that will solve the horizon problem (2.11), but not the curvature problem).

From the Friedmann equations (2.2), we observe that $\ddot{a} > 0$ can be achieved when

$$\rho + 3\,p < 0\,. \tag{2.13}$$

We will refer to this accelerated phase of expansion during the early universe as the inflationary epoch.

Besides solving the above mentioned problems of big-bang theory, inflation also provides a solution to the problem of unwanted/dangerous relics. At very high energies during the early universe, particle physics models predict existence of stable or metastable relics, such as monopoles, domain walls, gravitionos etc. These relics are either not observed today, contrary to the abundance that they should have, or their existence would have seriously affected the current observations within the big-bang cosmology; for example gravitinos might alter the big-bang nucleosynthesis, and the observed abundance of light elements would be predicted wrongly. Inflation solves these puzzles by diluting the relics and pushing them out of the scales corresponding to the current horizon.

2.2 The Physics of Inflation

As we have shown in the previous section, a solution to the puzzles within the big-bang theory can be achieved by an accelerated phase of expansion, which requires an equation

of state $\rho + 3\,p < 0$. As a first step to a more complete model, we can consider the extreme case when $\dot{\rho} = 0$, which corresponds to $\rho = -p =$ constant from equation (2.3). In this case, for a flat universe, [1] the scale factor expands exponentially and is given by

$$a(t) = a_i\, e^{H(t-t_i)} \tag{2.14}$$

where H is constant, and the resulting geometry of spacetime is known as the de-Sitter (dS) space-time. We can quantify the amount of inflationary expansion by the number of e-folds, which is defined as

$$N \equiv \mathrm{Ln}\left(\frac{a(t_{\rm end})}{a(t_i)}\right) \to H\ (t_{\rm end} - t_i) = H\,\Delta\, t_{\rm inf} \quad (\text{for dS}) \tag{2.15}$$

where $t_{\rm end}$ and t_i are the starting and ending time of inflation. Inflation solves the horizon problem if some physical length scale at t_i corresponding to the horizon scale today is smaller then the horizon scale at t_i. Namely,

$$\lambda_{H_0}(t_i) = H_0^{-1}\,\left(\frac{a(t_{\rm end})}{a(t_0)}\right)\,\left(\frac{a(t_i)}{a(t_{\rm end})}\right) = H_0^{-1}\,e^{-N}\,\frac{T_0}{T_{\rm end}} < H^{-1}(t_i) \tag{2.16}$$

where we have used the fact that $a(t_{\rm end})/a(t_0) = T_0/T_{\rm end}$. Then, using $T_0 \sim 10^{-4}\,\mathrm{eV}$ and $H_0 \sim 10^{-33}\,\mathrm{eV}$, the number of e-folds of inflation necessary to solve the horizon problem is given by

$$N \gtrsim \mathrm{Ln}\left(\frac{T_0}{H_0}\right) + \mathrm{Ln}\left(\frac{H(t_i)}{T_{\rm end}}\right) \simeq 67 + \mathrm{Ln}\left(\frac{H(t_i)}{T_{\rm end}}\right) \tag{2.17}$$

where the second term in the above inequality depends on the energy scale of inflation ($H(t_i)$) and the reheating temperature ($T_{\rm end}$), which is the temperature the universe attains after inflation is over. Therefore, up to a logarithmic dependence, we obtain $N \gtrsim 70$ is the necessary amount of inflation for the solution of the horizon problem. The same number of e-folds of inflation also provides a solution to the flatness problem. Noting that $\Omega - 1 \sim a^{-2}$ during inflation, we have

$$\frac{|\Omega - 1|_{t_{\rm end}}}{|\Omega - 1|_{t_i}} = \left(\frac{a(t_i)}{a(t_{\rm end})}\right)^2 = e^{-2\,N}\,. \tag{2.18}$$

We had $|\Omega - 1|_{t_{\rm end}} \sim 10^{-60}$ in the statement of the flatness problem from equation (2.8), so in order to have $|\Omega - 1|_{t_i}$ order unity, we find $N \sim 70$ from the above equation. Notice

[1] From now on, we will always work with a flat universe, assuming that any pre-existing curvature has already been washed away by the accelerated expansion.

that the above estimates for the required number of e-folds are only crude. We will provide a more precise estimate of the required amount of inflation, when we discuss quantum fluctuations in the next section, taking into account the largest observable scales in the sky.

Up to now, we have only discussed consequences of a generic inflationary model, without specifying the source (besides assuming a vacuum energy like equation of state $\rho = -p$). We will show that inflation can be achieved by a slowly rolling scalar field(inflaton), which is an approach taken by many authors so far, due to the simplicity of treating scalar fields. Therefore, we assume that inflation is driven by a scalar field, and all other matter fields have negligible energy densities. The action characterizing the dynamics of the scalar field is given by

$$S[\phi] = \int d^4x \sqrt{-g}\, \mathcal{L}[\phi] = \int d^4x \sqrt{-g} \left(-\frac{1}{2}\, \partial_\mu \phi\, \partial^\mu \phi - V(\phi) \right) . \tag{2.19}$$

The energy momentum tensor corresponding to the scalar field is therefore

$$T_{\mu\nu} = \partial_\mu \phi\, \partial_\nu \phi + \mathcal{L}[\phi]\, g_{\mu\nu} \tag{2.20}$$

where we have assumed that the background geometry is flat FRW ($k = 0$ in equation (2.1)). Since the background FRW geometry of the universe is homogeneous, the scalar field source must also be homogeneous, namely it depends only on time. Then, the corresponding energy density and pressure can be calculated from (2.20) as

$$\rho_\phi = \frac{1}{2}\, \dot{\phi}^2 + V(\phi) \quad , \quad p_\phi = \frac{1}{2}\, \dot{\phi}^2 - V(\phi)\, . \tag{2.21}$$

Moreover, extremezing the action (2.19), the scalar field obeys the evolution equation given by

$$\ddot{\phi} + 3H\, \dot{\phi} + V'(\phi) = 0\, . \tag{2.22}$$

The scalar field can drive an accelerated expansion of the universe if the equation of state approximately mimics that of vacuum energy, namely when $\rho_\phi \simeq -p_\phi$. This is achieved when $\dot{\phi}^2 \ll V(\phi)$ and $\ddot{\phi} \ll 3\, H\, \dot{\phi}$, and consequently equations (2.2) and (2.22) give

$$H \simeq \frac{\sqrt{V(\phi)}}{\sqrt{3}\, M_p} \quad , \quad \dot{\phi} \simeq -\frac{V'(\phi)}{3H}\, . \tag{2.23}$$

The conditions $\dot{\phi}^2 \ll V(\phi)$ and $\ddot{\phi} \ll 3\,H\,\dot{\phi}$ are known as the slow-roll conditions, and they can equivalently be formulated in terms of the smallness of the slow roll parameters ϵ and η, which are given by

$$\epsilon \equiv -\frac{\dot{H}}{H^2} = \frac{M_p^2}{2}\left(\frac{V'(\phi)}{V(\phi)}\right)^2 \quad , \quad \eta = M_p^2\,\frac{V''(\phi)}{V(\phi)}. \tag{2.24}$$

Inflation terminates when the slow-roll conditions are violated, namely when $\epsilon,\,\eta \sim 1$ and the universe starts to reheat. As a concrete example, we consider the case of massive chaotic inflation, where the potential term is given by $V(\phi) = m^2\,\phi^2/2$ [59]. In this case, slow-roll is achieved whenever $\phi \gg M_p$. This happens when the field ϕ is far away from the minimum and rolls slowly towards it. Inflation then terminates when the field starts oscillating around the minimum, and $\epsilon \gtrsim 1$. The condition $\phi \gg M_p$ does not mean that the Planck scale physics is necessarily relevant, since the energy density of the scalar field is much lower than the Planck scale as long as $m^2\,\phi^2 \ll M_p^4$, which is satisfied when $m/M_p \ll M_p/\phi$. We will discuss in the following section, that a mass which is a couple of orders of magnitude below the Grand Unified Theory (GUT) scale for the scalar field (which produces perturbations at the observed amount of inhomogeneity of $\sim 10^{-5}$), will satisfy this condition. The slow-roll approximation to the equations of motion for ϕ given in equations (2.23) reduces to

$$\dot{\phi} \simeq -\sqrt{\frac{2}{3}}\,m\,M_p \;\;,\;\; H \simeq \frac{m\,\phi}{\sqrt{6}\,M_p} \tag{2.25}$$

which are integrated to give

$$\begin{aligned} \phi &\simeq \phi_i - \sqrt{\frac{2}{3}}\,m\,M_p\;(t-t_i) \\ a(t) &\simeq a_i\,\exp\left[\frac{m\,\phi_i}{\sqrt{6}\,M_p}\,(t-t_i) - \frac{m^2}{6}\,(t-t_i)^2\right]. \end{aligned} \tag{2.26}$$

Inflation ends when $\phi(t_e) \sim 0$, so from the above equations we find

$$\Delta t_{\rm inf} = t_e - t_i \simeq \sqrt{\frac{3}{2}}\,\frac{\phi_i}{m\,M_p} \;\;,\;\; N = {\rm Ln}\left(\frac{a(t_e)}{a(t_i)}\right) \simeq \frac{\phi_i^2}{4M_p^2} \tag{2.27}$$

for the duration of inflation. We also show the phase space plot for the evolution of the scalar field in Figure 2.1, obtained by numerically integrating the equations (2.2)

and (2.22). The phase plot illustrate the attractor behavior of the evolution of the scalar field; arbitrary initial conditions quickly approach the slow-roll solution shown by the dashed line. After the slow-roll conditions are violated, the field ϕ starts to oscillate around the minimum, as can be seen from the elliptical motion in the phase plane in Figure 2.1. This behavior also explains why the name chaotic inflation is used to describe the model, since arbitrary initial conditions for the scalar field, as long as it obeys $\phi \gg M_p$, leads to slow-roll inflation.

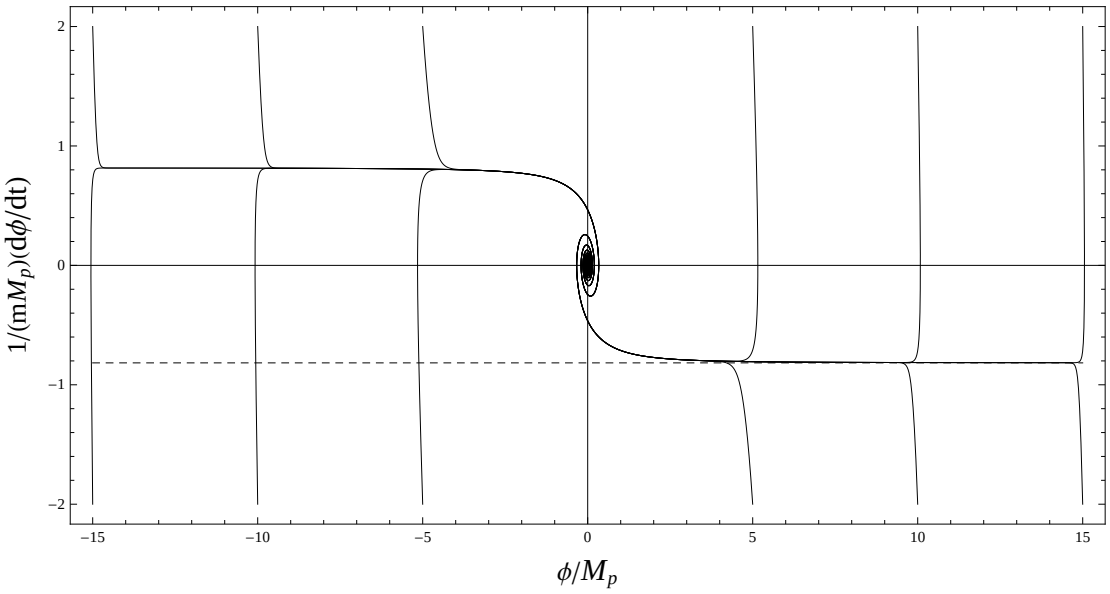

Figure 2.1: The phase plot $\phi - \dot{\phi}$ for massive chaotic inflation is shown. The value of ϕ is measured in units of M_p and time is measured in units of the mass of the scalar field m. The dashed line indicates the slow-roll solution.

As we have discussed previously, inflation also provides a natural mechanism for generation of cosmological perturbations. In the following sections we will discuss the quantum mechanical mechanism for the generation of these perturbations, starting from a simple case of a test field (neglecting gravity), and then developing the full theory including all associated degrees of freedom (including gravity).

2.3 Quantum Fields in a Cosmological Background

Consider the action for a massive scalar field ψ in a cosmological background, which is given by

$$S[\psi] = -\frac{1}{2}\int d^4x\,\sqrt{-g}\,\left[g^{\mu\nu}\,\partial_\mu\psi\,\partial_\nu\psi + m_\psi^2\,\psi^2\right] \tag{2.28}$$

where we choose to express the flat FRW metric $g_{\mu\nu}$ using conformal time η, which is defined by

$$ds^2 = a^2(\eta)\,\left(-d\eta^2 + d\vec{x}^2\right) \quad , \quad \eta \equiv \int \frac{dt}{a(t)}\,. \tag{2.29}$$

We assume that the energy density of the scalar field ψ is negligible, compared to the source that drives the expansion of the universe. Thus, we treat the field ψ as a quantum fluctuation in a classical cosmological background. The action (2.28) can be further expanded using the metric (2.29) to give

$$S[\psi] = \frac{1}{2}\int d^3x\,d\eta\,a^2(\eta)\,\left[(\partial_\eta\psi)^2 - (\vec{\nabla}\psi)^2 - m_\psi^2\,a^2(\eta)\,\psi^2\right]\,. \tag{2.30}$$

As can be seen from the above action, the kinetic term for the field ψ is not canonically normalized. Therefore, we define the field χ, which is given by $\chi = a(\eta)\,\psi$ and the action in terms of the new field reads

$$S[\chi] = \frac{1}{2}\int d^3x\,d\eta\,\left[(\partial_\eta\chi)^2 - (\vec{\nabla}\chi)^2 - \left(m_\psi^2 a^2(\eta) - \frac{a''(\eta)}{a(\eta)}\right)\,\chi^2\right] \tag{2.31}$$

up to a total time derivative. In the above action ($'$) denotes derivative with respect to conformal time η. Extremizing the above action, we obtain the classical evolution equation for the field χ, which is given by

$$\chi'' - \vec{\nabla}^2\,\chi + m_{\rm eff}^2\,\chi = 0 \;\;,\;\; m_{\rm eff}^2 \equiv m_\psi^2\,a^2 - \frac{a''}{a}\,. \tag{2.32}$$

The explicit time dependence for the mass of the field χ arises due to the interaction with the classical gravitational background. It is customary to work with a Fourier transformed field, which is defined through

$$\chi(\vec{x},\,\eta) = \int \frac{d^3k}{(2\pi)^{3/2}}\,\chi(\vec{k},\,\eta)e^{i\,\vec{k}\cdot\vec{x}} \tag{2.33}$$

where the Fourier transformed field obeys $\chi(-\vec{k},\,\eta) = \chi^*(\vec{k},\,\eta)$, due to reality of $\chi(\vec{x},\,\eta)$. The action (2.31) can be written in terms of the Fourier transformed modes as

$$S[\chi] = \frac{1}{2}\int d^3k\,d\eta\,\left[\dot{\chi}(\vec{k},\,\eta)\,\dot{\chi}^*(\vec{k},\,\eta) - \left(\vec{k}^2 + m_{\rm eff}^2\right)\,\chi(\vec{k},\,\eta)\,\chi^*(\vec{k},\,\eta)\right]\,. \tag{2.34}$$

Then, the classical equation of motion (2.32) can be expressed in terms of the Fourier transformed field as

$$\chi''(\vec{k},\eta) + \omega(k,\,\eta)^2\,\chi(\vec{k},\,\eta) = 0 \quad , \quad \omega(k,\,\eta)^2 \equiv \vec{k}^2 + m_{\rm eff}^2\,. \tag{2.35}$$

Therefore, we expand $\chi(\vec{k},\,\eta)$ as

$$\chi(\vec{k},\,\eta) = v(k,\,\eta)\,a(\vec{k}) + v^*(k,\,\eta)\,a^\dagger(-\vec{k}) \tag{2.36}$$

which satisfies the reality condition given above. In the above equation, a and $a^\dagger$ are expansion parameters for the moment, v's are known as the mode functions and they are solutions to the classical equation of motion (2.35) where $k \equiv |\vec{k}|$ since the classical equation of motion has only $\vec{k}^2 = k^2$ dependence. This is a result of the isotropy of the background geometry. Therefore, the original field can be written as

$$\chi(\vec{x},\,\eta) = \int \frac{d^3k}{(2\pi)^{3/2}}\,\left[v(k,\,\eta)\,a(\vec{k})\,e^{i\,\vec{k}\cdot\vec{x}} + v^*(k,\,\eta)\,a^\dagger(\vec{k})\,e^{-i\,\vec{k}\cdot\vec{x}}\right] \tag{2.37}$$

where we have changed the integration variable as $\vec{k} \to -\vec{k}$ in the second term and used the invariance of d^3k under this rotation. We now quantize the field χ by imposing bosonic commutation relations on χ and its canonical momentum $\pi_\chi \equiv \partial\mathcal{L}_\chi/\partial\chi'$ and promoting them to operators ($\chi \to \hat{\chi}$ and $\pi \to \hat{\pi}$) , namely

$$\begin{aligned}
&[\hat{\chi}(\vec{x},\,\eta),\,\hat{\pi}(\vec{y},\,\eta)] = \left[\hat{\chi}(\vec{x},\,\eta),\,\hat{\chi}'(\vec{y},\,\eta)\right] = i\,\delta(\vec{x}-\vec{y}) \\
&[\hat{\chi}(\vec{x},\,\eta),\,\hat{\chi}(\vec{y},\,\eta)] = [\hat{\pi}(\vec{x},\,\eta),\,\hat{\pi}(\vec{y},\,\eta)] = 0
\end{aligned} \tag{2.38}$$

which are equivalent to

$$\begin{aligned}
&\left[\hat{a}(\vec{k}),\,\hat{a}^\dagger(\vec{q})\right] = \delta(\vec{k}-\vec{q}) \\
&\left[\hat{a}(\vec{k}),\,\hat{a}(\vec{q})\right] = \left[\hat{a}^\dagger(\vec{k}),\,\hat{a}^\dagger(\vec{q})\right] = 0
\end{aligned} \tag{2.39}$$

whenever the mode function v satisfies the following relation

$$v(k,\,\eta)\,v^{*\prime}(k,\,\eta) - v^*(k,\,\eta)\,v'(k,\,\eta) = i\,. \tag{2.40}$$

The operators $\hat{a}$ and $\hat{a}^\dagger$ are the annihilation and creation operators, which annihilate/create particles with energy $\omega(k,\,\eta)$. Correspondingly, the vacuum state is defined to be

$$\hat{a}(\vec{k})|0>=0\,. \tag{2.41}$$

The Hamiltonian density ($\mathcal{H} \equiv \pi_\chi \, \dot{\chi} - \mathcal{L}$) can be integrated over the spatial coordinates to give the Hamiltonian operator ($\hat{H} = \int d^3x \, \mathcal{H}$) corresponding to the field χ is given by

$$\hat{H}(\eta) = \frac{1}{2} \int d^3x \, \left[\chi'^2 + (\vec{\nabla}\chi)^2 + m_{\rm eff}^2 \chi^2 \right] . \tag{2.42}$$

Inserting the expansion (2.37) into the Hamiltonian, we get

$$\begin{aligned} \hat{H}(\eta) \;\; = \;\; & \frac{1}{2} \int d^3k \left[\hat{a}(\vec{k}) \, \hat{a}(-\vec{k}) \, F(k, \, \eta) + \hat{a}^\dagger(\vec{k}) \, \hat{a}^\dagger(-\vec{k}) \, F^*(k, \, \eta) \right. \\ & \left. \left(\hat{a}(\vec{k}) \, \hat{a}^\dagger(\vec{k}) + \hat{a}^\dagger(\vec{k}) \, \hat{a}(\vec{k}) \right) \, E(k, \, \eta) \right] \end{aligned} \tag{2.43}$$

where

$$F(k, \, \eta) \equiv v'(k, \, \eta)^2 + \omega^2(k, \, \eta) \, v(k, \, \eta)^2 \;\; , \;\; E(k, \, \eta) \equiv |v'(k, \, \eta)|^2 + \omega^2(k, \, \eta) \, |v(k, \, \eta)|^2 \, . \tag{2.44}$$

The vacuum expectation value of the Hamiltonian operator is given by

$$< 0 | \hat{H}(\eta) | 0 > = \frac{1}{2} \, \delta(\vec{0}) \int d^3k \, E(k, \, \eta) \tag{2.45}$$

where $\delta(\vec{0})$ is the manifestation of the infinite volume of the 3-space and is harmless. The vacuum state would correspond to a state with minimum energy density $E(k, \, \eta)$. Parameterizing the mode function $v(k, \, \eta) = r_k \, e^{i \, s_k}$, the condition in equation (2.40) reduces to $r_k^2 \, s_k' = -1/2$ and $E(k, \, \eta)$ becomes

$$E(k, \, \eta) = r_k'^2 + r_k^2 \, \omega^2(k, \, \eta) + \frac{1}{4 r_k^2} \, . \tag{2.46}$$

$E(k, \, \eta)$ is minimized at a certain moment of time η_0 when

$$r_k'(\eta_0) = 0 \;\; , \;\; r_k = [2\omega(k, \, \eta_0)]^{-1/2} \rightarrow v(k, \, \eta_0) = [2\omega(k, \, \eta_0)]^{-1/2} \; e^{-i \, s_k(\eta_0)} \, . \tag{2.47}$$

This result shows that in general, the vacuum state can only be defined instantaneously. Therefore, the vacuum state defined at some time η_0 with $\hat{a}(\vec{k})_{(\eta_0)} | 0 > = 0$ contains particles at some time $\eta > \eta_0$ and $_{(\eta)} | 0 > \neq \, _{(\eta_0)} | 0 >$in general. Consequently, one can not define a global time independent vacuum and gravitational interactions with the classical background will lead to particle production. However, it is possible to define an adiabatic vacuum state if certain conditions are met and one would have

$_{(\eta)}|0>\approx {}_{(\eta_0)}|0>$, as we will discuss below. We can simplify the Hamiltonian (2.43) at η_0 using (2.47) which results in $F(k,\,\eta_0) = 0$ and $E(k,\,\eta_0) = \omega(k,\,\eta_0)$ and the Hamiltonian becomes

$$\hat{H}(\eta_0) = \frac{1}{2}\int d^3k\,\omega(k,\,\eta_0)\,\left[\hat{a}(\vec{k})\,\hat{a}^\dagger(\vec{k}) + \hat{a}^\dagger(\vec{k})\,\hat{a}(\vec{k})\right]. \tag{2.48}$$

Alternatively, we can rewrite the Hamiltonian in a normal ordered form to get rid of the divergent vacuum energy, which reads

$$:\hat{H}(\eta_0) := \int d^3k\,\omega(k,\,\eta_0)\,\hat{a}^\dagger(\vec{k})\,\hat{a}(\vec{k}) = \int d^3k\,\omega(k,\,\eta_0)\,\hat{n}(\vec{k}) \tag{2.49}$$

where $\hat{n}$ is the number operator. As we have pointed out, it is possible to define an adiabatic vacuum state, if the conditions (2.47) are approximately satisfied for a prolonged period, so they describe the minimum of energy. Below, we will show that this requirement is equivalent to $\omega(k,\,\eta)$ being a slowly varying function (see comment after equation (2.54)). Under this assumption, we can solve the classical equations of motion (2.35) for the mode function $v(k,\,\eta)$. In order to do so, we parameterize $v(k,\,\eta)$ as

$$v(k,\,\eta) = \frac{1}{\sqrt{2\Omega_k(\eta)}}\exp\left[-i\int_{\eta_0}^{\eta}\Omega_k(\eta')\,d\eta'\right] \tag{2.50}$$

and inserting into (2.35) results in

$$\omega^2(k,\,\eta) = \Omega_k^2(\eta) + \frac{\Omega_k''(\eta)}{2\Omega_k(\eta)} - \frac{3}{4}\left(\frac{\Omega_k'(\eta)}{\Omega_k(\eta)}\right)^2. \tag{2.51}$$

Using the fact that $\omega(k,\,\eta)$ is slowly varying, we can invert the above equation iteratively and neglect terms that are higher in time derivatives of ω, which gives

$$\Omega_k(\eta) = \omega(k,\,\eta)\,\left[1 - \frac{1}{4}\frac{\omega''(k,\,\eta)}{\omega^3(k,\,\eta)} + \frac{3}{8}\left(\frac{\omega'(k,\,\eta)}{\omega^2(k,\eta)}\right)^2 + \ldots\right] \tag{2.52}$$

which is valid as long as the adiabaticity conditions are satisfied, namely when

$$\frac{\omega'(k,\,\eta)}{\omega^2(k,\eta)} \ll 1\ ,\ \ \frac{\omega''(k,\,\eta)}{\omega^3(k,\,\eta)} \ll 1,\ \ \ldots \tag{2.53}$$

In general, only the first order term in the expansion (2.52) is taken into account, and the adiabatic solution for the mode function is given by

$$v(k,\,\eta) \simeq \frac{1}{\sqrt{2\omega}}\,e^{-i\int d\eta'\,\omega}. \tag{2.54}$$

Note that the conditions (2.47) are approximately met by the above mode function (up to an accuracy of ω'/ω^2 and ω''/ω^3), and therefore the vacuum state $|0>$ is well defined as long as conditions (2.53) are met. This result completely determines the mode expansion of the field χ in (2.37). Furthermore, using $\chi = a\,\psi$ we also determine the behavior of the starting field ψ in the adiabatic regime. The amplitude of fluctuations of the field χ is characterized by the two point correlation function, which is given by

$$< 0|\hat{\chi}(\vec{x},\,\eta)\,\hat{\chi}(\vec{y},\,\eta)|0 >= \int \frac{d^3k}{(2\pi)^3}\,|v(k,\,\eta)|^2 e^{i\,\vec{k}\cdot(\vec{x}-\vec{y})} \tag{2.55}$$

where we have explicitly used the mode expansion (2.37), and the commutation relations (2.39). We can further simplify the above expression by evaluating the angular integrals, which gives

$$< 0|\hat{\chi}(\vec{x},\,\eta)\,\hat{\chi}(\vec{y},\,\eta)|0 >= \frac{1}{2\pi^2}\int_0^\infty \frac{dk}{k}\,\frac{\sin kL}{kL}\,k^3\,|v(k,\,\eta)|^2 \equiv \int_0^\infty \frac{dk}{k}\,\frac{\sin kL}{kL}\,P_\chi(k) \tag{2.56}$$

where $L = |\vec{x}-\vec{y}|$ and $P_\chi(k)$ is known as the power spectrum and it corresponds to the typical contribution of the integrand to the full integral for scales $k \sim L^{-1}$.

Since the universe is expanding almost exponentially during slow-roll inflation, we apply the above results for a quasi de-Sitter expansion, when $\dot{H} = -\epsilon\,H^2$ with ϵ being the slow roll parameter defined in (2.24) and it is small during inflation. Solving $\dot{H} = -\epsilon\,H^2$ to first order in ϵ, we get $H = H_0(1-\epsilon\,H_0\,t^2)$ where H_0 is constant. Next, integrating $\dot{a}/a = H$ to first order in ϵ and then inserting the result to the definition of conformal time in (2.29), we get

$$a(\eta) = -\frac{1}{H\,\eta\,(1-\epsilon)}\,. \tag{2.57}$$

Using (2.32), the effective mass squared term $m^2_{\rm eff}$ becomes

$$m^2_{\rm eff} \simeq \left[\frac{m^2_\psi}{H^2} - 2 - 3\epsilon\right]\,\frac{1}{\eta^2} \tag{2.58}$$

at the linear order in ϵ [2] and consequently, the mode function $v(k,\,\eta)$ satisfies

$$v''(k,\,\eta) + \omega^2(k,\,\eta)\,v(k,\,\eta) = 0\ ,\ \ \omega^2(k,\ ,\eta) \simeq \left[k^2 + \left(\frac{m^2_\psi}{H^2} - 2 - 3\epsilon\right)\,\frac{1}{\eta^2}\right]\,. \tag{2.59}$$

[2] We neglected terms of order $\epsilon\,m_\psi$ because m_ψ is also assumed to be small, since the energy density of the field ψ, which is proportional to m^2_ψ, is neglected.

The conditions of adiabaticity given in equation (2.53) are readily satisfied by $\omega^2(k,\,\eta)$ defined in the above equation as long as the parameter ϵ is small, which is satisfied during inflation [3] . The substitution $v = \sqrt{k|\eta|}\, f_k(\eta)$ reduces the above equation, to the Bessel equation and $f_k(\eta)$ are solved in terms of the linear combinations of the Bessel functions of the first kind $J_n(k\,|\eta|)$ and the second kind $Y_n(k\,|\eta|)$, or by Hankel functions $H_n^{(1)} \equiv J_n + i\,Y_n$ and $H_n^{(2)} \equiv J_n - i\,Y_n$, namely

$$v(k,\,\eta) = \sqrt{k\,|\eta|}\,\left\{\delta_k\,H_n^{(1)}(k\,|\eta|) + \xi_k\,H_n^{(2)}(k\,|\eta|)\right\} \tag{2.60}$$

where

$$n \equiv \sqrt{\frac{9}{4} + 3\,\epsilon - \frac{m_\psi^2}{H^2}} \simeq \frac{3}{2} + \epsilon - \frac{m_\psi^2}{3H^2} \tag{2.61}$$

and we have assumed that $m_\psi/H \ll 3/2$, which reasonable since the energy density of the field is negligible. It is also useful to study the solution of (2.59) in two limiting cases when the physical momentum of the Fourier mode defined by k/a is (1) much larger than the horizon scale at early times ($k/a \gg H \;\Leftrightarrow\; k|\eta| \gg 1$) and (2) when it is much smaller then the horizon scale at late times ($k/a \ll H \;\Leftrightarrow\; k|\eta| \ll 1$). In the first case (sub-horizon or deep Ultraviolet (UV) regime), (2.59) reduces to

$$v''(k,\,\eta) + k^2\,v(k,\,\eta) \simeq 0 \tag{2.62}$$

whose properly normalized solution satisfying (2.54) and (2.40) is simply given by

$$v(k,\,\eta) \simeq \frac{1}{\sqrt{2k}}\,e^{-ik\,\eta}\,. \tag{2.63}$$

In the second case (super-horizon or Infrared (IR) regime), (2.59) reduces to

$$v''(k,\,\eta) - \left(2 + 3\epsilon - \frac{m_\psi^2}{H^2}\right)\,\frac{1}{\eta^2} \simeq 0 \tag{2.64}$$

whose solution is given by

$$v(k,\,\eta) \simeq \gamma_k\,|\eta|^{s_1} + \lambda_k\,|\eta|^{s_2}\;\;,\;\; s_{1,2} = \frac{1}{2} \pm n\,. \tag{2.65}$$

[3] Note that $\omega^2 =$ constant when $\epsilon = \dot{H} = 0$, which is the case for a de-Sitter spacetime. In this case, the vacuum state, which is known as the Bunch-Davies vacuum [60] is uniquely defined and is independent of time.

Since $\eta \to 0$ at late times when a grows (as can be seen from equation (2.57)), the s_2 term with the negative sign dominates in the super-horizon region regime and we have

$$v(k,\,\eta) \simeq \lambda_k\,|\eta|^{(1/2-n)} \propto [a(\eta)]^{(n-1/2)} \tag{2.66}$$

Note that we do not impose conditions (2.40) or (2.54) for super-horizon modes, since these solutions do not correspond to mode functions of quantum states. For super-horizon modes, $\omega^2 < 0$, and ω does not correspond to energy of particle excitations created by operating $\hat{a}^\dagger(\vec{k})$ on the vacuum. Therefore, a quantum to classical transition occurs at some moment during horizon crossing when $k/a \sim H$ [61]. This also means that initial conditions for the fluctuations are set quantum mechanically at small scales in the UV regime, but they behave like classical fields at large scales in the IR regime. Modes that already have a wavenumber $k/a_{\rm in} < H_{\rm in}$ initially are unobservable and irrelevant as we will discuss shortly. We can also determine the evolution of the original modes $\psi(k,\,\eta) = \chi(k,\,\eta)/a(\eta)$, which behaves according to

$$\psi(k,\,\eta) \propto \begin{cases} \frac{e^{-i\,k\,\eta}}{\sqrt{2k}\,a(\eta)} \\ [a(\eta)]^{(n-3/2)} \sim \text{constant} \end{cases} \tag{2.67}$$

where the second line is obtained using (2.61) and the fact that both ϵ and m/H are small. Therefore, $\psi(k,\,\eta)$ is oscillating with a decaying amplitude in the sub-horizon regime and stays constant (up to a small power law dependence on the ratio m/H and the slow roll parameter ϵ) in the super-horizon regime. Having understood the limiting behavior of the solutions to (2.59), we can set the unknown constants δ_k and ξ_k in the full solution (2.60) by considering the asymptotic expansions for the Hankel functions which are

$$\begin{aligned} H_n^{(1)}(k|\eta| \gg 1) &\simeq \sqrt{\frac{2}{\pi\,k\,|\eta|}}\,\exp\left[i\left(k\,|\eta| - \frac{n\,\pi}{2} - \frac{\pi}{4}\right)\right], \\ H_n^{(2)}(k|\eta| \gg 1) &\simeq \sqrt{\frac{2}{\pi\,k\,|\eta|}}\,\exp\left[-i\left(k\,|\eta| - \frac{n\,\pi}{2} - \frac{\pi}{4}\right)\right] \end{aligned} \tag{2.68}$$

where $\Gamma(n)$ is the Euler-Gamma function. Matching (2.60) with (2.63) in the sub-horizon/UV regime using the asymptotic expansions (2.68), we clearly see that $\xi_k = 0$ and δ_k is given by

$$\delta_k = \frac{\sqrt{\pi}}{2\,\sqrt{k}}\,\exp\left[i\,\left(\frac{n\,\pi}{2} + \frac{\pi}{4}\right)\right]. \tag{2.69}$$

Then, the mode function is fully determined as

$$v(k,\,\eta) = \frac{\sqrt{\pi}}{2}\,\sqrt{|\eta|}\exp\left[i\,\left(\frac{n\,\pi}{2}+\frac{\pi}{4}\right)\right]\,H_n^{(1)}\left(k\,|\eta|\right)\,. \tag{2.70}$$

Again, the original field can be obtained as $\psi(k,\,\eta) = \chi(k,\,\eta)/a(\eta)$. Using (2.70), and taking $\epsilon = m/H = 0$ (that is, de-Sitter space and massless field), which is approximately correct, we have plotted the evolution of the mode function corresponding to the field $\psi(k,\,\eta)$ in Figure 2.2, which shows agreement with the approximate result obtained in equation (2.67).

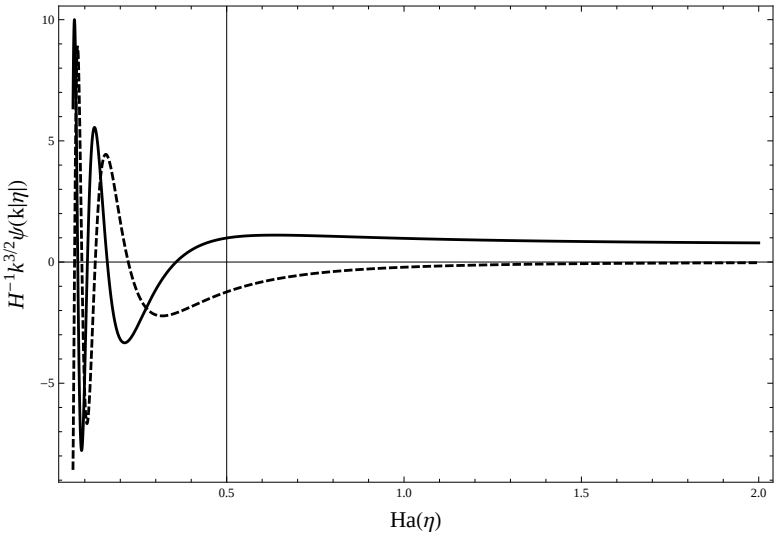

Figure 2.2: The real (dashed curve) and imaginary (continuous curve) parts of the mode function corresponding to the field ψ is shown. At small scales, the mode function is oscillatory with decreasing amplitude and at large scales it stays constant.

To compute the power spectrum at large scales when the field stays constant, we study the behavior of the full solution (2.70) by the asymptotic expansion of $H_n^{(1)}$ for small $k|\eta|$, which is

$$H_n^{(1)}(k|\eta| \ll 1) \simeq \sqrt{\frac{2}{\pi}}\,e^{-i\,\pi/2}\,2^{n-3/2}\,\frac{\Gamma(n)}{\Gamma(3/2)}\,(k\,|\eta|)^{-n}\,. \tag{2.71}$$

Using this expansion, the mode function $v(k,\,\eta)$ for $k\,|\eta| \ll 1$ is given by

$$v(k\,|\eta| \ll 1) \simeq e^{i(n/2-1/4)\pi}\,2^{n-3/2}\,\frac{\Gamma(n)}{\Gamma(3/2)}\,\frac{1}{\sqrt{2k}}\,(k\,|\eta|)^{1/2-n}\,. \tag{2.72}$$

Then, the power spectrum defined in (2.56) for χ at large scales (i.e super-horizon scales when the field ψ freezes out) can be calculated, which is roughly proportional to (neglecting the order unity numerical factors)

$$P_\chi \propto k^3 \, |v(k,\, \eta)|^2 \propto k^2 \, (k \, |\eta|)^{1-2n} \, . \tag{2.73}$$

Correspondingly, the power for the original field ψ can be computed using $\psi = \chi/a$ as

$$P_\psi = P_\chi/a^2 \propto H^2 \, (k \, |\eta|)^{3-2n} \simeq H^2 \, (k \, |\eta|)^{-2\epsilon+2m_\psi^2/3H^2} \, . \tag{2.74}$$

The power spectrum of ψ is nearly scale invariant up to the small k dependence which is known as the spectral index: $n_\psi = -2\epsilon + 2m_\psi^2/3H^2$. When $n_\psi > 0$, the spectrum is said to be blue tilted (more power in UV) and when $n_\psi < 0$ it is said to be red tilted (more power in IR).

The above results indicate that during the inflationary expansion, quantum fluctuations are produced at sub-horizon scales and they freeze out at horizon crossing. Namely, a mode with $k/a \gg H$ initially, will be generated quantum mechanically, and when $k/a \sim H$ due to the expansion of the universe, it will freeze out as can be seen in Figure 2.2. The mode will then stay constant as long as $k/a > H$ is satisfied. After inflation ends, the universe expands according to a power law, with $a \sim t^n$, $n < 1$ and $H^{-1} \sim a^{1/n} > a$. On the other hand, the physical length scale for the frozen out perturbations will grow as $\lambda \sim a/k$, so the horizon scale grows faster then the length scale of the perturbation. Consequently, there will be a moment when the perturbation re-enters the horizon and therefore it can be observed (Only modes that are inside the horizon can be observed, since the horizon sets the scale of casual processes). This also shows that modes that are initially in the super-horizon regime during inflation (which initially had $\omega^2(k,\, \eta) < 0$), will stay outside the observable horizon and therefore, they have no physical relevance as shown schematically in Figure 2.3. As pointed out earlier, it is possible to obtain an estimate for the required amount of inflation, taking into account the largest observable scales in the sky. Consider for example,

$$\frac{k}{a_0 \, H_0} = \frac{a_*}{a_{\rm end}} \, \frac{a_{\rm end}}{a_{\rm reh}} \, \frac{a_{\rm reh}}{a_0} \, \frac{H_*}{H_0} \tag{2.75}$$

where k is any horizon size co-moving scale, $a_0 \, H_0$ is the corresponding value of k today, $*$ denotes that the relevant quantity is evaluated at horizon crossing, and 0 denotes that

it is evaluated today. Note that in writing the above equation, we have followed the sequence of epochs after inflation (except the dark energy domination which is nearly today) shown in Figure. 2.3. A matter dominated epoch follows the end of inflation (due to oscillations of the inflaton around the minimum of its potential) and a radiation dominated era follows when the inflaton decays into radiation (reheating). The rest of the evolution is well described by the standard big-bang picture. In terms of energy densities ($\rho \sim a^{-3}$ during matter domination, $\rho \sim a^{-4}$ during radiation domination, and $H \sim \rho^{1/2}$ due to Friedman equation), equation (2.75) becomes

$$e^{N_*} = \frac{a_0\, H_0}{k} \left(\frac{\rho_{\rm ref}}{\rho_{\rm end}}\right)^{1/3} \left(\frac{\rho_{0r}}{\rho_{\rm reh}}\right)^{1/4} \left(\frac{\rho_*}{\rho_0}\right)^{1/2} \tag{2.76}$$

where we have used to fact that $a_{\rm end}/a_* = e^{N_*}$, N_* denotes the number of e-folds before the end of inflation, when the scale k crosses the horizon. Using the temperature today $T_0 \sim 10^{-4}$eV, $\rho_{0r} \sim T_0^4$ and $H_0 \sim 10^{-33}$eV the above equation can be re-written as [62]

$$N_* \simeq 62 - {\rm Ln}\left(\frac{k}{a_0\, H_0}\right) - {\rm Ln}\left(\frac{10^{16}\,{\rm GeV}}{\rho_*^{1/4}}\right) + {\rm Ln}\left(\frac{\rho_*^{1/4}}{\rho_{\rm end}^{1/3}}\right) - \frac{1}{3}\,{\rm Ln}\left(\frac{\rho_{\rm end}^{1/4}}{\rho_{\rm reh}^{1/4}}\right) . \tag{2.77}$$

For the largest observable scales when $k \sim a_0\, H_0$, the details of the mechanism of reheating introduces an order ~ 10 uncertainty in the number of necessary e-folds, leading to $50 \lesssim N_* \lesssim 70$.

Inflationary expansion provides an adiabatic vacuum state from which quantum fluctuations are generated and stretched to scales exceeding the horizon, as demonstrated in this chapter. These fluctuations then re-enter the horizon after the end of inflation and they can contribute to processes within the observable horizon. Therefore, if it is possible to connect the fluctuations of the field ψ to density fluctuations, they can lead to the formation of structure within the horizon. In the current setup, this is not possible since the energy density of the field ψ is neglected in the Einstein equations that determines the metric. Density perturbations can be described by the fluctuations in the metric which can be parameterized as

$$g_{\mu\nu}(t,\, \vec{x}) = g^{(0)}_{\mu\nu}(t) + \delta g_{\mu\nu}(t,\, \vec{x}) \tag{2.78}$$

where $g^{(0)}_{\mu\nu}$ is the background FRW metric. At linear order in fluctuations, the field ψ will be decoupled from the metric fluctuations $\delta g_{\mu\nu}$, so the generated field fluctuations

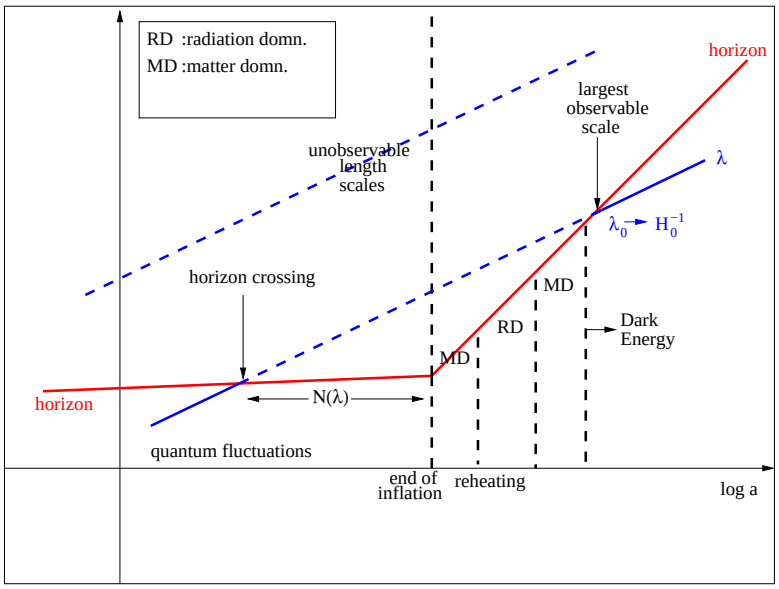

Figure 2.3: A schematic representation of the mechanism of generation of density fluctuations during inflation is shown. Modes that were already outside the horizon during inflation are not observable; only modes that were inside the horizon are observable today. The precise value of $N(\lambda)$, i.e the number of e-folds before the end of inflation when the largest observable perturbation left the horizon, is not precisely known, since the reheating mechanism is unknown.

can not source metric fluctuations during inflation. It is however possible to produce metric fluctuations after inflation, for example through the curvaton [63] and DGZK [49] mechanisms. In the curvaton scenario, density perturbations are produced when the energy density of a massive scalar field, like ψ, becomes significant after inflation, while it is oscillating. Then, the fluctuations in the scalar field are converted into density perturbations. The only requirement is that during inflation, the scalar field should acquire a nearly scale independent spectrum. In the DGZK mechanism, the decay rate of the field(s) driving inflation depends on on the value of a light scalar field (such couplings arise, for example in string theory models). Then, fluctuations in the light scalar field will lead to different reheating temperatures for different spatial regions in the universe. This in turn generates a density contrast and might lead to the observed spectrum of perturbations.

Another natural possibility is to consider quantum fluctuations of the inflaton field,

which sources the accelerated expansion of the universe. In this case, the inflaton field is given by $\varphi(t,\,\vec{x}) = \phi_0(t) + \delta\phi(t,\,\vec{x})$ where ϕ_0 is the homogeneous background value and $\delta\phi$ is a small fluctuation. In this case, the metric fluctuations $\delta g_{\mu\nu}$ and the inflaton fluctuation $\delta\phi$ are coupled at the linear order and density fluctuations are automatically generated during inflation. The treatment of this coupled system proves to be more involved, therefore we will discuss the formalism and basic results in the following section.

2.4 Quantum fluctuations of metric and scalar field during inflation

Consider the full action of the scalar field and gravitational degrees of freedom (through the Einstein-Hilbert action), which is given by

$$S[\phi,\,g_{\mu\nu}] = \int d^4x\,\sqrt{-g}\,\left[\frac{M_p^2}{2}\,R - \frac{1}{2}\,\partial^\mu\varphi\,\partial_\mu\varphi - V(\varphi)\right] \tag{2.79}$$

where R is the Ricci scalar curvature. Extremizing the action (2.79) with respect to the scalar field results in the evolution equations of φ and extremizing with respect to the metric tensor results in the Einstein equations which are respectively given by

$$\frac{1}{\sqrt{-g}}\,\partial_\mu\,\left[\sqrt{-g}\,g^{\mu\nu}\,\partial_\nu\,\varphi\right] + V'(\varphi) = 0 \tag{2.80}$$

$$G_{\mu\nu} = R_{\mu\nu} - \frac{1}{2}\,g_{\mu\nu}\,R = \frac{1}{M_p^2}\,T_{\mu\nu}(\varphi) \tag{2.81}$$

where $T_{\mu\nu}(\varphi)$ is given as in equation (2.20) with the replacement $\phi \to \varphi$. The metric $g_{\mu\nu}$ and the inflaton φ contain also the small perturbations, so they are given by

$$g_{\mu\nu} = g^{(0)}_{\mu\nu} + \delta g_{\mu\nu}\ ,\ \ \varphi = \phi_0 + \delta\phi\,. \tag{2.82}$$

The complete set of equations describing the evolution of the background, which are obtained by using the FRW metric and the homogeneous background value of the inflaton field ϕ_0 in (2.80) and (2.81), become

$$3\frac{a^{'2}}{a^2} = \frac{1}{M_p^2}\,\left(\frac{1}{2}\,\phi_0^{'2} + a^2\,V(\phi_0)\right)\ \ ,\ \ \phi_0^{''} + 2\,\frac{a'}{a}\,\phi_0' + a^2\,V'(\phi_0) = 0 \tag{2.83}$$

the inflationary solutions of which we have studied in detail in section (2.2). In order to study the linearized evolution of perturbations, we need to study the full action (2.79) at the quadratic level. This is also necessary in order to find the linear combinations of fields that canonically normalize the action, as we have done in section (2.3) when passing from field ψ to χ in order to obtain the action (2.31). This step is necessary, since only the canonically normalized fields can be properly quantized and initial conditions can be set accordingly.

The metric perturbations are described by a symmetric tensor $\delta g_{\mu\nu}$, which has in general 10 distinct entries. However, due to the general coordinate invariance in general relativity, 4 of these can be removed by coordinate transformations. Out of the remaining 6 perturbations, 4 of them correspond to nondynamical degrees of freedom, which can be best understood through the ADM formalism [64]. In the ADM formalism, the gravitational action is decomposed into the dynamical part containing the spatial metric δg_{ij} and a part containing the lapse ($N \equiv \delta g_{00}$) and shift functions ($N_i \equiv \delta g_{0i}$). The lapse and shift functions have no kinetic terms in the action, and they can be integrated out by solving their equations of motion [4] . This leaves only δg_{ij} as dynamical modes, which have only two degrees of freedom. In summary, the metric perturbations have only 2 dynamical degrees of freedom, which corresponds to the two polarizations of the graviton.

We decompose the metric fluctuations $\delta g_{\mu\nu}$ by exploiting the three-dimensional rotational symmetry of the background. In a more mathematical language, we consider irreducible representations of the $SO(3)$ group, therefore we can construct sets of perturbations that are decoupled at the linearized level. The decomposition we use can be parameterized as

$$\delta g_{\mu\nu} = \begin{pmatrix} -2\,a^2\,\Phi & a\,\left(\partial_i\,B + B_i\right) \\ & a^2\,\left(-2\,\Psi\,\delta_{ij} - 2\,\partial_i\,\partial_j\,E - \partial_i\,E_j - \partial_j\,E_i + h_{ij}\right) \end{pmatrix} \tag{2.84}$$

where the unperturbed metric $g^{(0)}_{\mu\nu}$ is given in conformal coordinates, and the scale factor a depends on η. The perturbations $\{\Phi,\, B,\, \Psi,\, E\}$ are scalar modes, $\{B_i,\, E_i\}$ are transverse vector modes satisfying $\partial_i\,B_i = \partial_i\,E_i = 0$ and h_{ij} is the transverse-traceless tensor mode satisfying $\partial_i\,h_{ij} = h^i_i = 0$. The naming of the modes is clear, and it is done

[4] The equations of motion derived from extremezing the gravitational action with respect to lapse and shift functions are known as the momentum and hamiltonian constraints.

with respect to their transformation properties under the $SO(3)$ group. Note that the tensor mode h_{ij} has two degrees of freedom, each vector mode has also two degrees of freedom, and each scalar mode has one degree of freedom. In total, the decomposition (2.84) provide us with $2 + 2 \times 2 + 4 \times 1 = 10$ degrees of freedom, which contains the total number of independent entries in $\delta g_{\mu\nu}$. Notice that the mode $\delta\phi$ is an additional scalar mode. As we have discussed earlier, the advantage of this decomposition is that perturbations are classified in decoupled sets at the linearized level. In addition, the scalar mode $a^2\,\Phi$ corresponds to the lapse function N and $a\,(\partial_i\,B + B_i)$ corresponds to the shift function N_i in the ADM formalism, so we can immediately claim that these modes are nondynamical. These claims will be proven explicitly when we calculate the quadratic action for perturbations below.

We have discussed in the beginning of this section that some of the perturbations in the decomposition (2.84) can be removed by coordinate transformations. This can be shown explicitly, by considering an infinitesimal coordinate transformation

$$x^\mu \to x^\mu + \epsilon^\mu \tag{2.85}$$

under which the metric and inflaton perturbations transform to linear order as

$$\delta g_{\mu\nu} \to \delta g_{\mu\nu} - g^{(0)}_{\mu\nu,\,\sigma}\,\epsilon^\sigma - g^{(0)}_{\mu\sigma}\,\epsilon^\sigma_{,\,\nu} - g^{(0)}_{\sigma\nu}\,\epsilon^\sigma_{,\,\mu} \tag{2.86}$$

$$\delta\phi \to \delta\phi - \phi_{0,\,\mu}\,\epsilon^\mu\ . \tag{2.87}$$

We can also decompose the infinitesimal transformation four-vector as

$$\epsilon^\mu = \left(\xi^0,\,\partial_i\,\xi + \xi^i\right)\ . \tag{2.88}$$

Therefore, the coordinate transformations (2.86) and (2.87) can be written explicitly as

$$\begin{aligned}
&\Phi \to \Phi - \frac{a'}{a}\,\xi^0 - \xi^{0\prime}\ \ ,\ \ B \to B + a\,\xi^0 - a\,\xi'\\
&\Psi \to \Psi + \frac{a'}{a}\,\xi^0\ \ ,\ \ E \to E + \xi\\
&E_i \to E_i + \xi^i\ \ ,\ \ B_i \to B_i - a\,\xi_i'\\
&\delta\phi \to \delta\phi - \phi_0'\,\xi^0\ \ ,\ \ h_{ij} \to h_{ij}\ .
\end{aligned} \tag{2.89}$$

As can be seen from (2.89), it is possible to fix the values of ξ^0, ξ, ξ^i to eliminate four perturbations. Another possibility is to form gauge invariant (gauge invariance with

respect to coordinate transformations) combinations of the above fields and study the action in terms of these variables. We choose the following gauge invariant combinations of the perturbations:

$$\hat{\Phi} \equiv \Phi + \Psi + \left(\frac{a}{a'}\,\Psi\right)' \;\;,\;\; \hat{B} \equiv B - \frac{a^2}{a'}\,\Psi + a\,E'$$
$$\hat{B}_i \equiv \hat{B}_i + a\,E_i' \;\;,\;\; \delta\hat{\phi} \equiv \delta\phi + \frac{a}{a'}\,\phi_0'\,\Psi \tag{2.90}$$

and h_{ij} is already gauge invariant. This choice of gauge invariant perturbations are different from those that are commonly used in the literature [5]. Our choice is motivated with the fact that it immediately defines the nondynamical modes of the system: it is possible to choose the gauge $E = E_i = \Psi = 0$ in which the gauge invariant combinations $\{\hat{\Phi},\, \hat{B}\}$ reduce to the nondynamical modes $\delta g_{0\,\mu}$. This choice provides a great advantage in calculating the quadratic action. In addition, we will show below that the quadratic action can be written solely in terms of the gauge invariant modes defined above.

We compute the action for perturbations by inserting the metric decomposition (2.84) and $\varphi = \phi_0 + \delta\phi$ into the action (2.79) and expanding it at quadratic order. We realize that the resulting quadratic action decomposes into three decoupled pieces, that only contain (1) scalar modes, (2) vector modes and (3) tensor modes. This proves the claim we have made before, and justifies the choice of the parameterization of the metric perturbations. In addition, we observe that the part of the action containing only the vector modes is just a total time derivative. This shows that vector modes are not generated during inflation, which is an expected result, since there are no vector sources.

We choose to study the quadratic action for perturbations in Fourier space:

$$\delta(\vec{x}) = \int \frac{d^3k}{(2\pi)^{3/2}}\,\delta(\vec{k})\,e^{i\,\vec{k}\cdot\vec{x}} \tag{2.91}$$

where δ denotes a generic perturbation and $\delta(-\vec{k}) = \delta^*(\vec{k})$ due to reality. In the subsections below, we study the scalar and tensor perturbations respectively.

2.4.1 Scalar Perturbations

We first study the action for scalar perturbations which, up to a total time derivative, is given in Fourier space as

$$\begin{aligned} S_{\rm sc} &= \frac{1}{2}\int d^3k\, d\eta\, a^2(\eta)\, \mathcal{L}_{\rm sc} \\ \mathcal{L}_{\rm sc} &= |\delta\hat{\phi}'|^2 - \phi_0'\,\left(\hat{\Phi}\,\delta\hat{\phi}' + \text{h.c.}\right) - \left(k^2 + a^2\,V''(\phi_0)\right)\,|\delta\hat{\phi}|^2 \\ &\quad -a^2\,V'(\phi_0)\,\left(\delta\hat{\phi}^*\,\hat{\Phi} + \text{h.c.}\right) - \frac{k^2}{a^2}\,\phi_0'\,\left(\delta\hat{\phi}^*\,\hat{B} + \text{h.c.}\right) \\ &\quad +2\,k^2\,M_p^2\,H\,\left(\hat{B}\,\hat{\Phi}^* + \text{h.c.}\right) - M_p^2\,a^2\,\left(6H^2 - \frac{\phi_0'^2}{a^2\,M_p^2}\right)\,|\hat{\Phi}|^2 \end{aligned} \tag{2.92}$$

where h.c. denotes hermitian conjugation. The steps leading to the above action, including removal of total derivatives, are straightforward but algebraically tedious. However, they can be quickly performed by implementing a simple script in a computer algebra package. The above action contains only the gauge invariant perturbations defined in (2.90), as we have claimed earlier. Notice that the modes $\hat{\Phi}$ and $\hat{B}$ does not have any kinetic terms, so they are nondynamical, as we have discussed when we motivated the choice of the gauge invariant modes (2.90). These modes can be integrated out by extremezing the action with respect to $\hat{B}$ (and its hermitian conjugate) which gives

$$\frac{\delta S_{\rm sc}}{\delta\hat{B}} = 0 \Rightarrow \hat{\Phi} = \frac{\phi_0'}{2M_p^2\,a\,H}\,\delta\hat{\phi} \quad (\text{and} \quad \text{h.c.})\ . \tag{2.93}$$

Inserting this solution back into the action eliminates the nondynamical modes and results in the following action

$$\begin{aligned} S_{\rm sc} = \frac{1}{2}\int d^3k\, d\eta\, a^2(\eta) \Bigg\{ &|\delta\hat{\phi}'|^2 - \frac{\phi_0'^2}{2M_p^2\,a\,H}\,\left(\delta\hat{\phi}^*\,\delta\hat{\phi}' + \text{h.c.}\right) \\ &- \left[k^2 + \frac{3\phi_0'^2}{2M_p^2} - \frac{\phi_0'^4}{2M_p^4\,a^2\,H^4} + \frac{a\,\phi_0'\,V'(\phi_0)}{M_p^2\,H} + a^2\,V''(\phi_0)\right]\,|\delta\hat{\phi}|^2\Bigg\}\,. \end{aligned} \tag{2.94}$$

We canonically normalize the kinetic term by defining

$$V = a\,\delta\hat{\phi}\,. \tag{2.95}$$

Therefore, up to a total time derivative, the action after insertion of the above definition, (2.94) reduces to

$$S_{\rm sc} = \frac{1}{2}\int d^3k\, d\eta \left\{ |V'|^2 - \left(k^2 - \frac{z''}{z}\right)|V|^2 \right\} \quad , \quad z \equiv \frac{a^2\,\phi_0'}{a'}\ . \tag{2.96}$$

This action is equal to the one obtained in reference (Mukhanov-Sasaki), using different gauge invariant perturbations. Clearly, the results are independent of the gauge invariant combinations or the gauge used in the calculations. The mode V is known as the Mukhanov-Sasaki variable, and it is connected to the comoving curvature perturbation $\mathcal{R}$ as

$$\mathcal{R} \equiv \Psi + \frac{a'}{a\,\phi_0'}\,\delta\phi = \frac{a'}{a\,\phi_0'}\,\delta\hat{\phi} = \frac{1}{z}\,V\,. \tag{2.97}$$

The reason for the name comoving curvature perturbation can be understood, by computing the spatial curvature ${}^{(3)}R$ which is given by

$${}^{(3)}R = \frac{4}{a^2}\,\partial^2\,\Psi. \tag{2.98}$$

The spatial curvature is a measure of the Newtonian potential, and thus related to the amount of density fluctuations. However, Ψ is not gauge invariant and therefore it does not have a clear physical interpretation. Let us consider the specific gauge, called the comoving gauge, where observers are freely falling so they do not observe the energy momentum tensor component $\delta T_{0i} \propto \partial_i\,\delta\phi$. Therefore, in the comoving gauge $\delta\phi_{\rm c.g.} = 0$, and using (2.87) we find

$$\xi^0_{\rm c.g.} = \frac{\delta\phi}{\phi_0'}. \tag{2.99}$$

Inserting this result into the gauge transformation of Ψ given in (2.89), we get

$$\Psi_{\rm c.g.} = \Psi + \frac{a'}{a}\,\xi^0_{\rm c.g.} = \Psi + \frac{a'\,\delta\phi}{a\,\phi_0'} = \mathcal{R} \tag{2.100}$$

which exactly reproduces (2.97), and is gauge invariant by construction. The power spectrum for scalar perturbations are generally defined using the comoving curvature perturbation, since it stays constant on super-horizon scales as we will demonstrate shortly.

In order to find the initial conditions on the scalar mode, we quantize the field V in (2.96) as we did before for the case of a simple decoupled scalar field in the previous

section, by defining the field operator $\hat{V}$ as

$$\hat{V}(k,\,\eta) = v(k,\,\eta)\,\hat{a}(\vec{k}) + v^{*}(k,\,\eta)\,\hat{a}^{\dagger}(-\vec{k}) \tag{2.101}$$

where $\hat{a}$ and $\hat{a}^{\dagger}$ satisfy the commutation relations given in (2.39) and the mode function v satisfies the classical field equation obtained from (2.96) which is

$$v'' + \left(k^2 - \frac{z''}{z}\right)\,v = 0\ . \tag{2.102}$$

Initial conditions are set in the deep sub-horizon regime when $k \gg a\,H$, which also implies $k^2 \gg z''/z$, and the properly normalized adiabatic solution to the mode function is given by

$$v \simeq \frac{1}{\sqrt{2k}}\,e^{-i\,k\,\eta} \tag{2.103}$$

At super-horizon scales when $k \ll a\,H$ so $k^2 \ll z''/z$, (2.102) approximately becomes

$$v'' - \frac{z''}{z}\,v \simeq 0 \tag{2.104}$$

whose general solution is given by

$$v \simeq \gamma_k\,z + \lambda_k\,z\int\frac{d\eta'}{z^2} \tag{2.105}$$

where γ_k and λ_k are constants. We can approximately compute the integral appearing in the second term using slow-roll approximation, which gives

$$\int\frac{d\eta'}{z^2} = \int da\,\frac{H}{a^4\,\dot{\phi}_0^2} \simeq -\frac{H}{3a^3\,\dot{\phi}_0^2} \tag{2.106}$$

where we have pulled out H and $\dot{\phi}_0$ out of the integral, since they are almost constant during slow-roll inflation. Then, (2.105) becomes

$$v \simeq \gamma_k\frac{a\,\dot{\phi}_0}{H} - \frac{\lambda_k}{3\,a^2\,\dot{\phi}_0} \rightarrow \gamma_k\,\frac{a\,\dot{\phi}_0}{H} = \gamma_k\,z \tag{2.107}$$

since the term with λ_k quickly vanishes as a grows. Using the sub and super-horizon solutions in the definition of the comoving curvature perturbation (2.97), we get

$$\mathcal{R} \propto \begin{cases} \frac{1}{\sqrt{2\,k}\,z}\,e^{-i\,k\,\eta} & ,\ k^2 \ll z''/z \\ \gamma_k & ,\ k^2 \gg z''/z \end{cases}\ . \tag{2.108}$$

As we have claimed before, the comoving curvature perturbation stays constant at super-horizon scales. Then, the relevant quantity to compute is the power spectrum of $\mathcal{R}$ at horizon crossing. The power spectrum of the comoving curvature spectrum is then calculated as

$$< 0|\hat{\mathcal{R}}(\vec{x})\,\hat{\mathcal{R}}(\vec{y})|0 >_* = \frac{1}{z_*^2} \; < 0|\hat{V}(\vec{x})\,\hat{V}(\vec{y})\,|0 >$$

$$\Rightarrow P_{\mathcal{R}} = \frac{1}{z_*^2}\,\frac{k_*^3}{2\,\pi^2}\,|v(k_*,\,\eta_*)|^2$$

where $*$ denotes that the quantities are evaluated at horizon crossing when $k_* \sim a_*\,H_*$. Then, approximating $v_* \sim 1/\sqrt{2\,k_*}$, and using the definition of z given in (2.96), the above equation becomes

$$P_{\mathcal{R}} \simeq \frac{H_*^2}{a_*^2\,\dot{\phi}_{0^*}2}\,\frac{1}{2k_*}\,\frac{k_*^3}{2\pi^2} \simeq \frac{H_*^4}{4\,\pi^2\,\dot{\phi}_{0*}^2} \propto k^{n_s-1} \tag{2.109}$$

which is nearly scale invariant and the deviation from scale invariance is encoded in the spectral index n_s, which can be calculated as

$$n_s - 1 = k_*\,\frac{d}{d\,k_*}\,\mathrm{Ln}\left(\frac{H_*^4}{\dot{\phi}_{0*}^2}\right) = k_*\,\frac{dt_*}{dk_*}\,\frac{d}{d\,t_*}\,\mathrm{Ln}\left(\frac{H_*^4}{\dot{\phi}_{0*}^2}\right) \tag{2.110}$$

using $dk_* = (a_*\,\dot{H}_* + a_*\,H_*^2)\,dt_* \simeq a_*\,H_*^2\,dt_*$, during slow-roll, the spectral index becomes

$$n_s - 1 \simeq -2\,\left(\frac{\dot{\phi}_{0*}^2}{M_p^2\,H_*^2} + \frac{\ddot{\phi}_{0*}}{\dot{\phi}_*\,H_*}\right) = 2\,(\eta - 3\,\epsilon) \tag{2.111}$$

where ϵ and η are slow-roll parameters defined in (2.24). The spectral index distinguishes different models of inflation and it is a measurable quantity. Thus, perturbation theory around an inflationary background has robust predictions for the spectrum of curvature perturbation and consequently on the density perturbation. As a concrete example, consider the case of massive chaotic inflation. It is possible to estimate the mass of the inflaton field taking into account the amount of inhomogeneities in the universe, which is of the 10^{-5} order. Under the assumptions that all the inhomogeneities are due to scalar modes (i.e. we neglect tensor modes, which are suppressed for single field, slow-roll inflation as we will demonstrate) and they are all sourced by the fluctuations of the inflaton field, we have

$$P_{\mathcal{R}} \sim \left(10^{-5}\right)^2 \tag{2.112}$$

up to an order unity factor which takes into account the evolution of perturbations from horizon crossing until today (This factor is known as the transfer function, and it is $\sim (9/10)^2$ for large scale perturbations). Using (2.109), the slow-roll relations $\dot{\phi}_0 \simeq -m^2\,\phi_0/3H$ and $H \simeq m\,\phi_0/\sqrt{6}M_p$ and the relation for the total number of e-folds of inflation given in (2.27) we get

$$P_{\mathcal{R}} \simeq \frac{1}{6\pi^2}\,\left(\frac{m}{M_p}\right)^2\,\left(\frac{\phi_{0*}^2}{4M_p^2}\right)^2 \simeq \frac{N_*^2}{6\pi^2}\,\left(\frac{m}{M_p}\right)^2 \sim 10^{-10}\ . \tag{2.113}$$

Assuming that $N_* \simeq 60$ from equation (2.77), the mass of the inflaton field satisfies

$$\frac{m}{M_p} \sim 10^{-6}\ \Rightarrow\ m \sim 10^{12}\mathrm{GeV} \tag{2.114}$$

which is mass below the Grand Unified Theory (GUT) scale ($\sim 10^{16}\,\mathrm{GeV}$).

2.4.2 Tensor Perturbations

The other nontrivial piece of the quadratic action comes from tensor perturbations. In this case, the action is much simpler and it is given, up to a total time derivative, by

$$S_{\mathrm{tens}} = \frac{M_p^2}{8}\,\int d^3x\,d\eta\,a^2(\eta)\,\left(h'_{ij}\,h'^{ij} + h^{ij}\,\partial^2\,h_{ij}\right) \tag{2.115}$$

where indices on h_{ij} are raised and lowered by the Kronecker delta δ_{ij} and $\partial^2 \equiv \delta^{ij}\,\partial_i\,\partial_j$. We again work with Fourier transformed fields, which are defined by

$$h_{ij}(k,\,\vec{x}) = \int \frac{d^3k}{(2\pi)^{3/2}}\,\sum_s\,\epsilon^s_{ij}(\vec{k})\,h_s(\vec{k},\,\eta)\,e^{i\,\vec{k}\cdot\vec{x}} \tag{2.116}$$

where $h^*_s(\vec{k},\eta) = h_s(-\vec{k},\,\eta)$ and the polarization tensor ϵ^s_{ij} satisfies

$$\epsilon^{s*}_{ij}\,\epsilon^{s'}_{ij} = 2\,\delta^{s\,s'}\ \ ,\ \ \epsilon^s_{ii} = k_i\,\epsilon^s_{ij} = 0\ \ ,\ \ \epsilon^s_{ij}(-\vec{k}) = \epsilon^{s*}_{ij}(\vec{k})\ . \tag{2.117}$$

Then, inserting (2.116) into (2.115), we obtain

$$S_{\mathrm{tens}} = \frac{M_p^2}{8}\,\int d^3k\,d\eta\,\sum_s\,a^2(\eta)\,\left[|h'_s|^2 - k^2\,|h_s|^2\right]\ . \tag{2.118}$$

We canonically normalize the above action, by defining

$$H_s = \frac{a\,M_p}{2}\,h_s \tag{2.119}$$

and the action, up to a total time derivative, becomes

$$S_{\rm tens} = \sum_s \frac{1}{2} \int d^3k\, d\eta \left[|H_s'|^2 - \left(k^2 - \frac{a''}{a} \right) |H_s|^2 \right] . \tag{2.120}$$

Again, we canonically quantize H_s to find the initial conditions. In order to do so, we define the following field operators

$$\hat{H}^s(\vec{k},\, \eta) = v_h(k,\, \eta)\, \hat{a}_s(\vec{k}) + v_h^*(k,\, \eta)\, \hat{a}_s^\dagger(-\vec{k}) \tag{2.121}$$

where the creation and annihilation operators $\hat{a}_s$, $\hat{a}_s^\dagger$ satisfy the following commutation relations

$$\begin{aligned} \left[\hat{a}_s(\vec{k}),\, \hat{a}_{s'}^\dagger(\vec{q}) \right] &= \delta_{s\, s'}\, \delta(\vec{k} - \vec{q}) \\ \left[\hat{a}_s(\vec{k}),\, \hat{a}_{s'}(\vec{q}) \right] &= \left[\hat{a}_s^\dagger(\vec{k}),\, \hat{a}_{s'}^\dagger(\vec{q}) \right] = 0 \end{aligned} \tag{2.122}$$

and the mode function v_h satisfy the evolution equation obtained from (2.120), which is

$$v_h'' + \left(k^2 - \frac{a''}{a} \right) v_h = 0 . \tag{2.123}$$

As we have done previously for the scalar mode, we can determine the evolution of the mode function v_h, by studying the sub and super-horizon limits of (2.123). In the sub-horizon regime when $k^2 \gg a''/a$, the properly normalized mode function is simply given by

$$v_h \simeq \frac{1}{\sqrt{2\, k}}\, e^{-i\, k\, \eta} \tag{2.124}$$

and in the super-horizon regime, we obtain (similarly to (2.105) and (2.107))

$$v_h \simeq \gamma_k\, a + \lambda_k\, a \int \frac{d\eta'}{a^2} \simeq \gamma_k\, a - \frac{\lambda_k}{3\, a^2\, H} \to \gamma_k\, a . \tag{2.125}$$

Therefore, the evolution of the original tensor mode h_s, related to the canonically normalized field H_s through equation (2.119), is given by

$$h_s \propto \begin{cases} \frac{1}{\sqrt{2\, k}\, a}\, e^{-i\, k\, \eta} & ,\ k^2 \ll a''/a \\ \gamma_k & ,\ k^2 \gg a''/a \end{cases} . \tag{2.126}$$

As in the case of the comoving curvature perturbation, the tensor modes stay constant at superhorizon scales. Therefore, we compute the power spectrum of tensor modes at horizon crossing as

$$P_T = 2 \times \frac{4}{a_*^2\, M_p^2} \times \frac{k_*^3}{2\pi^2}\, |v_h(k_*,\, \eta_*)|^2 \tag{2.127}$$

where the factor 2 in front accounts for the number of polarizations of tensor modes, and the factor $4/a_*^2 M_p^2$ comes from the definition of the canonical mode given in (2.119). Following similar steps that led to the result (2.109), the tensor power reduces to

$$P_T = \frac{2\,H_*^2}{\pi^2\,M_p^2} \propto k^{n_T} \tag{2.128}$$

where n_T is the tensor spectral index, which can be calculated as

$$n_T = k_* \frac{d}{dk_*} \mathrm{Ln}\left(H_*^2\right) = 2\,k_* \frac{dt_*}{dk_*} \frac{d}{dt_*} \mathrm{Ln}\, H_* \simeq -2\frac{\dot{H}_*}{H_*^2} = -2\,\epsilon \tag{2.129}$$

where ϵ is again the slow-roll parameter defined in (2.24). The spectrum of tensor modes is almost scale invariant and unlike the spectrum of curvature perturbations, which is enhanced by the factor $1/\dot{\phi}_{0*}^2$, the tensor spectrum depends only on the Hubble rate during inflation, namely the energy scale of inflation. Therefore, a direct detection of inflationary gravity waves would lead to the determination of the energy scale, consequently the amplitude of the potential energy of the inflaton.

Finally, we discuss the inflationary consistency relation, which holds for all single field inflationary models, and is given by the ratio of scalar and tensor powers obtained using (2.128) and (2.109)

$$r = \frac{8\,\dot{\phi}_{0*}^2}{M_p^2\,H_*^2} = -16\,\frac{\dot{H}_*}{H_*^2} = 16\,\epsilon\,. \tag{2.130}$$

The scalar spectral index n_s along with the tensor-to-scalar ratio r are generally used to constrain inflationary models by observations [2]. We also provide the power spectra of the scalar and tensor modes, obtained by numerically integrating the equations (2.102) and (2.123) and the results are shown in Figure 2.4.

In order to compute the numerical power spectra shown in Figure. 2.4, we integrated the evolution equations of the mode functions numerically in cosmic time, namely

$$\ddot{u} + H\,\dot{u} + \left(\frac{k^2}{a^2} - f^2(t)\right) u = 0 \;\;,\;\; f^2(t) = \begin{cases} \frac{a''}{a} \;\;,\;\; u = v \text{ (scalar)} \\ \frac{z''}{z} \;\;,\;\; u = v_h \text{ (tensor)} \end{cases}$$

$$\frac{a''}{a} = 2H^2 - \frac{\dot{\phi}_0^2}{2M_p^2},$$

$$\frac{z''}{z} = 2H^2 - \frac{7\dot{\phi}_0^2}{2M_p^2} + \frac{\dot{\phi}_0^4}{2H^2\,M_p^4} - \frac{2\,\dot{\phi}_0\,V''(\phi_0)}{H\,M_p^2} - V''(\phi_0)\;.$$

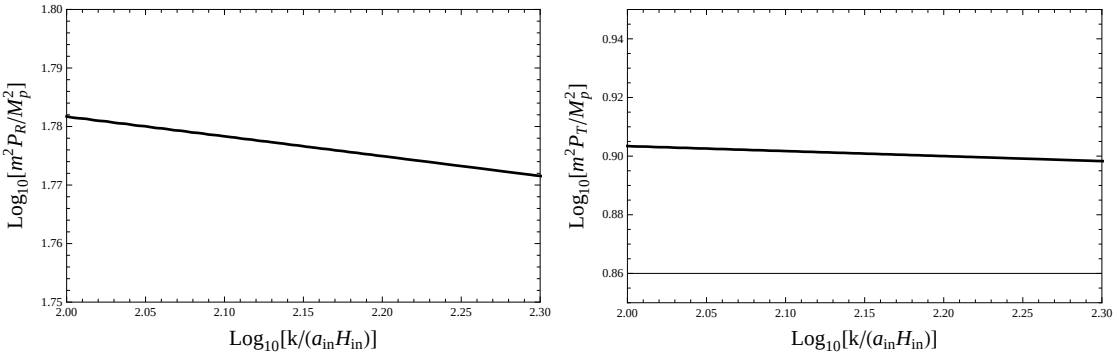

Figure 2.4: Left panel shows the spectrum of scalar perturbations and the right panel shows the spectrum of tensor perturbations. The slope of the curves coincide with the estimates given in (2.111) and (2.129).

These equations are integrated together with the background equations numerically with the following initial conditions:

$$u_{\mathrm{in}} = \frac{1}{\sqrt{2\,k}} \;\;,\;\; \dot{u}_{\mathrm{in}} = \frac{1}{\sqrt{2\,k}} \left(-i\,\frac{k}{a_{\mathrm{in}}}\right) \;\;,\;\; a_{\mathrm{in}} = 1,\;\;,\;\; \phi_{\mathrm{in}} = 16\,M_p \;\;,\;\; \dot{\phi}_{\mathrm{in}} = -\sqrt{\frac{2}{3}}\,m\,M_p \tag{2.131}$$

where initial conditions on u are obtained by the sub-horizon adiabatic solution, initial condition on the inflaton field is set by the desired amount of N-folds of inflation ($\phi_{\mathrm{in}} = 16M_p$ gives ~ 60 e-folds of inflation) and the initial condition on the derivative of the inflaton field is obtained by slow-roll approximation. The initial condition on the scale factor is arbitrary and set to unity for brevity. The range of co-moving momenta where the mode functions are numerically integrated is given by $100 < k/(a_{\mathrm{in}}H_{\mathrm{in}}) < 200$ at 100 values. As can be seen in Figure 2.4 the spectra are nearly scale invariant. The slopes of the spectra, which correspond to n_s and n_T are approximately equal to the estimates obtained in equations (2.111) and (2.129).

In the next chapter, we will briefly study the CMB anisotropies resulting from the primordial perturbations and discuss the experimental status of inflationary models.

Chapter 3

The Cosmic Microwave Background

The cosmic microwave background (CMB) radiation was formed when the protons and electrons were decoupled from the photons when the universe sufficiently cooled down at around $z_{\rm CMB} \sim 1100$. The moment of time when the CMB was formed is also known as the last scattering surface, since photons freely stream without scattering after this moment. Today, we observe the CMB radiation in the blackbody spectrum peaked at a temperature of $T_0 \sim 2.7$K. The CMB is homogeneous and isotropic, with a 10^{-5} level of anisotropy which was first measured by the COBE satellite [3] and later by various experiments. In the previous chapter, we have introduced the inflationary mechanism of generation of fluctuations, which has been very successful in explaining the origin of the anisotropies observed by experiments. In this chapter, we will first introduce the basic physics behind the formation of the CMB anisotropies. Then, we will review the basic outcomes of the CMB experiments relevant for inflation, and finally discuss some of the debated features emerged in some studies of the CMB data, that seem to be anomalous in the standard inflationary picture. These features in part motivated the study of vector fields and anisotropic inflationary models, which we will discuss in the following chapters.

3.1 Formation of CMB anisotropies

The photons from the CMB travel along null geodesics with a tangential four vector $k^\mu = d\,x^\mu\,/d\lambda$, which satisfy the normalization condition given by

$$g_{\mu\nu}\,k^\mu\,k^\nu = 0 \tag{3.1}$$

where, λ is an affine parameter, different from the proper time $d\tau = \sqrt{-g_{\mu\nu}\,dx^\mu\,dx^\nu}$ used for parameterizing time-like geodesics (which define the path of physical co-moving observers) and $g_{\mu\nu}$ is the FRW metric given in (2.1). We again work with the flat metric for $k = 0$. Figure. 3.1 schematically illustrates the world-lines of photons emitted from the last scattering surface and the comoving observers. The world-lines are null geodesics for photons (with $k^\mu = d\,x^\mu\,/d\lambda$) and time-like geodesics for observers ($U^\mu = dx^\mu/d\tau$). Using the fact that null geodesics are conformally invariant (which we will prove below), we define two metrics

$$\begin{aligned} ds^2 &= \bar{g}_{\mu\nu}\,dx^\mu\,dx^\nu = a^2(\eta)\,\left(-d\eta^2 + d\vec{x}^2\right) \\ \bar{g}_{\mu\nu} &= a^2\,g_{\mu\nu} \qquad , \qquad g_{\mu\nu} = \eta_{\mu\nu} = -d\eta^2 + d\vec{x}^2. \end{aligned} \tag{3.2}$$

The barred metric is therefore the physical metric and the unbarred metric corresponds to the conformal frame. We further define barred and unbarred four-vectors $\bar{k}^\mu$ and k^μ as

$$k^\mu = \frac{dx^\mu}{d\lambda}\ ,\ \bar{k}^\mu = \frac{dx^\mu}{d\bar{\lambda}}\ ,\ \eta_{\mu\nu}\,k^\mu\,k^\nu = \bar{g}_{\mu\nu}\,\bar{k}^\mu\,\bar{k}^\nu = 0\,. \tag{3.3}$$

The barred vector $\bar{k}^\mu$ is parameterized by a different affine parameter $\bar{\lambda}$, which is related to the parameter λ through

$$\bar{k}^\mu = C(\eta)\,k^\mu\ ,\ \frac{dx^\mu}{d\bar{\lambda}} = C(\eta)\,\frac{dx^\mu}{d\lambda}\ \Rightarrow C(\eta) = \frac{d\lambda}{d\bar{\lambda}}\,. \tag{3.4}$$

The four vector $\bar{k}^\mu$ satisfies the geodesic equation given by

$$\frac{d\bar{k}^\mu}{d\bar{\lambda}} + \bar{\Gamma}^\mu_{\alpha\beta}\,\bar{k}^\alpha\,\bar{k}^\beta = 0 \tag{3.5}$$

where $\bar{\Gamma}^\mu_{\alpha\beta}$'s are Christoffel symbols calculated using the physical metric. Using (3.2), the barred Christoffel symbols are given by

$$\bar{\Gamma}^\mu_{\alpha\beta} = \Gamma^\mu_{\alpha\beta} + \frac{1}{a}\,\left(\delta^\mu_\alpha\,\partial_\beta\,a + \delta^\mu_\beta\,\partial_\alpha\,a - g_{\alpha\beta}\,\partial^\mu\,a\right) \tag{3.6}$$

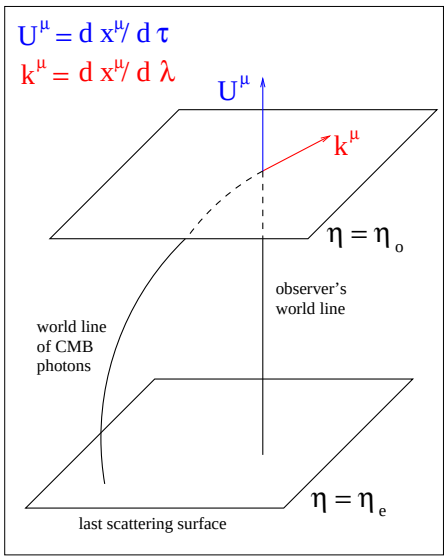

Figure 3.1: The world-line of CMB photons and co-moving observers are shown schematically. Photons are emitted at conformal time $\eta = \eta_e$ and reach the observer today at conformal time $\eta = \eta_0$.

where $\Gamma^{\mu}_{\alpha\beta}$'s are the Christoffel symbols calculated using the conformal metric. Then, using the above equation with (3.4) in (3.5) we get

$$C^2 \left[\frac{dk^\mu}{d\lambda} + \Gamma^{\mu}_{\alpha\beta}\, k^\alpha\, k^\beta\right] + C\,\frac{dC}{d\lambda}\, k^\mu + \frac{C^2}{a}\,\left[2\,(\partial_\beta\, a)\, k^\mu\, k^\nu\right] = 0\,. \tag{3.7}$$

The first term in the brackets vanishes identically, since it is the geodesic equation for the vector k^μ in the conformal frame. Using the fact that $k^\nu = dx^\nu/d\lambda$, the above equation is solved up to a nonphysical constant as

$$C = \frac{1}{a^2} \;\;\Rightarrow\;\; k^\mu = a^2\,\bar{k}^\mu\,. \tag{3.8}$$

This result shows that the physical frame and the conformal frame has the same geodesics, with the tangent four-vectors in each frame related to each other through (3.4). Notice that no assumption about the metric is made in deriving the above relation and therefore the result is generic. In the present case, since the conformal metric is just the Minkowski metric, where the Christoffel symbols $\Gamma^{\mu}_{\alpha\beta} = 0$ identically, and the fact that the geodesics are the same with the physical metric, it proves to be useful to work in the conformal frame. Then, the geodesic equation in the conformal frame

reduces to

$$\frac{dk^\mu}{d\lambda} = 0 \tag{3.9}$$

which has a simple solution given by

$$k^\mu = (1,\, \vec{n}) \qquad \text{with} \qquad \vec{n}^2 = 1\,. \tag{3.10}$$

The frequency (energy) of the photons measured by the co-moving observers are proportional to the projection of the physical four-vector $\bar{k}^\mu$ on the observer's four velocity $\bar{U}^\mu$. The observed frequency ω is then given by

$$\omega = -\bar{g}_{\mu\nu}\, \bar{U}^\mu\, \bar{k}^\nu \tag{3.11}$$

and also schematically represented in Figure. 3.2. The quantity ω is not the actual frequency of the photon, it just represents the geometric dependence of it. However, as long as the photon spectrum is fixed, ratios of ω is equal to the ratios of the frequencies, a fact which we will use extensively.

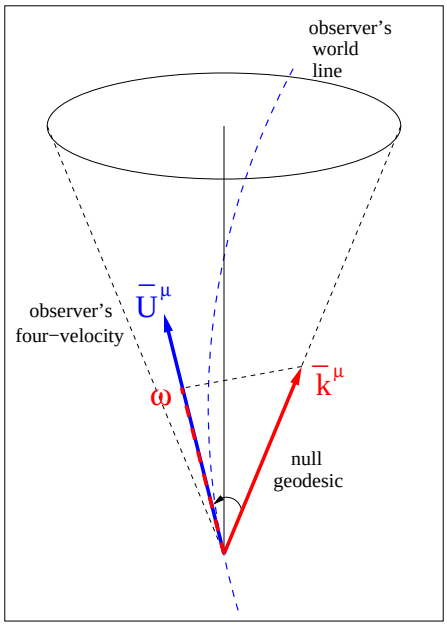

Figure 3.2: The frequency of photons measured by co-moving observers are proportional to the projection of the wave-vector $\bar{k}^\mu$ on the four-velocity $\bar{U}^\mu$, which is schematically shown.

Using equations (3.2) and (3.8), (3.11) reduces to

$$\omega = -g_{\mu\nu}\,\bar{U}^{\mu}\,k^{\nu}\,. \tag{3.12}$$

The four-velocity of the co-moving observers can be determined from the normalization condition given by

$$\bar{g}_{\mu\nu}\,\bar{U}^{\mu}\,\bar{U}^{\nu} = -1\,. \tag{3.13}$$

The vector $\bar{U}^{\mu}$ has only its zeroth component to be non-vanishing, since it describes the world-lines of co-moving observers. Then, $\bar{U}^{\mu}$ is given by

$$\bar{U}^{\mu} = \frac{1}{a}\,\left(1,\,\vec{0}\right)\,. \tag{3.14}$$

Therefore, the frequency of the photons are obtained from (3.12) as

$$\omega = \frac{1}{a} \qquad \text{(arbitrary units)} \tag{3.15}$$

which simply shows the redshift factor that scales the energy of the photons. The spectrum of photons are given by the Planck distribution $f = (e^{\omega/T} - 1)^{-1}$, where T is the temperature. We assume that this spectrum is fixed, that is $df/dt = 0$ (i.e. Liouville's equation is satisfied), since photons free-stream after the last scattering surface [1] . Therefore, the ratio ω/T is fixed and we have

$$T_o = \frac{\omega_o}{\omega_e}\,T_e \tag{3.16}$$

where T_o, T_e are the temperatures at the observation and emission points (last scattering surface) and ω_o, ω_e are the frequencies measured at the observation and emission points respectively (see Figure. 3.1). This relation also verifies the a^{-1} dependence of the temperature, previously shown in Section. 2.1.

We are interested in the anisotropies of the temperature observed today, which can be obtained by perturbing the relation (3.16). However, neither ω nor T is a gauge invariant quantity, and they change under coordinate (gauge) transformations. In order to determine how they transform under a coordinate transformation, we rewrite equation (3.16) in the following form

$$\omega = -\bar{g}_{00}\,\bar{U}^{0}\,\bar{k}^{0} = -\bar{k}_{0}\,\bar{U}^{0} = -\frac{\bar{k}_{0}}{\sqrt{-\bar{g}_{00}}}\,. \tag{3.17}$$

[1] We neglect small scale effects like the Sunyaev-Zeldovich effect [66], which accounts for the inverse Compton scattering of CMB photons with ionized gas.

Consider transformed coordinates $\tilde{x}^\mu = x^\mu + \xi^\mu$. The metric and wave-vector in the transformed coordinates ($\tilde{x}$) are given by

$$\tilde{\bar{k}}_0 = \bar{k}_0 - \bar{k}_\mu \, \xi^{\mu\,\prime} \;\; , \;\; \tilde{\bar{g}}_{00} = \bar{g}_{00} - 2\,\bar{g}_{00}\,\xi^{0\,\prime} \tag{3.18}$$

Inserting (3.18) into (3.17) and expanding in first oder, we get

$$\tilde{\omega} = \omega \left(1 - \xi^{i\,\prime}\,\frac{\bar{k}_i}{\bar{k}_0}\right) . \tag{3.19}$$

The temperature can be perturbatively expanded as $T(\eta, \vec{x}) = T_0(\eta) + \delta T(\eta, \vec{x})$, and since the distribution function is a scalar, so is the ratio ω/T, we have

$$\tilde{T}(\tilde{x}^\mu) = T(x^\mu)\,\frac{\tilde{\omega}}{\omega} . \tag{3.20}$$

Then, using (3.19) and expanding $\tilde{T}(\tilde{x}^\mu)$ to first order, we have

$$\delta\tilde{T} = \delta T - T_0'\,\xi^0 - T_0\,\xi^{i\,\prime}\,\frac{\bar{k}_i}{\bar{k}_0} . \tag{3.21}$$

This result clearly shows that the temperature fluctuations are gauge dependent. However, if we decomposed both sides of (3.21) in spherical harmonics, only the monopole (ξ^i-independent $l = 0$ term) and the dipole (ξ^i-dependent $l = 1$ term) are gauge dependent, and higher multipoles are not. Notice that the monopole term can be removed by a redefinition of the background temperature, so it is of no physical interest. The dipole depends on the motion of the observer in the rest frame of the CMB and it is not related to cosmological physics [2] . The dipole can be measured by determining the velocity of the observer in the CMB rest frame, and can be subtracted from the data. Therefore, the lowest physically interesting component of the temperature anisotropy is the quadrupole ($l = 2$) and it is gauge independent (along with higher multipoles).

We now return to equation (3.16) and perturb it in linear order to obtain

$$\frac{\delta T_o}{T_o} = \frac{\delta\omega_o}{\omega_o} - \frac{\delta\omega_e}{\omega_e} + \frac{\delta T_e}{T_e} . \tag{3.22}$$

This equation determines the relation of the temperature anisotropies observed today, to the anisotropies at the emission point. We further define $\delta\hat{T} \equiv \delta T/T$ for shortness

[2] There are however some claimed anomalies, like a dipolar power asymmetry in the northern and southern galactic planes, which could be attributed to some modifications in the inflationary physics. See the next section for a brief discussion of this effect.

and perturbatively expand ω, $\bar{U}^\mu$ and k^μ in (3.12) as

$$\omega = \omega^{(0)} + \omega^{(1)} \;\;,\;\; \bar{U}^\mu = \bar{U}^{(0)\mu} + \bar{U}^{(1)\mu} \;\;,\;\; k^\mu = k^{(0)\mu} + k^{(1)\mu} \tag{3.23}$$

where the superscript (0) denotes the background value and the superscript (1) denotes the first order perturbation. Then, (3.12) reduces to

$$\omega^{(1)} = -\delta g_{\mu\nu}\, \bar{U}^{(0)\mu}\, k^{(0)\nu} - \eta_{\mu\nu}\, \bar{U}^{(0)\mu}\, k^{(1)\nu} - \eta_{\mu\nu}\, \bar{U}^{(1)\mu}\, k^{(0)\nu}\,. \tag{3.24}$$

We can determine $\bar{U}^{(1)\mu}$ by perturbing the normalization condition $g_{\mu\nu}\, \bar{U}^\mu\, \bar{U}^\nu = -1$ to first order which gives

$$\bar{U}^{(1)\,0} = \frac{\delta g_{00}}{2\,a}\,. \tag{3.25}$$

Notice that we have not obtained any condition on the spatial components $\bar{U}^{(1)i}$. However, these components are related to the peculiar motion of the observer and thus affects only the dipole term, so we disregard them. Similarly, we expand the normalization condition for k^μ to first order, which gives

$$k^{(1)0} = \frac{1}{2}\,\delta g_{00} + \delta g_{0i}\, n^i + \frac{1}{2}\,\delta g_{ij}\, n^i\, n^j\,. \tag{3.26}$$

As we will demonstrate below, the components $k^{(1)\,i}$ will not appear in the final result, therefore we do not need their explicit forms. Then, inserting (3.26) and (3.25) into (3.24), and using the fact that $\omega^{(0)} = a^{-1}$, we get

$$\frac{\omega^{(1)}}{\omega^{(0)}} = -\frac{1}{2}\,\delta g_{00} - \delta g_{0i}\, n^i + k^{(1)0} \tag{3.27}$$

which, when inserted in (3.22) gives

$$\delta\hat{T}_o = \left[-\frac{1}{2}\,\delta g_{00} - \delta g_{0i}\, n^i + k^{(1)0}\right]_e^o + \delta\hat{T}_e \tag{3.28}$$

In order to determine the dependence of $k^{(1)0}$ on the components of the metric, we need to solve the perturbed geodesic equation, which is given by

$$\frac{d}{d\lambda}\, k^{(1)\mu} + \delta\Gamma^\mu_{\alpha\beta}\, k^{(0)\alpha}\, k^{(0)\beta} = 0\,. \tag{3.29}$$

Notice that terms like $\Gamma^\mu_{\alpha\beta}\, k^{(0)\,\alpha}\, k^{(1)\,\beta}$ and $\partial_\sigma\, \Gamma^\mu_{\alpha\beta}\, k^{(0)\alpha}\, k^{(0)\beta}\, x^{(1)\sigma}$ (this term takes into account the perturbed position of the geodesic; $x^\mu = x^{(0)\mu} + x^{(1)\mu}$) does not appear in

the above equation, since we are in the conformal frame where the Christoffel symbols vanish [3] . In order to compute the perturbed Christoffel symbols, we fix the coordinate gauge freedom, and write the metric in the following form

$$ds^2 = -\,(1+2\phi_L)\;d\eta^2 + (1-2\psi_L)\;d\vec{x}^2 \tag{3.30}$$

which is also known as the longitudinal gauge. Then, making use of the background solution for $k^{(0)\mu}$ given in (3.10), the perturbed geodesic equation for $k^{(1)0}$ becomes

$$\frac{d}{d\lambda}k^{(1)0} + \phi_L' + 2\,n^i\,\partial_i\,\phi_L - \psi_L' = 0\,. \tag{3.31}$$

Using the identity $df/d\lambda = f' + n^i\,\partial_i\,f$, the above equation is integrated to give

$$k^{(1)0}\Big|_e^o = -\phi_L\Big|_e^o + \int_e^o d\lambda\;\left(\phi_L' + \psi_L'\right) \tag{3.32}$$

Finally, inserting (3.32) and the metric (3.30) into (3.28), we obtain

$$\delta\hat{T}_o(\eta_o,\,x_o^i,\,n^i) = \phi_L(\eta_e,\,x_e^i,\,n^i) - \phi_L(\eta_o,\,x_o^i) + \int_e^o d\lambda\;\left(\phi_L' + \psi_L'\right) + \delta\hat{T}_e\,. \tag{3.33}$$

The term $\phi_L(\eta_o,\,x_o^i)$ depends only on the coordinates of the observer, and therefore contributes only to the monopole term since x_o^i has no n^i dependence (i.e dependence on the direction of photons from the emission surface). $\phi_L(\eta_e,\,x_e^i)$ is the ordinary Sachs-Wolfe contribution and $\delta\hat{T}_e$ is the intrinsic temperature fluctuation on the last scattering surface and is determined by the physics of the baryon-radiation plasma. This term has to be treated properly using the Boltzmann equations for the baryon-photon plasma distributions (i.e $df/dt = C[f]$ instead of the collisionless Liouville equation) and is beyond the scope of this thesis. However, at large scales it is possible to approximate $\delta\hat{T}_e$ in Fourier space, and it is given by [68]

$$\delta\hat{T}(\eta_e,\,\vec{k}) \simeq -\frac{2}{3}\,\phi_L(\eta_e,\,\vec{k})\,. \tag{3.34}$$

The integral term in (3.33) is known as the integrated Sachs-Wolfe effect, and accounts for the evolution of gravitational potential from the last scattering surface until today. The integrated Sachs-Wolfe (ISW) effect has two type of contributions. The early time ISW effect accounts for the fact that the last scattering is not a sharp moment

[3] For a more detailed analysis of perturbed geodesics for higher orders, see for example [67]

in time, but rather has a spread during which potentials evolve. The late time ISW effect accounts for the fact that the potentials decay at late times when cosmological constant/dark energy dominates the energy content of the universe. Neglecting the effect of late time cosmological constant/dark energy, we ignore the ISW effect, which is sub dominant compared to the ordinary SW contribution in this case at large scales where the perturbations are constant. Then, using (3.34), the temperature fluctuations at the observation point is given by

$$\delta\hat{T}_o(\eta_o,\, x^i_o,\, n^i) \simeq \frac{1}{3}\int \frac{d^3k}{(2\pi)^{3/2}}\,\phi_L(\eta_e,\,\vec{k})\exp\left[i\,\vec{k}\cdot(\vec{x}_o-\vec{n}\,(\eta_e-\eta_o))\right] \tag{3.35}$$

where we have used the fact that the photons move along geodesics ($x^i = x^i_o - n^i\,(\eta-\eta_o)$) obtained from integrating (3.10). We compute the two point correlation function for the temperature fluctuations today, using the fact that $\eta_o \gg \eta_e$, which gives

$$\left\langle \delta\hat{T}(\vec{n}_1)\,\delta\hat{T}(\vec{n}_2)\right\rangle = \frac{1}{9}\int \frac{d^3k\,d^3q}{(2\pi)^3}\left\langle \phi_L(\eta_e,\,\vec{k})\,\phi_L(\eta_e,\,\vec{q})\right\rangle e^{i\,\vec{k}\cdot(\vec{x}_o+\vec{n}_1\,\eta_o)}\,e^{i\,\vec{q}\cdot(\vec{x}_o+\vec{n}_2\,\eta_o)}\,. \tag{3.36}$$

Since we assume that the perturbations are generated quantum mechanically during inflation, the correlator appearing in the above equation should obey $\left\langle \phi_L(\eta_e,\,\vec{k})\,\phi_L(\eta_e,\,\vec{q})\right\rangle = |\phi_L(\eta_e,\,\vec{k})|^2\,\delta(\vec{k}+\vec{q})$. Then we have

$$\begin{aligned}\left\langle \delta\hat{T}(\vec{n}_1)\,\delta\hat{T}(\vec{n}_2)\right\rangle &= \frac{1}{9}\int \frac{d^3k}{(2\pi)^3}\,|\phi_L(\eta_e,\,\vec{k})|^2\,e^{i\vec{k}\cdot(\vec{n}_1-\vec{n}_2)\eta_o} \\ &= \frac{1}{9}\int_0^\infty \frac{dk}{k}\,P_\phi\,\frac{1}{4\pi}\int d\Omega_k\,e^{i\,\vec{k}\cdot(\vec{n}_1-\vec{n}_2)\eta_o}\end{aligned} \tag{3.37}$$

where we have used the definition of the power spectrum $P_\phi \equiv k^3\,|\phi_L(\eta_e,\,\vec{k})|^2/(2\pi^2)$. Now, we use the spherical harmonic expansion of plane waves for the above equation to get

$$\begin{aligned}e^{i\,\vec{k}\cdot\vec{n}_1\,\eta_o} &= 4\pi\sum_{l,\,m} i^l\,j_l(k\eta_o)\,Y^*_{lm}(\theta_k,\,\phi_k)\,Y_{lm}(\theta_1,\,\phi_1) \\ e^{-i\,\vec{k}\cdot\vec{n}_2\,\eta_o} &= 4\pi\sum_{l',\,m'} (-i)^{l'}\,j_{l'}(k\eta_o)\,Y_{l'm'}(\theta_k,\,\phi_k)\,Y^*_{l'm'}(\theta_2,\,\phi_2)\end{aligned} \tag{3.38}$$

where $(\theta_k,\,\phi_k)$ denote angular coordinates of the vector $\vec{k}$ and $(\theta_{1,2},\,\phi_{1,2})$ denote angular coordinates of $\vec{n}_{1,2}$. Then the angular integral appearing in (3.37) can be evaluated as

$$\frac{1}{4\pi}\int d\Omega_k\,e^{i\,\vec{k}\cdot(\vec{n}_1-\vec{n}_2)\eta_o} = 4\pi\sum_{l,m} j^2_l(k\eta_o)\,Y_{lm}(\theta_1,\,\phi_1)\,Y^*_{lm}(\theta_2,\,\phi_2)$$

$$= \sum_l (2l+1)\, j_l^2(k\eta_o)\, P_l(\cos\gamma) \tag{3.39}$$

where we have used the fact that $\int d\Omega_k\, Y^*_{lm}(\theta_k,\phi_k)\, Y_{l'm'}(\theta_k,\phi_k) = \delta_{ll'}\,\delta_{mm'}$ in obtaining the first line and the spherical harmonic addition theorem for obtaining the second line, which is

$$4\pi \sum_m Y_{lm}(\theta_1,\,\phi_1)\, Y^*_{lm}(\theta_2,\,\phi_2) = (2l+1)\, P_l(\cos\gamma) \quad , \quad \cos\gamma = \vec{n}_1\cdot\vec{n}_2\,. \tag{3.40}$$

Then, the correlator of temperature fluctuations become

$$\left\langle \hat{\delta T}(\vec{n}_1)\, \hat{\delta T}(\vec{n}_2) \right\rangle = \sum_l (2l+1)\, P_l(\cos\gamma)\, \frac{1}{9} \int_0^\infty \frac{dk}{k}\, P_\phi\, j_l^2(k\eta_o)\,. \tag{3.41}$$

This result can be compared with a direct expansion of temperature fluctuations in spherical harmonics, which is

$$\hat{\delta T}(\vec{n}_{1,2}) = \sum_{l,m} a_{lm}\, Y_{lm}(\theta_{1,2},\,\phi_{1,2})\,. \tag{3.42}$$

Then, assuming statistical isotropy, namely

$$\langle a^*_{lm}\, a_{l'm'} \rangle = C_l\, \delta_{ll'}\, \delta_{mm'} \tag{3.43}$$

the correlator of temperature fluctuations become

$$\begin{aligned} \left\langle \hat{\delta T}(\vec{n}_1)\, \hat{\delta T}(\vec{n}_2) \right\rangle &= \sum_{l,m} C_l\, Y^*_{lm}(\theta_1,\,\phi_1)\, Y_{lm}(\theta_2,\,\phi_2) \\ &= \frac{1}{4\pi} \sum_l (2l+1)\, P_l(\cos\gamma)\, C_l \end{aligned} \tag{3.44}$$

where we have used (3.38) again in obtaining the second line. Then, comparing (3.41) and (3.44) we get

$$C_l = \frac{4\pi}{9} \int_0^\infty \frac{dk}{k}\, P_\phi\, j_l^2(k\eta_o)\,. \tag{3.45}$$

Assuming that P_ϕ is approximately scale independent (which is true for inflationary scenarios), we pull it out of the integral and use the well known result for spherical Bessel functions given by

$$\int_0^\infty x^{n-1}\, j_l^2(x)\, dx = 2^{n-3}\, \pi\, \frac{\Gamma(2-n)\,\Gamma(l+n/2)}{\Gamma^2(\frac{3-n}{2})\,\Gamma(l+2-n/2)} \tag{3.46}$$

to get

$$C_l \simeq \frac{\pi}{l\,(l+1)}\,P_\phi \;\;\Rightarrow\;\; l\,(l+1)\,C_l \simeq \text{constant} \tag{3.47}$$

which holds for small enough l's, namely at sufficiently large scales, where the above approximations hold. Notice that, the above result is in agreement with the numerically obtained spectra for C_l's shown in Figure. 3.3 for $l \lesssim 30$. For the calculation without any cosmological constant/dark energy (the blue curve in Figure. 3.3) the quantity $l(l+1)C_l$ is precisely constant at small multipoles. When the contribution of cosmological constant is taken into account, the late time ISW effect, which is ignored in obtaining (3.47), lifts $l(l+1)C_l$ for small multipoles. The oscillatory behavior of the spectrum at large multipoles/small scales is a feature of the oscillations in the baryon-photon plasma at the last scattering surface and each peak in the spectrum is known as an acoustic peak. The first acoustic peak corresponds to angular scale of the last scattering surface, using which the moment of time when photons decoupled and CMB is formed can be determined. Notice that in obtaining the above result, we have neglected the effect of tensor modes, which can be calculated as an additional contribution, since tensor and scalar modes are decoupled at the linearized level. However, since the tensor-to-scalar ratio r is small for single field slow-roll inflationary models as shown in the previous chapter, this approximation is valid.

We have also limited our discussion only on the temperature correlations, and did not discuss the polarization spectra, since it is beyond the scope of this thesis [4] . The polarization spectra of the CMB is a very promising tool, since its measurement might lead to detection of primordial gravitational waves and open a new era in precision cosmology [4]. For this reason, there are numerous new experiments planned for the detection of the polarization of the CMB.

In the next section, we will discuss some of the observational tests of the inflationary cosmology from recently obtained data. As will be shown, the data is in impressive agreement with the predictions of inflation. There are however a few unexplained and controversial features in the data, which have motivated a series of studies that consider modifications of the standard inflationary picture, inducing the analysis of inflationary vector fields (which have several other motivations to be studied). We will also briefly discuss these issues, and comment on the significance of such features.

[4] See for example reference [70] for a discussion of polarization spectra.

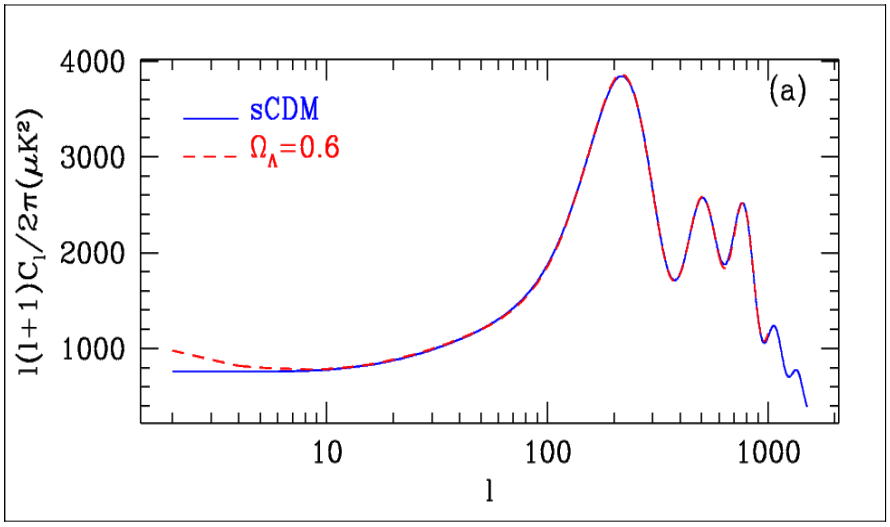

Figure 3.3: Numerically determined C_l's are shown. The blue curve is obtained by only assuming cold-dark matter and no cosmological constant/dark energy. The red curve is obtained by taking into account cosmological constant that dominates the energy density of the universe today with $\Omega_\Lambda = 0.6$. Notice that both models agree at large multipoles or small scales. The figure is taken from reference [69].

3.2 CMB Observations and Inflation

As we have discussed previously, the inflationary paradigm has became a widely accepted description of the early universe, not only because of its success in solving the classical problems of the big-bang cosmology (as discussed in the previous chapter), but also for providing a natural mechanism of generation of primordial perturbations. The spectrum of perturbations generated during inflation is very close to Gaussian (for single field slow-roll inflationary models) and almost scale independent. The deviation from scale independence depends on the curvature of the potential for single field inflationary models, namely to the slow-roll parameters. Single field models can be completely characterized by three parameters, the scalar spectral index n_s, tensor-to-scalar ratio r and the number of e-folds before the end of inflation N. For example, when $V(\phi) \sim \phi^\alpha$, using (2.111), (2.130) and the definition of slow-roll parameters (2.24) we find

$$r = \frac{4\alpha}{N_*} \qquad , \qquad n_s - 1 = -\frac{2+\alpha}{N_*} \tag{3.48}$$

where $N_* \simeq \phi_0^2/(2\alpha M_p^2)$ corresponds to the number of e-folds before the end of inflation, when the largest observable scale $k_0 \sim a_0 H_0$ left the horizon. We show in Figure. 3.4 the 68% and 95% confidence level constraints on several single inflationary models with $V(\phi) \sim \phi^\alpha$ determined by the seven-year data of the WMAP satellite [6]. The constraints are plotted for both $N_* = 50, 60$, since there is an order 10 uncertainty due to the unknown details of reheating (see equation (2.77)).

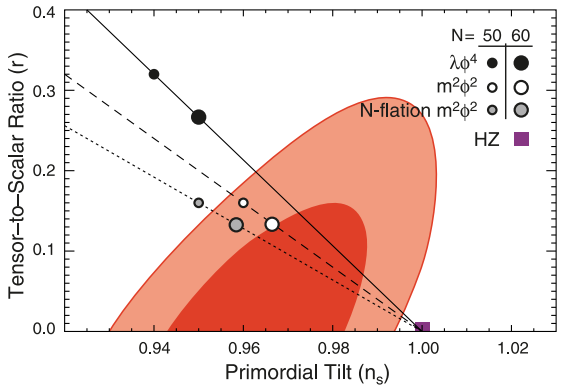

Figure 3.4: Constraints on the scalar spectral index and tensor-to-scalar ratio at the 68% and 95% confidence levels are shown for models with the potential $V(\phi) \sim \phi^\alpha$ (No running of spectral index is taken into account). Notice that $\alpha = 4$ is excluded by the data. $\alpha = 2$ is almost below and $\alpha = 2$ N-field inflation is below the 95% confidence level. Figure is taken from reference [6].

Reference [6] has analyzed the seven year data from the WMAP satellite, combined it with the luminosity distance data of the type Ia Supernovae (SNIa) and angular diameter distance data from baryon acoustic oscillations (BAO) to put constraints on the primordial power spectra. The summary of their analysis is shown in Table 3.1. In the analysis, the power spectrum for scalar perturbations is parameterized as

$$P_{\mathcal{R}}(k) = P_{\mathcal{R}}(k_0) \left(\frac{k}{k_0}\right)^{n_s(k_0)-1+\frac{1}{2}\frac{dn_s}{d\ln k}\ln(k/k_0)} \tag{3.49}$$

where $k_0 = 0.002\text{Mpc}^{-1}$ and the amplitude today is determined as

$$P_{\mathcal{R}}(k_0) = 2.441^{+0.088}_{-0.092} \times 10^{-9} \tag{3.50}$$

from the combined WMAP7+SNIa+BAO data [5] . If both the tensor contribution and the running of spectral index is assumed to be zero, then the scalar spectral index is

[5] The SNIa data is obtained from the direct measurement of the Hubble parameter from the

determined as

$$n_s = 0.963 \pm 0.012 \qquad (r = 0, \ \frac{dn_s}{d\ln k} = 0) \tag{3.51}$$

from the WMAP7+SNIa+BAO data, which is the first entry in Table. 3.1. Taking into account the tensor contributions sets an upper limit on the tensor-to-scalar ratio given by

$$r < 0.24 \ \ (95\% \ \text{confidence level}) \tag{3.52}$$

and the spectral index in this case is determined to be

$$n_s = 0.973 \pm 0.0014\,. \tag{3.53}$$

Table 3.1: WMAP 7-year constraints for n_s, r and $dn_s/d\ln k$ are shown.

Model	Parameters	WMAP+BAO+SNIa
Power-law	n_s	0.963 ± 0.012
Running	n_s	1.008 ± 0.042
	$dn_s/d\ln k$	-0.022 ± 0.020
Tensor	n_s	0.973 ± 0.014
	r	< 0.24
Running	n_s	1.070 ± 0.060
+Tensor	r	< 0.49
	$dn_s/d\ln k$	-0.042 ± 0.024

The possibility of the running of the spectral index is also analyzed and summarized in Table. 3.1. The analysis shows that the running of the index is consistent with zero and therefore there is no evidence for running. Tensor modes are also not detected, and observations can only set an upper limit on the tensor-to-scalar ratio r currently. Notice that observations are now at a stage to rule out some of the inflationary models; for instance $V(\phi) \sim \phi^\alpha$ potentials with $\alpha \geq 4$ has been ruled out as can be seen from Figure. 3.4. Therefore, observations not only support inflationary predictions, but also able to distinguish and even rule out some of the models. New observations of the

luminosity distances of type Ia supernovae [71]. The Baryon Acoustic Oscillation (BAO) data is obtained from the matter power spectrum from the clustering of galaxies, where there is a bump at the scale corresponding to the last scattering, which gives a measurement of z_{CMB} [72].

CMB will improve the status of observational cosmology, especially upcoming CMB polarization experiments [4] will introduce tighter limits on r.

In spite of the fact that the CMB data is in impressive agreement with the inflationary picture, there have been several features emerged in some studies of the data which seem to be anomalous within the inflationary picture. Some of the reported features include

- Low power in the quadrupole moment [14, 15, 16, 17, 18],
- The alignment of the lowest multipoles and claims of statistical anisotropy [18, 19, 20, 21, 22, 23, 24],
- An asymmetry in power between the northern and southern hemispheres [25, 26, 27, 28, 29, 30, 31],
- A nongaussian deviation in the southern hemisphere, known as the 'cold-spot' [6] [32, 33, 34, 35, 36, 37].

The statistical significance of these effects has been highly debated in the literature. In many cases, the outcome of statistical analyses are affected from a posteriori choices or from filtering methods, which prevent a concise conclusion to be reached. Systematic effects or a foreground signal affecting the analysis of data seem to be a possible explanation of these features. However, a complete study explaining the above mentioned features due to systematic effects or a foreground signal is still lacking. For this reason, many authors considered the possibility that these features might have a cosmological origin.

The low power in the quadrupole moment was known since it was first measured by the COBE satellite [14]. This feature stimulated several works in the literature, which explain the low quadrupole by a modification of the standard inflationary picture. For instance, references [73, 74, 75, 76, 77] assumed a short period of inflation, which would lead to a cut-off in the large scale power. Among these, reference [73] assumed that initial conditions for the inflaton field are set away from the attractor solution, therefore initially the inflaton field is not slowly rolling (More precisely, the inflaton field will start from one of the branches that quickly approach to the flat attractor shown in

[6] This feature is most probably a late time effect and has no relevance to inflationary physics.

Figure 2.1). Then, slow-roll conditions are violated initially and the curvature spectrum is suppressed by a factor of $1/\dot{\phi}$ as can be seen from equation (2.109). Consequently, the fluctuations that left the horizon during this fast-roll stage would result in a suppressed power at the largest observable scales. Since the attractor is very quickly reached (in a few e-folds) starting from fast-roll initial conditions, the largest observable scales are affected if inflation lasted just around $N \sim 60$ (i.e 60 e-folds before the end of inflation, when the largest observable scale left the horizon). If inflation lasted longer, then the fast-roll stage would have no observable effect at all. For this reason, the models that explain the low-quadrupole by a cut-off in the power spectrum has to be fine tuned.

Although the low quadrupole power attracted considerable attention, the latest analysis by the WMAP team indicates that this feature is not anomalous [78]. Reference [78] concludes that, although a model predicting a lower quadrupole might fit to the specific part of the data better than a standard inflationary scenario, such a model cannot be favored just on the basis of low quadrupole power. The standard best fit ΛCDM cosmological data fits to the data at the 2σ level, as found by the WMAP team.

The alignment of the quadrupole and octupole moments and claims of breakage of statistical isotropy, has also attracted considerable interest in the literature. The possibility of these features being related to an existence of a preferred direction, attracted many author's interest on anisotropic models of inflation, which we will discuss in the next chapter in detail. The alignment of the lowest multipoles was realized by determining the "direction of the lowest multipoles". The "direction of a multipole" is determined by rotating the coordinate system until $|a_{l,l}|^2+|a_{l,-l}|^2$ is maximized for fixed l, where a_{lm}'s are defined in (3.42) [7] . It has been found that the $l = 2$ (quadrupole) and the $l = 3$ (octupole) components are aligned at a level $< 1^\circ$, and the probability of such an event is around 0.001% [19, 20, 22, 23]. The aligned $l = 2$ and $l = 3$ multipoles can also be seen in Figure. 3.5. Recently, WMAP team has also analyzed the the quadrupole-octupole alignment and verified that it is statistically significant. In Figure. 3.5, the $l = 2$ and $l = 3$ components are added and shown over top of the cleaned full sky map and it was realized that the $l = 2$ and $l = 3$ components are also aligned with the cool fingers in the full sky map (shown within white curves in the right

[7] The reason being that, among the different values for m, spherical harmonics $Y_{l\,m}$ with $m = \pm l$ are the most planar ones.

figure). Therefore, it is possible that the alignment might be related to the cold fingers in the southern hemisphere. Existence of such cold features are expected, however, their non-existence in the northern hemisphere might be an unusual situation [78]. Recently, reference [79] has estimated the local density field of galaxies for $z < 0.3$ and used this estimate to calculate the resulting ISW effect. Subtracting the ISW estimate from the WMAP data showed that the quadrupole-octupole alignment on the last scattering surface becomes insignificant. Therefore, it is possible that the alignment might be related to nonlinearities in the late universe era, or even to the existence of a preferred direction today (see for example [80]).

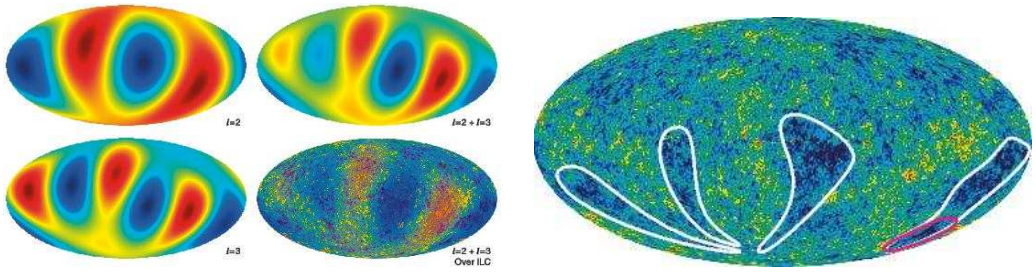

Figure 3.5: The left figure shows the $l = 2$, $l = 3$, $(l = 2) + (l = 3)$ and $(l = 2) + (l = 3)$ over top of the full sky maps respectively. The right figure shows the cleaned full sky map. Regions inside the white curves indicate the cold fingers, which are by themselves expected CMB fluctuations. The region enclosed by the red curve is the cold-spot, which is claimed to be anomalous by many authors. Figure is taken from reference [78].

Assuming statistical isotropy (i.e $< a^*_{lm}\, a_{l'm'} >= C_l\, \delta_{ll'}\, \delta_{mm'}$), one expects that the a_{lm} coefficients have random directions. Therefore, this feature has risen the question whether the statistical isotropy predicted by standard inflationary scenarios might be broken at the largest scales. The breakage of statistical isotropy can be related to an anisotropic phase of inflation, which has been first studied in references [38, 39, 40, 41, 46, 11] and we will discuss these anisotropic inflationary models in detail in the next chapter. Among these, reference [46] has predicted a modified power spectrum resulting from an anisotropic stage of inflation given by $P'(\mathbf{k}) = P(k)\, \left(1 + g_*\, (\hat{\mathbf{k}} \cdot \mathbf{n})^{\mathbf{2}}\right)$, where $P(k)$ is the standard spectrum, $\hat{\mathbf{k}}$ is the direction of the vector $\mathbf{k}$ and $\hat{\mathbf{n}}$ is the preferred direction. Using the anisotropic form of the power spectrum, reference [47] found an evidence for a preferred direction in the data at the 3.8σ level and determined the orientation of the preferred direction. The resulting preferred direction was not aligned

with the ecliptic plane, suggesting the possibility that it could have a cosmological origin. However, an algebraic factor was forgotten in the analysis. This factor was corrected in references [48, 81, 82] and the evidence for the preferred direction increased to 9σ level, but the new direction was pointing along the ecliptic poles. This result suggests that the effect is more likely to be of astrophysical origin. References [81, 82] claimed that the beam asymmetry effect is large enough to explain this signal, although reference [48] has reached the opposite conclusions about the effect of beam asymmetries. However, the subject is still debated and different authors have different conclusions. Therefore, to reach a more concrete conclusion about these features, it is sensible to wait for the data from the Planck experiment, which will have totally different systematics from WMAP.

Another unconventional feature of the CMB data that has been largely debated is the asymmetry in power between northern and southern hemispheres. The significance of this effect has been reported to be up to 3.8σ [29]. This feature has inspired a series of works [83, 84, 85], where a superhorizon perturbation creates a gradient in the sky which modulates the CMB power spectrum. The spatial gradient is generated by a curvaton field, which accounts for the power asymmetry in these works. Recently, WMAP team has revisited the analysis of the power asymmetry effect and concluded that the anomaly is not significant, when the a posteriori choices are removed from the analysis [78].

Finally, we discuss the cold-spot, a non-Gaussian deviation in the southern galactic hemisphere which is shown within the red circle in the right panel of Figure. 3.5. Although this anomaly is not a large scale effect, and most probably has no relevance to inflationary physics, we briefly discuss its significance for the sake of completeness. The significance of this feature is still debated, for example reference [86] indicate that there is no statistical evidence for the cold-spot, and the previous findings are related to the a posteriori choices of the filter used. The cold-spot motivated several papers which seek to explain the mechanism behind it. For example, references [36, 37] suggested that the cold-spot might result from the existence of a topological defect in the form of cosmic texture. Reference [87] suggested that the cold-spot might originate from a large void between our observation point and the last scattering surface. The cold-spot is then a result of energy loss of photons traveling through the void (ISW effect). Their claim

was supported by a deficit in the brightness of galaxies in the direction of the cold-spot. However, reference [88] has reached opposite conclusions after accounting for systematic effects and elimination of a posteriori choices for statistical analysis. Furthermore, reference [89] has found no observational evidence for a void along the direction of the CMB cold-spot. Thus, the subject is still under debate and future data from new experiments might resolve these issues.

Although the subject of CMB anomalies is under debate, one should keep an open mind about the possibility that these effects might have a cosmological origin. This might change if new data will resolve these features by attributing them to systematic effects. We will discuss in the following chapters that the existence of inflationary vector fields or an anisotropic stage of inflation, initially motivated by the claims of breakage of statistical isotropy, have other important motivations to be studied. Moreover, such models would have signatures not only on the temperature spectrum, but also on the polarization spectrum provided that gravity waves are discovered. In the near future, it will be possible to test the predictions from these models and maybe to rule out or support some of them. Therefore, we believe that the study of anisotropic models of inflation and inflationary vector fields is still relevant and promising.

Chapter 4

The Ackerman-Carroll-Wise Model and its Stability

In this chapter we study the Ackerman-Carroll-Wise (ACW) model [46] which was originally formulated in order to adress the alignment of the multipoles in the CMB data which was discussed in the previous chapter. The ACW model has attracted considerable interest, since the type of the power spectrum predicted by this model was shown to be consistent with the CMB data [47, 48, 81, 82] (See previous chapter for more details). In the ACW model, the background geometry is anistropic, which is supported by a fixed norm vector field. The anisotropy of the background leads to the breakage of statistical isotropy, which can be demonstrated by considering a simple geometry with a residual 2-dimensional isotropy. Without loss of generality, let us assume that the anisotropic direction is aligned with the z-axis and the $x-y$ plane is still isotropic. The power spectrum of the fields that produce the density perturbations (either $\delta\chi$ or gravitaional fields) would clearly have an angular dependence of the form $P(k,\,\cos\theta_k)$ where $k=|\vec{k}|$ and θ_k is the angle between $\vec{k}$ and the anisotropic z direction. Therefore, equation (3.37) in the isotropic case is modified as

$$\left\langle \hat{\delta T}(\vec{n}_1)\,\hat{\delta T}(\vec{n}_2)\right\rangle = \frac{1}{9}\int \frac{d^3k\,d^3q}{(2\pi)^3}\,\frac{2\pi^2}{k^3}\,P_\phi(k,\,\cos\theta_k)\,\delta(\vec{k}+\vec{q})\,e^{i\,\vec{k}\cdot(\vec{n}_1-\vec{n}_2)\,\eta_0}\,. \qquad (4.1)$$

Inverting the relation (3.42) and computing the generalized $< a^*_{lm}\, a_{l'm'} >$ covariance gives

$$C_{l\,l'\,m\,m'} = \langle a^*_{lm}\, a_{l'm'} \rangle = \int d\Omega_1\, d\Omega_2\, Y^*_{lm}(\theta_1,\, \phi_1)\, Y_{l'm'}(\theta_2,\, \phi_2)\, \left\langle \delta\hat{T}(\vec{n}_1)\, \delta\hat{T}(\vec{n}_2) \right\rangle . \quad (4.2)$$

Then, using (3.38) in (4.1) we get

$$\left\langle \delta\hat{T}(\vec{n}_1)\, \delta\hat{T}(\vec{n}_2) \right\rangle = \frac{4\pi}{9} \int d(\cos\theta_k)\, d\phi_k\, \frac{dk}{k}\, P_\phi(k,\, \cos\theta_k) \sum_{l,l',m,m'} i^{(l-l')}\, j_l(k\,\eta_0)\, j_{l'}(k\,\eta_0) \times Y^*_{lm}(\theta_k,\, \phi_k)\, Y_{lm}(\theta_1,\, \phi_1)\, Y_{l'm'}(\theta_k,\, \phi_k)\, Y^*_{l'm'}(\theta_2,\, \phi_2) . \quad (4.3)$$

Using the fact that

$$Y_{lm}(\theta,\, \phi) = e^{i\,m\,\phi} \sqrt{\frac{(2l+1)\,(l-m)!}{4\pi\,(l+m)!}}\, P^m_l(\cos\theta) \quad (4.4)$$

where P^m_l's are associated Legendre functions, integrating over the ϕ_k variable reduces (4.3) to

$$\frac{2\pi}{9} \int d(\cos\theta_k)\, \frac{dk}{k}\, P_\phi(k,\, \cos\theta_k) \sum_{l,l',m} \sqrt{\frac{(2l+1)\,(2l'+1)\,(l-m)!\,(l'-m)!}{(l+m)!\,(l'+m)!}}\, i^{(l-l')} \times j_l(k\,\eta_0)\, j_{l'}(k\,\eta_0)\, P^{m*}_l(\cos\theta_k)\, P^m_{l'}(\cos\theta_k)\, Y_{lm}(\theta_1,\, \phi_1)\, Y^*_{l'm'}(\theta_2,\, \phi_2) . \quad (4.5)$$

Inserting (4.5) into (4.2) and integrating over the angular variables Ω_1 and Ω_2 we get

$$\begin{aligned} C_{ll'mm'} &= \delta_{mm'}\, \frac{2\pi}{9}\, i^{(l-l')} \sqrt{\frac{(2l+1)\,(2l'+1)\,(l-m)!\,(l'-m)!}{(l+m)!\,(l'+m)!}} \int \frac{dk}{k}\, d(\cos\theta_k) \\ &\quad \times P_\phi(k,\, \cos\theta_k)\, j_l(k\,\eta_0)\, j_{l'}(k\,\eta_0)\, P^{m*}_l(\cos\theta_k)\, P^m_{l'}(\cos\theta_k) \\ &\equiv \delta_{m\,m'}\, C_{l\,l'} . \end{aligned} \quad (4.6)$$

Note that the standard case is recovered when $P_\phi(k,\, \cos\theta_k) \to P_\phi(k)$. To see this, we use the following orthogonality relation for associated Legendre functions;

$$\int_{-1}^{1} d(\cos\theta_k)\, P^{m*}_l(\cos\theta_k)\, P^m_{l'}(\cos\theta_k) = \frac{2\,(l+m)!}{(2l+1)\,(l-m)!}\, \delta_{l\,l'} . \quad (4.7)$$

Then, (4.6) in the isotropic limit reduces to

$$C_{ll'mm'} = \delta_{mm'}\, \delta_{ll'}\, \frac{4\pi}{9} \int_0^\infty \frac{dk}{k}\, P_\phi(k)\, j^2_l(k\,\eta_0) \quad (4.8)$$

which is equal to the previously found result (3.45) in the standard case. Thus, a simple extension of a flat FRW geometry introduces correlators that have non-vanishing values for $l \neq l'$. Therefore, an inflationary expansion that took place anisotropically, might have some relevance to the alignment of multipoles.

The vector field in the ACW model only acts as to introduce a small anisotropy, the overall expansion of the universe is driven by an unspecified field, taken to be a cosmological constant in the original paper for simplicity. The power spectrum was obtained by studying the evolution of a test field $\delta\chi$ (as we have done in chapter 2 for the isotropic case) in the anisotropic background. It was assumed that the spectrum of $\delta\chi$ is converted into density perturbations after inflation by the DGZK [49] mechanism(we have briefly discussed the DGZK mechanism in chapter 2). Due to the anistropy in the background geometry, the resulting power spectrum breaks statistical isotropy. However, during inflation, metric perturbations (which are coupled to the perturbations of the fixed norm vector field as we will show below) are also generated, therefore in order that the ACW model to be successful, the metric perturbations must be subdominant compared to the test field $\delta\chi$. In order to verify this assumption, references [50, 51] studied the stability of the ACW model, taking into account all the degrees of freedom (arising from gravity and vector field). The equations of perturbations were studied both in the sub-horizon and super-horizon regimes and it was concluded that the ACW model is stable. However, references [52, 53] studied both the quadratic action and the linearized Einstein equations taking into account all the degrees of freedom in the model, and found that close to horizon crossing, the perturbations were divergent. This was due to the fact that one of the vector field perturbations become a ghost (an excitation with negative kinetic energy, which indicates the instability of the vacuum, since energy is unbounded from below.) at that moment when perturbations diverge, which was discovered by the study of the quadratic action. This instability was missed in references [50, 51], since the regime when instability arises was not studied. Below, we will first discuss the original ACW model and then the results of the references [52, 53] for the satibility of the model in detail.

4.1 The ACW model

The ACW model is defined by the action,

$$S = \int d^4x \sqrt{-g} \left[\frac{M_p^2}{2} R - \frac{1}{4} F_{\mu\nu} F^{\mu\nu} + \lambda \left(A^2 - m^2 \right) - V_0 \right] \tag{4.9}$$

where $A^2 \equiv A_\mu A^\mu$ and V_0 is a constant vacuum energy (which is assumed to approximate a slow-roll inflationary phase). This action is a special case of the one considered in [46], which contains generalized kinetic terms. [1] The field equations that describe the evolution of the system is obtained from extremizing the action (4.9) with respect to the metric tensor $g^{\mu\nu}$, the vector field A_μ and the lagrange multiplier field λ, which gives

$$\begin{aligned} & G_{\mu\nu} = \frac{1}{M_p^2} \left[F_{\mu\alpha} F_\nu{}^\alpha - 2\lambda A_\mu A_\nu + g_{\mu\nu} \left(-\frac{1}{4} F^2 + \lambda \left(A^2 - m^2 \right) - V_0 \right) \right] \\ & \frac{1}{\sqrt{-g}} \partial_\nu \left[\sqrt{-g} F^{\mu\nu} \right] = 2 \lambda A^\mu \\ & A^2 = m^2 \end{aligned} \tag{4.10}$$

respectively. The background metric is the special case of a Bianchi-I metric with a residual $2d$ isotropy in the $y - z$ plane and the vacuum expectation value (vev) of the vector field is along the x-direction. They are given by

$$\begin{aligned} g_{\mu\nu} &= \mathrm{diag}(-1,\, a(t)^2,\, b(t)^2,\, b(t)^2) \\ A_\mu &= (0,\, M_p\, a(t)\, B_1(t),\, 0,\, 0) \end{aligned} \tag{4.11}$$

where in the vev for the vector field $A_1 \equiv M_p\, a\, B_1$ we rescaled out the scale factor a and the reduced Planck mass M_p for algebraic convenience (since the background equations of motion are simpler when written in terms of B_1 ; we also note that B_1 is a dimensionless quantity). The last of (4.10) enforces a constant value for B_1,

$$B_1 = \frac{m}{M_p} \equiv \mu \,. \tag{4.12}$$

[1] Specifically, the general kinetic term for the vector field considered in [46] is $\mathcal{L} = -\beta_1 \nabla^\mu A^\nu \nabla_\mu A_\nu - \beta_2 \left(\nabla_\mu A^\mu \right)^2 - \beta_3 \nabla^\mu A^\nu \nabla_\nu A_\mu$. Reference [50] showed that the cases $\beta_1 < 0$ and $\beta_1 + \beta_2 + \beta_3 \neq 0$ have ghosts. Therefore, we consider only the case of a standard kinetic term, with $\beta_1 = -\beta_3 = 1/2$, $\beta_2 = 0$.

Denoting the two expansion rates $H_a \equiv \dot{a}/a$ and $H_b \equiv \dot{b}/b$, where dot is a time derivative, the nontrivial equations in (4.10) are [2]

$$
\begin{aligned}
& 2H_a\, H_b + H_b^2 = \frac{1}{2}\, H_a^2\, \mu^2 + \frac{V_0}{M_p^2} \\
& 2\dot{H}_b + 3H_b^2 = \frac{1}{2}\, H_a^2\, \mu^2 + \frac{V_0}{M_p^2} + 2\,\lambda\,\mu^2 \\
& \dot{H}_a + \dot{H}_b + H_a^2 + H_a\, H_b + H_b^2 = -\frac{1}{2}\, H_a^2\, \mu^2 + \frac{V_0}{M_p^2} \\
& \lambda = H_a\, H_b + \frac{1}{2}\, \dot{H}_a\,.
\end{aligned}
\tag{4.13}
$$

The equations are solved by exponentially expanding scale factors $a \propto e^{H_a\, t}$ and $b \propto e^{H_b\, t}$, with constant Hubble rates

$$
H_a^2 = \frac{2\, V_0}{M_p^2}\, \frac{1}{6 + 7\mu^2 + 2\mu^4} \;\;,\;\; H_b = \left(1 + \mu^2\right)\, H_a\,. \tag{4.14}
$$

The rate H_b which characterizes the expansion of the two dimensional $y - z$ plane is larger than H_a, the expansion rate of the anisotropic x-direction. The difference is proportional to the background expectation value of the vector field. The overall inflationary expansion is supported by the vacuum energy $V_0 > 0$, which approximates an inflaton field.

In the next section, we will provide a simple demonstration of the instability arising in the ACW model, by neglecting the gravitational degrees of freedom, and just solving the evolution equations of the vector field perturbations around the anisotropic background. Although this type of analysis is incomplete, it captures the basic physics of the instability and is agreement with the full calculation, which we will perform later in section 4.3.

4.2 Instability from a simplified computation

We start from the ACW background, given in equations (4.11), (4.12), and (4.14). The most general decomposition of the perturbations of the vector field is

$$
\delta A_\mu = (\alpha_0,\, \alpha_1,\, \partial_i \alpha) \tag{4.15}
$$

[2] Specifically, eqs. (4.13) are, respectively, the 00 , 11 , 22 Einstein equations, and the $x-$ component of the vector field equation.

where the index $i = 2, 3$ spans the isotropic $y - z$ plane, and $\partial_i \alpha_i = 0$ (so, α_i encodes 1 degree of freedom each). The decomposition of δA_i exploits the fact that, due to the symmetry of the background, the mode α_i is decoupled from the other perturbations at the linearized level. The solution for α_i remains finite, therefore we do not discuss it here. We study the rest of the perturbations in the momentum space, where

$$\delta(t,\, \vec{x}) = \int \frac{d^3k}{(2\pi)^{3/2}}\, \delta(t,\, \vec{k})\, e^{-i\,\vec{k}\cdot\vec{x}} \tag{4.16}$$

where δ denotes any of the above perturbations. We denote by k_L the component of the comoving momentum in the x-direction, and by k_T the component in the orthogonal $y-z$ plane. The corresponding components of the physical momentum are $p_L = k_L/a(t)$ and $p_T = k_T/b(t)$. The square magnitudes of the comoving/physical momenta are given by $k^2 = k_L^2 + k_T^2$ and $p^2 = p_L^2 + p_T^2$, respectively. Finally $k_{Ti}\,(p_{Ti})$ denotes the comoving (physical) momentum in the $y(i = 2)$ or $z(i = 3)$ direction.

The constraint equation enforced by the lagrange multiplier, namely, the third equation in (4.10), once linearized in the perturbations, gives $\alpha_1 = 0$. We then perturb the equation for the vector field (the second equation in (4.10)) to obtain [3]

$$\begin{aligned} & p_T^2\,\dot{\alpha} - \left[p_L^2 + p_T^2 - 2\,\left(1+\mu^2\right)\,H_a^2\right]\,\alpha_0 = 0 \\ & \ddot{\alpha} + H_a\,\dot{\alpha} - \dot{\alpha}_0 + \left[p_L^2 - 2\left(1+\mu^2\right)\,H_a^2\right]\,\alpha - H_a\,\alpha_0 = 0\,. \end{aligned} \tag{4.17}$$

We proceed by differentiating the first equation with respect to time, and by combining it with the second equation so to eliminate the $\ddot{\alpha}$ term. In this way we get two first order differential equations:

$$\begin{aligned} \dot{\alpha} &= \frac{p_L^2 + p_T^2 - 2\left(1+\mu^2\right)\,H_a^2}{p_T^2}\,\alpha_0 \\ \dot{\alpha}_0 &= -\frac{\left(1+2\,\mu^2\right)\,p_L^2 - 2\,\left(1+\mu^2\right)\,\left(3+2\,\mu^2\right)\,H_a^2}{p_L^2 - 2\,\left(1+\mu^2\right)\,H_a^2}\,H_a\,\alpha_0 - p_T^2\,\alpha\,. \end{aligned} \tag{4.18}$$

This set of equations has a singular point when $p_L^2 = 2\,\left(1+\mu^2\right)\,H_a^2 = 2\,H_a\,H_b$. We set the origin of time at the singularity, so that the physical momenta are

$$p_L = \sqrt{2\,(1+\mu^2)}\,H_a\,\mathrm{e}^{-H_a\,t} \quad , \quad p_T = p_{T0}\,\mathrm{e}^{-\left(1+\mu^2\right)H_a\,t} \tag{4.19}$$

[3] We do not need to introduce explicitly the perturbation of the Lagrange multiplier in this equation, since we can first eliminate λ as will be explained in section 4.3

where p_{T0} is the value of p_L at the singularity.

Once expanded close to the singularity, the system (4.18) becomes

$$\dot{\alpha} \approx \alpha_0 \quad , \quad \dot{\alpha}_0 \approx -\frac{\alpha_0}{t} - p_{T0}^2\,\alpha \tag{4.20}$$

which we can combine into (we obtain the same result if we first combine the two equations (4.18) into a unique equation for α, and we then expand that one)

$$\ddot{\alpha} + \frac{\dot{\alpha}}{t} + p_{T*}^2\,\alpha \approx 0 \tag{4.21}$$

which is in turn solved by

$$\alpha \approx C_1\,J_0\left(p_{T*}\,t\right) + C_2\,Y_0\left(p_{T*}\,t\right) \tag{4.22}$$

where $C_{1,2}$ are constants to be determined from initial conditions. While the J_0 solution is constant at $t = 0$, the Y_0 solution has a logarithmic divergence. In principle, one may imagine arranging the initial conditions, so that the solution will be regular ($C_2 = 0$) at $t = 0$. One would need to do so for both the real and imaginary parts of α and for all modes (namely, for all values of the comoving momenta). There is however no physical reason for this tuning; the initial conditions are given when the mode is deeply inside the horizon, well before the equations become singular (there is no reason why the mode should initially "know" about the singularity that will happen close to horizon crossing). Moreover, as we will see, the solution is clearly divergent ($C_2 \neq 0$) if the initial conditions are chosen in the adiabatic vacuum. Therefore, α has a logarithmic divergence, and $\alpha_0 \approx \dot{\alpha}$ has a linear $1/t$ divergence close to horizon crossing, which indicates that the background solution is unstable. This result is confirmed by the numerical solutions below. Moreover, this degree of divergence is the same as the one obtained in the complete computation of section 4.3.

To find the initial conditions, and to understand the reason for the instability, we compute the quadratic action for the perturbations (namely, we insert the decomposition (4.15) into the action (4.9), disregarding the decoupled mode α_i). After imposing the linearized constraint equation $\alpha_1 = 0$, the action becomes (up to boundary terms)

$$\begin{aligned} S_s \;=\; \frac{1}{2}\int d^3k\,dt\,a\,b^2 \Big\{ & p_T^2\,|\dot{\alpha}|^2 - p_T^2\,\left(\alpha_0^*\,\dot{\alpha} + \text{h.c.}\right) - p_T^2\,\left[p_L^2 - 2\,\left(1+\mu^2\right)\,H_a^2\right]\,|\alpha|^2 \\ & + \left[p_L^2 + p_T^2 - 2\,\left(1+\mu^2\right)\,H_a^2\right]\,|\alpha_0|^2 \Big\}\,. \end{aligned} \tag{4.23}$$

This actions leads to the equations (4.18), when it is extremized. The mode α_0 appears without any time derivatives in the action, therefore it can be integrated out by solving its equation of motion, which gives

$$\alpha_0 = \frac{p_T^2}{p_L^2 + p_T^2 - 2\,(1+\mu^2)\,H_a^2}\,\dot{\alpha}\,. \tag{4.24}$$

Inserting this solution back into the action we get

$$S_s = \frac{1}{2}\int d^3k\,dt\,a\,b^2\,p_T^2\,\left(p_L^2 - 2\,\left(1+\mu^2\right)\,H_a^2\right)\,\left[\frac{|\dot{\alpha}|^2}{p_L^2 + p_T^2 - 2\,(1+\mu^2)\,H_a^2} - |\alpha|^2\right]\,. \tag{4.25}$$

In the early-time/UV limit when $p_{L,T}^2 \gg H_a^2$, this action is ghost free and α is stable. However, there is a moment later in the evolution, close to horizon crossing, when the longitudinal physical momentum becomes $p_L = \sqrt{2\,(1+\mu^2)}\,H_a$ and the action vanishes. This generates the singularity in the equations (4.18). In addition, α becomes a ghost after the action vanishes, since the kinetic term becomes negative. [4]

We define the mode α_c, which canonically normalizes the kinetic terms in the above action, given by

$$\alpha_c \equiv \sqrt{a}\,b\,p_T\,\sqrt{\frac{p_L^2 - 2\,(1+\mu^2)\,H_a^2}{p_L^2 + p_T^2 - 2\,(1+\mu^2)\,H_a^2}}\,\alpha\,. \tag{4.26}$$

Inserting this into the action (4.25) we get (up to a boundary term)

$$S_s = \frac{1}{2}\int d^3k\,dt\,\left(|\dot{\alpha}_c|^2 - \omega_c^2\,|\alpha_c|^2\right)\,. \tag{4.27}$$

The exact expression of ω_c is rather involved, and we do not report it here. The first two terms in the early time/subhorizon expansion ($H \ll p$) are

$$\omega_c = p\left[1 - \frac{\left(9+8\mu^2\right)p_L^4 + \left(3+2\mu^2\right)^2 p_T^4 + 2\left(9+10\mu^2-4\mu^4\right)p_L^2\,p_T^2}{8p^4}\,\frac{H_a^2}{p^2} + \mathrm{O}\left(\frac{H_a^4}{p^4}\right)\right]\,. \tag{4.28}$$

The frequency ω_c is adiabatically evolving at early times, $\dot{\omega_c} \ll \omega_c = \mathrm{O}\,(H/p) \ll 1\,.$ Therefore, we can set the initial conditions for the canonical variable α_c in the adiabatic vacuum

$$\alpha_{\mathrm{c,\,in}} = \frac{1}{\sqrt{2\,\omega_c}}\,\mathrm{e}^{-i\,\int^t \omega_c\,dt}\,. \tag{4.29}$$

[4] The kinetic term also diverges when $p = \sqrt{2\,(1+\mu^2)}\,H_a$ (where $p = \sqrt{p_L^2 + p_T^2}$); this is due to the fact that α_0 cannot be integrated at this point. However, this happens after the singularity we are interested in.

This gives the initial values of α_c and $\dot{\alpha}_c$ as we have discussed in chapter 2. From (4.27) and its time derivative we then obtain the initial values of α and $\dot{\alpha}$. Finally, from (4.24) we obtain the initial value of α_0. Specifically, we find

$$\mathrm{Im}\,(\alpha_0/\alpha)_{\rm in} = -\frac{p_T^2}{p}\left[1+\mathrm{O}\left(\frac{H^2}{p^2}\right)\right] \quad , \quad \mathrm{Re}\,(\alpha_0/\alpha)_{\rm in} = -\frac{\mu^2\,p_T^4}{2\,p^3}\,\frac{H_a}{p}\left[1+\mathrm{O}\left(\frac{H^2}{p^2}\right)\right] . \tag{4.30}$$

The overall phase of the modes is unphysical, and we can always choose $\alpha_{\rm in}$ to be real. Since the coefficients of (4.18) are real, we need to evolve this system twice, one for the real part and one for the imaginary parts of the modes. We did so starting from $t=-7/H_a$, so that $H/p=\mathrm{O}\left(10^{-3}\right)$ initially. For definiteness, we take $\mu=0.1$, $p_{T0}=H_a$. We show the solutions for the real part in Figure 4.1. The right panel is a close up near the singularity (which, in logarithmic units, occurs at $-\ln\left(-H_a\,t\right)=+\infty$). The two solutions have been re-scaled so to make the degree of divergence manifest. The imaginary part presents an analogous divergence.

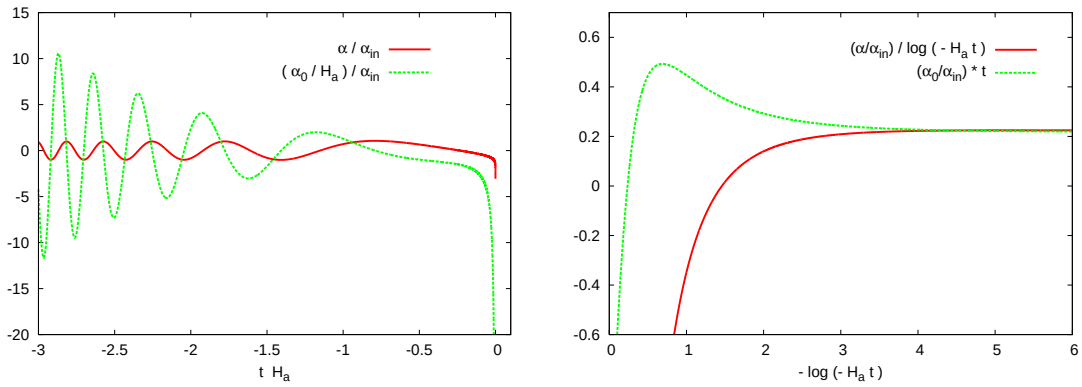

Figure 4.1: The right panel shows a zoom of the left panel in the region $-1 \le H_a\,t \le -2.5{\cdot}10^{-3}$ (the time is shown in log units). Both modes blow up when the system (4.18), becomes singular, $\alpha \propto \log t$ and $\alpha_0 \propto 1/t$, in agreement with the analytic approximate solution (4.22). Notice also that $\alpha_0 \approx \dot{\alpha}$ close to the singularity, in agreement with the analytic computation.

4.3 Instability from the full linearized equations

In this section we show that the instability found from the simplified computation presented in the previous section appears also in the full stability calculation. We

do so by writing down and solving the linearized equations for the most general set of perturbations of the ACW background solution. We first introduce the decomposition of perturbations, relevant for Bianchi-I spacetimes. In decomposing the perturbations, we exploit the left-over $2d$ isotropy of the background solution which leads to two decoupled sets of perturbations. One of the decoupled sets have a stable evolution, so we will disregard them. The other set will be proven to exhibit the instability. Some of the intermediate steps in of this computation are very lengthy, therefore they are presented in Appendix A.

4.3.1 Classification of the perturbations

We generalize to the present case, the standard computation of cosmological perturbations in the case of a scalar field on an isotropic background studied in chapter 2. As usual, it is convenient to exploit the symmetry of the background spacetime in this computation. The three dimensional rotational symmetry of the isotropic background was used when the perturbations were classified as scalar, vector and tensor modes. Since the modes in that decomposition form a complete basis for the perturbations, we could still use them here. However, this would be of no practical advantage, since modes belonging to different representations would now be coupled to each other. We can however still exploit the residual symmetry of the ACW background solution (4.11) in the $y-z$ plane, and classify the perturbations according to how they transform with respect to rotations in this plane [39]. Modes transforming differently under these rotations are decoupled at the linearized level, as we will explicitly demonstrate below.

Specifically, we write the most general perturbations of the metric and of the vector field as

$$\begin{aligned}
\delta g_{\mu\nu} &= \begin{pmatrix} -2\Phi & a\,\partial_1\chi & b\,(\partial_i B + B_i) \\ & -2\,a^2\,\Psi & a\,b\,\partial_1\left(\partial_i \tilde{B} + \tilde{B}_i\right) \\ & & b^2\,(-2\Sigma\,\delta_{ij} - 2\,\partial_i\,\partial_j\,E - \partial_i\,E_i - \partial_j\,E_i) \end{pmatrix} \\
\delta A_\mu &= (\alpha_0,\, \alpha_1,\, \partial_i\alpha + \alpha_i)
\end{aligned} \tag{4.31}$$

where $i,j = 1,2$ span the isotropic coordinates. [5]

[5] We chose to insert a ∂_1 derivative in the δg_{01} and δg_{1i} metric perturbations for algebraic convenience. For instance, we could have equivalently denoted $\delta g_{01} = \chi_1$. More precisely, we only study

The perturbations $\{\Phi,\, \chi,\, B,\, \Psi,\, \tilde{B},\, \Sigma,\, E,\, \alpha_0,\, \alpha_1,\, \alpha\}$ are 2d scalar modes: they encode 1 degree of freedom (d.o.f.) each. The perturbations $\{B_i,\, \tilde{B}_i,\, E_i,\, \alpha_i\}$ are 2d vector modes. Due to the transversality condition ($\partial_i B_i = \ldots = 0$), they also encode 1 d.o.f. each. Notice that, contrary to the 3d case, there are no 2d tensor modes, since the transversality and traceless conditions eliminate all possible degrees of freedom. Altogether, we have 10 d.o.f. in the 2d scalar sector, and 4 d.o.f. in the 2d vector sector. These add up to 14 d.o.f., which is the number of initial independent entries in the metric and in the vector field.

The set of perturbations just given is redundant, since modes can be transformed into each other through infinitesimal coordinate transformations $x^\mu \to x^\mu + \xi^\mu$. Under this change

$$\delta g_{\mu\nu} \to \delta g_{\mu\nu} - g^{(0)}_{\mu\nu,\alpha}\,\xi^\alpha - g^{(0)}_{\mu\alpha}\,\xi^\alpha_{,\nu} - g^{(0)}_{\alpha\nu}\,\xi^\alpha_{,\mu} \quad , \quad \delta A_\mu \to \delta A_\mu - A^{(0)}_{\mu,\alpha}\,\xi^\alpha - A^{(0)}_\alpha\,\xi^\alpha_{,\mu} \tag{4.32}$$

where $g^{(0)}_{\mu\nu}$ and $A^{(0)}_\mu$ are the background metric and vev of the vector field respectively. We decompose also the components of the infinitesimal parameter ξ^μ in the $y-z$ plane in a 2d scalar plus 2d vector part. In this way 2d scalar (vector) modes manifestly transform into 2d scalar (vector) modes. More explicitly,

$$\xi^\mu = \left(\xi^0,\, \partial_1\,\xi^1,\, \partial_i\,\xi + \xi^i\right) \tag{4.33}$$

and the modes defined in (4.32) transform as

$$\begin{aligned}
&\Phi \to \Phi - \dot{\xi}^0 \qquad , \qquad \chi \to \chi + \frac{1}{a}\,\xi^0 - a\,\dot{\xi}^1 \\
&B \to B + \frac{1}{b}\,\xi^0 - b\,\dot{\xi} \qquad , \qquad B_i \to B_i - b\,\dot{\xi}^i \\
&\Psi \to \Psi + \frac{\dot{a}}{a}\,\xi^0 + \partial_1^2\,\xi^1 \qquad , \qquad \tilde{B} \to \tilde{B} - \frac{a}{b}\,\xi^1 - \frac{b}{a}\,\xi \\
&\tilde{B}_i \to \tilde{B}_i - \frac{b}{a}\,\xi^i \qquad , \qquad E \to E + \xi \\
&E_j \to E_j + \xi^j \qquad , \qquad \Sigma \to \Sigma + \frac{\dot{b}}{b}\,\xi^0 \\
&\alpha_0 \to \alpha_0 - A^{(0)}_1\,\partial_1\,\dot{\xi}^1 \qquad , \qquad \alpha_1 \to \alpha_1 - \dot{A}^{(0)}_1\,\xi^0 - A^{(0)}_1\,\partial_1^2\,\xi^1 \\
&\alpha \to \alpha - A^{(0)}_1\,\partial_1\,\xi^1 \qquad , \qquad \alpha_i \to \alpha_i\,.
\end{aligned} \tag{4.34}$$

the modes of the perturbations which have a nonvanishing momentum component both along the x direction and in the $y-z$ plane (in coordinate space, they have a nontrivial dependence both on x and at least on one between y and z).

To eliminate the redundancy, we can specify a gauge that completely fixes the freedom of general coordinate reparametrization (this was the procedure chosen in [39], where the choice $E = \Sigma = \tilde{B} = E_i = 0$ was made). Equivalently, we can construct gauge invariant combinations of the above perturbations ("gauge invariance" here means invariance with respect to general coordinate transformations; there is no gauge U(1) symmetry associated to the vector field, due to its mass term). We choose this second procedure here: each linearized equation can be written as "left hand side = 0"; therefore the equation must be gauge invariant. This means that the perturbations must enter in the linearized equations in such a way that these equations can be written in terms of the gauge invariant combinations only (the same is true for the quadratic action that we compute in the next section). This provides a nontrivial check on our algebra.

Using the transformations given in (4.34) and the fact that $A_1^{(0)} = a\, M_p\, B_1$, we find the following set of gauge invariant modes

$$\begin{aligned}
\hat{\Phi} &= M_p \left[\Phi + \left(\frac{\Sigma}{H_b}\right)^{\bullet}\right] \\
\hat{\Psi} &= M_p \left[\Psi - \frac{H_a}{H_b}\,\Sigma + \frac{b}{a}\,\partial_1^2 \left(\tilde{B} + \frac{b}{a}\,E\right)\right] \\
\hat{B} &= -\frac{M_p^2}{b}\,\vec{\partial}_T^2 \left[B - \frac{1}{b\,H_b}\,\Sigma + b\,\dot{E}\right] \\
\hat{\chi} &= -\frac{M_p}{a}\,\partial_1^2 \left[\chi - \frac{1}{a\,H_b}\,\Sigma - a\left(\frac{b}{a}\left(\tilde{B} + \frac{b}{a}\,E\right)\right)^{\bullet}\right] \\
\hat{\alpha}_1 &= -\frac{1}{a}\left[\alpha_1 + a\,M_p\,\frac{\dot{B}_1 + H_a\,B_1}{H_b}\,\Sigma - b\,M_p\,B_1\,\partial_1^2 \left(\tilde{B} + \frac{b}{a}\,E\right)\right] \\
\alpha &= -\frac{1}{a}\,\partial_1 \left[\alpha - b\,M_p\,\partial_1 \left(\tilde{B} + \frac{b}{a}\,E\right)\right] \\
\hat{\alpha}_0 &= \frac{1}{a}\,\partial_1 \left[\alpha_0 - a\,M_p\,B_1\,\partial_1 \left(\frac{b}{a}\left(\tilde{B} + \frac{b}{a}\,E\right)\right)^{\bullet}\right]
\end{aligned} \tag{4.35}$$

(where the bullet denotes time derivative, and $\vec{\partial}_T^2 \equiv \partial_2^2 + \partial_3^2$) in the 2d scalar sector, and

$$\begin{aligned}
\hat{B}_i &= B_i + b\,\dot{E}_i \\
\hat{\tilde{B}}_i &= a\left(\tilde{B}_i + \frac{b}{a}\,E_i\right) \\
\hat{\alpha}_i &= \frac{\alpha_i}{M_p}
\end{aligned} \tag{4.36}$$

in the 2d vector sector. The prefactors in front of these modes do not affect their gauge invariance, but have been chosen for algebraic convenience.

Since we started from ten 2d scalars and four 2d vectors, and since there are three infinitesimal 2d scalar transformations, and one infinitesimal 2d vector transformation, we end up with seven 2d scalar gauge invariant modes, and three 2d vector gauge invariant modes. One could have equivalently chosen other gauge invariant combinations of the initial modes. However, they can be obtained from those given here. The choice of the above variables is again motivated by the fact that when ($E = \Sigma = \tilde{B} = E_i = 0$) is chosen as a gauge, the gauge invariant variables $\{\hat{\Phi},\, \hat{B},\, \hat{\chi}\}$ reduce to the nondynamical modes $\delta g_{0\,\mu}$ as was the case when we studied the standard case in chapter 1.

We perform the computations in the momentum space, defined in equation (4.16) (see the paragraph after that equation for our definitions of the various components of the comoving and physical momentum). As we have already mentioned, modes with different momenta are decoupled from each other at the linearized level. In momentum space, the transversality condition on any $2d$ vector mode v_i reads

$$k_{Ti}\, v_i = p_{Ti}\, v_i = 0 \tag{4.37}$$

4.3.2 Solutions to the linearized equations for the perturbations

We perturb the metric and the vector field as in equation (4.31). We want to solve the system of linearized equations for these modes. We multiply the second line of (4.10) by A_μ and we replace A^2 by m^2 on the right hand side. In this way we obtain an expression for λ in terms of the vector field and the metric (this is the procedure also adopted in [90] to study a similar model, and it has the advantage that we do not have to introduce explicitly the perturbation of the lagrange multiplier). In this way, the first and second line of (4.10) become

$$\begin{aligned} & G_{\mu\nu} = \frac{1}{M_p^2}\, T_{\mu\nu} = \frac{1}{M_p^2}\, \left[F_{\mu\alpha}\, F_\nu{}^\alpha - \frac{1}{\mu^2\, M_p^2}\, A_\alpha\, \nabla_\beta\, F^{\alpha\beta}\, A_\mu\, A_\nu + g_{\mu\nu}\, \left(-\frac{1}{4}\, F^2 - V_0 \right) \right] \\ & \partial_\nu \left[\sqrt{-g}\, F^{\lambda\nu} \right] \left(m^2\, \delta^\mu_\lambda - A_\lambda\, A^\mu \right) = 0\,. \end{aligned} \tag{4.38}$$

We then linearize these equations, and we go to momentum space as indicated in (4.16). We denote the resulting equations as [6]

$$\mathrm{Eq}_{\mu\nu} : \delta \left(G_{\mu\nu} - \frac{1}{M_p^2}\, T_{\mu\nu} \right) = 0 \quad , \quad \mathrm{Eq}_{\mu} : \delta \left(\frac{\delta S}{\delta A_\mu} \right) = 0 \,. \tag{4.39}$$

The explicit expressions are given in equations (A.1) in Appendix A. The expressions pass two crucial tests: we initially wrote them in terms of the original perturbations (4.31); with some algebra, we have been able to write them solely in terms of the gauge invariant combinations (4.35) and (4.36). As a second test, we show explicitly in Appendix A that the set of 2d scalar and 2d vector perturbations decouple in these equations. We verified that the system of 2d vectors is stable. For brevity, we do not report those computations here. We also show in Appendix A that not all the equations (4.39) are independent (due to the perturbed Bianchi identities). A set of independent equations is

$$\mathrm{Eq}_1 : \quad \hat{\alpha}_1 - \mu\, \hat{\Psi} = 0 \tag{4.40}$$

$$\begin{aligned} \mathrm{Eq}_{00} : \quad & \left(2+\mu^2\right) H_a\, \dot{\hat{\Psi}} + p_T^2\, \hat{\Psi} + \left(2+\mu^2\right)\, \left(3+2\mu^2\right)\, H_a^2\, \hat{\Phi} \\ & -2\left(1+\mu^2\right) H_a\, \hat{\chi} - \left(2+\mu^2\right) H_a\, \hat{B} - \mu\, H_a\, \hat{\alpha}_0 = 0 \end{aligned} \tag{4.41}$$

$$\begin{aligned} \mathrm{Eq}_{01} : \quad & 2\left(1+\mu^2\right) H_a \hat{\Phi} + \frac{1}{2\, p_L^2} \left[p_T^2 - 4\,\mu^2 \left(1+\mu^2\right) H_a^2 \right] \hat{\chi} - \frac{\hat{B}}{2} \\ & -2\mu \left(1+\mu^2\right) \frac{H_a^2}{p_L^2} \hat{\alpha}_0 = 0 \end{aligned} \tag{4.42}$$

$$\mathrm{Eq}_{0i} : \quad \dot{\hat{\Psi}} + \left(2+\mu^2\right) H_a\, \hat{\Phi} - \frac{\hat{\chi}}{2} + \frac{p_L^2}{2 p_T^2}\, \hat{B} - \mu\, H_a\, \hat{\alpha} = 0 \tag{4.43}$$

$$\begin{aligned} \mathrm{Eq}_{11} : \quad & \mu^2\, \ddot{\hat{\Psi}} + \mu^2 \left(3+2\,\mu^2\right) H_a \dot{\hat{\Psi}} + \mu^2\, p_T^2\, \hat{\Psi} - \left(2+\mu^2\right) H_a\, \dot{\hat{\Phi}} \\ & + \left[p_T^2 - \left(2+\mu^2\right)\, \left(3+2\mu^2\right)\, H_a^2 \right] \hat{\Phi} + \dot{\hat{B}} + \left(3+2\,\mu^2\right) H_a\, \hat{B} + \mu\, \dot{\hat{\alpha}}_0 \\ & +\mu \left(3+2\,\mu^2\right) H_a\, \hat{\alpha}_0 - \mu\, p_T^2\, \hat{\alpha} = 0 \end{aligned} \tag{4.44}$$

$$\begin{aligned} \mathrm{Eq}_{0} : \quad & \dot{\hat{\alpha}} + H_a\, \hat{\alpha} + \frac{1}{p_T^2} \left[p^2 - 2\left(1+\mu^2\right) H_a^2 \right] \hat{\alpha}_0 + \mu\, \frac{p_L^2}{p_T^2}\, \dot{\hat{\Psi}} + \mu\, \frac{p_L^2}{p_T^2}\, H_a\, \hat{\Phi} \\ & -\mu \left(1+\mu^2\right) \frac{2\, H_a^2}{p_T^2}\, \hat{\chi} = 0 \end{aligned} \tag{4.45}$$

$$\mathrm{Eq}_i : \quad \ddot{\hat{\alpha}} + 3 H_a\, \dot{\hat{\alpha}} + \dot{\hat{\alpha}}_0 + \left(p_L^2 - 2\,\mu^2\, H_a^2\right)\, \hat{\alpha} - \mu\, p_L^2\, \hat{\Psi} + \mu\, \frac{p_L^2}{p_T^2}\, H_a\, \hat{B}$$

[6] After we eliminated λ, the linearization of the third of (4.10) coincides with Eq_1.

$$+2H_a\,\hat{\alpha}_0 = 0\,. \tag{4.46}$$

We have used (4.40) to eliminate $\hat{\alpha}_1$ in favor of $\hat{\Psi}$ in all the other equations. Therefore, we do not need to consider this equation further in the following.

We now solve the set of equations (4.41)-(4.46). We need to rearrange them in a system that can be numerically integrated. There are several equivalent ways to proceed. We could either integrate all the above equations numerically, or we could solve some of them analytically. We choose this second option (in this way, we reduce the number of equations to be numerically integrated, but we generally obtain more involved expressions). We start by solving equations (4.42) and (4.43) for $\hat{\chi}$ and $\hat{B}$. We find

$$\begin{aligned}
\hat{\chi} &= \frac{p_T^2}{2\,\mu^2\,(1+\mu^2)\,H_a^2}\dot{\hat{\Psi}} + \frac{1}{\mu^2\,H_a}\left[p^2 - \frac{\mu^2}{2\,(1+\mu^2)}p_T^2\right]\hat{\Phi} - \frac{p_T^2}{2\,\mu\,(1+\mu^2)\,H_a}\hat{\alpha} - \frac{\hat{\alpha}_0}{\mu} \\
\hat{B} &= \frac{1}{2\,\mu^2\,H_a^2}\,\frac{p_T^2}{p_L^2}\left(\frac{p_T^2}{1+\mu^2} - 4\,\mu^2\,H_a^2\right)\dot{\hat{\Psi}} \\
&\quad + \frac{1}{\mu^2\,H_a}\,\frac{p_T^2}{p_L^2}\left[p^2 - \frac{\mu^2}{2\,(1+\mu^2)}p_T^2 - 2\left(2+\mu^2\right)\mu^2\,H_a^2\right]\hat{\Phi} \\
&\quad - \frac{1}{2\,\mu\,H_a}\,\frac{p_T^2}{p_L^2}\left(\frac{p_T^2}{1+\mu^2} - 4\,\mu^2\,H_a^2\right)\hat{\alpha} - \frac{p_T^2}{p_L^2}\,\frac{\hat{\alpha}_0}{\mu}\,.
\end{aligned} \tag{4.47}$$

Inserting these solutions into the remaining equations (4.41), (4.44), (4.45), and (4.46), we have now a system of 4 equations in terms of the four unknown modes $\hat{\Psi}$, $\hat{\alpha}$, $\hat{\Phi}$, and $\hat{\alpha}_0$. These equations are explicitly given in Appendix A, eqs. (A.6) - (A.9). As we show in Appendix A, by simple algebraic manipulation of these equations we obtain the system

$$\mathcal{M}_\kappa \begin{pmatrix} \ddot{\hat{\alpha}} \\ \dot{\hat{\alpha}}_0 \\ \ddot{\hat{\Psi}} \\ \dot{\hat{\Phi}} \end{pmatrix} = \begin{pmatrix} f_1 \\ f_2 \\ f_3 \\ f_4 \end{pmatrix} \quad , \quad \mathcal{M}_\kappa \equiv \begin{pmatrix} 1 & 1 & 0 & 0 \\ 0 & \kappa_{22} & \kappa_{23} & \kappa_{24} \\ 1 & \kappa_{32} & \kappa_{33} & \kappa_{34} \\ 0 & \kappa_{42} & \kappa_{43} & \kappa_{44} \end{pmatrix} \tag{4.48}$$

(for reasons explained in the next section, there are no second time derivatives of $\hat{\alpha}_0$ and $\hat{\Phi}$ in these equations). The entries of $\mathcal{M}_\kappa$, given in eq. (A.10) depend on background quantities, while the four expressions at right hand side, given in eq. (A.11), are linear combinations of the unknown quantities $\left\{\hat{\alpha},\, \dot{\hat{\alpha}},\, \hat{\alpha}_0,\, \hat{\Psi},\, \dot{\hat{\Psi}},\, \hat{\Phi}\right\}$ (also the coefficients of

these linear combinations depend on background quantities). It is now straightforward to invert $\mathcal{M}_\kappa$, and to integrate the system numerically.

It is easy to see that, in general, the solutions of (4.48) diverge close to horizon crossing. Indeed,

$$\det \mathcal{M}_\kappa = \frac{p_T^2}{p_L^2}\,\frac{1+\mu^2}{\mu^2}\,\left[p_L^2 - \left(2+\mu^2\right)\,H_a\,H_b\right] \tag{4.49}$$

so that, when we invert this matrix, we encounter a singularity when $p_L = \sqrt{2+\mu^2}\,\sqrt{H_a\,H_b}$.

We evolve the system, starting from the adiabatic vacuum initial conditions discussed in chapter 2 deeply inside the horizon (eqs. (A.12) and (A.17)). The two components of the physical momentum evolve as

$$\begin{aligned} p_L\,(t) &= \frac{k_L}{a\,(t)} = p_{L0}\,\mathrm{e}^{-H_a\,t} \\ p_T\,(t) &= \frac{k_T}{b\,(t)} = p_{T0}\,\mathrm{e}^{-H_b\,t} = p_{T0}\,\mathrm{e}^{-\left(1+\mu^2\right)H_a\,t} \end{aligned} \tag{4.50}$$

where p_{L0}, p_{T0} are the values of these components when $t = 0$, and where we have used the background relation (4.14) between the two Hubble constants. We are free to choose the origin of the time. We set $t = 0$ at the moment in which $\det \mathcal{M}_\kappa = 0$. This fixes $p_{L0} = \sqrt{2+\mu^2}\,\sqrt{H_a\,H_b}$. The mode is then completely specified by giving the ratio p_{T0}/p_{L0}. For definiteness, we choose $\mu = 0.1$ (giving an $\mathrm{O}\left(10^{-2}\right)$ anisotropy), and $p_{T0} = H_a$ (so that the two components of the momentum are comparable to each other in the time range considered). We start the numerical evolution at $t = -7/H_a$, so that $H/p = \mathrm{O}\left(10^{-3}\right)$ initially, and the modes are well inside the horizon.

The left panel of Figure 4.2 shows that the modes $\hat{\alpha}_0$ and $\hat{\Phi}$ indeed diverge when $\det \mathcal{M}_\kappa = 0$. The right panel gives the behavior close to the singularity. We give time in log units, so that $t = 0$ is mapped at $-\log\left(-H_a\,t\right) = \infty$. We see that both $\hat{\alpha}_0$ and $\hat{\Phi}$ diverge linearly. The two modes $\hat{\alpha}$ and $\hat{\Psi}$ (not shown here) diverge logarithmically. The modes $\hat{\alpha}$ and $\hat{\alpha}_0$ present an identical divergence in the simplified computation of Section 4.2. For that simplified analysis, we have also obtained the divergence analytically. It is also clear from there that the solutions diverge for generic initial conditions (we have also verified this in the numerical solutions of the system (4.48)).

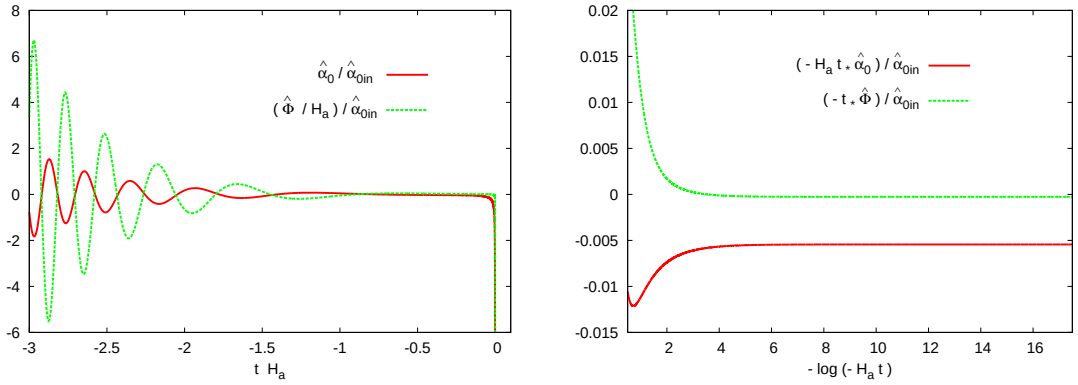

Figure 4.2: The right panel shows a zoom of the left panel in the region $-0.6 \leq H_a\, t \leq -10^{-5}$ (the time is shown in log units). Both modes show a 1/t divergence.

4.4 Ghost from the quadratic equation

To gain a better understanding on the nature of the instability, we computed the quadratic action for the perturbations. We inserted the expression (4.11) and (4.31) in the action (4.9). We expanded at the second order in the perturbations. We disregarded the 2d vector modes, which are decoupled from the 2d scalars. We also eliminated the mode $\hat{\alpha}_1$ through the constraint equation (4.40). We then Fourier transformed the perturbations as in (4.16). The final result is, up to boundary terms,

$$
\begin{aligned}
S_{2\rm dS} &= \frac{1}{2}\int d^3k\, dt\, a\, b^2\, \mathcal{L}_{2\rm dS} \\
\mathcal{L}_{2\rm dS} &= \mu^2\, |\dot{\hat{\Psi}}|^2 + \frac{p_T^2}{p_L^2}\, |\dot{\hat{\alpha}}|^2 - H_a \left(\hat{\Psi}^*\, \dot{\hat{\Psi}} + \text{h.c.}\right) - \left(2+\mu^2\right)\, H_a \left(\hat{\Phi}^*\, \dot{\hat{\Psi}} + \text{h.c.}\right) \\
&\quad + \left(\hat{B}^*\, \dot{\hat{\Psi}} + \text{h.c.}\right) + \mu \left(\hat{\alpha}_0^*\, \dot{\hat{\Psi}} + \text{h.c.}\right) + \frac{p_T^2}{p_L^2}\, H_a \left(\hat{\alpha}^*\, \dot{\hat{\alpha}} + \text{h.c.}\right) \\
&\quad + \frac{p_T^2}{p_L^2} \left(\hat{\alpha}_0\, \dot{\hat{\alpha}} + \text{h.c.}\right) - \left[\mu^2\, p_T^2 + \left(3+2\mu^2\right)\, H_a^2\right]\, |\hat{\Psi}|^2 - p_T^2 \left(\hat{\Phi}^*\, \hat{\Psi} + \text{h.c.}\right) \\
&\quad + \mu\, p_T^2 \left(\hat{\alpha}^*\, \hat{\Psi} + \text{h.c.}\right) - \left(2+\mu^2\right)\, \left(3+2\mu^2\right)\, H_a^2\, |\hat{\Phi}|^2 \\
&\quad + 2\, \left(1+\mu^2\right)\, H_a \left(\hat{\chi}^*\, \hat{\Phi} + \text{h.c.}\right) + \left(2+\mu^2\right)\, H_a \left(\hat{B}^*\, \hat{\Phi} + \text{h.c.}\right) \\
&\quad + \mu\, H_a \left(\hat{\alpha}_0^*\, \hat{\Phi} + \text{h.c.}\right) + \frac{p_T^2 - 4\mu^2\, \left(1+\mu^2\right)\, H_a^2}{2p_L^2}\, |\hat{\chi}|^2 - \frac{1}{2} \left(\hat{B}^*\, \hat{\chi} + \text{h.c.}\right) \\
&\quad - \frac{2\mu\, \left(1+\mu^2\right)\, H_a^2}{p_L^2}\, \left(\hat{\chi}^*\, \hat{\alpha}_0 + \text{h.c.}\right) + \frac{p_L^2}{2p_T^2}\, |\hat{B}|^2 - \mu\, H_a \left(\hat{B}^*\, \hat{\alpha} + \text{h.c.}\right)
\end{aligned}
$$

$$-\frac{p_T^2}{p_L^2}\,\left[p_L^2-\left(3+2\mu^2\right)\,H_a^2\right]\,|\hat{\alpha}|^2+\frac{p_T^2}{p_L^2}\,H_a\,\left(\hat{\alpha}_0^*\,\hat{\alpha}+\text{h.c.}\right)$$
$$+\frac{p^2-2\,\left(1+\mu^2\right)\,H_a^2}{p_L^2}\,|\hat{\alpha}_0|^2\,. \tag{4.51}$$

The computation is conceptually straightforward, although technically involved. The resulting action passes several nontrivial checks. Firstly, the perturbations rearrange so that the action can be written solely in terms of gauge invariant combinations. Secondly, extremizing the action with respect to these modes gives precisely the linearized equations (4.41) - (4.46). Thirdly, the action correctly identifies the nondynamical variables of the system. The nondynamical modes are the modes entering in the action (4.51) without time derivatives. They do not correspond to propagating dynamical degrees of freedom (since the nondynamical modes can be obtained from the dynamical ones by their own equations of motion, that are algebraic - since they enter without time derivatives in the action).

Whether a mode is dynamical or not depends on the initial kinetic terms. For instance, from the field strength $F_{\mu\nu}=\partial_\mu A_\nu-\partial_\nu A_\mu$ we immediately see that the temporal component of the vector field is nondynamical. By direct inspection, we can also verify that the Ricci scalar does not lead to time derivatives for any of the $g_{0\mu}$ entry of the metric (this is most easily seen through the ADM formalism [64]). The gauge choice of [39] ($E=\Sigma=\tilde{B}=E_i=0$) preserves all the $\delta g_{0\mu}$ modes, as well as δA_0 , namely the modes Φ, χ, B, B_i, α_0. These perturbations are the nondynamical fields in that gauge. Therefore, the combinations $\hat{\Phi}$, $\hat{\chi}$, $\hat{B}$, $\hat{B}_i$, $\hat{\alpha}_0$ given in (4.35) and (4.36) are nondynamical (since they are gauge invariant, and since they reduce to the nondynamical modes of the system once the gauge choice of [39] is made). This is explicitly verified by the quadratic action (4.51). We integrate the nondynamical modes out of the action (4.51). Namely, we express them as a function of the dynamical modes by using their own algebraic equations of motion.

To be more explicit, the 2d modes entering in (4.51) can be divided in the two sets of dynamical $Y=\left\{\hat{\Psi},\,\hat{\alpha}\right\}$ and nondynamical $N=\left\{\hat{\Phi},\,\hat{\chi},\,\hat{B},\,\hat{\alpha}_0\right\}$ modes. The action (4.51) is formally of the type

$$S^{(2)}_{YN}\;=\;\int dt\,d^3k\Big[a_{ij}\,\dot{Y}_i^*\,\dot{Y}_j+\left(b_{ij}\,N_i^*\,\dot{Y}_j+\text{h. c.}\right)+c_{ij}\,N_i^*\,N_j+\left(d_{ij}\,\dot{Y}_i^*\,Y_j+\text{h. c.}\right)$$

$$+e_{ij}\,Y_i^*\,Y_j+\left(f_{ij}\,N_i^*\,Y_j+\text{h. c.}\right)\Big] \tag{4.52}$$

where the matrices formed by the a, c, e coefficients are hermitian. The equations of motion for the nondynamical modes are

$$\frac{\delta S_{YN}^{(2)}}{\delta N_i^*}=0 \quad \Rightarrow \quad c_{ij}\,N_j=-b_{ij}\,\dot{Y}_j-f_{ij}\,Y_j\,. \tag{4.53}$$

These equations are precisely Eqs. (4.41), (4.42), (4.43), and (4.45) of the linearized system that we have solved (notice that, indeed, they do not contain any time derivative of the nondynamical modes). We solve them to express the nondynamical modes in terms of the dynamical ones. Inserting these expressions back into (4.52), we obtain the action for the dynamical modes. This action is formally of the type

$$S_Y^{(2)}=\frac{1}{2}\int dt\,d^3k\left[\dot{Y}_i^*\,K_{ij}\,\dot{Y}_j+\left(\dot{Y}_i^*\,X_{ij}\,Y_j+\text{h. c.}\right)-Y_i^*\,\Omega_{ij}^2\,Y_j\right] \tag{4.54}$$

where (up to boundary terms) the matrices K and Ω^2 are hermitian, while X anti-hermitian and they are given by

$$\begin{aligned}
K_{ij}&\equiv a_{ij}-\left(b^\dagger\right)_{ik}\left(c^{-1}\right)_{km}\,b_{mj}\\
X_{ij}&\equiv d_{ij}-\left(b^\dagger\right)_{ik}\left(c^{-1}\right)_{km}\,f_{mj}\\
\Omega_{ij}^2&\equiv -e_{ij}+\left(f^\dagger\right)_{ik}\left(c^{-1}\right)_{km}\,f_{mj}
\end{aligned} \tag{4.55}$$

Extremizing this action we find

$$\begin{aligned}
\frac{\delta S_Y^{(2)}}{\delta Y_i^*}=0 \quad &\Rightarrow \quad K_{ij}\,\ddot{Y}_j+\left(\dot{K}_{ij}+X_{ij}-X_{ji}^*\right)\dot{Y}_j+\left(\dot{X}_{ij}+\Omega_{ij}^2\right)Y_j=0\\
&\Rightarrow \quad \ddot{Y}_i=-\left[K^{-1}\left(\dot{K}+X-X^\dagger\right)\right]_{ij}\dot{Y}_j-\left[K^{-1}\left(\dot{X}+\Omega^2\right)\right]_{ij}Y_j\,.
\end{aligned} \tag{4.56}$$

These two equations are precisely the linearized equations (4.44) and (4.46), after we have inserted in them the expressions for the nondynamical modes.

It is straightforward to obtain the expressions of these matrices from the terms in the action (4.51). However, they are rather involved, and not needed for the present discussion. We list instead the expression for the determinant of the kinetic matrix

$$\det K=\frac{p_T^6\,\left(1+\mu^2\right)^2}{2\,\Delta\,p_L^2\,p^2}\,\left[p_L^2-H_a^2\,\left(1+\mu^2\right)\,\left(2+\mu^2\right)\right]$$

$$\Delta \equiv \left[2\,p^2+\mu^2\,\left(p^2+p_L^2\right)\right]^2 \\ -2H_a^2\,\left(1+\mu^2\right)\,\left(2+\mu^2\right)\,\left[2p_L^2\,(1+\mu^2)^2+p_T^2\,(2+\mu^2)\,(1+2\mu^2)\right] \quad (4.57)$$

One can verify that the determinant starts positive at $p \gg H$, and becomes zero precisely when $p_L = \sqrt{2+\mu^2}\,\sqrt{H_a\,H_b} = \sqrt{2+\mu^2}\,\sqrt{1+\mu^2}\,H_a$. As it is clear from the general form (4.56) of the equations, one expect that the solutions diverge at this moment. This is precisely what we have found by explicitly solving these equations in the previous section.

We also see that the determinant of the kinetic matrix becomes negative after this moment. Therefore, one of the physical modes of the system becomes a ghost. This by itself signals an instability of the ACW vacuum.

We have thus concluded that the ACW background solution is unstable by explicitly solving the linearized equations for the most general set of perturbations and by studying the quadratic action for perturbations. The linearized equations and their solutions diverge close to horizon crossing at some time t_* (this occurs for any mode in the Fourier decomposition; we stress that all the modes are decoupled from each other at the linearized level). The computations presented in this chapter prove by themselves that the background is unstable. It is possible that the divergency does not occur at the full nonlinear level. However, when the nonlinear interactions become important, the solution will be substantially different from the ACW background solution. Therefore, phenomenological predictions based on the ACW background will be unreliable. We have also shown that one of the dynamical variables in the system of perturbations becomes a ghost precisely at t_* when the solutions to the linearized equations diverge. The kinetic term for this mode vanishes at t_* which explain why the corressponding equation of motion, and the solution diverge at this point. We stress that the presence of a ghost indicates on its own an instability of the vacuum. We will dicuss the problems related with the appearence of the ghost in the next chapter.

In a loose sense, the ACW model is "doubly unstable", since the linearized equations for the perturbations diverge - we call this "instability I"- and since it has a ghost - "instability II" (in a generic model either instability may appear without the other one). Motivated by this finding, we investigated whether other models with vector fields play some role during inflation are also unstable. To our knowledge, the first model where

anistropic inflation is due to a vector field is one of Ford [45]. In the next subsection, we will briefly discuss the background and perturbations of this model, and show that it is plauged by a ghost instability.

4.4.1 Ghost instabilities in some other models

This section is devoted to a study of vector field driven models of inflation originally discussed in [45]. The discussions made here are also relevant for models of vector like dark energy models [91], which use a similar construction. We first discuss the background evolution and then the scalar perturbations around the background below.

The model is described by the action

$$S = \int d^4x \sqrt{-g} \left[\frac{M_p^2}{2} R - \frac{1}{4} F_{\mu\nu} F^{\mu\nu} - V(A^2) \right] . \tag{4.58}$$

The field equations are obtained by extremizing the action with respect to the metric tensor and the vector field, which are

$$\begin{aligned} G_{\mu\nu} &= \frac{1}{M_p^2} \left[F_{\mu\alpha} F_\nu{}^\alpha + 2 \frac{\partial V}{\partial A^2} A_\mu A_\nu + g_{\mu\nu} \left(-\frac{1}{4} F^2 - V\left(A^2\right) \right) \right] \\ & \frac{1}{\sqrt{-g}} \partial_\mu \left[\sqrt{-g} F^{\mu\nu} \right] - 2 \frac{\partial V}{\partial A^2} A^\nu = 0 . \end{aligned} \tag{4.59}$$

The metric and the vector field are again assumed to be given as in equation (4.11). Then, the above equations become,

$$\begin{aligned} 3H^2 - 3h^2 &= \frac{V}{M_p^2} + \frac{1}{2} \dot{B}_1^2 + (H - 2h) \, B_1 \dot{B}_1 + \frac{1}{2} \left(H^2 - 4H\,h + 4h^2 \right) B_1^2 \\ 2\dot{H} + 3H^2 + 3h^2 &= \frac{V}{M_p^2} - \frac{2\,B_1^2\,V'}{3M_p^2} - \frac{1}{6} \dot{B}_1^2 - \frac{1}{3} \, (H - 2h) \, B_1 \dot{B}_1 - \frac{1}{6} \, (H - 2h)^2 \, B_1^2 \\ \dot{h} + 3H\,h &= -\frac{2\,B_1^2\,V'}{3M_p^2} + \frac{1}{3} \dot{B}_1^2 + \frac{2}{3} \, (H - 2h) \, B_1 \dot{B}_1 + \frac{1}{3} \, (H - 2h)^2 \, B_1^2 \\ \ddot{B}_1 + 3H \, \dot{B}_1 &+ \left[\frac{2V'}{M_p^2} - 4h^2 - 2H\,h + 2H^2 - 2\dot{h} + \dot{H} \right] B_1 = 0 \end{aligned} \tag{4.60}$$

where two expansion rates H and h are defined as $H = (H_a + 2H_b)/3$ and $h = (H_b - H_a)/3$ and $V' \equiv \partial V / \partial B_1^2$. Namely, H measures the overall volume expansion rate of the universe and h measures the anistropy. A possible solution to the above equations, which

provides a prolonged anisotropic expansion is obtained when the system is stationary. Namely, when $\ddot{B}_1 = \dot{B}_1 = \dot{H} = \dot{h} = 0$. Then, the last of (4.60) requires

$$\frac{V'}{M_p^2} = -H^2 + H\,h + 2h^2 = -H_a\,H_b < 0 \tag{4.61}$$

which will be shown to be related to the appearence of a ghost in the perturbations of the model. It is convenient to define the parameter

$$\gamma \equiv -\frac{V_0'}{V_0} \tag{4.62}$$

where $V_0 \equiv V\left(B_{1,0}^2\right)$ and $B_{1,0}$ is the stationary solution for the vector filed. Then, equations (4.60) are easily solved to give

$$\begin{aligned}
H_0 &= \frac{2-\gamma+\sqrt{4-12\gamma+\gamma^2}}{3\left[2-3\gamma+\sqrt{4-12\gamma+\gamma^2}\right]^{1/2}}\,\frac{\sqrt{V_0}}{M_p} \\
h_0 &= \frac{2-7\gamma+\sqrt{4-12\gamma+\gamma^2}}{6\left[2-3\gamma+\sqrt{4-12\gamma+\gamma^2}\right]^{1/2}}\,\frac{\sqrt{V_0}}{M_p} \\
B_{1,0}^2 &= \frac{2-7\gamma+\sqrt{4-12\gamma+\gamma^2}}{4\gamma} \quad , \quad 0 \leq \gamma \leq \frac{1}{3}\,.
\end{aligned} \tag{4.63}$$

Whether or not these solutions exist depend on the specific potential chosen; indeed, since for any given potential γ is only a function of $B_{1,0}$, the third of (4.63) may or may not be solvable. When the solution exists, we note that the expansion rate of the two isotropic directions is greater then of the anisotropic one, $H_{b0} > H_{a0}$, which can be inferred from (4.63) since $H_{b0} = H_{a0}\,(1 + B_{1,0}^2)$ so $h_0 > 0$. Note that there is also an isotropic solution when $\gamma = 1/3$. Even though the vector field $B_{1,0}$ vanishes in this particular case, the non-vanishing value of V_0' indicates that an additional degree of freedom exists compared to the standard case when the potential is independent of A (due to the lack of the symmetry $A_\mu \to A_\mu + \partial_\mu\lambda$). Therefore, we expect that, if the model is plagued by a ghost instability around the anisotropic background, this would indicate that the isotropic background solution with $\gamma = 1/3$ has the same problems (and vice versa). Therefore, it is actually possible to limit the study to the isotropic limit when $\gamma = 1/3$, however we study here a generic value of γ for the sake of completeness. Besides the solution (4.63), it is also possible that the system admits the standard dS

solution with $\gamma = B_{1,0} = 0$, so that V_0 plays the role of the cosmological constant (unlike the dS solution with $\gamma = 1/3$, this second dS solution is not continuously connected to the family of solutions (4.63), therefore problems encountered for perturbations around the anisotropic background solution will not appear in this case, as expected).

As in the case of the ACW model, the $2d$ vector perturbations are free of instabilities, therefore we do not discuss them here. We study the $2d$ scalar perturbations by inserting the metric and vector field decompositions (4.31) into the action (4.58) and expand it to second order. We observe that, up to a total time derivative, the action can be written solely in terms of the gauge invariant variables introduced in (4.35). The resulting action in Fourier space is given by

$$
\begin{aligned}
S_{2\mathrm{dS}} &= \frac{1}{2}\int d^3k\, dt\, a\, b^2\, \mathcal{L}_{2\mathrm{dS}} \\
\mathcal{L}_{2\mathrm{dS}} &= |\dot{\hat{\alpha}}_1|^2 + \frac{p_T^2}{p_L^2}\,|\dot{\hat{\alpha}}|^2 + \left(\dot{\hat{\alpha}}_1\,\hat{\alpha}_0^* + \mathrm{h.c.}\right) + H_a\,\left(\dot{\hat{\alpha}}_1\,\hat{\alpha}_1^* + \mathrm{h.c.}\right) \\
&\quad + H_a\,B_0\,\left(\dot{\hat{\alpha}}_1\,\hat{\Phi}^* + \mathrm{h.c.}\right) - H_a\,B_0\,\left(\dot{\hat{\alpha}}_1\,\hat{\Psi}^* + \mathrm{h.c.}\right) + \frac{p_T^2}{p_L^2}\,\left(\dot{\hat{\alpha}}\,\hat{\alpha}_0^* + \mathrm{h.c.}\right) \\
&\quad + H_a\,\frac{p_T^2}{p_L^2}\,\left(\dot{\hat{\alpha}}\,\hat{\alpha}^* + \mathrm{h.c}\right) + \left(\dot{\hat{\Psi}}\,\hat{B}^* + \mathrm{h.c.}\right) - 2\left(1+B_0^2\right)\,H_a\,\left(\dot{\hat{\Psi}}\,\hat{\Phi}^* + \mathrm{h.c.}\right) \\
&\quad - H_a\,\left(\dot{\hat{\Psi}}\,\hat{\Psi}^* + \mathrm{h.c.}\right) + \left(\left(3+2B_0^2\right)\,H_a^2 - p_T^2 - 4B_0^2\,\frac{V_0''}{M_p^2}\right)\,|\hat{\alpha}_1|^2 \\
&\quad + p_T^2\,\left(\hat{\alpha}_1\,\hat{\alpha}^* + \mathrm{h.c.}\right) - \left(\left(3+2B_0^2\right)\,H_a^2 - 4B_0^2\,\frac{V_0''}{M_p^2}\right)\,B_0\,\left(\hat{\alpha}_1\,\hat{\Psi}^* + \mathrm{h.c.}\right) \\
&\quad + \frac{p_T^2}{p_L^2}\,\left(\left(3+2B_0^2\right)\,H_a^2 - p_L^2\right)\,|\hat{\alpha}|^2 + \left(\left(2B_0^4 + B_0^2 - 3\right)\,H_a^2 - 4B_0^4\frac{V_0''}{M_p^2}\right)\,|\hat{\Psi}|^2 \\
&\quad - \left(1+2B_0^2\right)\,B_0\,H_a^2\,\left(\hat{\alpha}_1\,\hat{\Phi}^* + \mathrm{h.c.}\right) + H_a\,B_0\,\left(\hat{\alpha}_1\,\hat{B}^* + \mathrm{h.c.}\right) \\
&\quad + H_a\,\left(\hat{\alpha}_1\,\hat{\alpha}_0^* + \mathrm{h.c.}\right) - H_a\,B_0\,\left(\hat{\alpha}\,\hat{B}^* + \mathrm{h.c.}\right) + H_a\,\frac{p_T^2}{p_L^2}\,\left(\hat{\alpha}\,\hat{\alpha}_0^* + \mathrm{h.c.}\right) \\
&\quad + \left(\left(1+2B_0^2\right)\,H_a^2\,B_0^2 - p_T^2\right)\,\left(\hat{\Psi}\,\hat{\Phi}^* + \mathrm{h.c.}\right) - H_a\,B_0^2\,\left(\hat{\Psi}\,\hat{B}^* + \mathrm{h.c.}\right) \\
&\quad - H_a\,B_0\,\left(\hat{\Psi}\,\hat{\alpha}_0^* + \mathrm{h.c.}\right) - \left(6+7B_0^2+2B_0^4\right)\,H_a^2\,|\hat{\Phi}|^2 \\
&\quad + 2\left(1+B_0^2\right)\,H_a\,\left(\hat{\Phi}\,\hat{\chi}^* + \mathrm{h.c.}\right) + \left(2+B_0^2\right)\,H_a\,\left(\hat{\Phi}\,\hat{B}^* + \mathrm{h.c.}\right) \\
&\quad + H_a\,B_0\,\left(\hat{\Phi}\,\hat{\alpha}_0^* + \mathrm{h.c.}\right) + \left(\frac{p_T^2}{2p_L^2} - \frac{2B_0^2\,\left(1+B_0^2\right)\,H_a^2}{p_L^2}\right)\,|\chi|^2
\end{aligned}
$$

$$-\frac{1}{2}\,\left(\hat{\chi}\,\hat{B}^{*}+\text{h.c.}\right)-2\,\frac{H_a^2}{p_L^2}\,B_0\,\left(1+B_0^2\right)\,\left(\hat{\chi}\,\hat{\alpha}_0^{*}+\text{h.c.}\right)$$
$$+\frac{p_L^2}{2p_T^2}\,|\hat{B}|^2+\left(\frac{p^2}{p_L^2}-2\left(1+B_0^2\right)\,\frac{H_a^2}{p_L^2}\right)\,|\hat{\alpha}_0|^2\,. \tag{4.64}$$

In writing the above action, we made use of the background equation $-V_0'/M_p^2 = H_a\,H_b = H_a^2\,(1+B_0^2)$. We see that the modes $\hat{\Phi}$, $\hat{\chi}$, $\hat{B}$ and $\hat{\alpha}_0$ are nondynamical and can be integrated out. The above action can be expanded at early times as described by the method outlined for the ACW model in Appendix A , which gives

$$\begin{aligned} S_{\text{2dS ,early}} &= \frac{1}{2}\int d^3k\,dt\,\left(|\dot{H}_+|^2-p^2\,|H_+|^2\right)+\frac{1}{2}\int d^3k\,dt\,\left(|\dot{\Delta}_+|^2-p^2\,|\Delta_+|^2\right) \\ &\quad -\frac{1}{2}\int d^3k\,dt\,\left[|\dot{\Delta}_-|^2-\left(p^2-2\,\frac{B_0^2\,p_L^2\,V_0''}{\left(1+B_0^2\right)\,H_a^2\,M_p^2}\right)\,|\Delta_-|^2\right] \end{aligned} \tag{4.65}$$

where the canonical modes are defined by,

$$\begin{aligned} \hat{\Psi} &= \frac{1}{\sqrt{a}\,b}\,\frac{\left(2p_L^2+p_T^2\right)\,V_0'/M_p^2-H_a^2\,p_T^2}{\sqrt{2}\,p_T^2\,V_0'/M_p^2}\,H_+ \\ \hat{\alpha}_1 &= \frac{1}{\sqrt{a}\,b}\,\left[-\frac{B_0\,H_a^2}{2\,\sqrt{2}\,V_0'/M_p^2}\,H_+ +\frac{p}{2p_T}\,\Delta_+ +\frac{p_L\,M_p}{\sqrt{2}\,\sqrt{-V_0'}}\,\Delta_-\right] \\ \hat{\alpha} &= \frac{1}{\sqrt{a}\,b}\,\left[\frac{B_0\,H_a^2}{2\,\sqrt{2}\,V_0'/M_p^2}\,H_+ -\frac{p}{2p_T}\,\Delta_+ +\frac{p_L\,M_p}{\sqrt{2}\,\sqrt{-V_0'}}\,\Delta_-\right]\,. \end{aligned} \tag{4.66}$$

Therefore, we see that the mode Δ_- is a ghost, since its kinetic energy is negative. We have checked that the linearized perturbations do not diverge in this case, however the computation is very extensive and proceeds in a manner similar to the case of the ACW model, therefore we only report the result here. Consequently, this model has only type-II instability, unlike the ACW case which has both type-I and type-II.

In the next chapter, we will discuss another class of models, charaterized by the coupling of the vector field to the curvature. We will show that models in this class, that are of cosmological interest also suffer from instabilities. We will also provide a generic discussion for theories which have ghosts and study the possibility whether they can be considered as low energy effective theories. We will show that even such an interpretation of theories with ghosts are not viable, since they prove to have phenomenological problems.

Chapter 5

Models with vector fields non-minimally coupled to the curvature

In this chapter we study vector fields which are coupled nonminimally to curvature during the inflationary epoch. The non-minimal coupling of the vector field enters in the mass term, which is of the form $M_A^2 \sim m^2 - R/6$, where R is the scalar curvature. The non-minimal coupling can provide either a slow-roll phase for the vector field so that it can drive inflationary expansion, or a nearly scale-free spectrum for a vector curvaton. This is achieved if $m^2 < R/6$, and in turn the mass squared term becomes negative. Unlike for scalar fields, where a negative mass squared term leads to tachyonic excitations, for vector fields, when the mass squared term is negative, the longitudinal polarization becomes a ghost. A ghost in the spectrum indicates the instability of the vacuum of the theory, and by itself a problem of quantum theory of fluctuations around the background solution. The formalism we have presented in chapter 2 for determining initial conditions on perturbations, which crucially depends on the definition of a stable adiabatic vacuum, fails when there are ghosts in the spectrum. Therefore, predictions based on models with a ghost in its spectrum are not reliable. Although it is possible to view these models as effective theories below a cut-off scale, we will provide a discussion below to argue that such an intepretation has strict phenomenological limits.

The models we study in this chapter can be divided into two classes, depending on whether the vector fields have a vanishing or non-vanishing vacuum expectations values (vevs). We show that the two classes of models are plagued both by a ghost instability and an instability at the classical level, when one of the perturbations diverge. We do so by studying the quadratic action and linearized equations for the perturbations.

5.1 General discussion of ghost instabilities

In this section, we give a general discussion of vector field models that are plagued by ghost instabilities. We will show, by three different methods, that when the effective mass squared term of a vector field is negative, the longitudinal polarization is a ghost. This signals the instability of the vacuum of the theory and therefore, predictions based on cosmological models with ghost instabilities are unreliable.

Consider a generic model, where the vector field has a vev along the x-direction parameterized as $\langle A_x \rangle = a\, M_p\, B$, where $a(t)$ is the scale factor along the x-direction. Due to the breakage of rotational symmetry by the vector field, the background geometry is assumed to be the Bianchi-I metric given in (4.11), where the scale factor in the $y-z$ plane is $b(t)$ and different from $a(t)$. For the models we are considering, the anisotropy satisfies $h/H = \mathrm{O}(B^2)$, where $H = (H_a + 2H_b)/3$ is the average expansion rate and $h = (H_b - H_a)/3$ is the anisotropic expansion rate. The rescaled vev of the vector field B is assumed to be slowly rolling (for models of interest) and we consider the phenomenologically relevant case of moderate anisotropy, $B < 1$.

Before studying the anisotropic models, consider a massive vector field in an isotropic background ($a = b$)

$$S = \int d^4x\, \sqrt{-g}\, \left[-\frac{1}{4}\, F_{\mu\nu}\, F^{\mu\nu} - \frac{M^2}{2}\, A_\mu\, A^\mu \right] \tag{5.1}$$

We assume that A_μ has vanishing vev, and we decompose its fluctiations as

$$A_\mu = \left(\alpha_0,\, \partial_i\, \alpha + \alpha_i^T \right) . \tag{5.2}$$

Using this decomposition, the action (5.1) in conformal time separates into two decoupled pieces,

$$S \;=\; \int d\eta d^3x \Bigg\{ \frac{1}{2} \left[\alpha_i'^2 - (\partial_i \alpha_j)^2 - M^2 \alpha_i^2 \right] + \frac{1}{2} \Bigg[\left(\partial_i \alpha' \right)^2 - 2 \partial_i \alpha' \partial_i \alpha_0$$

$$
\begin{aligned}
& -M^2\,(\partial_i\alpha)^2 + (\partial_i\alpha_0)^2 + M^2\,\alpha_0\Big]\Big\} \\
= \int d\eta d^3k \Big\{ & \frac{1}{2}\left[|\alpha_i'|^2 - \left(\vec{k}^2 + M^2\right)|\alpha_i|^2\right] \\
& + \frac{1}{2}\left[\vec{k}^2|\alpha'|^2 - \vec{k}^2\left(\alpha'^*\,\alpha_0 + \text{h.c.}\right) - M^2\,\vec{k}^2|\alpha|^2 + \left(\vec{k}^2 + M^2\right)|\alpha_0|^2\right]\Big\}
\end{aligned}
\tag{5.3}
$$

where the prime denotes the derivative with respect to conformal time, and in the final expression we have Fourier transformed the modes as in (4.16). The first decoupled part governs the two transverse polarizations, which are well behaved. The second part contains only one physical mode, since α_0 enters without time derivatives and must be integrated out. The equation of motion for this field obtained from (5.3) is

$$
\alpha_0 = \frac{\vec{k}^2}{\vec{k}^2 + M^2}\,\alpha' \,. \tag{5.4}
$$

Inserting this back into the second part of (5.3), we obtain

$$
S_{\text{longitudinal}} = \int d\eta\, d^3k\, \frac{\vec{k}^2\,M^2}{2}\left[\frac{|\alpha'|^2}{\vec{k}^2 + M^2} - |\alpha|^2\right] . \tag{5.5}
$$

The longitudinal vector mode exists due to the mass term, so it is not a surprise that M^2 multiplies the kinetic term. We see that this mode is a ghost when $M^2 < 0$. The ghost disappears in the limit when $M^2 \to 0$, since in this case the action is $U(1)$ invariant, and the vector has only the 2 transverse degrees of freedom.

Another possible way to see that the negative mass squared term leads to a ghost instability is to compute the propogator. For simplicity, consider for example, the action (5.1) in a pure de-Sitter spacetime which is given by

$$
S = \int d\eta\, d^3x\, \left[-\frac{1}{4}\,F_{\mu\nu}\,F^{\mu\nu} - \frac{1}{2}\,M^2\,A_\mu\,A^\mu\right] \tag{5.6}
$$

where $M^2 = -2\,a^2\,H^2$. The quadratic Lagrangian in (5.6) can be cast in the form $(1/2)\,A^\mu\,P^{-1}_{\mu\nu}\,A^\nu$, where

$$
P_{\mu\nu} = -\frac{\eta_{\mu\nu} - k_\mu\,k_\nu/M^2}{k^2 + M^2} \tag{5.7}
$$

where $k^2 \equiv k_\mu\, k^\mu$ and $P_{\mu\nu}$ is the propogator. In general, the propogator needs to be diagonalized. However, we can choose a frame in which it is diagonal (clearly, the number and nature of physical modes do not depend on the frame). For a positive M^2, the pole is at $k^2 = -M^2 < 0$, and we can go in the rest frame, where $k^\mu = -k_\mu = (M,\, 0,\, 0,\, 0)$. In this case, $-(\eta_{\mu\nu} + k_\mu\, k_\nu/M^2) = \mathrm{diag}(0,\, -1,\, -1,\, -1)$, indicating that the theory has three well-behaved particles (-1 indicates a well-behaved mode due to signature; cf. the propogator for a scalar particle). For $M^2 < 0$, we cannot go in the rest frame; however, we can choose a frame where the energy vanishes, $k^\mu = k_\mu = (0,\, 0,\, 0,\, M)$. In this case, $-\left(\eta_{\mu\nu} + k_\mu k_\nu/M^2\right) = \mathrm{diag}\,(1,\, -1,\, -1,\, 0)$, indicating that one mode (the longitudinal vector) is a ghost.

The ghost also appears in the Stuckelberg formalism. For simplicity, here M is treated a constant (the time dependence of M does not modify the quadratic kinetic term, but it complicates the diagonalization). If we redefine

$$A_\mu = B_\mu + \frac{1}{M}\partial_\mu \phi \tag{5.8}$$

we promote the action (5.6) to a gauge invariant action, with the symmetry

$$\phi \to \phi + \xi \quad , \quad B_\mu \to B_\mu - \frac{1}{M}\partial_\mu \phi \tag{5.9}$$

The action (5.6) is recovered in the unitary gauge, $\phi = 0$. But one can also choose a gauge in which B_μ is transverse, $\partial^\mu B_\mu = 0$. In this gauge, the action of the system is

$$S = \int d\eta\, d^3x \left[-\frac{1}{4}F\,(B)^2 - \frac{M^2}{2}\,B^2 \mp \frac{1}{2}\,(\partial\phi)^2\right] \tag{5.10}$$

where the field strength $F_{\mu\nu}$ does not contain ϕ, and where the kinetic term of ϕ has opposite sign to M^2. We stress that the two actions (5.6) and (5.10) describe the same theory in two different gauges. We again see that the longitudinal component ϕ is a normal field for $M^2 > 0$, and a ghost for $M^2 < 0$.

Let us return back to the models with anistropic background solutions. The two models [45] and [11] can be studied together, using the generic action

$$S = \int d^4x\, \sqrt{-g}\, \left[\frac{M_p^2}{2}\,R - \frac{1}{4}\,F_{\mu\nu}\,F^{\mu\nu} - V\left(A^2\right) + \frac{\xi}{2}\,R\,A^2\right] \tag{5.11}$$

Expanding the potential at quadratic order in A_μ, and comparing with equation (5.1), this action leads to the mass term

$$M^2 = 2\,\frac{\partial V}{\partial A^2} - \xi\,R = 2\,\frac{\partial V}{\partial A^2} - 6\,\xi\,\left(2H^2 + h^2 + \dot{H}\right)\,. \tag{5.12}$$

The equations of motion for the rescaled vev B obtained from (5.11) is

$$\begin{aligned} &\ddot{B} + 3\,H\,\dot{B} + \mathcal{Q}\,B = 0 \\ &\mathcal{Q} \equiv 2\,\frac{\partial V}{\partial A^2} - 2\,H\,h - 5\,h^2 - 2\,\dot{h} + (1-6\,\xi)\,\left(2\,H^2 + h^2 + \dot{H}\right) \end{aligned} \tag{5.13}$$

Slow roll of B requires $\mathcal{Q} \ll H^2$ (since $3\,H\,\dot{B}$ term provides a "friction" to the motion). This is achieved in two different ways by [45] and [11]. In the model of reference [45], which we have studied in section (4.4.1), solutions with constant $H_{a,b}$ in absence of the $A^2\,R$ term, $\xi = 0$ were considered. This requires $\mathcal{Q} = 0$, or, in other terms

$$\frac{\partial V}{\partial A^2} = -H^2 + H\,h + 2h^2 = -H_a\,H_b < 0\,. \tag{5.14}$$

This leads to a negative mass squared term in equation (5.12). From our previous discussion of the action (5.1), we immediately see that the longitudinal vector polarization is a ghost in the limit of isotropic background ($B = 0$). When the vev B is not neglected, the background becomes anisotropic. We have studied the perturbations of this complete case in section (4.4.1), taking into account metric perturbations, and verified that the ghost also exists in this case.

In reference [11], the choice $\xi = 1/6$ is made, so that (following the idea of [8]) the $\mathrm{O}(H^2)$ contribution is absent from $\mathcal{Q}$. Then, slow roll is achieved in the case of small anisotropy, $B \ll 1$, and for $\partial V/\partial A^2 \ll H^2$. We then see that the square mass parameter (5.12) is negative in this limit, indicating that the longitudinal vector polarization is a ghost in the isotropic limit in this case too. A more detailed study in the following sections, including also the metric perturbations, shows that the ghost instability persists also for moderate anisotropy.

5.2 Review of some models with a $R\,A^2$ term

In this Section, we briefly review the reasons for introducing a nonminimal coupling of a vector field to the curvature. We start from the quadratic action of a vector field with

a generic time-dependent mass:

$$S = \int d^4x\sqrt{-g}\left[-\frac{1}{4}F_{\mu\nu}\,F^{\mu\nu} - \frac{1}{2}\,M\,(t)^2\,A_\mu\,A^\mu\right] \tag{5.15}$$

leading the equations of motion

$$\frac{1}{\sqrt{-g}}\,\partial_\nu\left(\sqrt{-g}\,F^{\mu\nu}\right) + M^2\,A^\mu = 0\,. \tag{5.16}$$

Moreover, due to its antisymmetry, the field strength $F_{\mu\nu}$ satisfies the identity

$$\partial_\mu\,F_{\rho\nu} + \partial_\nu\,F_{\mu\rho} + \partial_\rho\,F_{\nu\mu} = 0\,. \tag{5.17}$$

Turner and Widrow [55] suggested a mechanism for the generation of primordial magnetic fields during inflation, starting from the action (5.15). [1] In this mechanism, the vector field A_μ is the electromagnetic field, and the mass term is proportional to the scalar curvature R. Following [55], we use conformal time η, defined by the line element $ds^2 = a^2\,(\eta)\left(-d\eta^2 + d\vec{x}^2\right)$ in the present discussion, so that the electric and magnetic fields are ($\epsilon_{123} = +1$)

$$F_{i0} = a^2\,E_i \quad , \quad F_{ij} = a^2\,\epsilon_{ijk}\,B_k\,. \tag{5.18}$$

The two equations (5.16) and (5.17) can be easily combined into an equation for the magnetic field [55]:

$$\left(\partial_\eta^2 - \partial_{\vec{x}}^2 + a^2\,M^2\right)\left(a^2\vec{B}\right) = 0\,. \tag{5.19}$$

From this equation, we find the well known result that, in the massless case ($M^2 = 0$), and in the large wavelength limit (i.e. negligible spatial gradient) , the amplitude of a magnetic field decreases as $\propto a^{-2}$. Correspondingly, its energy density decreases as $\propto a^{-4}$. Consider instead the mass term [55]

$$M^2 = \xi\,R = 6\,\xi\,\frac{a''}{a^3} \tag{5.20}$$

where ξ is a constant, and prime denotes derivative wrt η. The equation of motion for the magnetic field then becomes

$$\left(\partial_\eta^2 - \partial_{\vec{x}}^2 + 6\,\xi\,\frac{a''}{a}\right)\left(a^2\vec{B}\right) = 0\,. \tag{5.21}$$

[1] More precisely, ref. [55] studied a more general action with a quadratic term of the type $R_{\mu\nu}A^\mu A^\nu$ also included; we disregard this term in the present work.

During inflation, $a = -1/(H\,\eta)$ where the Hubble rate H is nearly constant; inserting this into the equation of motion (and treating H as constant), we find that, in the large wavelength regime, the energy density of the magnetic field behaves as

$$\rho_B \propto \vec{B}^2 \propto a^{-5+\sqrt{1-48\,\xi}}\,. \tag{5.22}$$

Therefore, for $\xi < 0$ - corresponding to a negative M^2 in the action (5.15) - ρ_B is less affected by the expansion with respect to the massless case.

It is instructive to compare the behavior of the magnetic field with respect to that of a massless scalar field coupled to the curvature, characterized by the action

$$S = \int d^4x\,\sqrt{-g}\left[-\frac{1}{2}\partial_\mu\phi\partial^\mu\phi - \frac{1}{2}\,\xi_s\,R\,\phi^2\right] \tag{5.23}$$

This leads to the equation of motion

$$\left(\partial_\eta^2 - \partial_{\vec{x}}^2 + (6\xi_s - 1)\,\frac{a''}{a}\right)(a\,\phi) = 0\,. \tag{5.24}$$

By comparing this equation with the analogous expression for the vector field [2] , it has been noted [55] that a vector field with $\xi = -1/6$ behaves analogously to a scalar field minimally coupled to the curvature ($\xi_s = 0$). Conversely, the standard vector field $\xi = 0$ is analogous to a conformally coupled scalar, $\xi_s = 1/6$ (therefore, no magnetic field is produced by the inflationary expansion in the standard case).

This analogy has been recently exploited in [8], that proposed a mechanism of inflation driven by a combination of N nonminimally coupled vector fields. The mass term of the vectors comprises of the coupling to the curvature plus a constant term:

$$S = \int d^4x\,\sqrt{-g}\,\sum_{a=1}^{N}\left[-\frac{1}{4}\,F^{(a)}_{\mu\nu}\,F^{(a)\,\mu\nu} - \frac{1}{2}\,\left(\xi\,R + m^2\right)\,A^{(a)}_\mu\,A^{(a)\mu}\right]\,. \tag{5.25}$$

The simplest case, and the one which has been most studied in [8], is characterized by three mutually orthogonal vectors with equal vev:

$$\langle A^{(1)}_\mu\rangle = (0,\,\mathcal{A},\,0,\,0) \quad,\quad \langle A^{(2)}_\mu\rangle = (0,\,0,\,\mathcal{A},\,0) \quad,\quad \langle A^{(3)}_\mu\rangle = (0,\,0,\,0,\,\mathcal{A}) \quad,$$
$$\mathcal{A} \equiv M_p\,a\,(t)\;B\,(t)\;. \tag{5.26}$$

[2] It is appropriate to compare the behavior of $a^2\vec{B}$ with that of $a\,\phi$, since, due to the different structures of the kinetic terms, these are the canonically normalized fields in the two cases.

These sources allow for a FRW background, controlled by the equations of motion (we switch to physical time, and we denote by a dot derivative with respect to it)

$$H^2 - \frac{\dot{B}^2}{2} - \frac{1}{2}\, m^2\, B^2 = \frac{1+6\,\xi}{2}\, H\, B\, \left(2\,\dot{B} + H\, B\right)$$
$$\ddot{B} + 3\, H\, \dot{B} + m^2\, B = -\,(1+6\,\xi)\, B\, \left(\dot{H} + 2\, H^2\right)\,. \tag{5.27}$$

For $\xi = -1/6$, and upon the identification $B = \phi/\left(\sqrt{3} M_p\right)$, we recover the same equations as those of chaotic inflation driven by a minimally coupled scalar field ϕ.

Another compelling feature of the proposal of [8] is that it can naturally give a small violation of isotropy. Indeed, for a large number N of vectors with random orientations and vev, one expects an almost isotropic expansion, with a deviation $\Delta H/H = \mathrm{O}\left(1/\sqrt{N}\right)$ between the expansion rates of the different directions. Ref. [11] provides a slightly different mechanism in which a single nonminimally couple vector breaks the isotropy in one spatial direction, while a scalar field with greater energy density is responsible for the overall nearly isotropic expansion.

Vector fields with nonminimal coupling to the curvature have also been recently employed for the generation of a nearly scale invariant spectrum of perturbations [13]. Consider the action (5.25) for a single field ($N = 1$) and with $\xi = 1/6$. Following the discussion of [13], we compute the evolution of the perturbations δA_μ assuming that the vev $\langle A_\mu \rangle$ can be neglected . In this way, the perturbations of the vector do not mix with those of the metric at the linearized level. Moreover, with a negligible vector vev, we can study the evolution of δA_μ in an unperturbed FRW background. In the present discussion, we only consider the transverse components of the perturbations, $\delta A_\mu = \left(0,\, \delta \vec{A}^T\right)$, with $\partial_i\, \delta A_i^T = 0$, since, as we will show in the following Section, there are serious problems with the longitudinal mode in these models. Due to the $\xi = -1/6$ choice, the equation for this mode is identical to that of a minimally coupled curvaton scalar field:

$$\left[\partial_\eta^2 - \partial_{\vec{x}}^2 + a^2\, \left(m^2 - \frac{a''}{a^3}\right)\right]\, \delta A_i^T = 0\,. \tag{5.28}$$

We proceed as in the scalar curvaton case. For simplicity, we assume a dS background; in momentum space, the Fourier transform of δA_i^T (denoted by $\delta \tilde{A}_i^T$) obeys to the equation

$$\left(\partial_\eta^2 + k^2 - \frac{2\,\mu^2}{\eta^2}\right)\, \delta \tilde{A}_i^T = 0 \quad , \quad \mu^2 \equiv 1 - \frac{m^2}{2H^2}\,. \tag{5.29}$$

As we have done in chaper 2, among the two solutions of this equation, we chose the one that reduces to the adiabatic vacuum at early times, when the mode is deeply inside the horizon:

$$\delta\tilde{A}_i^T = \frac{\sqrt{\pi}}{2}\,\sqrt{|\eta|}\,H^{(1)}_{\frac{1}{2}\sqrt{1+8\mu^2}}\left(|k\,\eta|\right) \tag{5.30}$$

where $H^{(1)}$ is the Hankel function of the first kind. Indeed, up to an irrelevant phase, this solution reduces to $\mathrm{e}^{-ik\eta}/\sqrt{2k}$ for $|k\eta| \gg 1$. In the opposite late time / super horizon regime ($|k\eta| \ll 1$), from the asymptotic expansion of the Hankel function, we then find the power spectrum for the transverse modes [13]

$$P_{Ti} \propto k^3\,|\delta\tilde{A}_i^T|^2 \propto k^{3-\sqrt{1+8\,\mu^2}} = k^{\frac{2m^2}{3H^2}+\mathrm{O}\left(\frac{m^4}{H^4}\right)}\,. \tag{5.31}$$

Namely, $m \ll H$ provides a small departure from scale invariance. We remark that this result follows from the solution (5.30). Indeed, eq. (5.29) has two solutions with two undetermined (and, in principle, $k-$dependent) integration constants. As it is customary, we chose the linear combinations of these solutions which reduces to the adiabatic vacuum in the early time sub-horizon regime. The phenomenological prediction (5.31) crucially relies on the fact that the theory must be under control in this regime.

For all the models we have reviewed, the discussion presented in this Section disregards the role of the longitudinal polarization of the vector field(s). In the next Sections we show that, for all the models discussed, this mode turns out to be a ghost.

5.3 Identification of ghosts, and their associated instability

In the next two Sections, we will see that the models described in the previous Section have ghosts. We outline here the method we employ to find the ghosts, and the instability associated with them. The ghosts are among the physical excitations of the background geometries of the various models. Therefore, we need to compute the spectrum of these theories. To do so, we perturb the background solutions of a given model, and we expand the action at quadratic order in the perturbations, as we have done for the ACW model in the previous chapter. This is the free action for the perturbations (interaction among these fields come from expanding the initial action to higher

orders), and the spectrum follows from the diagonalization of this action. Moreover, extremizing this action with respect to the perturbations, we obtain the linearized Einstein equations as described in equations (4.56) in the previous chapter. We study two classes of models, the first one for which $\langle A_\mu \rangle = 0$ relevant for the vector curvaton and inflationary magnetic fields and the second one $\langle A_\mu \rangle \neq 0$ relevant for the case of vector inflation.

5.4 Ghost instability for $\langle A_\mu \rangle = 0$

We start our analysis from the case in which the vector field has no vev. This is the case for the computations presented in [55, 13] to study the evolution of the modes. On a technical level, the assumption of zero vev drastically simplifies the computation. Indeed, the actions we are studying (cf. eqs. (5.15) and (5.25)), are quadratic in the vectors; therefore, for $\langle A_\mu \rangle = 0$, the perturbations of the vector(s) are decoupled from those of any other field at the linearized level. [3] Therefore, the action for the vector field already starts at quadratic order in the perturbations, and we can simply study the evolution of δA_μ in an unperturbed FRW background. The more involved case of $\langle A_\mu \rangle \neq 0$ is studied in the following Section.

Consider the action

$$S = \int d^4x\sqrt{-g}\left[-\frac{1}{4}F_{\mu\nu}\,F^{\mu\nu} - \frac{1}{2}\,M^2\,A_\mu\,A^\mu\right] \quad , \quad M^2 = -\frac{R}{6} + m^2 \tag{5.32}$$

in the FRW background, $ds^2 = -dt^2 + a\,(t)^2\,d\vec{x}^2$. We parametrize the fluctuations of the vector field as in equation (4.15). As was the case for the ACW model, the transverse polarizations α_i^T are well behaved in all regimes, so we only study here the nature and evolution of the longitudinal mode and the temporal component.

It is well known that a massive vector has three physical degrees of freedom. The two transverse ones are encoded in α_i^T. Therefore, the two perturbations α_0 and α encode only one physical mode, which is the longitudinal polarization of the massive vector. This can be immediately seen from the equations of motion for the two perturbations

[3] In the mechanism of [55], the full action in not quadratic in A_μ, since the photon is obviously coupled to the current of charged fields. This coupling is important from reheating on, when the conductivity of the charged particles become high, and affects the evolution of the magnetic field. However, the presence of these fields can be disregarded during the inflationary stage, as done in [55].

following from (5.32), which, in Fourier space, read [4]

$$\alpha_0 = \frac{p^2}{p^2 + M^2}\dot{\alpha} \tag{5.33}$$

$$\ddot{\alpha} + \frac{\left(3p^2 + M^2\right) H + p^2 \frac{\frac{d\,M^2}{dt}}{M^2}}{p^2 + M^2}\dot{\alpha} + \left(p^2 + M^2\right)\alpha = 0 \tag{5.34}$$

where $p = k/a$ is the physical momentum of the perturbation, and, as usual, $H = \dot{a}/a$. While equation (5.34) is a second order differential equation, equation (5.33) is an algebraic equation in α_0. Therefore, α_0 does not introduce additional degrees of freedom, but it is completely determined once α is known (compare these equations with the formal set of equations (4.53) and (4.56)). This was also the case for the simplified calculation we have performed for the ACW model in the previous chapter.

We can also see this from the quadratic action for the perturbations. Inserting the decomposition $A_\mu = (\alpha_0,\, \partial_i\,\alpha)$ in (5.32), and Fourier transforming the spatial coordinates, we find

$$S = \frac{1}{2}\int dt\, d^3k\, \left[p^2|\dot{\alpha}|^2 - p^2M^2|\alpha|^2 - p^2\left(\alpha_0^*\,\dot{\alpha} + \text{h. c.}\right) + \left(p^2 + M^2\right)|\alpha_0|^2\right]\,. \tag{5.35}$$

The mode α_0 enters in the action without time derivatives, confirming that it is a nondynamical mode. We integrate it out: we compute its equation of motion from this action (namely, eq. (5.34) given above), we solve it, and we insert the solution back into (5.35). This leads to the action for the longitudinal mode: [5]

$$S = \frac{1}{2}\int dt\, d^3k\, p^2\, M^2\left(\frac{|\dot{\alpha}|^2}{p^2 + M^2} - |\alpha|^2\right)\,. \tag{5.36}$$

The extremization of this action reproduces the equation of motion (5.34). [6] We remark that the lagrangian in (5.36) is proportional to the M^2 term, and that, for $p^2 > |M^2|$, the longitudinal mode is a ghost (i.e. a field with negative energy, not simply a tachyon) whenever $M^2 < 0$ [52, 53].

[4] The first equation is $\delta S/\delta A_0$; the second equation has been obtained by combining $\delta S/\delta A_0$ and $\delta S/\delta A_i$.

[5] We remark that, in going from the action (5.35) to the action (5.36), we are precisely following the general procedure that we outlined at a formal level in the previous Section.

[6] This equation, in conformal time, was already given in [13]; this confirms our algebra. The action for the longitudinal mode could be also written starting from this equation, up to an overall factor. The procedure described here provides the complete action. We also note that the Ref. [13] did not solved the equation at the moment in which the total mass of the vector vanishes; as we show here, the solution diverges at this moment.

The presence of a ghost signals the instability of the vacuum of the model, due to its (UV-divergent) decay in ghost-nonghost excitations. In addition, the equation of motion (5.34) indicates that the system may be unstable already at the linearized level, whenever $\omega^2 \equiv p^2 + M^2$ or M^2 vanish. Let us first discuss when this occurs. During inflation, $m^2 \ll R$ for the models we are studying. As a consequence, during inflation, $M^2 = m^2 - R/6 \simeq -2H^2 < 0$, while $\omega^2 = p^2 + M^2 \simeq p^2 - 2H^2$ goes from positive to negative. We denote by $t_{\omega 1}$ the moment at which ω^2 vanishes; we note that this happens when the mode is close to horizon crossing, and that ω^2 remains negative from $t_{\omega 1}$ until a time well after the end of inflation (since the mode is well outside the horizon, $p \ll H$, when inflation ends). After inflation, $R/6 = \mathrm{O}\left(H^2\right)$ decreases as the universe expands, and it eventually drops below m^2. At this moment, which we denote by t_M, the mass term M^2 goes from negative to positive. Therefore, $\omega^2 = p^2 + M^2 > 0$ for all times $t \geq t_M$. Since we saw that $\omega^2 < 0$ at the end of inflation, there is a moment after the end of inflation, and before t_M, at which ω^2 vanishes for the second time. We denote this moment by $t_{\omega 2}$. In summary, M^2 vanishes at $t = t_M$, while ω^2 vanishes at $t = t_{\omega 1}, t_{\omega 2}$. Denoting by t_{end} the moment at which inflation finishes, and by t_0 the present time, we have $t_{\omega 1} < t_{\mathrm{end}} < t_{\omega 2} < t_M < t_0$. [7]

To see whether the linearized system diverges when either ω^2 or M^2 vanish, we study the equation of motion (5.34) for a finite interval of time close to $t_{\omega i}$ $(i = 1, 2)$ or t_M. We assume that the equation of state w of the source driving the expansion can be treated as constant in this interval (which is certainly true, provided the interval is not too extended). We also assume that $-1 < w < 1/3$. This is a rather general assumption, since it includes the following cases: inflation (with $w \gtrsim -1$), coherent oscillations of the inflaton after inflation (which, for a quadratic inflaton potential, give an average $w = 0$), matter domination (if m^2 is sufficiently small, so that M^2 vanishes at this stage), and also radiation domination (for which the equation of state is slightly smaller than 1/3, due to the masses of the particles in the thermal bath).

We summarize the results for the two cases as:

Behavior of the linearized system for $p^2 + M^2 \to 0$. The scale factor evolves

[7] One may imagine that m is so small, so that t_M has not occurred yet. In this case the longitudinal polarization is still a ghost today; we disregard this possibility, due to the stringent limits on theories with ghosts found by [97].

as

$$a = a_{\omega i} \left(\frac{t}{t_{\omega i}} \right)^{\frac{2}{3(1+w)}} \tag{5.37}$$

were we recall that $t_{\omega i}$ is either of the times at which $\omega^2 = 0$, and $a_{\omega i}$ is the value of the scale factor at that time. The mass and frequency squared are given by

$$M^2 = m^2 - \frac{R}{6} = m^2 - \frac{2}{9\,t^2} \frac{1-3w}{(1+w)^2} \tag{5.38}$$

$$\omega^2 = p^2 + M^2 = p_{\omega i}^2 \left(\frac{t_{\omega i}}{t} \right)^{\frac{4}{3(1+w)}} + m^2 - \frac{2}{9\,t^2} \frac{1-3w}{(1+w)^2} \tag{5.39}$$

where $p_{\omega i}$ is the value of the physical momentum at $t_{\omega i}$. We then find

$$\omega\left(t_{\omega i}\right) = 0 \quad \Rightarrow \quad t_{\omega i} = \frac{\sqrt{2}\,\sqrt{1-3\,w}}{3\,\sqrt{m^2 + p_{\omega i}^2}\,(1+w)} \tag{5.40}$$

We insert these expression for the momentum and the total mass in eq. (5.34), and we Taylor expand the resulting expression for $t \simeq t_{\omega i}$. We find:

$$\ddot{\alpha} - \frac{\dot{\alpha}}{t - t_{\omega i}} + C\,\left(t - t_{\omega i}\right)\,\alpha \approx 0 \tag{5.41}$$

where

$$C = \sqrt{\frac{2\left(m^2 + p_{\omega i}^2\right)}{1-3w}}\,\left[3m^2\,(1+w) + p_{\omega i}^2\,(1+3\,w)\right] \tag{5.42}$$

Eq. (5.41) is solved by

$$\alpha \approx C_1\,Ai'\left[(-C)^{1/3}\,(t - t_{\omega i})\right] + C_2\,Bi'\left[(-C)^{1/3}\,(t - t_{\omega i})\right] \tag{5.43}$$

where $C_{1,2}$ are two integration constants, and Ai' and Bi' the derivatives of the Airy functions Ai and Bi, respectively. These two solutions are regular at $t = t_{\omega i}$, where they have the expansion series Ai', $Bi' = \text{const.} + \mathrm{O}\left(t - t_{\omega i}\right)^2$. Since the linearized term is absent, we find that $\alpha_0 \propto \dot{\alpha}/\left(t - t_{\omega i}\right)$ also remains finite as $t = t_{\omega i}$.

Behavior of the linearized system for $M^2 \to 0$. The scale factor evolves as

$$a = a_M \left(\frac{t}{t_M} \right)^{\frac{2}{3(1+w)}} \tag{5.44}$$

were we recall that t_M is the times at which $M^2 = 0$, given by

$$t_M = \frac{\sqrt{2}}{3\,m}\,\frac{\sqrt{1-3w}}{1+w} \tag{5.45}$$

(cf. equation (5.38)), and a_M is the value of the scale factor at t_M. We Taylor expand eq. (5.34) for $t \simeq t_M$:

$$\ddot{\alpha} + \frac{\dot{\alpha}}{t - t_M} + p_M^2\,\alpha \approx 0 \tag{5.46}$$

where p_M is the value of the physical momentum of the mode at t_M . This equation is integrated to give

$$\alpha \approx C_1\,J_0\left(p_M\,(t_M - t)\right) + C_2\,Y_0\left(p_M\,(t_M - t)\right) \tag{5.47}$$

where J_0, Y_0 are, respectively, the Bessel functions of the first and second kinds of order 0, and $C_{1,2}$ are integration constants. While the J_0 solution is regular at $t = t_M$, the Y_0 solution has a logarithmic divergence. Correspondingly, the mode α_0 exhibits a linear divergence, as can be seen from equation (5.33).

The only way to avoid the singularity is to arrange the initial conditions so that $C_2 = 0$. This must be done for every mode (namely, for any comoving momentum k) and for both the real and imaginary parts of the perturbations. We regard this as a completely unnatural assumption, since there is no reason why the initial conditions (set during inflation) should "know" about the singularity which is to occur later on when M^2 vanishes.

In conclusion, the solutions of the linearized system remain finite when $\omega^2 = p^2 + M^2 = 0$, while they diverge when $M^2 = 0$. To verify this behavior, we performed a numerical evolution of equations (5.34) for the specific case of $w = 0$, $p_M = 2$. We then have $t_{\omega 2} \simeq 0.058/m$ and $t_M \simeq 0.47/m$. We set the initial conditions $\alpha = 1$, $\dot{\alpha} = 0$ at $t_M/100$. [8] We plot in Figure 5.1 the resulting evolution of α and α_0. We see that the system is regular at $t_{\omega 2}$, while it diverges at t_M (we verified that α_0 diverges linearly, and, correspondingly, α diverges logarithmically).

It is worth noting that the solutions diverge when the kinetic term of the longitudinal mode vanishes, cf. equation (5.36). On the basis of what we wrote at the end of the

[8] The parameters of the evolution have no particular relevance, and have been chosen only for illustrative purposes. We have verified that other choices of parameters also confirm the behavior we have obtained analytically.

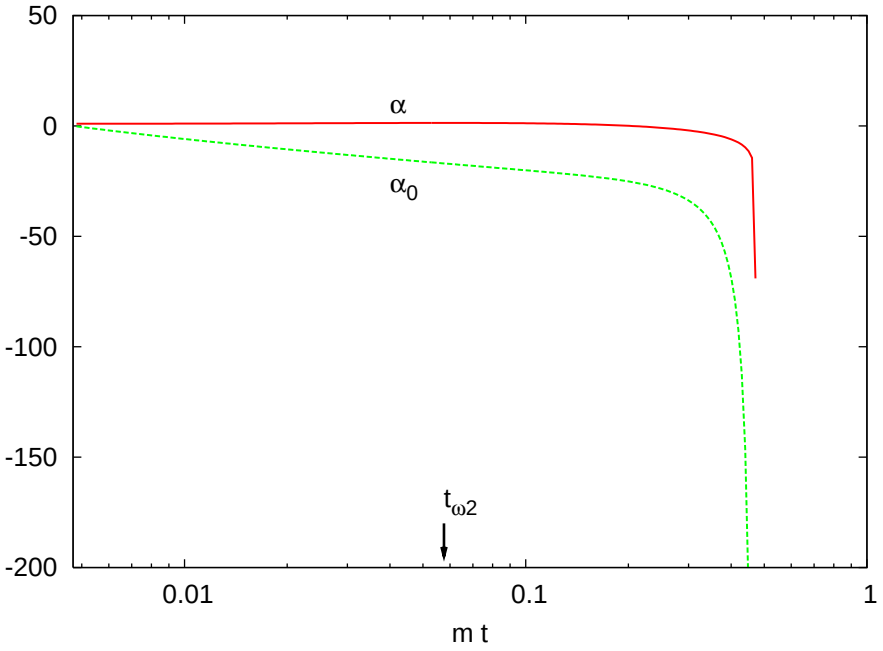

Figure 5.1: Behavior of the linearized solutions representing the longitudinal mode. The system remains finite at the point $t_{\omega i}$, when the frequency vanishes, but it diverges at t_M, when the mass term M^2 of the vector vanishes. See the main text for the parameters chosen.

previous Section, one should expect that this happens also for the cases in which the vector field(s) has a nonvanishing expectation value. We verify this explicitly in Section 5.5.1, for the simplest possible case of a vector field and a cosmological constant.

5.5 Ghost instability for $\langle A_\mu \rangle \neq 0$

As we mentioned, when the vector field(s) has a vev, its perturbations mix with those of the metric already at the linearized level. The computation then becomes significantly harder than that discussed in the previous Section for the case of vanishing vev. Besides the increased number of perturbations, the spatial vev of the vector(s) breaks the isotropy of the background, so that, in general, one needs to study the cosmological perturbations of a non FRW space.

We start by studying the case of a single vector field with a vev along one spatial

direction. The background has a 2d isotropy in the other two directions. We study the perturbations of the background by the formalism introduced in the previous chapter in subsection 4.3.1. We verified that one subset of perturbations, which includes the transverse vector modes, is well behaved, and, for brevity, we disregard it in the following discussions. The other subset, which we discuss in details, includes the longitudinal polarization of the vector.

In Subsection 5.5.1 we apply this formalism to the simplest case of a single vector field plus a cosmological constant. In Subsection 5.5.2 we study the case in which the cosmological constant is replaced by a scalar inflaton, which is the model proposed in [11]. Finally, in Subsection 5.5.3 we study the model of vector inflation [8] (for which the formalism of Subsection 4.3.1 does not apply; for this reason, this Subsection is a self-contained study).

5.5.1 One vector plus a cosmological constant

We study the simplest model in which a nonminimally coupled vector field with a spatial vev provides an anisotropic expansion. Besides the vector field, there is a vacuum energy V_0 which is responsible for an overall accelerated expansion. The Subsection is divided into three parts. We first present the model, and discuss the background evolution. We then solve the linearized system of equations for the perturbations, and find that it diverges at some point close to horizon crossing. We finally compute the kinetic term K of the quadratic action of the perturbations, and show (i) that the divergence of the linearized system takes place precisely when one eigenvalue of K vanishes, and (ii) that one of the perturbations is a ghost for some moment of time.

The model and the background solution

The action of the model

$$S = \int d^4x \left[-\frac{1}{4} F_{\mu\nu} F^{\mu\nu} - V_0 - \frac{1}{2} \left(m^2 - \frac{R}{6} \right) A_\mu A^\mu \right] \tag{5.48}$$

gives the equations of motion

$$G_{\mu\,\nu} = \frac{1}{M_p^2} \left[-V_0\, g_{\mu\nu} + T^{(A)}_{\mu\nu} \right]$$

$$T^{(A)}_{\mu\nu} \equiv F_\mu{}^\sigma\, F_{\nu\sigma} - \frac{1}{4}\, F_{\alpha\beta}\, F^{\alpha\beta}\, g_{\mu\nu} + \left(m^2 - \frac{R}{6}\right)\, A_\mu\, A_\nu - \frac{1}{2}\, m^2\, A_\alpha\, A^\alpha\, g_{\mu\nu}$$
$$-\frac{1}{6}\left(R_{\mu\nu} - \frac{1}{2}\, R\, g_{\mu\nu}\right)\, A_\alpha\, A^\alpha - \frac{1}{6}\, \left(g_{\mu\nu}\, \Box - \nabla_\mu\, \nabla_\nu\right)\, A_\alpha\, A^\alpha$$
$$\frac{1}{\sqrt{-g}}\, \partial_\mu\, \left[\sqrt{-g}\, F^{\mu\nu}\right] - \left(m^2 - \frac{R}{6}\right)\, A^\nu = 0 \qquad (5.49)$$

If we assume that the background solutions depend only on time, then the ν component of the last of (5.49) gives $A^0 = 0$. For a homogeneous background, the vev of the vector is everywhere in the same direction; we choose the coordinates such that this direction coincides with the $x-$axis. We look for background solutions of the form (4.11), and we define

$$H_a \equiv \frac{\dot{a}}{a} \quad , \quad H_b \equiv \frac{\dot{b}}{b} \quad , \quad H \equiv \frac{H_a + 2\, H_b}{3} \quad , \quad h \equiv \frac{H_b - H_a}{3} \qquad (5.50)$$

Namely, H is the average expansion rate, while h parametrizes the departure from isotropy. The regime of small isotropy corresponds to $h \ll H$. In terms of these quantities, and for the background (4.11), equations (5.49) give [9]

$$H^2 - h^2 = \frac{V_0}{3\, M_p^2} + \frac{1}{6}\dot{B}_1^2 - \frac{2}{3} h\, B_1\, \dot{B}_1 + \frac{1}{6}\, B_1^2\, \left(m^2 - 4Hh + 5h^2\right)$$
$$\dot{h} + 3Hh = \frac{1}{3} B_1^2 \left(\dot{H} - \frac{\dot{h}}{2}\right) + \frac{1}{3}\dot{B}_1^2 + \frac{1}{3}\, (2H - 5h)\, B_1 \dot{B}_1$$
$$+\frac{1}{3}\left(3H^2 - \frac{11}{2} Hh + 5h^2 - m^2\right) B_1^2$$
$$2\dot{H} + 3H^2 + 3h^2 = \frac{V_0}{M_p^2} - \frac{1}{2}\dot{B}_1^2 - \frac{1}{3} B_1 \left[\ddot{B}_1 + (3H - 2h)\, \dot{B}_1\right]$$
$$+\frac{1}{6}\left(4Hh - 5h^2 + m^2\right) B_1^2$$
$$\ddot{B}_1 + 3\, H\, \dot{B}_1 + \left(m^2 - 5h^2 - 2\, h\, H - 2\, \dot{h}\right)\, B_1 = 0 \qquad (5.51)$$

One of the last three equations can be obtained from the other equations in (5.51) due to a nontrivial Bianchi identity. We see from the second of (5.51) that the anisotropy of the background is indeed supported by the vector vev B_1.

[9] The first of (5.51) is the 00 Einstein equation; the second is the linear combination of the (11)-(22) Einstein equations; the third equation is the linear combination of the $(11) + 2 \times (22)$ Einstein equations . Finally, the fourth equation is the $x-$ component of the equations for the vector field (the 33 Einstein equation coincides with the 22 one, while the remaining equations are trivial).

Below, when we study the perturbations of this model, we use the exact background equations (5.51). However, only for this discussion, we present the inflationary solution of (5.51) in the slow roll approximation (slow motion of B_1 towards zero, so that the anisotropy is not quickly damped away) and for small anisotropy. Specifically, we disregard the time derivatives of H, h, and look for expansion series solutions of the type

$$H = H_0 + c_H\, B_1^2 + \mathrm{O}\left(B_1^4\right) \quad , \quad h = c_h\, B_1^2 + \mathrm{O}\left(B_1^4\right) \quad , \quad \dot{B}_1 \simeq c_B\, H_0\, B_1 \quad , \\ \text{with} \;\; B_1,\, c_B \ll 1 \tag{5.52}$$

We insert these expressions in the last equation of (5.51) and expand in B_1. This gives $3c_B H_0^2 + c_B^2\, H_0^2 + m^2 = 0$. Since, $c_B \ll 1$, this gives $c_B = -\frac{m^2}{3\, H_0^2}$. Therefore, slow roll requires $m \ll H_0$. We then insert (5.52) in the first of (5.51), expand in B_1, and neglect m vs. H_0. We find $H_0 = \sqrt{V_0}/\left(\sqrt{3}\, M_p\right)$, $c_H = m^2/\left(12\, H_0\right)$. Finally, we insert (5.52) in the second and third of (5.51), expand in B_1, and again neglect m vs. H_0. These equations then become identical, and give $c_h = H_0/3$. Therefore,

$$H = H_0 + \frac{m^2}{12\, H_0}\, B_1^2 + \mathrm{O}\left(B_1^4\right) \quad , \quad h = \frac{H_0}{3}\, B_1^2 + \mathrm{O}\left(B_1^4\right) \quad , \quad \dot{B}_1 = -\frac{m^2}{3\, H_0} B_1 + \mathrm{O}\left(B_1^3\right) \tag{5.53}$$

where H_0 is the expansion rate in absence of the vector field.

Before moving to the study of the perturbation, we note that the mass parameter m of the vector field must satisfy

$$B_1\, H_0^2 \lesssim m^2 \ll H_0^2 \tag{5.54}$$

The second condition is due to the slow roll requirement, as we already pointed out. The first condition comes from requiring that the "mass term" for B_1 in the last of (5.51) is positive, so that B_1 evolves towards the origin (so that the anisotropy decreases during inflation rather than increasing).

Instability from the linearized equations

We now expand the field equations (5.49) at first order in the 2d scalar perturbations of the metric and the vector field. [10] We denote the resulting linearized equations as

$$\mathrm{Eq}_{\mu\nu} : \delta\left(G_{\mu\nu} - \frac{1}{M_p^2}\,\left(-V_0\, g_{\mu\nu} + T^{(A)}_{\mu\nu}\right)\right) = 0 \quad , \quad \mathrm{Eq}_{\mu} : \delta\left(\frac{\delta S}{\delta A_\mu}\right) = 0 \tag{5.55}$$

We study the linearized equations in Fourier space defined in equation (4.16). The explicit expressions of the linearized equations for the scalar sector are given in equations (B.1) of Appendix B. We could express these equations solely in terms of the gauge invariant modes defined in (4.35). This is a nontrivial check on our algebra. Here, we disregard some of the equations in (B.1) which can be obtained from the remaining ones (due to Bianchi identities). The (complete) set of independent linearized equations which we choose to integrate is

$$\begin{aligned}
\mathrm{Eq}_{00} : \quad & \left[\left(1-\frac{B_1^2}{3}\right) H + \left(1+\frac{B_1^2}{6}\right) h + \frac{1}{6}\,\dot{B}_1\, B_1\right] \dot{\hat{\Psi}} \\
& + \frac{1}{2}\left[p_T^2 + \left(m^2 - \frac{p_T^2+2p_L^2}{6} + 5h^2 - 4\,h\,H\right)\, B_1^2 - 4\,h\,B_1\,\dot{B}_1 + \dot{B}_1{}^2\right]\hat{\Psi} \\
& + \left[3H^2 - \left(3+\frac{5}{2}\,B_1^2\right)\, h^2 - \frac{1}{2}\,\dot{B}_1^2 + 2\,\left(B_1\,H + \dot{B}_1\right)\, B_1\, h\right]\,\hat{\Phi} \\
& - \left[\left(1+\frac{B_1^2}{6}\right)\,(H+h) + \frac{1}{6}\,B_1\,\dot{B}_1\right]\,\hat{\chi} \\
& - \left[\left(1+\frac{B_1^2}{6}\right)\,\left(H - \frac{1}{2}\,h\right) + \frac{1}{6}\,B_1\,\dot{B}_1\right]\,\hat{B} \\
& - \left[\left(\frac{1}{2}\,H - h\right)\, B_1 + \frac{1}{2}\,\dot{B}_1\right]\,\hat{\alpha}_0 - \left(\frac{1}{2}\,\dot{B}_1 - B_1\,h\right)\,\dot{\hat{\alpha}}_1 \\
& + \left[\frac{1}{2}\,\left(\frac{p^2}{3} - m^2 - 5h^2 + 4\,h\,H\right)\, B_1 + h\,\dot{B}_1\right]\,\hat{\alpha}_1 = 0
\end{aligned}$$

$$\begin{aligned}
\mathrm{Eq}_{01} : \quad & \frac{1}{6}\,\left(\dot{\hat{\alpha}}_1 - B_1\,\dot{\hat{\Psi}}\right)\, B_1 + \frac{B_1}{6}\,\left(B_1\,H - 2\,B_1\,h - 2\,\dot{B}_1\right)\,\hat{\Psi} \\
& + \left(1+\frac{B_1^2}{6}\right)\,\left(H + h + \frac{B_1\,\dot{B}_1}{6+B_1^2}\right)\,\hat{\Phi} + \frac{1}{6}\,\left(-B_1\,H + 2\,h\,B_1 + \dot{B}_1\right)\,\hat{\alpha}_1
\end{aligned}$$

[10] As we mentioned, the 2d vector perturbations are decoupled from the 2d scalar ones; we have verified that the 2d vectors do not develop any instability; for brevity, we do not present this computations here.

$$+\left(\frac{p_T^2}{4p_L^2}+\frac{p_T^2}{24p_L^2}\,B_1^2-\frac{1}{3}\,\mathcal{D}_{\chi\chi}\right)\,\hat{\chi}-\frac{6+B_1^2}{24}\,\hat{B}-\frac{B_1}{3}\,\mathcal{D}_{\alpha_0\alpha_0}\,\hat{\alpha}_0=0$$

$$\mathrm{Eq}_{0i}:\quad \frac{1}{2}\,\left(1-\frac{B_1^2}{6}\right)\,\dot{\hat{\Psi}}+\frac{1}{6}\,B_1\,\dot{\hat{\alpha}}_1+\left[\frac{B_1}{6}\,\left(H\,B_1-2\,\dot{B}_1\right)-\left(\frac{3}{2}+\frac{B_1^2}{12}\right)\,h\right]\,\hat{\Psi}$$
$$+\left[\left(\frac{1}{3}\,H-\frac{7}{6}\,h\right)\,B_1+\frac{2}{3}\,\dot{B}_1\right]\,\hat{\alpha}_1+\left[\left(h-\frac{H}{2}\right)\,B_1-\frac{\dot{B}_1}{2}\right]\,\hat{\alpha}$$
$$+\left[-\left(\frac{1}{2}+\frac{B_1^2}{12}\right)\,h+\left(1+\frac{B_1^2}{6}\right)\,H+\frac{1}{6}\,B_1\,\dot{B}_1\right]\,\hat{\Phi}-\frac{1}{4}\,\left(1+\frac{B_1^2}{6}\right)\,\hat{\chi}$$
$$+\frac{p_L^2}{4p_T^2}\,\left(1+\frac{B_1^2}{6}\right)\,\hat{B}=0$$

$$\mathrm{Eq}_{0}:\quad \dot{\hat{\alpha}}_1+\left(2\,h\,B_1-H\,B_1-\dot{B}_1\right)\,\hat{\Psi}+(H-2h)\,\hat{\alpha}_1+\frac{p_T^2}{p_L^2}\,\dot{\hat{\alpha}}+\frac{p_T^2}{p_L^2}\,(H-2h)\,\hat{\alpha}$$
$$+\left(H\,B_1-2h\,B_1+\dot{B}_1\right)\,\hat{\Phi}-\frac{2}{3B_1}\,\mathcal{D}_{\chi\chi}\,\hat{\chi}+\left(1+\frac{p_T^2}{p_L^2}-\frac{2}{3}\,\mathcal{D}_{\alpha_0\alpha_0}\right)\,\hat{\alpha}_0=0$$

$$\mathrm{Eq}_{11}:\quad \frac{1}{2}\,B_1\,\left(\ddot{\hat{\alpha}}_1-2\,B_1\,\ddot{\hat{\Psi}}\right)-\left(3\,H\,B_1+2\,\dot{B}_1\right)\,B_1\,\dot{\hat{\Psi}}+\frac{1}{2}\,\left(-H\,B_1+8\,h\,B_1-\dot{B}_1\right)\,\dot{\hat{\alpha}}_1$$
$$+\left(\mathcal{M}_{\Psi\Psi}-p_T^2\,B_1^2\right)\,\hat{\Psi}+\left(\mathcal{M}_{\Psi\alpha_1}+\frac{p_T^2}{2}\,B_1\right)\,\hat{\alpha}_1$$
$$+\left[\left(3+\frac{1}{2}\,B_1^2\right)\,h+\left(3-B_1^2\right)\,H+\frac{1}{2}\,B_1\,\dot{B}_1\right]\,\dot{\hat{\Phi}}$$
$$+\left[\left(-\frac{9}{4}\,m^2+\frac{p_T^2+2p_L^2}{4}-\frac{15}{4}\,h^2+3\,h\,H\right)\,B_1^2+3\,h\,B_1\,\dot{B}_1\right.$$
$$\left.-3\,\left(\frac{p_T^2}{2}\,-\frac{V_0}{2M_p^2}+\frac{3}{2}\,h^2-\frac{3}{2}\,H^2+\frac{1}{4}\,\dot{B}_1^2\right)\right]\,\hat{\Phi}-\left(\frac{3}{2}-\frac{1}{4}\,B_1^2\right)\,\dot{\hat{B}}+\frac{1}{2}\,B_1^2\,\dot{\hat{\chi}}$$
$$+(2H-h)\,B_1^2\,\hat{\chi}-\left[\left(\frac{9}{2}+\frac{1}{4}\,B_1^2\right)\,h+\left(\frac{9}{2}-\frac{5}{4}\,B_1^2\right)\,H+\frac{1}{2}\,B_1\,\dot{B}_1\right]\,\hat{B}$$
$$+\frac{3}{2}\,\left(2h\,B_1-H\,B_1-\dot{B}_1\right)\,\hat{\alpha}_0=0$$

$$\mathrm{Eq}_{1}:\quad \ddot{\hat{\alpha}}_1-\frac{1}{3}\,B_1\,\ddot{\hat{\Psi}}+3H\,\dot{\hat{\alpha}}_1+\left(\frac{8}{3}\,B_1\,h-\frac{7}{3}\,B_1\,H-\dot{B}_1\right)\,\dot{\hat{\Psi}}+\left(\mathcal{M}_{\alpha_1\alpha_1}+p_T^2\right)\,\hat{\alpha}_1\hat{\Psi}$$
$$-\frac{B_1}{3}\,p_T^2\,+\left(\dot{B}_1-2\,B_1\,h\right)\,\dot{\hat{\Phi}}+\frac{B_1}{3}\,\left(\dot{\hat{B}}+\dot{\hat{\chi}}\right)+\dot{\hat{\alpha}}_0+\frac{B_1}{3}\,\left(p^2-6m^2\right)\,\hat{\Phi}$$
$$+\frac{1}{3}\,\left(7\,B_1\,h+B_1\,H-3\dot{B}_1\right)\,\hat{B}+\frac{2}{3}\,(2H-h)\,B_1\,\hat{\chi}-p_T^2\,\hat{\alpha}+2\,(h+H)\,\hat{\alpha}_0=0$$

$$\text{Eq}_i: \quad \ddot{\hat{\alpha}} + 3\,(H-2h)\,\dot{\hat{\alpha}} + \left(\mathcal{M}_{\alpha\alpha} + p_L^2\right)\,\hat{\alpha} - p_L^2\,\hat{\alpha}_1 + \frac{p_L^2}{p_T^2}\,\left(B_1\,H - 2\,B_1\,h + \dot{B}_1\right)\,\hat{B}$$
$$+\dot{\hat{\alpha}}_0 + (2H-4h)\,\hat{\alpha}_0 = 0 \tag{5.56}$$

where $\mathcal{D}_{\chi\chi}$, $\mathcal{D}_{\alpha_0\alpha_0}$, $\mathcal{M}_{\Psi\Psi}$, $\mathcal{M}_{\Psi\alpha_1}$, $\mathcal{M}_{\alpha_1\alpha_1}$, $\mathcal{M}_{\alpha\alpha}$ depend on the background quantities and are explicitly given in equations (D.5) and (B.3) in Appendix B. In writing (5.56), we have also made use of the physical momenta, defined previously as $p_L = k_L/a$, $p_T = k_T/b$ and $p^2 = p_L^2 + p_T^2$.

We now solve the system of equations (5.56) numerically. We start by noting that the first four equations in (5.56) contain at most a single time derivative for the perturbations, and do not contain any time derivative of the modes $\{\hat{\Phi},\, \hat{\chi},\, \hat{B},\, \hat{\alpha}_0\}$; these are the nondynamical modes of the system, and these first four equations can also be obtained by extremizing the quadratic action for the perturbations (equation (5.63) below) with respect to these modes. These equations are precisely of the type (4.53) given above where we discussed the linearized equations at a formal level. Compare also with eq. (5.33) for the nondynamical mode α_0 in the simpler case studied in Section 5.4.

One can choose to solve these four constraint equations for $\{\hat{\Phi},\, \hat{\chi},\, \hat{B},\, \hat{\alpha}_0\}$, and insert the solutions in the remaining equations in (5.56). In this way, we obtain a closed system of equations for the dynamical modes. A different but equivalent way to integrate the system (5.56) is to differentiate the constraint equations, so as to obtain differential equations for the nondynamical modes too. Combined with the remaining equations in (5.56), one then obtains a closed system that can be numerically integrated (the constraint equations need to be imposed as initial condition). In the first method mentioned, one obtains a system with fewer but more complicated equations. On the other hand, the second method results in a larger set of less complicated equations. Here, we adopt an "intermediate" method, which we have found to be convenient for the numerical integration. We solve the second of (5.56) for $\hat{\chi}$ (unlike what we have for the case of the ACW model in the previous chapter, where we have solved for $\hat{\chi}$ and $\hat{B}$):

$$\hat{\chi} \;=\; \frac{p_L^2}{\mathcal{D}}\left[\left(6 + B_1^2\right)\,\hat{B} + 8B_1\,\mathcal{D}_{\alpha_0\alpha_0}\,\hat{\alpha}_0 + 4\,\left(\left(H-2h\right)B_1 - \dot{B}_1\right)\,\hat{\alpha}_1\right.$$

$$-4\,B_1\,\left((H-2h)\,B_1-2\dot{B}_1\right)\,\hat{\Psi}-4\,\left(6+B_1^2\right)\,\mathcal{H}\,\hat{\Phi}-4\,B_1\,\dot{\hat{\alpha}}_1+4B_1^2\,\dot{\hat{\Psi}}\Bigg] \tag{5.57}$$

where the time dependent coefficients $\mathcal{D}_{\alpha_0\alpha_0}$, $\mathcal{D}$ and $\mathcal{H}$ are given in equations (D.5) and (B.4) of Appendix B.

It is important to verify that the second of (5.56) can indeed be solved in terms of $\hat{\chi}$; namely, that $\mathcal{D}\neq 0$. The easiest way to verify this is to use the slow-roll solutions (5.53) in the expression (B.4) for $\mathcal{D}$, since we are working in a regime in which these slow-roll solutions are highly accurate. This gives

$$\mathcal{D}=6p_T^2+\left(p_T^2-24\,H^2+12m^2\right)\,B_1^2+\mathrm{O}\left(B_1^4\right)\,. \tag{5.58}$$

We can integrate out $\hat{\chi}$ provided that $\mathcal{D}\neq 0$. We see that $\mathcal{D}$ is positive at least as long as $p_T\gtrsim 2\,H\,B_1$ (when the two terms become equal, the negative term dominates the $\mathcal{O}\left(B_1^2\right)$ expression, an the expression cancels with the positive $\mathcal{O}\left(B_1^0\right)$ term. At this point, the expansion series (5.58) breaks down). As we show below, the computation we are performing shows that the linearized perturbations blow up when $p_L\approx\sqrt{12}\,H/B_1$. Since integrating out $\hat{\chi}$ is a step of this computation, our result can be trusted as long as $p_T>2\,H\,B_1$ when $p_L\approx\sqrt{12}\,H/B_1$. Namely, we consider modes for which $p_T>\left(B_1^2/\sqrt{3}\right)p_L$ at that moment. This is not a strong restriction, since $B_1\ll 1$.

We insert the solution (5.57) into the other equations in (5.56), and we differentiate the three remaining constraint equations (we stress that we do not lose any information, provided that these equations are imposed as initial conditions). In this way, we obtain a system of 6 differential equations, which can be formally written as

$$\mathcal{M}_\kappa\begin{pmatrix}\ddot{\hat{\Psi}}\\ \ddot{\hat{\alpha}}_1\\ \ddot{\hat{\alpha}}\\ \dot{\hat{\Phi}}\\ \dot{\hat{B}}\\ \dot{\hat{\alpha}}_0\end{pmatrix}=\begin{pmatrix}f_1\\ f_2\\ f_3\\ f_4\\ f_5\\ f_6\end{pmatrix}\quad,\quad \mathcal{M}_\kappa\equiv\begin{pmatrix}\kappa_{11}&\kappa_{12}&0&\kappa_{14}&\kappa_{15}&\kappa_{16}\\ \kappa_{21}&\kappa_{22}&0&\kappa_{24}&\kappa_{25}&\kappa_{26}\\ 0&0&1&0&0&1\\ \kappa_{41}&\kappa_{42}&0&\kappa_{44}&\kappa_{45}&\kappa_{46}\\ \kappa_{51}&\kappa_{52}&0&\kappa_{54}&\kappa_{55}&\kappa_{56}\\ \kappa_{61}&\kappa_{62}&\kappa_{63}&\kappa_{64}&\kappa_{65}&\kappa_{66}\end{pmatrix} \tag{5.59}$$

which correspond, respectively, to Eq_{11}, Eq_1, Eq_i, and to the dime derivatives of Eq_{00}, Eq_{0i}, and Eq_0.

The elements of the matrix $\mathcal{M}_\kappa$ depend on the background quantities. The functions on the right hand side of (5.59) f_i are expressed as linear combinations of $\{\dot{\hat{\Psi}},\ \hat{\Psi},\ \dot{\hat{\alpha}}_1,\ \hat{\alpha}_1,\ \dot{\hat{\alpha}},\ \hat{\alpha},\ \hat{\Phi},\ \hat{B},\ \hat{\alpha}_0\}$ whose coefficients also depend on the background quantities. The explicit expressions for the matrix $\mathcal{M}_\kappa$ and the coefficients f_i are given in equations (B.8) and (B.11) of Appendix B.

We invert $\mathcal{M}_\kappa$, and integrate the system numerically. The determinant of $\mathcal{M}_\kappa$ vanishes at some given time. As we approach that time, $\mathcal{M}_\kappa^{-1}$ diverges. Correspondingly, the numerical solutions of the system also diverge.

By inserting the explicit expressions for the entries of $\mathcal{M}_\kappa$ given in Appendix B, we find:

$$\det\mathcal{M}_\kappa = \frac{p_T^2\ \left(6+B_1^2\right)^2}{864\mathcal{D}}\ (h+H)^2\ \left[72\,\mathcal{D}_{\alpha_0\alpha_0} - 6\,B_1^2\ (3-2\mathcal{D}_{\alpha_0\alpha_0}) - B_1^4\ (3-8\mathcal{D}_{\alpha_0\alpha_0})\right] \tag{5.60}$$

Using the expressions for $\mathcal{D}_{\alpha_0\alpha_0}$ and $\mathcal{D}$ given in (D.5) and (B.4), we then find that the determinant vanishes when

$$\begin{aligned} p_L^2 = p_{L*}^2 \quad \equiv \quad & \frac{1}{B_1^2\ \left(6+B_1^2\right)} \Bigg\{ -18\ \left(2m^2 - 4H^2 + 4h^2 + \dot{B}_1^2\right) \\ & - \left(6m^2 - 12H^2 - 72\,h\,H + 102\,h^2 + 7\dot{B}_1^2\right)\ B_1^2 \\ & - \left(4H^2 - 28\,h\,H + 31\,h^2\right)\ B_1^4 + 48\,h\,B_1\,\dot{B}_1 \\ & + 4\,(7h-2H)\ B_1^3\,\dot{B}_1 \Bigg\}. \end{aligned} \tag{5.61}$$

This expression for p_{L*} is exact. Using the slow-roll solutions (5.53), we obtain the approximate expression:

$$p_{L*}^2 \simeq \frac{6\left(2\,H_0^2 - m^2\right)}{B_1^2} + \mathrm{O}\left(B_1^0\right)\ . \tag{5.62}$$

To confirm that the linearized modes indeed blow up at p_{L*}, we integrate the system (5.59) for a specific choice of parameters (the parameters we use have no particular relevance, and are chosen only for illustrative purposes). We choose a small anisotropy, $(h/H)_{\rm in} = \mathrm{O}\left(B_{1,\rm in}^2\right) \simeq 10^{-2}$, and an initial value for the momentum, $p_{\rm in} \simeq 10^3\,H_{\rm in}$, so that the mode is initially deeply inside the horizon. As we verify in Appendix C, the frequency for the modes is initially adiabatically evolving, so that we can choose the

initial conditions for the dynamical modes $\hat{\Psi}$, $\hat{\alpha}_1$, $\hat{\alpha}$ and their derivatives according to the adiabatic vacuum prescription described in chapter 2. We then use the constraint equations (the first, the third, and the fourth of (5.56)), to provide the initial conditions for the three nondynamical modes $\hat{\Phi}$, $\hat{B}$, $\hat{\alpha}_0$ of the system. The resulting evolution of the "relativistic Newtonian potential" $\hat{\Phi}$, and of two other 2d scalar modes are shown in Figure 5.2. We see that the modes indeed diverge at some given time. We verified that $p_L = p_{L*}$ at this moment. This is confirmed by the time evolution of one of the eigenvalue of the kinetic matrix of the dynamical perturbations (computed in 5.5.1) shown in the left panel of the Figure. We see that the linearized solutions blow up precisely when the system (5.59), or equivalently, the kinetic matrix, becomes singular.

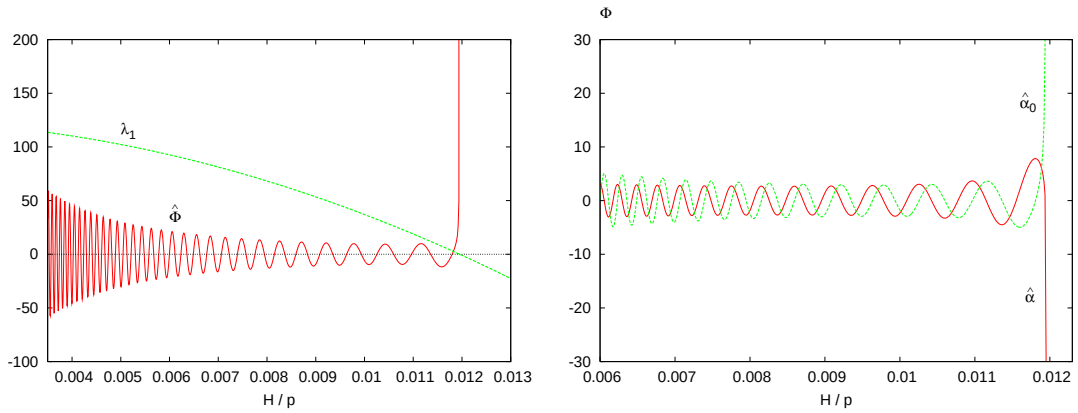

Figure 5.2: Results from a numerical simulation with $m^2 = 0.1\, H_0\, B_{\rm in} = 0.1$, $p_{L,{\rm in}} = 400 H_{\rm in}$, $p_{T,{\rm in}} = 900 H_{\rm in}$, (corresponding to $H/p \simeq 10^{-3}$; the modes are initially in the adiabatic vacuum; only the final part of the evolution is shown in the two figures). Since H/p grows during inflation, we use this quantity as "time variable" in the Figure. Left panel: gauge invariant relativistic gravitational potential $\hat{\Phi}$. We show the real part in units of $\hat{\Psi}_{\rm in}$. We also show the eigenvalue λ_1 of the kinetic matrix (multiplied by 3×10^5, so that it is visible in the figure). We see that $\hat{\Phi}$ diverges when $\lambda_1 = 0$. Right panel: real parts of the modes $\hat{\alpha}_0$ (in units of $100\, H_0\, \hat{\Psi}_{\rm in}$) and $\hat{\alpha}$ (in units of $\hat{\Psi}_{\rm in}$) . Also these modes (as all the modes of the system) diverge when $\lambda_1 = 0$.

Ghost from the quadratic action

In order to understand the physical reasons behind the instability we have just found, we compute the quadratic action for the perturbations. We expand the action (5.48) at quadratic order in the perturbations (4.31). The resulting action can be expressed

solely in terms of the gauge invariant modes defined in (4.35)-(4.36). This provides a nontrivial check on our algebra. We also find that the action is the sum of two separate parts, one involving only the 2d scalar modes, and one the 2d vectors. We disregard this second piece in the following discussion. The action for the 2d scalars reads

$$
\begin{aligned}
S_{\rm 2dS} &= \frac{1}{3}\int d^3k\, dt\, a\, b^2\, \mathcal{L}_{\rm 2dS} \\
\mathcal{L}_{2dS} &= B_1^2\,|\dot{\hat\Psi}|^2 - \frac{B_1}{2}\left(\dot{\hat\Psi}\,\dot{\hat\alpha}_1^* + \text{h.c.}\right) + \frac{3p_T^2}{2p_L^2}\,|\dot{\hat\alpha}|^2 \\
&+ \frac{3}{2}\,|\dot{\hat\alpha}_1|^2 - \frac{3}{2}\left(1+\frac{1}{2}\,B_1^2\right)\left(H - 2\,h - \frac{2\,B_1\,\dot B_1}{2+B_1^2}\right)\left(\dot{\hat\Psi}^*\,\hat\Psi + \text{h.c.}\right) \\
&- \left(B_1\,h - \frac{1}{2}\,B_1\,H + \frac{1}{2}\,\dot B_1\right)\left(\dot{\hat\Psi}^*\,\hat\alpha_1 + \text{h.c.}\right) \\
&- \left[\left(3+\frac{1}{2}\,B_1^2\right)\,h + \left(3-B_1^2\right)\,H + \frac{1}{2}\,B_1\,\dot B_1\right]\left(\dot{\hat\Psi}^*\,\hat\Phi + \text{h.c.}\right) \\
&- \frac{B_1^2}{2}\left(\dot{\hat\Psi}^*\,\hat\chi + \text{h.c.}\right) + \frac{1}{4}\left(6-B_1^2\right)\left(\dot{\hat\Psi}^*\,\hat B + \text{h.c.}\right) \\
&+ \frac{3p_T^2}{2p_L^2}\,(H-2\,h)\left(\dot{\hat\alpha}^*\,\hat\alpha + \text{h.c.}\right) + \frac{3p_T^2}{2p_L^2}\left(\dot{\hat\alpha}^*\,\hat\alpha_0 + \text{h.c.}\right) \\
&- \frac{3}{2}\left(B_1\,H - 2\,B_1\,h + \dot B_1\right)\left(\dot{\hat\alpha}_1^*\,\hat\Psi + \text{h.c.}\right) + \frac{3}{2}\,(H-2\,h)\left(\dot{\hat\alpha}_1^*\,\hat\alpha_1 + \text{h.c.}\right) \\
&+ \frac{3}{2}\left(\dot B_1 - 2\,B_1\,h\right)\left(\dot{\hat\alpha}_1^*\,\hat\Phi + \text{h.c.}\right) + \frac{B_1}{2}\left(\dot{\hat\alpha}_1^*\,\hat\chi + \text{h.c.}\right) + \frac{B_1}{2}\left(\dot{\hat\alpha}_1^*\,\hat B + \text{h.c.}\right) \\
&+ \frac{3}{2}\left(\dot{\hat\alpha}_1^*\,\hat\alpha_0 + \text{h.c.}\right) - \left(\mathcal{D}_{\Psi\Psi} + p_T^2\,B_1^2\right)\,|\hat\Psi|^2 \\
&- \left(\mathcal{D}_{\Psi\alpha_1} - \frac{1}{2}\,p_T^2\,B_1\right)\left(\hat\Psi^*\,\hat\alpha_1 + \text{h.c.}\right) \\
&+ \left[\left(-\frac{3}{2}\,m^2 + \frac{2p_L^2+p_T^2}{4} - \frac{15}{2}\,h^2 + 6\,h\,H\right)\,B_1^2 + 6\,h\,B_1\,\dot B_1 - \frac{3}{2}\left(p_T^2 + \dot B_1^2\right)\right] \\
&\qquad \times\left(\hat\Psi^*\,\hat\Phi + \text{h.c.}\right) \\
&- \left(h\,B_1^2 - \frac{1}{2}\,B_1^2\,H + B_1\,\dot B_1\right)\left(\hat\Psi^*\,\hat\chi + \text{h.c.}\right) \\
&- \left(\frac{9}{2}\,h + \frac{1}{4}\,(h-2H)\,B_1^2 + B_1\,\dot B_1\right)\left(\hat\Psi^*\,\hat B + \text{h.c.}\right) \\
&- \frac{3}{2}\left(B_1\,H - 2B_1\,h + \dot B_1\right)\left(\hat\Psi^*\,\hat\alpha_0 + \text{h.c.}\right) \\
&- \left(\mathcal{D}_{\alpha\alpha} + \frac{3}{2}\,p_T^2\right)\,|\hat\alpha|^2 + \frac{3}{2}\,p_T^2\,\left(\hat\alpha^*\,\hat\alpha_1 + \text{h.c.}\right)
\end{aligned}
$$

$$
\begin{aligned}
&+ \quad \frac{3}{2}\left(2\,h\,B_1 - B_1\,H - \dot{B}_1\right)\left(\hat{\alpha}^*\,\hat{B} + \text{h.c.}\right) + \frac{3p_T^2}{2p_L^2}\,(H - 2\,h)\,(\hat{\alpha}^*\,\hat{\alpha}_0 + \text{h.c.}) \\
&- \quad \left(\mathcal{D}_{\alpha_1\alpha_1} + \frac{3}{2}\,p_T^2\right)|\hat{\alpha}_1|^2 \\
&+ \quad \left[\left(\frac{3}{2}\,m^2 - \frac{p^2}{2} + \frac{15}{2}\,h^2 - 6\,h\,H\right)B_1 - 3h\,\dot{B}_1\right]\left(\hat{\alpha}_1^*\,\hat{\Phi} + \text{h.c.}\right) \\
&- \quad \frac{1}{2}\left(H\,B_1 - 2h\,B_1 - \dot{B}_1\right)(\hat{\alpha}_1^*\,\hat{\chi} + \text{h.c.}) \\
&+ \quad \frac{1}{2}\left(2\,H\,B_1 - 7h\,B_1 + 4\dot{B}_1\right)\left(\hat{\alpha}_1^*\,\hat{B} + \text{h.c.}\right) \\
&+ \quad \frac{3}{2}\,(H - 2\,h)\,(\hat{\alpha}_1^*\,\hat{\alpha}_0 + \text{h.c.}) \\
&+ \quad \left[\left(9 + \frac{15}{2}\,B_1^2\right)h^2 - 9\,H^2 + \frac{3}{2}\,\dot{B}_1^2 - 6\,h\,B_1\,(H\,B_1 + \dot{B}_1)\right]|\hat{\Phi}|^2 \\
&+ \quad \frac{1}{2}\left(6 + B_1^2\right)\left(H + h + \frac{B_1\,\dot{B}_1}{6 + B_1^2}\right)\left(\hat{\Phi}^*\,\hat{\chi} + \text{h.c.}\right) \\
&+ \quad \frac{1}{2}\left(6 + B_1^2\right)\left(H - \frac{1}{2}\,h + \frac{B_1\,\dot{B}_1}{6 + B_1^2}\right)\left(\hat{\Phi}^*\,\hat{B} + \text{h.c.}\right) \\
&- \quad \left(3\,h\,B_1 - \frac{3}{2}\,H\,B_1 - \frac{3}{2}\,\dot{B}_1\right)\left(\hat{\Phi}^*\,\hat{\alpha}_0 + \text{h.c.}\right) \\
&- \quad \left(\mathcal{D}_{\chi\chi} - \frac{6 + 8B_1^2}{8p_L^2}\,p_T^2\right)|\hat{\chi}|^2 - \frac{1}{8}\left(6 + B_1^2\right)\left(\hat{\chi}^*\,\hat{B} + \text{h.c.}\right) - \mathcal{D}_{\chi\alpha_0}\,(\hat{\chi}^*\,\hat{\alpha}_0 + \text{h.c.}) \\
&+ \quad \frac{p_L^2}{p_T^2}\,\frac{6 + B_1^2}{8}\,|\hat{B}|^2 - \left(\mathcal{D}_{\alpha_0\alpha_0} - \frac{3p^2}{2\,p_L^2}\right)|\hat{\alpha}_0|^2
\end{aligned}
\tag{5.63}
$$

where the coefficients $\{\mathcal{D}_{\Psi\Psi},\, \mathcal{D}_{\Psi\alpha_1},\, \mathcal{D}_{\alpha\alpha},\, \mathcal{D}_{\alpha_1\alpha_1},\, \mathcal{D}_{\chi\chi},\, \mathcal{D}_{\alpha_0\alpha_0},\, \mathcal{D}_{\chi\alpha_0}\}$ depend on the background quantities (and, hence, are functions of time), and their explicit forms are given in equations (D.5) of Appendix B. As a further check on our algebra, we explicitly verified that the extremization of this action with respect to the fields included in it reproduces the system of linearized equations (5.56).

In the previous chapter in section 4.4, we outlined at a formal level the computation that we are now performing. We expressed the quadratic action in equation (4.52), where we distinguished between the dynamical fields Y_i and the nondynamical ones N_i. The action (5.63) is the explicit form of the action (4.52) for the model we are studying. The variables $\{\hat{\Phi},\, \hat{\chi},\, \hat{B},\, \hat{\alpha}_0\}$ are the nondynamical modes $\{N_i\}$, since they enter into the action (5.63) without time derivatives. Starting from the action (5.63),

we integrate out the nondynamical modes, and compute the action for the dynamical modes, following the same steps that lead from equation (4.52) to equation (4.54). In practice, we read the coefficients a_{ij}, ..., f_{ij} from the action (5.63), by comparing it with the formal expression (4.52); we then compute the combinations $K = a - b^\dagger\, c^{-1}\, b$, $X = d - b^\dagger\, c^{-1}\, f$, $\Omega^2 = -e + f^\dagger\, c^{-1}\, f$ (cf. equations (4.55)) that characterize the action of the dynamical modes. This computation is a straightforward algebraic manipulation; the resulting coefficients K_{ij}, X_{ij}, Ω^2_{ij} are extremely lengthy, and we do not report them here.

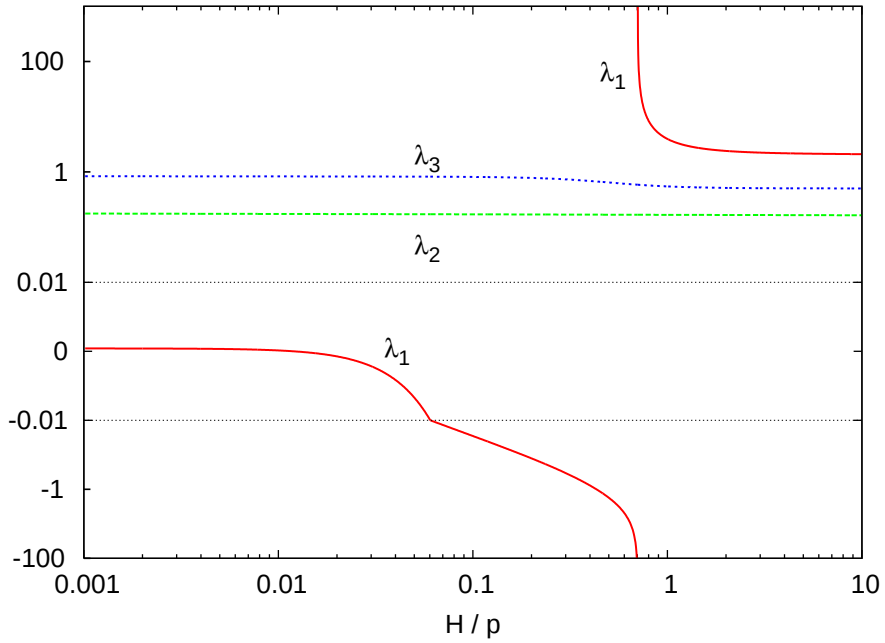

Figure 5.3: Evolution of the eigenvalues of the kinetic matrix. The parameters and initial conditions are as in Figure 5.2. Due to the wide range spanned by the eigenvalues, in the y axis, we have used a linear scale inside the interval $[-0.01,\, 0.01]$, and a logarithmic scale outside.

The instability emerged from the linearized equations can be understood by studying the kinetic matrix K. In Figure 5.3 we show the three eigenvalues of this matrix, for the same numerical evolution (i.e., for the same parameters and initial conditions) as the one leading to Figure 5.2. We see that the two eigenvalues $\lambda_{2,3}$ are always positive, indicating that the two corresponding eigenmodes are well behaved positive-energy fields. On the

contrary, the eigenvalue λ_1 vanishes close to horizon crossing. The system of linearized equations becomes singular at this point (cf. the formal equations (4.56); they are singular if the matrix K is noninvertible), and the linearized solutions diverge. We also see from the Figure that the eigenvalue λ_1 is negative for some time after this moment. The corresponding eigenmode is a ghost in this time interval.

Although the exact expression for K is rather lengthy, it is possible to obtain a simple expansion series for its determinant, in the sub-horizon / early time limit:

$$\det\left(\frac{K}{a\,b^2}\right) = \frac{p_T^6\,B_1^2}{96\,p^6} - \frac{\left(2H_0^2 - m^2\right)p_T^6}{16\,p_L^2\,p^6} + \mathrm{O}\left(\frac{H_0^4}{p^4}\right) \tag{5.64}$$

To obtain this expression, we first expanded the exact expression for the determinant in a power series of the momenta; we then simplified each term in the series by using the slow roll solutions (5.53), and finally kept for each term only the leading expression for $B_1^2 \ll 1$ (which corresponds to small anisotropy, since $h/H = \mathrm{O}\left(B_1^2\right)$). The terms of $\mathrm{O}\left(H_0^4/p^4\right)$ are parametrically suppressed with respect to the second term in (5.64) for $H_0 \ll p$. Therefore, the first two terms in (5.64) provide an accurate approximation of the determinant in the whole sub-horizon regime.

Eq. (5.64) shows that the determinant is positive at sufficiently early times, and it then becomes negative in the later part of the sub-horizon regime. This confirms the behavior of λ_1 seen in Figure 5.3 (since $\lambda_{2,3} > 0$, the sign of the determinant coincides with that of λ_1). The determinant vanishes when the two leading terms in (5.64) are (approximately) equal; this happens for $p_L^2 \simeq 6\left(2H_0^2 - m^2\right)/B_1^2$. Not surprisingly, this is precisely the approximate value (5.62) of p_L at which the linearized system (5.59) becomes singular.

In Figure 5.4, we compare the approximate expression for the determinant - the first two terms in (5.64) - with the exact one (not reported here). We see that the approximated expression is extremely accurate in the range of our interest.

5.5.2 One vector plus a scalar inflaton

The model proposed in ref. [11] is very similar to the one we have studied in the previous Subsection, with the only difference that the vacuum energy that we have included is replaced there by a slowly rolling inflaton field. We expect that the same instability that we have found above is present also for this model. The study presented in this

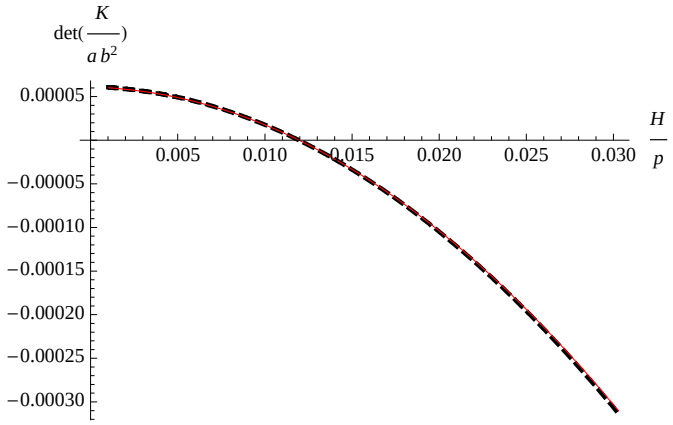

Figure 5.4: Determinant of the kinetic matrix, for the same choice of parameters and initial conditions as in the previous Figure. Compared with the previous figure, we show a close up of early times, around the point where the determinant vanishes. The black dashed curve shows the exact determinant, while the red curve shows the approximate expression given in eq. (5.64).

Subsection confirms this. We first briefly review the model and its slow roll solution. We then show that one of the 2d scalar modes is a ghost. More precisely, as in the case studied above, the mode is well behaved in the deep UV regime, but it becomes a ghost close to horizon crossing. When this happens, the system of linearized equations becomes singular.

The model and the background solution

The model of ref. [11] is characterized by the action:

$$S = \int d^4x \left[-\frac{1}{4} F_{\mu\nu} F^{\mu\nu} - \frac{1}{2} \partial_\mu \phi \, \partial^\mu \phi - V(\phi) - \frac{1}{2} \left(m^2 - \frac{R}{6} \right) A_\mu A^\mu \right] . \tag{5.65}$$

The inflaton field ϕ replaces the vacuum energy V_0 that we considered in the action (5.48). In this way, one can have a graceful exit from inflation. The field equations following from this action are

$$G_{\mu\,\nu} = \frac{1}{M_p^2} \left[T^{(\phi)}_{\mu\nu} + T^{(A)}_{\mu\nu} \right] \quad , \quad T^{(\phi)}_{\mu\nu} \equiv \partial_\mu \phi \, \partial_\nu \phi - g_{\mu\nu} \left(\frac{1}{2} \, \partial_\alpha \phi \, \partial^\alpha \phi + V(\phi) \right)$$
$$\frac{1}{\sqrt{-g}} \, \partial_\mu \left[\sqrt{-g} \, F^{\mu\nu} \right] - \left(m^2 - \frac{R}{6} \right) A^\nu = 0 \quad , \quad \frac{1}{\sqrt{-g}} \, \partial_\mu \left[\sqrt{-g} \, g^{\mu\nu} \, \partial_\nu \, \phi \right] - V'(\phi) = 0 \tag{5.66}$$

where $T^{(A)}_{\mu\nu}$ is defined as in (5.49). The background solution is again of the form (4.11), giving

$$
\begin{aligned}
3H^2-3h^2 &= \frac{1}{M_p^2}\left(\frac{1}{2}\,\dot\phi^2+V\left(\phi\right)\right)+\frac{1}{2}\,\dot B_1^2-2h\,B_1\,\dot B_1+\frac{1}{2}\,\left(m^2+5h^2-4h\,H\right)\,B_1^2\\
\dot h+3Hh &= \frac{1}{3}B_1^2\left(\dot H-\frac{\dot h}{2}\right)+\frac{1}{3}\dot B^2\\
&\quad+\frac{1}{3}\left(2H-5h\right)B_1\dot B_1+\frac{1}{3}\left(3H^2-\frac{11}{2}Hh+5h^2-m^2\right)B_1^2\\
2\dot H+3H^2+3h^2 &= \frac{1}{M_p^2}\,\left(-\frac{1}{2}\,\dot\phi^2+V\left(\phi\right)\right)-\frac{1}{2}\dot B_1^2-\frac{1}{3}B_1\left[\ddot B_1+\left(3H-2h\right)\dot B_1\right]\\
&\quad+\frac{1}{6}\left(4Hh-5h^2+m^2\right)B_1^2\\
\ddot B_1+3H\,\dot B_1+&\left(m^2-5h^2-2h\,H-2\dot h\right)\,B_1=0\\
\ddot\phi+3H\,\dot\phi+&\,V'\left(\phi\right)=0
\end{aligned}
\tag{5.67}
$$

where we have used the same combinations of Einstein equations we have written in (5.51).

We assume that the inflaton field is in the slow roll regime, $\dot\phi\approx -V'(\phi)/3H$, leading to inflation. For what concerns the evolution of the vector field, and of the anisotropy, all the considerations done for the model (5.48) are valid also in the present case, with the only difference that the vacuum energy V_0 is now replaced by the slowly decreasing potential energy of the inflaton. This leads to the slow roll and small anisotropy ($B_1 \ll 1$) background evolution

$$
\begin{aligned}
&H\approx H_0+\frac{m^2}{12\,H_0}\,B_1^2+\mathrm{O}\left(B_1^4\right)\quad,\quad h\approx\frac{H_0}{3}\,B_1^2+\mathrm{O}\left(B_1^4\right)\quad,\quad \dot B_1\approx-\frac{m^2}{3\,H_0}B_1+\mathrm{O}\left(B_1^3\right)\\
&\dot\phi\approx-\frac{V'(\phi)}{3H_0}+\mathrm{O}\left(B_1^2\right)\quad,\quad H_0\equiv\frac{\sqrt{V\left(\phi\right)}}{\sqrt{3}\,M_p}
\end{aligned}
\tag{5.68}
$$

Ghost instability from the quadratic action

We now study the perturbations of the background solution. We again decompose the perturbations as in (4.31), disregard the well behaved system of 2d vector modes, and construct the gauge invariant combinations (4.35). We have an additional gauge

invariant mode coming from the perturbation of the inflaton field, which is defined as

$$\delta\hat{\phi} = \delta\phi + \frac{\dot{\phi}}{H_b}\,\Sigma\,. \tag{5.69}$$

We proceed as in 5.5.1 by expanding the action of the model at quadratic order in the 2d scalar modes, and by rewriting it solely in terms of the gauge invariant modes (which provides a nontrivial check on our algebra). We find

$$\begin{aligned}
S_{\rm 2dS} &= \frac{1}{2}\int d^3k\,dt\,a\,b^2\,\mathcal{L}_{\rm 2dS} \\
\mathcal{L}_{\rm 2dS} &\supset |\dot{\hat{\delta\phi}}|^2 + \frac{2}{3}\,B_1^2\,|\dot{\hat{\Psi}}|^2 + \frac{p_T^2}{p_L^2}\,|\dot{\hat{\alpha}}|^2 + |\dot{\hat{\alpha}}_1|^2 \\
&\quad -\frac{1}{3}\,B_1\,\left(\dot{\hat{\Psi}}^*\,\dot{\hat{\alpha}}_1 + \text{h.c.}\right) - \frac{\dot{\phi}}{M_p}\,\left(\dot{\hat{\delta\phi}}^*\,\hat{\Phi} + \text{h.c.}\right) \\
&\quad +\frac{1}{3}\,\left(2\left(B_1^2-3\right)\,H - \left(6+B_1^2\right)\,h - B_1\,\dot{B}_1\right)\,\left(\dot{\hat{\Psi}}^*\,\hat{\Phi} + \text{h.c.}\right) \\
&\quad -\frac{B_1^2}{3}\,\left(\dot{\hat{\Psi}}^*\,\hat{\chi} + \text{h.c.}\right) + \left(1-\frac{B_1^2}{6}\right)\,\left(\dot{\hat{\Psi}}^*\,\hat{B} + \text{h.c.}\right) + \frac{p_T^2}{p_L^2}\,\left(\dot{\hat{\alpha}}^*\,\hat{\alpha}_0 + \text{h.c.}\right) \\
&\quad +\left(\dot{B}_1 - 2B_1\,h\right)\,\left(\dot{\hat{\alpha}}_1^*\,\hat{\Phi} + \text{h.c.}\right) + \frac{B_1}{3}\,\left(\dot{\hat{\alpha}}_1^*\,\hat{\chi} + \text{h.c.}\right) + \frac{B_1}{3}\,\left(\dot{\hat{\alpha}}_1^*\,\hat{B} + \text{h.c.}\right) \\
&\quad +\left(\dot{\hat{\alpha}}_1^*\,\hat{\alpha}_0 + \text{h.c.}\right) \\
&+ \quad \left(-6H^2 + \left(6+5B_1^2\right)\,h^2 + \dot{B}_1^2 - 4B_1\,\left(\dot{B}_1 + H\,B_1\right)\,h + \frac{\dot{\phi}^2}{M_p^2}\right)\,|\hat{\Phi}|^2 \\
&\quad +\frac{1}{3}\,\left(\left(6+B_1^2\right)\,(H+h) + B_1\,\dot{B}_1\right)\,\left(\hat{\Phi}^*\,\hat{\chi} + \text{h.c.}\right) \\
&\quad +\frac{1}{6}\,\left(\left(6+B_1^2\right)\,(2H-h) + 2\,B_1\,\dot{B}_1\right)\,\left(\hat{B}\,\hat{\Phi}^* + \text{h.c.}\right) \\
&\quad +\left(\dot{B}_1 + (H-2h)\,B_1\right)\,\left(\hat{\Phi}^*\,\hat{\alpha}_0 + \text{h.c.}\right) + \left(\Delta + \frac{p_T^2}{12p_L^2}\,\left(6+B_1^2\right)\right)\,|\hat{\chi}|^2 \\
&\quad -\frac{1}{2}\,\left(1+\frac{B_1^2}{6}\right)\,\left(\hat{\chi}^*\,\hat{B} + \text{h.c.}\right) + \frac{\Delta}{B_1}\,\left(\hat{\chi}^*\,\hat{\alpha}_0 + \text{h.c.}\right) \\
&\quad +\frac{p_L^2}{12p_T^2}\,\left(6+B_1^2\right)\,|\hat{B}|^2 + \left(\frac{\Delta}{B_1^2} + \frac{p^2}{p_L^2}\right)\,|\hat{\alpha}_0|^2 + \dots
\end{aligned} \tag{5.70}$$

where we have defined

$$\begin{aligned}
\Delta = \frac{1}{p_L^2\,\left(18+3B_1^2+2B_1^4\right)}\,\Bigg\{ & 3\left(6m^2 + 12h^2 - 12H^2 + 3\dot{B}_1^2 + 3\frac{\dot{\phi}^2}{M_p^2}\right)\,B_1^2 - 24h\,B_1^3\,\dot{B}_1 \\
& +2\,(2H-7h)\,B_1^5\,\dot{B}_1
\end{aligned}$$

$$+3\left(m^2+17h^2-12h\,H-2H^2+\frac{7}{6}\dot{B}_1^2+\frac{\dot{\phi}^2}{2M_p^2}\right)B_1^4$$
$$+\left(\frac{31}{2}h^2-14h\,H+2H^2\right)B_1^6\Bigg\}$$

In the action (5.70), we included only the terms that contribute to the kinetic matrix of the dynamical modes; the remaining terms, denoted by the dots, are omitted for brevity. Specifically, the terms included in (5.70) are those proportional to the coefficients a_{ij}, b_{ij}, and c_{ij} in eq. (4.56), where the quadratic action is written at a formal level. These are the only terms entering in the kinetic matrix K of the dynamical modes, see eqs. (4.55) and (4.54). It is immediate to compute K from (5.70). However, the explicit entries of this matrix are very involved, and not illuminating. For this reason, we do not report them here. We can however compute the eigenvalues of this matrix numerically for any given choice of parameters (namely, for any background evolution, and momentum of the perturbation). In addition, it is possible to obtain a simple approximation for the determinant of K

$$\det\left(\frac{K}{a\,b^2}\right)=\frac{p_T^6\,B_1^2}{192\,p^6}-\frac{\left(2H_0^2-m^2\right)p_T^6}{32\,p_L^2\,p^6}+\mathrm{O}\left(\frac{H_0^4}{p^4}\right) \tag{5.71}$$

where H_0 has been defined in eq. (5.68). This expression is accurate in the sub-horizon regime during inflation, in the limit of small anisotropy. More specifically, we obtained it using the same steps outlined after the analytic expression for the determinant of the model considered in the previous Subsection, eq. (5.64). It is worth noting that (5.71) differs from (5.64) only by an extra factor of $1/2$; this is the original factor in the kinetic term of the inflaton (which is the only additional field in the model we are considering in this Subsection). This suggests that the perturbation $\hat{\delta}\phi$ is decoupled from the other ones at leading order.

In figure 5.5 we present the results of a numerical evolution for a given set of parameters and initial conditions (starting from inflation, in the slow roll regime). The left panel shows the evolution of various background quantities. The right panel shows instead the determinant of the kinetic matrix for a mode with $p_L = 100H$, $p_T = 200H$ at the initial time (both the exact value, obtained from a numerical evaluation of the kinetic matrix, and the approximated value (5.71), are shown). We see that the determinant vanishes and becomes negative in the sub-horizon regime, when $H/p \sim B_1$.

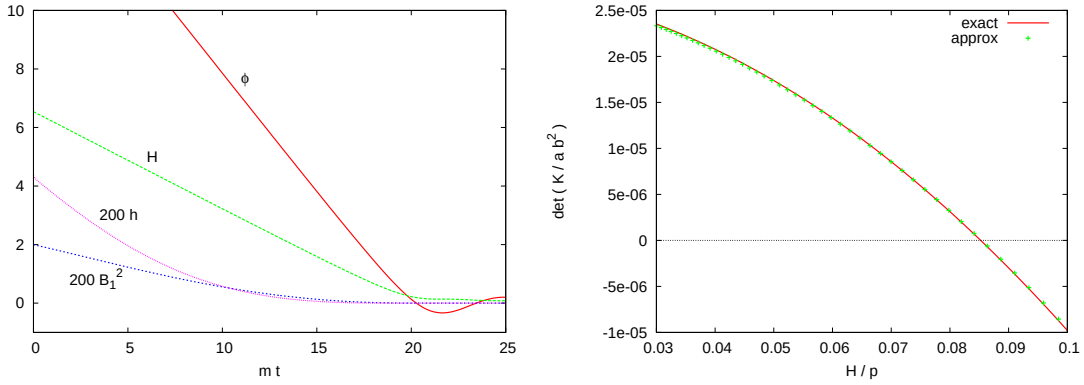

Figure 5.5: Results from a numerical simulation starting at $t = 0$ from $\phi = 16$ (providing about 60 e-folds of inflationary expansion), $B_1 = 0.1$ (providing a $\sim B_1^2 \simeq 1\%$ anisotropy). More precisely, we have considered a massive inflaton potential, with the inflaton mass equal to m. Left panel: inflaton (in units of M_p), hubble parameters (in units of m), and dimensionless rescaled vectorB_1. The anisotropic rate h and the vector are rescaled so that they are visible in the figure. Right panel: determinant of the kinetic matrix of the perturbations, for modes with initial momenta $p_{L,\rm in} = 100 H_{\rm in}$, $p_{T,\rm in} = 200 H_{\rm in}$, . The red curve shows the exact determinant, while the green points show the approximate expression given in eq. (5.71). The determinant vanishes at the time $m\,t \simeq 0.16$.

In Figure 5.6 we show the evolution of the four eigenvalues of the kinetic matrix; notice that there is an additional dynamical mode, supported by the inflaton field, with respect to the model studied in the previous Subsection. However, as for that case, one mode is a ghost for some time. We know that the system of linearized equations for the perturbations become singular when the eigenvalue λ_1 crosses zero. We expect that also the solutions diverge at that point, analogously to the study of the previous Subsection.

5.5.3 Vector inflation

We now study the simplest realization of the idea of vector inflation proposed in [8]. It is characterized by three mutually orthogonal vector fields nonminimally coupled to the curvature. The three fields have equal vev, providing a FRW background. Despite the background solution is isotropic, the model suffers of the same ghost instability as the models studied above. The discussion is divided in two parts. We first introduce the model, and discuss the background evolution. We then study the spectrum of

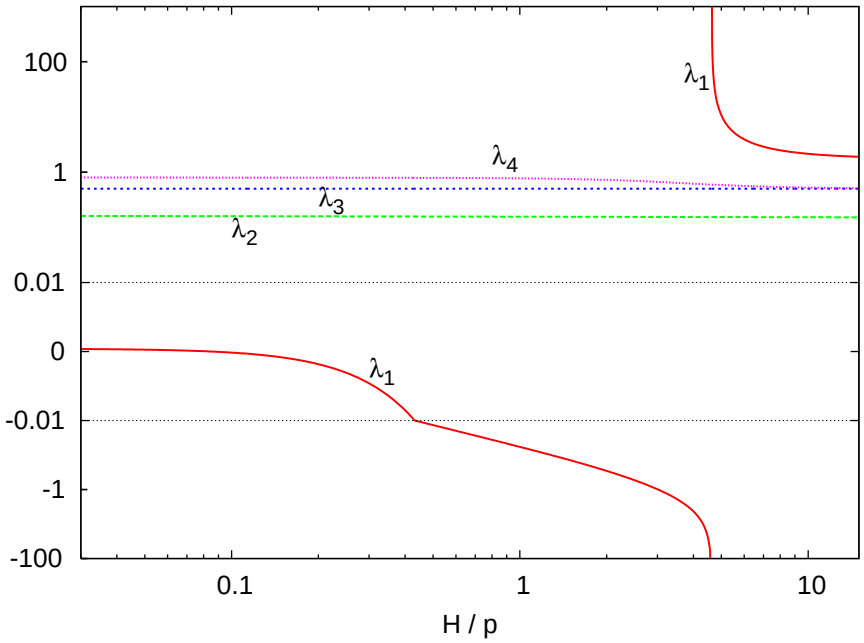

Figure 5.6: Eigenvalues of the kinetic matrix, for the same choice of parameters and initial conditions as in the right panel of Figure 5.5. The eigenvalues $\lambda_{2,3,4}$ are always positive, so that the sign and the behavior of the determinant are determined by λ_1. This eigenvalue is initially positive, crosses zero at $H/p \simeq 0.082$ (see the previous figure), and diverges at $H/p \simeq 4.6$. In the y axis, we have used a linear scale inside the interval $[-0.01,\, 0.01]$, and a logarithmic scale outside.

perturbations around this background solution.

The model and the background solution

The action of the model is given in eq. (5.25), with $\xi = -1/6$, and $N = 3$:

$$S = \int d^4x \sqrt{-g} \sum_{a=1}^{3} \left[-\frac{1}{4} F^{(a)}_{\mu\nu} F^{(a)\,\mu\nu} - \frac{1}{2} \left(-\frac{R}{6} + m^2 \right) A^{(a)}_{\mu} A^{(a)\mu} \right] \tag{5.72}$$

The background vev of the three vectors is chosen as in eq. (5.26), while the background geometry is $ds^2 = -dt^2 + a^2(t)\, d\vec{x}^2$. The system is governed by the equations

$$G_{\mu\nu} = \frac{1}{M_p^2} \sum_{a=1}^{3} T^{(a)}_{\mu\nu}$$

$$T^{(a)}_{\mu\nu} \equiv F^{(a)\,\sigma}_{\mu}\, F^{(a)}_{\nu\sigma} - \frac{1}{4}\, F^{(a)}_{\alpha\beta}\, F^{(a)\,\alpha\beta}\, g_{\mu\nu} + \left(m^2 - \frac{R}{6}\right)\, A^{(a)}_{\mu}\, A^{(a)}_{\nu} - \frac{1}{2}\, m^2\, A^{(a)}_{\alpha}\, A^{(a)\,\alpha}\, g_{\mu\nu}$$
$$-\frac{1}{6}\left(R_{\mu\nu} - \frac{1}{2}\, R\, g_{\mu\nu}\right)\, A^{(a)}_{\alpha}\, A^{(a)\,\alpha} - \frac{1}{6}\, \left(g_{\mu\nu}\,\Box - \nabla_{\mu}\,\nabla_{\nu}\right)\, A^{(a)}_{\alpha}\, A^{(a)\,\alpha}$$
$$\frac{1}{\sqrt{-g}}\,\partial_{\mu}\,\left[\sqrt{-g}\, F^{(a)\,\mu\nu}\right] - \left(m^2 - \frac{R}{6}\right)\, A^{(a)\,\nu} = 0 \tag{5.73}$$

For the background under considerations, the 00 Einstein equation and the $i-th$ spatial component of the equation for the $i-th$ vector give

$$H^2 = \frac{1}{2}\,\left(\dot{B}^2 + m^2\, B^2\right)$$
$$\ddot{B} + 3H\,\dot{B} + m^2\, B = 0 \tag{5.74}$$

As always for a FRW geometry, the diagonal ii Einstein equations does not provide additional information (due to a nontrivial Bianchi identity). The remaining equations vanish identically. Upon the identification $B = \phi_{\rm eff}/\left(\sqrt{3}M_p\right)$, we recover the same equations as those of chaotic inflation driven by a minimally coupled scalar field $\phi_{\rm eff}$ (where the suffix stands for "effective") with potential $V = m^2\phi^2_{\rm eff}/2$. Inflation is therefore characterized by the slow roll evolution

$$H^2 \approx \frac{m^2}{2}\, B^2 \quad , \quad \dot{B} \approx -\frac{m^2}{3H}\, B \tag{5.75}$$

which applies as long as the slow roll conditions [11]

$$\epsilon \equiv \frac{M_p^2}{2}\left(\frac{\frac{dV}{d\phi_{\rm eff}}}{V}\right)^2 = \frac{2\, M_p^2}{\phi_{\rm eff}{}^2} = \frac{2}{3\, B^2} \ll 1$$
$$\eta \equiv M_p^2\, \frac{\frac{d^2V}{d\phi^2_{\rm eff}}}{V} = \frac{2\, M_p^2}{\phi_{\rm eff}{}^2} = \frac{2}{3\, B^2} \ll 1 \tag{5.76}$$

are valid. After that, B performs damped coherent oscillations around $B = 0$ (see for instance [94]):

$$B = \left(\frac{\sqrt{8}}{3\, m\, t} + {\rm O}\left(\frac{1}{m^2\, t^2}\right)\right)\, \sin\left(m\, t + \xi_0\right) \tag{5.77}$$

where ξ_0 is a phase (irrelevant for this discussion). The coherent oscillations provide a stage of effective matter domination ($w = 0$ once averaged over a few oscillations) [94].

[11] See [93] for more detailed studies of initial and slow-roll conditions for vector inflation.

It is expected that the vectors then decay into the visible matter (either perturbatively, or nonperturbatively) giving rise to the radiation dominated stage of cosmology.

From the slow roll conditions, we see that $H^2 \gg m^2$ during most of the inflationary stage. At these times, the mass term for the vectors is negative, $-R/6 + m^2 \simeq -2H^2 + m^2 < 0$. However, R decreases as B rolls towards the origin, while m remains constant. We find numerically that $-R/6 + m^2 = 0$ when $B \simeq 1.048$. This happens towards the end of inflation.

Ghost instability from the quadratic action

We now study the perturbations of the model (5.72) around the background solution just discussed. Since the background geometry is FRW, one may choose to adopt the standard decomposition of metric perturbations, and decompose them into scalar, vector, and tensor modes with respect to 3d spatial rotations, as we did in chapter 2. While this is possible, one should however bear in mind that, contrary to the standard case, these three groups of modes cannot be studied separately even at the linearized level. Consider for instance the tensor perturbations h_{ij}^{TT}, introduced as the traceless ($h_{ii}^{TT} = 0$), and transverse ($\partial_j h_{ij}^{TT} = 0$) part of the spatial metric perturbations, $\delta g_{ij} = a^2 h_{ij}^{TT}$. While in the case of scalar field inflation these modes are decoupled from the other perturbations, and can be studied separately, in the case under consideration they are coupled to the perturbations of the vector fields. Namely, we find the following coupling in the quadratic action $\delta_2 S$ of the perturbations:

$$\delta_2 S \supset -\frac{M_p}{2} \int d^4x\, a^2 \left[\left(\dot{B} + H\, B \right) \delta \dot{A}_j^{(i)} + \left(2H^2 + \dot{H} - m^2 \right) B\, \delta A_j^{(i)} + (i \leftrightarrow j) \right] h_{ij}^{TT} \,. \tag{5.78}$$

As a consequence, the perturbations of the vector fields must be included in the linearized equations of motion for the tensor metric perturbations. In turn, the perturbations of the vector fields are coupled to the scalar and vector perturbations of the metric. One then finds that all the perturbations of the system need to be studied together, even at the linearized level. [12]

[12] Ref. [95] studied the tensor modes alone, arguing that the effect of the coupling to the $\delta A_\mu^{(a)}$ perturbations can be "averaged away" in the limit of many vectors. However, each vector introduces a coupling of h_{ij}^{TT} with its own perturbations, and perturbations of different vectors cannot cancel against each other in the study of the spectrum (and, therefore, of the stability) of the theory.

This makes the study extremely hard, and indeed no complete computation existed until [54]. The metric has 10 perturbations, while each vector introduces 4 perturbations. Thus, in this simplest realization of vector inflation, one starts with a system of 22 coupled modes. Four perturbations can be removed by fixing the freedom of general coordinate transformations, leading to a system of 18 coupled modes. Not all these modes are dynamical. The nondynamical modes originate from the initial perturbations $\delta g_{0\mu}$ and $\delta A_0^{(a)}$, which enter in the quadratic action of the perturbations without time derivatives. As we now show, it is possible to choose gauge invariant perturbations which associate a gauge invariant combination to each of the $\delta g_{0\mu}$ and $\delta A_0^{(a)}$ modes. These seven gauge invariant combinations are also nondynamical fields. We integrate them out as outlined in Section 5.3, and obtain the quadratic action for the dynamical modes. From the study of the kinetic matrix of this system, we find that three modes become ghosts for some time during inflation.

Since the usual decomposition in scalar/vector/tensor modes does not provide decoupled sets of perturbations, we do not employ it, and simply decompose the perturbations as

$$g_{\mu\nu} = \begin{pmatrix} -1-2\Phi & a\chi_1 & a\chi_2 & a\chi_3 \\ & a^2\,(1-2\Psi) & a^2\,\partial_1\,\partial_2\,E_3 & a^2\,\partial_1\,\partial_3\,E_2 \\ & & a^2\,(1-2\Sigma) & a^2\,\partial_2\,\partial_3\,E_1 \\ & & & a^2\,[1-2\,(T-\Psi-\Sigma)] \end{pmatrix}$$

$$A_\mu^{(a)} = A_\mu^{0\,(a)} + \alpha_\mu^{(a)} = a\,M_p\,B\,\delta_\mu^a + \alpha_\mu^{(a)} \tag{5.79}$$

where $A_\mu^{0\,(a)}$ denotes background values of the vector fields. The parametrization of the δg_{33} component has chosen so that $\delta g_i^i = -2\,T$. Moreover, for algebraic convenience, some $\delta g_{\mu\nu}$ entry has been written with spatial derivatives (in practice, we assume that the momentum of the modes - after Fourier transforming - has nonvanishing components in all three directions, k_x, k_y, $k_z \neq 0$).

We need to fix the gauge freedom associated with general coordinate transformations. Consider the infinitesimal transformation $x^\mu \to x^\mu + \xi^\mu$, under which the perturbations of the metric and the vector field transform as $\delta g_{\mu\nu} \to \delta g_{\mu\nu} - g^{(0)}_{\mu\nu\,,\alpha}\xi^\alpha - g^{(0)}_{\mu\alpha}\xi^\alpha_{,\nu} - g^{(0)}_{\alpha\nu}\xi^\alpha_{,\mu}$, and $\delta A_\mu^{(a)} \to \delta A_\mu^{(a)} - A^{(a)}_{\mu,\alpha}\xi^\alpha - A^{(a)}_\alpha\,\xi^\alpha_{,\mu}$. Due to the assumption of the modes we are studying, we need to consider infinitesimal transformations with nontrivial spatial dependence

along all the three directions. We can therefore parametrize the transformation parameter as $\xi^\mu = \left(\xi^0,\, \partial_1\xi^1,\, \partial_2\xi^2,\, \partial_3\xi^3\right)$. The explicit transformations of the modes in (5.79) are then

$$\begin{aligned}
&\Phi \to \Phi - \partial_0\xi^0 \quad , \quad \chi_i \to \chi_i + \frac{1}{a}\,\partial_i\xi^0 - a\,\partial_0\,\partial_i\,\xi^i \;\; \text{(no sum over } i\text{)} \\
&E_1 \to E_1 - \xi_2 - \xi_3 \;\; , \;\; E_2 \to E_2 - \xi_1 - \xi_3 \;\; , \;\; E_3 \to E_3 - \xi_1 - \xi_2 \;\; , \\
&\Psi \to \Psi + H\,\xi^0 + \partial_1^2\xi^1 \;\; , \;\; \Sigma \to \Sigma + H\,\xi^0 + \partial_2^2\xi^2 \;\; , \;\; T \to T + 3\,H\,\xi^0 + \partial_i^2\xi^i \\
&\alpha_\mu^{(i)} \to \alpha_\mu^{(i)} - \partial_0\,(a\,M_p\,B)\,\xi^0\,\delta_\mu^i - a\,M_p\,B\,\partial_\mu\,\partial_i\xi^i \;\; \text{(no sum over } i\text{)}
\end{aligned} \tag{5.80}$$

We consider the combinations

$$\begin{aligned}
&C^1 \equiv \frac{E_1 - E_2 - E_3}{2} \;\; , \;\; C^2 \equiv \frac{E_2 - E_1 - E_3}{2} \;\; , \;\; C^3 \equiv \frac{E_3 - E_1 - E_2}{2} \;\; , \\
&C^0 \equiv \frac{1}{3\,H}\left[T - \partial_i^2\,C^i\right]
\end{aligned} \tag{5.81}$$

that transform as $C^\mu \to C^\mu + \xi^\mu$. Then, the modes

$$\begin{aligned}
\hat{\Phi} &\equiv M_p\left(\Phi + \partial_0\,C^0\right) \\
\hat{\chi}_i &\equiv M_p\left(\chi_i - \frac{1}{a}\,\partial_i\,C^0 + a\,\partial_0\,\partial_i\,C^i\right) \;\; \text{(no sum over } i\text{)} \\
\hat{\Psi} &\equiv M_p\left(\Psi - H\,C^0 - \partial_1^2\,C^1\right) \\
\hat{\Sigma} &\equiv M_p\left(\Sigma - H\,C^0 - \partial_2^2\,C^2\right) \\
\hat{\alpha}_\mu^{(i)} &\equiv \alpha_\mu^{(i)} + \partial_0\,(a\,M_p\,B)\,C^0\,\delta_\mu^i + a\,M_p\,B\,\partial_\mu\,\partial_i C^i \;\; \text{(no sum over } i\text{)}
\end{aligned} \tag{5.82}$$

are gauge invariant (all these modes have mass dimension $+1$).

We expanded the metric and vector fields according to (5.79), and computed the quadratic action for the perturbations. We verified that the perturbations rearrange so that the quadratic action can be written solely in terms of the gauge invariant modes (5.82) (this is a nontrivial check on our algebra). In this way, we have eliminated the redundancy associated to general coordinate transformations. [13] The action in Fourier space reads

$$\delta_2 S \;\; = \;\; \int d^3k\,dt\,a^3\,\mathcal{L}$$

[13] Notice that the procedure we adopted is equivalent to choose the gauge $E_1 = E_2 = E_3 = T = 0$. It is easy to see from (5.80) that this choice can always be made, and it completely fixes the gauge freedom.

$$
\begin{aligned}
\mathcal{L} \;=\; & \frac{1}{2}\,\left(2+B^2\right)\,\left(|\dot{\hat{\Psi}}|^2+|\dot{\hat{\Sigma}}|^2\right)+\frac{1}{2a^2}\,\sum_{j,a=1}^{3}|\dot{\hat{\alpha}}_j^{(a)}|^2+\frac{1}{4}\,\left(2+B^2\right)\,\left(\dot{\hat{\Psi}}^*\,\dot{\hat{\Sigma}}+\text{h.c.}\right)\\
& -\frac{1}{4}\,\left(2+B^2\right)\,\left[i\,\dot{\hat{\Psi}}^*\,\left(p_1\,\hat{\chi}_1-p_3\,\hat{\chi}_3\right)+i\dot{\hat{\Sigma}}^*\,\left(p_2\,\hat{\chi}_2-p_3\,\hat{\chi}_3\right)+\text{h.c.}\right]\\
& +\frac{1}{2a}\,\sum_{j,a,=1}^{3}\left(i\,p_j\,\dot{\hat{\alpha}}_j^{(a)*}\,\hat{\alpha}_0^{(a)}+\text{h.c.}\right)-\frac{1}{2\,a}\,\dot{B}\,\sum_{j=1}^{3}\left(\dot{\hat{\alpha}}_j^{(j)*}\,\hat{\Phi}+\text{h.c.}\right)\\
& +\frac{B}{6\,a}\,\sum_{j,a,=1}^{3}\left(ip_j\,\hat{\chi}_j^*\,\dot{\hat{\alpha}}_a^{(a)}\;+\text{h.c.}\right)-\frac{3}{2}\,m^2\,B^2\,|\hat{\Phi}|^2\\
& -\frac{1}{2}\,\left(H\,B+\dot{B}\right)\,\sum_{j=1}^{3}\left(i\hat{\Phi}^*\,p_j\,\hat{\alpha}_0^{(j)}+\text{h.c.}\right)\\
& +\frac{1}{2}\,\left[B\,\dot{B}+\left(2+B^2\right)\,H\right]\,\sum_{j=1}^{3}\left(i\hat{\Phi}^*\,p_j\,\hat{\chi}_j+\text{h.c.}\right)\\
& +\frac{1}{2}\,\left(p^2+m^2+H^2-\frac{3}{2}\,m^2\,B^2\right)\,\sum_{a=1}^{3}|\hat{\alpha}_0^{(a)}|^2\\
& -\frac{B}{2}\,\left(H^2+m^2-\frac{3}{2}\,m^2\,B^2\right)\,\sum_{j=1}^{3}\left(\hat{\alpha}_0^{(j)*}\,\hat{\chi}_j+\text{h.c.}\right)\\
& +\frac{1}{4}\,\sum_{j=1}^{3}\left[p^2+\frac{1}{2}\,\left(p^2+4m^2\right)\,B^2-3\,m^2\,B^4+2\,H^2\,B^2\right]\,|\hat{\chi}_j|^2\\
& -\frac{1}{8}\,\left(2+B^2\right)\,\sum_{i,j=1}^{3}p_i\,p_j\,\hat{\chi}_i\,\hat{\chi}_j^*+\ldots
\end{aligned}
\tag{5.83}
$$

where we have used the physical momenta $p_i \equiv k_i/a$. Eq. (5.83) actually is not the full quadratic action of the perturbations, but some terms (denoted by dots) are omitted. Let us clarify this. We find that no time derivatives of the combinations $\hat{\Phi}$, $\hat{\chi}_i$, $\hat{\alpha}_0^{(a)}$ enter in the quadratic action (neither in the terms shown here, nor in those omitted). These are the nondynamical gauge invariant modes of the system. [14] The remaining modes are dynamical. Eq. (5.83) is the action for all the gauge invariant modes of the system (both the dynamical, and the nondynamical ones). However, it contains only the terms that contribute to the kinetic matrix of the action for the dynamical modes,

[14] Notice that they corresponds to the nondynamical perturbations $\delta g_{0\mu}$ and $\delta A_0^{(a)}$ in the gauge $E_1 = E_2 = E_3 = T = 0$.

once the nondynamical modes have been integrated out. [15] These terms are given without any omission, nor approximation, so that eq. (5.83) contains all the necessary information for the exact computation of the kinetic matrix of the dynamical modes.

Before integrating out the nondynamical modes, we can easily see that 5 dynamical modes decouple from the remaining ones in the part of the action shown. There are 9 dynamical modes in the spatial perturbations of the three vector fields, $\hat{\alpha}_j^{(a)}$. These perturbations enter in the action (5.83) with a diagonal quadratic term (the second term, $\propto |\hat{\alpha}_j^{(a)}|^2$). Then, they are coupled with the remaining modes only in the third line of (5.83)). We see that, out of the nine modes $\hat{\alpha}_j^{(a)}$, only the four linear combinations $p_j \dot{\hat{\alpha}}_j^{(a)}$ $(a = 1, 2, 3)$ and $\dot{\hat{\alpha}}_j^{(j)}$ are involved in these couplings. The remaining 5 linear combinations are decoupled. Therefore, we can rotate the fields $\hat{\alpha}_j^{(a)}$ into the coupled and decoupled linear combinations:

$$
\begin{aligned}
\hat{\alpha}_1^{(1)} &= \frac{p_{23}^2}{\sqrt{2}\,p^2}\,\hat{v}_1 + \frac{p_1}{p}\,\hat{v}_2 + \frac{p_{12}\,p_{23}}{p\,\sqrt{p_{12}^2+p_{23}^2}}\,\hat{v}_8 - \frac{p_{13}\,p_{23}^2}{\sqrt{2}\,p^2\,\sqrt{p_{12}^2+p_{23}^2}}\,\hat{v}_9 \\
\hat{\alpha}_2^{(1)} &= -\frac{p_1\,p_2}{\sqrt{2}\,p^2}\,\hat{v}_1 + \frac{p_2}{p}\,\hat{v}_2 + \frac{p_3}{p_{23}}\,\hat{v}_5 - \frac{p_1\,p_2\,p_{12}}{p_{23}\,p\,\sqrt{p_{12}^2+p_{23}^2}}\,\hat{v}_8 + \frac{p_1\,p_2\,p_{13}}{\sqrt{2}\,p^2\,\sqrt{p_{12}^2+p_{23}^2}}\,\hat{v}_9 \\
\hat{\alpha}_3^{(1)} &= -\frac{p_1\,p_3}{\sqrt{2}\,p^2}\,\hat{v}_1 + \frac{p_3}{p}\,\hat{v}_2 - \frac{p_2}{p_{23}}\,\hat{v}_5 - \frac{p_1\,p_{12}\,p_3}{p_{23}\,p\,\sqrt{p_{12}^2+p_{23}^2}}\,\hat{v}_8 + \frac{p_1\,p_3\,p_{13}}{\sqrt{2}\,p^2\,\sqrt{p_{12}^2+p_{23}^2}}\,\hat{v}_9 \\
\hat{\alpha}_1^{(2)} &= -\frac{p_1\,p_2}{\sqrt{2}\,p^2}\,\hat{v}_1 + \frac{p_1}{p}\,\hat{v}_3 - \frac{p_3}{p_{13}}\,\hat{v}_6 - \frac{p_1\,p_2\,\sqrt{p_{12}^2+p_{23}^2}}{\sqrt{2}\,p_{13}\,p^2}\,\hat{v}_9 \\
\hat{\alpha}_2^{(2)} &= \frac{p_{13}^2}{\sqrt{2}\,p^2}\,\hat{v}_1 + \frac{p_2}{p}\,\hat{v}_3 + \frac{p_{13}\,\sqrt{p_{12}^2+p_{23}^2}}{\sqrt{2}\,p^2}\,\hat{v}_9 \\
\hat{\alpha}_3^{(2)} &= -\frac{p_2\,p_3}{\sqrt{2}\,p^2}\,\hat{v}_1 + \frac{p_3}{p}\,\hat{v}_3 + \frac{p_1}{p_{13}}\,\hat{v}_6 - \frac{p_2\,p_3\,\sqrt{p_{12}^2+p_{23}^2}}{\sqrt{2}\,p_{13}\,p^2}\,\hat{v}_9 \\
\hat{\alpha}_1^{(3)} &= -\frac{p_1\,p_3}{\sqrt{2}\,p^2}\,\hat{v}_1 + \frac{p_1}{p}\,\hat{v}_4 + \frac{p_2}{p_{12}}\,\hat{v}_7 + \frac{p_1\,p_3\,p_{23}}{p_{12}\,p\,\sqrt{p_{12}^2+p_{23}^2}}\,\hat{v}_8 + \frac{p_1\,p_3\,p_{13}}{\sqrt{2}\,p^2\,\sqrt{p_{12}^2+p_{23}^2}}\,\hat{v}_9 \\
\hat{\alpha}_2^{(3)} &= -\frac{p_2\,p_3}{\sqrt{2}\,p^2}\,\hat{v}_1 + \frac{p_2}{p}\,\hat{v}_4 - \frac{p_1}{p_{12}}\,\hat{v}_7 + \frac{p_2\,p_3\,p_{23}}{p_{12}\,p\,\sqrt{p_{12}^2+p_{23}^2}}\,\hat{v}_8 + \frac{p_2\,p_3\,p_{13}}{\sqrt{2}\,p^2\,\sqrt{p_{12}^2+p_{23}^2}}\,\hat{v}_9 \\
\hat{\alpha}_3^{(3)} &= \frac{p_{12}^2}{\sqrt{2}\,p^2}\,\hat{v}_1 + \frac{p_3}{p}\,\hat{v}_4 - \frac{p_{12}\,p_{23}}{p\,\sqrt{p_{12}^2+p_{23}^2}}\,\hat{v}_8 - \frac{p_{12}^2\,p_{13}}{\sqrt{2}\,p^2\,\sqrt{p_{12}^2+p_{23}^2}}\,\hat{v}_9
\end{aligned}
\tag{5.84}
$$

where for brevity we have defined $p_{ij} \equiv \sqrt{p_i^2 + p_j^2}$.

[15] For clarity, compare with the formal discussion of Section 5.3. The action (5.83) given here corresponds to the formal action (4.52), with only the terms proportional to the coefficients a_{ij}, b_{ij}, and c_{ij} included. Those are the only terms necessary to compute the kinetic matrix K of the dynamical modes, cf. equations (4.55) and (4.54).

The combinations $\hat{v}_1, \ldots, \hat{v}_4$ are the coupled modes, while $\hat{v}_5, \ldots, \hat{v}_9$ are decoupled from the remaining perturbations. One can check that the matrix relating the vector $\left\{\hat{\alpha}_1^{(1)}, \hat{\alpha}_2^{(1)}, \hat{\alpha}_3^{(1)}, \hat{\alpha}_1^{(2)}, \ldots, \hat{\alpha}_3^{(3)}\right\}$ to the vector $\{\hat{v}_1, \ldots, \hat{v}_9\}$ is orthogonal. Therefore, the quadratic term $\propto \sum_{j,a} |\hat{\alpha}_j^{(a)}|^2$ becomes $\propto \sum_i |\hat{v}_i|^2$. As a consequence, the modes $\hat{v}_5, \ldots, \hat{v}_9$ enter only through the term

$$\mathcal{L} \supset \frac{1}{2\,a^2} \sum_{i=5}^{9} |\dot{\hat{v}}_i|^2 \tag{5.85}$$

and are therefore decoupled from the other modes in the part of the action shown in (5.83) (we stress that this part is all we need to compute the kinetic term for the dynamical modes). Since the coefficient in front of each term in the sum (5.85) is positive, we see that these modes are well behaved (positive energy) excitations. Let us now focus on the coupled system of the remaining modes (which includes the remaining 6 dynamical modes, and the 7 nondynamical modes). The next step is to integrate out the nondynamical modes as outlined formally in equations form (4.52) to (4.54). Doing so, we end up with a rather long kinetic matrix for the six dynamical modes $\{\hat{\Psi}, \hat{\Sigma}, \hat{v}_i\}$ $(i = 1, 2, 3, 4)$. We were unable to perform analytical simplifications of this matrix, as those leading to the expressions (5.64) and (5.71) for the simpler models studied above. However, we can evaluate this matrix numerically for any given choice of parameters.

More specifically, we show the results of a numerical evolution starting from $B_{in} = 10$, $\dot{B}_{\rm in} = -\sqrt{2}\,m/3$ according to the slow roll conditions (5.75), and with momentum of the modes initially satisfying $p_1 = 100\,H$, $p_2 = 80\,H$, $p_3 = 60\,H$ (these values have be chosen only for illustrative purposes and have no particular relevance, other that we require the mode to be well inside the horizon initially; we verified that other choices of the momenta lead to the same conclusions as those shown here). We show in Figures 5.7 and 5.8 the evolution of the eigenvalues of the kinetic matrix (the second Figure is a close-up of the first one where the eigenvalue λ_3 crosses zero) close to horizon crossing. [16]

We see that two eigenvalues $\lambda_{1,2}$ are initially negative; the corresponding eigenvalues are ghosts at these times. These eigenvalues become positive without crossing zero (they diverge). A third eigenvalue λ_3 is initially positive, but it becomes negative crossing

[16] The overall factor a^3 appearing in (5.83) has not been included in this computation. This is irrelevant for our discussion, since this factor simply rescales all eigenvalues by a common positive number.

zero. It then diverges and becomes again positive. As the formal equations (4.56) show, the linearized system of equations becomes singular when this eigenvalue crosses zero. We expect that also the linearized solutions diverge at this point (cf. the explicit solutions given in the model of Subsection 5.5.1).

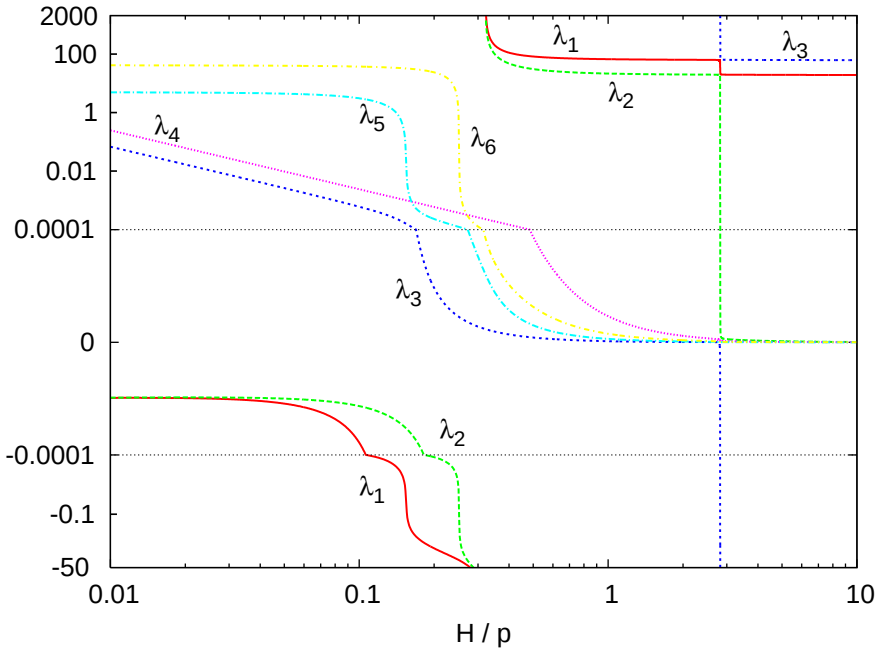

Figure 5.7: Eigenvalues of the kinetic matrix for the dynamical and gauge invariant perturbations $\hat{\Psi}$, $\hat{\Sigma}$, $\hat{v}_{1,\ldots,4}$ for the model of vector inflation (5.72), and for one specific choice of initial conditions (see the main text). Since H/p increases with time during the stage shown, we use it as a "time variable" in this and the next Figure. The eigenmodes corresponding to $\lambda_{1,2}$ are ghosts at the earliest times shown (low H/p). The mode corresponding to λ_3 becomes a ghost close to horizon crossing. This eigenvalues (and the determinant of the kinetic matrix) crosses zero at this point, signaling an instability of the system also at the linearized level. The kinetic matrix, and its eigenvalues, are dimensionless. Notice that we use linear units in the interval $[-0.0001, 0.0001]$, and logarithmic units outside.

The study so far concentrated on the nature of the modes at horizon crossing, in an inflationary regime for which the total mass term of the vectors was negative, $-R/6 + m^2 \simeq -2H^2 + m^2 < 0$. However, as we discussed after eq. (5.77), $-R/6 + m^2$ vanishes towards the end of inflation.We studied the behavior of the eigenvalues of the kinetic matrix also around this point. We considered the same background evolution as

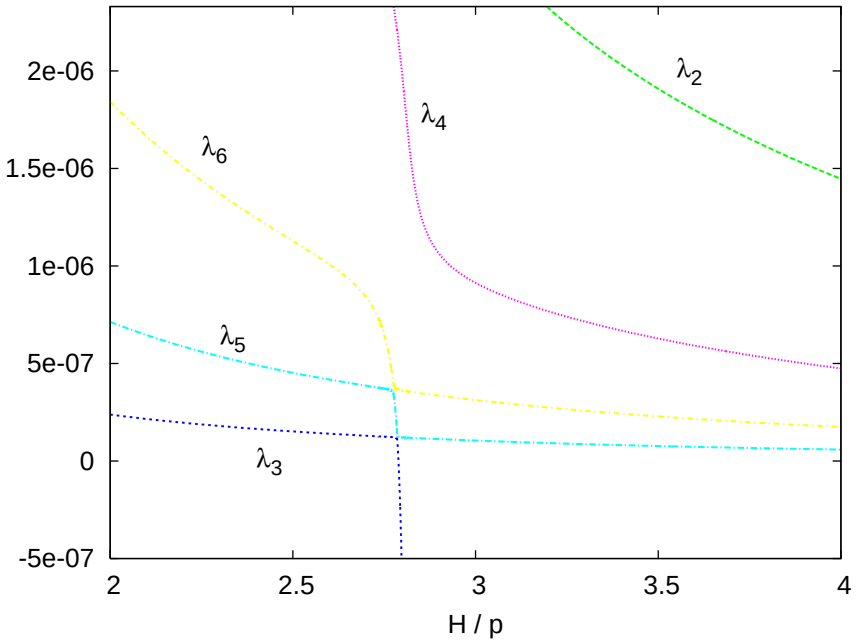

Figure 5.8: Close up of the previous Figure where λ_3 vanishes. A further close up shows that λ_5 and λ_6, and, later, λ_3 and λ_5 do not cross each other, although they appear to do so in the Figure.

for the previous plot, but smaller values of the momenta, so that H/p is not exponentially small at the times shown (we want to avoid that our results are affected by numerical inaccuracies). As shown in Figure 5.9, we find that two eigenvalues cross zero precisely when the total mass vanishes. Also at this point, the system of equations for the eigenvalues becomes singular We expect that the linearized solutions diverge also at this point.

It is interesting to compare the behavior of the eigenvalues shown in these Figures with that obtained for the previous models. We find that the two eigenvalues $\lambda_{1,2}$ behave precisely as in the case of zero vev studied in the previous Section: they are negative in the deep sub-horizon regime, they diverge close to horizon crossing, and they cross zero when the total mass vanishes. On the contrary, the eigenvalue λ_3 behaves precisely as in the cases of a single vector with nonvanishing vev studied above (cf. Figures 5.3 and 5.6): it is positive in the deep sub-horizon regime, it crosses zero close to horizon crossing, and it remains negative for some time afterwards. It appears from these behaviors that

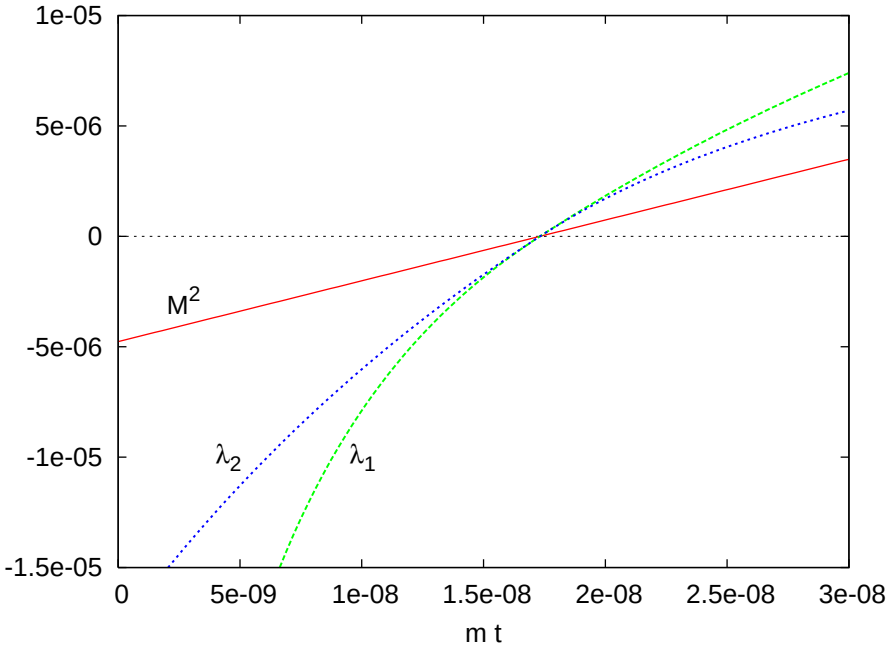

Figure 5.9: Two eigenvalues vanish when the mass term $M^2 = m^2 - R/6$ of the vector fields vanishes. The mass M^2 is shown in units of $m^2/300$. We have $B \simeq 1.048$ when the total mass vanishes (this occurs still during inflation). The mode has been chosen to be outside the horizon when the total mass vanishes ($H/p \simeq 1872$ at the time shown, and $k_1 : k_2 : k_3 = 10 : 8 : 4$).

the mixing with gravity affects only one linear combination of the three ghosts.

5.6 Discussion

Although the paradigm of inflation is well supported by the observational data, we still do not know the actual particle physics mechanism behind the inflationary expansion, and the generation of cosmological perturbations. It is customary to parametrize our ignorance in terms of scalar fields: they may be fundamental fields, or simply order parameters which provide an effective description of some degrees of freedom in the theory (for instance, the brane-antibrane separation in some string motivated models of inflation). However, it may well be possible that these two key elements of cosmology are due to higher spin fields. Vector fields are probably the simplest possibility after scalars. They can in principle leave a distinct signature from the scalar case, since a

nonvanishing spatial vev of a vector breaks the isotropy of space. This can provide anisotropic expansion, and / or generate a spectrum of primordial perturbations that breaks statistical isotropy. The main obstacle faced by explicit realizations of this idea is that, in the standard case, vector fields decrease too quickly due to the expansion of the universe. Therefore, suitable modifications of the standard action need to be made.

We have studied a class of models in which the vector is nonminimally coupled to the curvature, $\mathcal{L} \supset R/12\, A^\mu\, A_\mu$. Indeed, for this specific coupling, the vev of the vector evolves as that of a minimally coupled scalar field; this offers the possibility of realizing an inflationary background, with a controllable anisotropy [8, 11]. In addition, the transverse perturbations of the vector behave as the perturbations of a minimally coupled scalar; this is the basis of the mechanism of vector curvaton [13] for the generation of a nearly scale invariant spectrum of primordial perturbations. To our knowledge, the analogy between the $R/12\, A^\mu\, A_\mu$ coupling and the minimally couple scalar field first appeared in the 1987 work by Turner and Widrow [55], where it was exploited for the generation of a primordial magnetic field during inflation. The renewed interest in this mechanism is mostly motivated by some features in the WMAP data that hint for a small break of statistical isotropy.

All of the mentioned works suggested new interesting mechanisms, and a complete check of the stability of these proposals was beyond their scope. It is tempting to assume that these models should be well behaved due to the strong analogy with the minimally coupled scalar field case. There is however a crucial difference between these two cases, and between the case of a minimally vs a nonminimally couple vector; it is due to the longitudinal vector polarization. In the above works, the vector has a U(1) invariant kinetic term $\mathcal{L} \supset -1/4 F_{\mu\nu} F^{\mu\nu}$. If only this term was present, the vector would only have the two transverse polarizations. However, the nonminimal coupling to the curvature breaks the U(1) symmetry, and gives rise to an additional, longitudinal, polarization. The nature of this mode is controlled by the sign of the mass term, which, for these mechanisms to work, needs to be negative. For the scalar case, a negative mass squared means that the field is a tachyon; for a vector field, a negative mass squared means that the longitudinal polarization is a ghost.

Motivated by this initial consideration, we studied the stability of this class of theories. We did so by computing the free action for the dynamical (physically propagating)

modes of such theories, around the background solutions considered in the various proposals. The sign of the eigenvalues of the kinetic matrix of these action indicates whether the corresponding eigenmode is a positive or negative energy excitation. Our computations confirmed that there is a ghost for each nonminimally coupled vector field in the model. As we already mentioned previously, theories with ghosts can only be consistent only as effective theories, valid below some energy scale Λ. Inflationary predictions heavily rely on the initial conditions; for instance, the vector curvaton mechanism of [13] results in a scale invariant spectrum because of the specific choice of initial adiabatic vacuum. This choice is made in the quantized theory for the perturbations, which is performed in the deep UV regime (energy $\gg H^{-1}$) [5]. In presence of a cut-off, the initial adiabatic vacuum cannot be imposed at arbitrarily early times, and, depending on the precise numerical value of the cut-off, it may not be possible to impose it at all. This casts doubts on the phenomenological predictions obtained for such models.

In fact, all theories with an explicit mass M for the vector require a cut-off which makes them invalid at high energies, irrespectively of the sign of the mass term. We can see this based on the behavior of massive vector fields at high energies. The explicit mass breaks the gauge invariance in a hard way. It is well known that, in such case, the interactions of the longitudinal bosons violate unitarity at a scale which is parametrically set by M, leading to a quantum theory out of control. For the present models, M is the Hubble rate or below, so that the entire sub-horizon regime may be ill-defined. At high energies, the longitudinal mode will also interact strongly with the other fields in the theory (this will renormalize the coupling constants). Then, depending on exactly when this happens, the quantum theory of the perturbations may be out of control throughout the entire short wavelength regime. If this is the case, all initial conditions would become unjustified, and the theory would lose its predictive power. Although this problem is present for both positive and negative mass terms, a theory which has a hard vector mass and a ghost is more problematic than a theory with only a hard vector mass. The most immediate UV completion of a theory with a hard mass is through a Higgs mechanism. The mass would be then due to the vev of a scalar field that becomes dynamical above the scale M. In this way the theory remains under control also in the short wavelength regime, and one can apply all the standard computations valid for scalar fields during inflation. However, if M^2 needs to have the wrong sign, the scalar

field in this UV completed theory needs to be a ghost. In fact, we are not aware of any well behaved UV completion of a theory with a ghost.

The most obvious problem associated to a ghost is the instability of the vacuum. If a ghost is coupled to a normal field (and, in all the above theories, there are at least gravitational couplings), the vacuum will decay in ghost-nonghost excitations, with a rate which is UV divergent. This is simply due to phase space considerations. In normal situations, a source of any given energy can produce quanta up to some given momentum; this cuts-off the phase space available to the decay products. However, the quanta of a ghost field have negative energy: the higher their momentum, the more negative the energy is. Therefore, even a zero energy source decays into ghost-nonghost excitations conserving both energy and momentum. One may hope that the nonlinear interactions may somewhat arrange to cancel the total decay rate. However, this does not appear likely. The usual approach is to regard theories with ghosts as effective theories, valid only below some energy scale. For instance, a theory with a ghost today, coupled only gravitationally to satndard model fields, is only valid for energies $E \lesssim 3\,\mathrm{MeV}$, otherwise we would see signatures of the vacuum decay in the diffuse γ-ray background [97]. A stronger coupling would result in a tighter bound on E.

We stress that this instability is not related to the classical behavior of the solutions of the linearized equations for the perturbations, and it would be present even if the latter remained finite. However, we argued that, for the models considered here, also the linearized solutions diverge. This is a second instability that adds up to the one we have just discussed. This instability appears because the eigenvalues corresponding to the ghosts do not remain negative over the whole evolution, but change sign, and cross zero at some finite moment of time t_* (there are two such moments in the model of vector inflation considered here). We showed that the linearized equations are singular at t_*, and we expect that the linearized solutions diverge for $t \to t_*$. While it is possible that the divergency does not occur at the full nonlinear level, this instability also invalidates all the phenomenological signatures of these models which are based on the linearized computation (as for instance the primordial spectrum of perturbations). We solved the linearized equations only in the simplest cases of a vector field with no vev, and of a vector field with vev plus a cosmological constant. We did not solve them for the models

[8, 11]. We have shown however that the linearized equations become singular also in these cases. It is important to stress that even if, due to some unexpected cancellation, the solutions to these equations would remain finite, this would not eliminate the ghost instability that we have discussed in the two previous paragraphs, and that we have proven to be present for all the models studied here.

We conclude the discussion with some remarks on models different from those considered here. The instability we pointed out motivates the study of such models, as for instance vector fields with nonstandard kinetic terms [46, 98, 99] (although, some of these proposals are also unstable), nonabelian vectors with nonminimal coupling to the curvature [100] [17] , spinors [7], or higher $p-$forms [44, 9, 101] [18] . Of particular interest, in our opinion, is a class of models characterized by a function of a scalar field multiplying the kinetic terms of the vectors, $f^2(\phi) F^{\mu\nu} F_{\mu\nu}$, but no potential term for the vector [99, 12]. U(1) invariance is preserved in these models, and the problematic longitudinal mode is absent. A complete study of the cosmological perturbations (conducted along the lines described here) is the next necessary step for obtaining the phenomenological predictions of these models. In the following chapters, we study the background and perturbations of these models. We will demonstrate that they are stable as expected, and we compute the relevant spectra of perturbations.

[17] The stability analysis performed here applies also to the nonabelian model of [100] if the vectors have no vev (since, in this case, the nonabelian structure does not affect the quadratic action for the perturbations); however, the case with a nonvanishing vev requires a separate investigation.

[18] The vector case is $p = 1$; Ref. [101] generalized the arguments of [52, 53], and pointed out that also the $p = 2$ case contains ghosts.

Chapter 6

Models with vector fields kinetically coupled to a scalar field

In this chapter we study a class of models, where the vector field is coupled kinetically to a scalar field which drives an inflationary expansion. These types of models are recenlty discussed by references [12, 56]. The coupling is of the form $f^2(\phi)\, F_{\mu\nu}\, F^{\mu\nu}$, and therefore the $U(1)$ gauge invariance of the vector field is unbroken. This means that the longitudinal mode, which was related to the instabilities we have discussed before, does not exist. However, the conformal invariance of the vector field is broken, which has interesting consequences. The scalar field ϕ drives the inflationary expansion in these models. When the vector field has a non-vanishing vev along one of the spatial directions, the model possess an anisotropically expanding attractor solution. The anisotropy in the attractor is initially small, but it increases towards the end of inflation; therefore this is a counter example to the cosmic no hair conjecture (See [44] for a another example). The breaking of the conformal invariance due to the scalar-vector coupling can also be used to generate magnetic fields from inflation, as discussed in reference [55] and more recently in [56]. These models are expected to be free from ghost-instabilities as long as the coupling to the scalar field remains positive. In this chapter, we perform the full perturbative analysis of these models following references [57, 58]. We will prove

that the model is stable by studying the quadratic action for perturbations and solving the linearized Einstein equations. We find that all the perturbations have regular kinetic terms (there are no ghosts) and their evolution is stable and free of instabilities. In addition, we will compute the power spcetrum of a single gravity wave mode as an example in a model where there are two scalar fields. In the next chapter, we will give a complete analysis of power spectra in these type of models.

6.1 Anisotropic inflationary expansion due to coupled vector and scalar fields

The models we discuss in this chapter and the next are generically described by the following action

$$\begin{aligned} S &= \int d^4x\,\sqrt{-g}\left[\frac{M_p^2}{2}\,R-\sum_{a=1}^{N}\left(\frac{1}{2}\,\partial_\mu\phi_a\,\partial^\mu\phi_a+V_a(\phi_a)\right)\right. \\ &\qquad \left.-\frac{1}{2}\,\partial_\mu\phi\,\partial^\mu\phi-V(\phi)-\frac{1}{4}\,f^2(\phi)\,F_{\mu\nu}\,F^{\mu\nu}\right] \end{aligned} \tag{6.1}$$

The original discussion of these coupled vector-scalar field theories in an anisotropic inflationary background was given in [12], where there is only the single scalar field ϕ in the action. We assume that only one of the scalar fields (or only one linear combination) enters in the kinetic function f for the vector field. We denote the remaining scalars with ϕ_a $(a=1,\ldots,N)$. The metric ansatz is taken to be the homogeneous but anisotropic Bianchi-I metric given by

$$ds^2=-dt^2+e^{2\alpha(t)}\,\left[e^{-4\sigma(t)}\,dx^2+e^{2\sigma(t)}\,\left(dy^2+dz^2\right)\right] \tag{6.2}$$

In the above metric α measures the number of e-folds of average isotropic expansion of the universe and σ measures the anisotropy. This metric also possesses a left over $2d$ isotropy in the $y-z$ plane (which we make use of when decomposing the perturbations). We can also identify (6.2) with (4.11), then we would

$$a=e^{\alpha-2\sigma}\ ,\ b=e^{\alpha+\sigma}\ ,\ H\equiv\frac{H_a+2H_b}{3}=\dot{\alpha}\ ,\ h\equiv\frac{H_b-H_a}{3}=\dot{\sigma} \tag{6.3}$$

where $H_a=\dot{a}/a$, $H_b=\dot{b}/b$, H is the average isotropic expansion rate, and h is the anisotropic expansion rate. An isotropic flat FRW universe is the limiting case when

$h \to 0$. We will make use of both representations of the Bianchi-I metric in the following discussions. The field equations obtained from the action (6.1) are

$$\begin{aligned}
G_{\mu\nu} &= \frac{1}{M_p^2}\left[\partial_\mu\phi\,\partial_\nu\phi - g_{\mu\nu}\,\left(\frac{1}{2}\,\partial_\alpha\phi\,\partial^\alpha\phi + V\,(\phi)\right) + \sum_{a=1}^{N} T^{(a)}_{\mu\nu}\right. \\
&\qquad \left. + f^2\,(\phi)\;F_\mu^{\ \alpha}\,F_{\nu\,\alpha} - \frac{1}{4}\,g_{\mu\nu}\,f^2\,(\phi)\;F_{\alpha\,\beta}\,F^{\alpha\,\beta}\right] \\
&\frac{1}{\sqrt{-g}}\,\partial_\mu\,\left[\sqrt{-g}\,g^{\mu\nu}\,\partial_\nu\,\phi\right] - V'\,(\phi) - \frac{f(\phi)\,f'(\phi)}{2}\,F_{\alpha\,\beta}\,F^{\alpha\,\beta} = 0 \\
&\frac{1}{\sqrt{-g}}\,\partial_\mu\,\left[\sqrt{-g}\,g^{\mu\nu}\,\partial_\nu\,\phi_a\right] - V_a'\,(\phi_a) = 0 \\
&\frac{1}{\sqrt{-g}}\,\left[\sqrt{-g}\,f^2\,(\phi)\;F^{\mu\nu}\right] = 0
\end{aligned} \tag{6.4}$$

where

$$T^{(a)}_{\mu\nu} = \partial_\mu\phi_a\,\partial_\nu\phi_a - g_{\mu\nu}\,\left(\frac{1}{2}\,\partial_\alpha\phi_a\,\partial^\alpha\phi_a + V_a(\phi_a)\right) \tag{6.5}$$

and $f'(\phi) \equiv df/d\phi$. We assume that all the scalar fields are homogeneous so that $\phi = \phi(t)$ and $\phi_a = \phi_a(t)$ for all a. The vector field is assumed to have a homogeneous vacuum expectation value along the x-direction so $A_\mu = (0,\, A_1(t),\, 0,\, 0)$ (a homogeneous A_0 does not enter into the field equations, and can be set to zero by using the $U(1)$ gauge invariance). With the metric and vector field ansatz, the last of (6.4) can be integrated to give

$$\dot{A}_1 = f^{-2}\,(\phi)\;p_A\,e^{-\alpha-4\sigma} \tag{6.6}$$

where p_A is an integration constant. We use (6.6) and the metric ansatz (6.2) in the field equations (6.4) to obtain the evolution equations

$$\begin{aligned}
&3\dot{\alpha}^2 - 3\dot{\sigma}^2 = \frac{1}{M_p^2}\,\left[\frac{1}{2}\,\dot{\phi}^2 + V\,(\phi) + \sum_{a=1}^{N}\,\rho_a(t)\right] + \frac{\tilde{p}_A^2}{2M_p^2}\,f^{-2}\,(\phi) \\
&2\ddot{\alpha} + 3\dot{\alpha}^2 + 3\dot{\sigma}^2 = \frac{1}{M_p^2}\,\left[-\frac{1}{2}\,\dot{\phi}^2 + V\,(\phi) - \sum_{a=1}^{N}\,p_a(t)\right] - \frac{\tilde{p}_A^2}{6M_p^2}\,f^{-2}\,(\phi) \\
&\ddot{\sigma} + 3\dot{\alpha}\,\dot{\sigma} = \frac{\tilde{p}_A^2}{3M_p^2}\,f^{-2}\,(\phi) \\
&\ddot{\phi} + 3\dot{\alpha}\,\dot{\phi} + V'\,(\phi) - \tilde{p}_A^2\,f^{-3}\,(\phi)\;f'\,(\phi) = 0 \\
&\ddot{\phi}_a + 3\,\dot{\alpha}\,\dot{\phi}_a + V_a'(\phi_a) = 0 \quad , \quad a = 1, \ldots, N
\end{aligned} \tag{6.7}$$

where we have defined

$$\rho_a \equiv \frac{1}{2}\,\dot{\phi}_a^2 + V_a(\phi_a) \quad , \quad p_a \equiv \frac{1}{2}\,\dot{\phi}_a^2 - V_a(\phi_a) \quad , \quad \tilde{p}_A \equiv p_A\, e^{-2\,(\alpha+\sigma)} \tag{6.8}$$

The values of the functions α and σ are nonphysical; what is physical is their time derivatives. Therefore physics is the same under a constant shift $\alpha(t) \to \alpha(t) + \alpha_0$ and $\sigma(t) \to \sigma(t) + \sigma_0$ (This corresponds to a rescaling of the spatial coordinates by two constant factors.). Clearly, the value of the constant p_A is nonphysical, and it changes under a coordinate transformation. We can deduce its transformation properties by imposing invariance of $F_{\alpha\beta}\,F^{\alpha\beta}$ which reduces to the condition

$$F_{\alpha\beta}\,F^{\alpha\beta} \to F_{\alpha\beta}\,F^{\alpha\beta} \quad \text{under} \quad \{\alpha \to \alpha + \alpha_0,\ \sigma \to \sigma + \sigma_0\} \quad \Rightarrow \quad , \quad p_A \to p_A\, e^{2\,(\alpha_0+\sigma_0)} \tag{6.9}$$

Thus, $\tilde{p}_A$ is a physical parameter invariant under the constant coordinate rescaling. For this reason, it is the combination which enters in the field equations (6.7).

We will discuss inflationary solutions of (6.7), with appropriate choices of $f(\phi)$ for both single field (only ϕ) and two field models (a=1) respectively.

6.1.1 Single Scalar Field Inflationary Background

In this subsection, we review and discuss the background evolution of the original model [12] with a single scalar field ϕ coupled to the vector field. As described in [12], we look for solutions that have a slow-roll regime and small anisotropy. Thus, we neglect $\dot{\sigma}$, $\dot{\phi}$ in the first and $\ddot{\alpha}$ in the last of (6.7) to get

$$3\dot{\alpha}^2 \approx \frac{V(\phi)}{M_p^2} + \frac{\tilde{p}_A^2}{2M_p^2}\,f^{-2}(\phi) \quad , \quad 3\,\dot{\alpha}\,\dot{\phi} \approx -V'(\phi) - \tilde{p}_A^2\,f^{-3}(\phi)\,f'(\phi) \tag{6.10}$$

Up to now, $f(\phi)$ has been arbitrary. We now specify it so to obtain the desired anisotropic background solution. To do so, we first assume that the effect of the vector field is completely negligible, and the resulting equations can be solved approximately in the standard slow-roll approximation, given by

$$\alpha \approx -\frac{1}{M_p^2}\int \frac{V(\phi)}{V'(\phi)}\,d\phi \tag{6.11}$$

The case $\dot{\sigma} = 0$ corresponds to the isotropic FRW background. A prolonged anisotropic inflation requires $\dot{A}_1$ to be nearly constant. From equation (6.6) we see that this can be

achieved if we choose

$$f(\phi) \sim e^{-2\alpha} \sim \text{Exp}\left[\frac{2}{M_p^2}\int \frac{V(\phi)}{V'(\phi)}\,d\phi\right] \tag{6.12}$$

For instance, when $V \propto \phi^n$, this becomes $f \sim e^{\phi^2/nM_p^2}$. Furthermore, one can sUp to now, $f(\phi)$ has been arbitrary. We now specify it so to obtain the desired anisotropic background solution. To do so, we first assume that the effect of the vector field is completely negligible, and the resulting equations can be solved approximately in the standard slow-roll approximation, given by

$$\alpha \approx -\frac{1}{M_p^2}\int \frac{V(\phi)}{V'(\phi)}\,d\phi \tag{6.13}$$

The case $\dot{\sigma} = 0$ corresponds to the isotropic FRW background. A prolonged anisotropic inflation requires $\dot{A}_1$ to be nearly constant. From equation (6.6) we see that this can be achieved if we choose

$$f(\phi) \sim e^{-2\alpha} \sim \text{Exp}\left[\frac{2}{M_p^2}\int \frac{V(\phi)}{V'(\phi)}\,d\phi\right] \tag{6.14}$$

For instance, when $V \propto \phi^n$, this becomes $f \sim e^{\phi^2/nM_p^2}$. Furthermore, one can set $f \sim e^{c\phi^2/nM_p^2}$ (where c is a constant) and for $c > 1$, the anisotropy is expected to grow. From now on, we assume that the functional form of $f(\phi)$ is given by

$$f(\phi) = \text{Exp}\left[\frac{2c}{M_p^2}\int \frac{V(\phi)}{V'(\phi)}\,d\phi\right] \tag{6.15}$$

We now return back to equations (6.10) and look for solutions that have small anisotropy, but the vector field contribution is not totally negligible. We specify the scalar field potential as $V(\phi) = m^2\,\phi^2/2$ and set $f = e^{c\,\phi^2/2M_p^2}$ from now on. The vector field modifies the evolution of the scalar field, if the terms $V'(\phi)$ and $\tilde{p}_A^2\,f^{-3}(\phi)\,f'(\phi)$ are comparable. Namely, for our choice of the potential and $f(\phi)$

$$m^2 \sim \frac{c\,\tilde{p}_A^2}{M_p^2}\,e^{-c\,\phi^2/M_p^2} \tag{6.16}$$

For such type of solutions, we can compare the energy densities of the scalar and vector fields. The ratio, (when the scalar field is still in the slow-roll regime and the anisotropy is small) is given by

$$\frac{\rho_A}{\rho_\phi} \approx \frac{\tilde{p}_A^2\,e^{-c\,\phi^2/M_p^2}}{m^2\,\phi^2} \approx \frac{M_p^2}{c\,\phi^2} \tag{6.17}$$

where, the second approximate equality is obtained from (6.16). This ratio is much smaller than 1 during inflation, since $\phi/M_p \gg 1$. Thus, even when the dynamics of the scalar field is modified by the action of the vector field, as long as the anisotropy is kept small enough, the energy density of the vector field can be neglected. Therefore, we can rewrite equations (6.10) by neglecting the effect of the vector field only in the first equation as

$$\dot{\alpha}^2 \approx \frac{m^2\,\phi^2}{6M_p^2} \quad , \quad 3\,\dot{\alpha}\,\dot{\phi} \approx -m^2\,\phi + \frac{c\,\tilde{p}_A^2}{M_p^2}\,\phi\,e^{-c\,\phi^2/M_p^2} \tag{6.18}$$

These equations are integrated to give

$$e^{c\,\phi^2/M_p^2+4\,\alpha} = \frac{c^2\,p_A^2}{m^2\,M_p^2\,(c-1)} + D\,e^{-4\,(c-1)\,\alpha} \tag{6.19}$$

where D is an integration constant. When the second term in the right hand side of the above equality is dominant we get

$$\frac{c\,\phi^2}{M_p^2} + 4\,c\,\alpha \sim \text{constant} \quad \rightarrow \quad \dot{\phi} \approx -\sqrt{\frac{2}{3}}\,m\,M_p \tag{6.20}$$

which is the standard slow-roll relation. The second term in the right hand side of (6.19) will eventually be subdominant for $c > 1$, since the universe expands and α grows. Therefore, the first term eventually dominates and we have

$$e^{c\,\phi^2/M_p^2} \approx \frac{c^2\,\tilde{p}_A^2}{m^2\,M_p^2\,(c-1)} \quad \rightarrow \quad \dot{\phi} \approx -\sqrt{\frac{2}{3}}\,\frac{m\,M_p}{c} \tag{6.21}$$

which has an extra $1/c$ factor compared to the standard slow-roll solution (6.20). Using the third of (6.7), for small and slowly varying anisotropy we have

$$3\,\dot{\alpha}\,\dot{\sigma} \approx \frac{\tilde{p}_A^2}{3M_p^2}\,e^{-c\,\phi^2/M_p^2} \tag{6.22}$$

Moreover, combining this result with (6.21) and the first of (6.18) we find that the anisotropy obeys

$$\frac{\dot{\sigma}}{\dot{\alpha}} = \frac{\tilde{p}_A^2\,e^{-c\,\phi^2/M_p^2}}{9\,M_p^2\,\dot{\alpha}^2} \approx \frac{2}{3}\,\frac{M_p^2\,(c-1)}{c^2\,\phi^2} \propto \frac{\rho_A}{\rho_\phi} \ll 1 \tag{6.23}$$

which is always satisfied (either in the region described by (6.20) or (6.21)). Also, note that the anisotropy is slowly increasing with time, since ϕ is decreasing towards the

end of inflation. The slow-roll solutions described by (6.20) is the standard isotropic inflationary attractor and the solutions described by (6.21) is the anisotropic inflationary attractor. We are interested in configurations that start close to the attractor solution (6.21). For illustration, we solve the system (6.7) numerically by setting the initial conditions on the attractor solution. Namely, we set initial conditions as

$$\begin{aligned}\dot{\phi}_{in} &= -\frac{m^2}{3c\,\dot{\alpha}_{in}}\,\phi_{in} \\ \dot{\sigma}_{in} &= \frac{m^2\,(c-1)}{9c^2\,\dot{\alpha}_{in}} \\ \frac{\tilde{p}^2_{A\,in}}{M_p^2\,f^2(\phi)} &= \frac{m^2\,(c-1)}{c^2}\end{aligned} \tag{6.24}$$

Inserting (6.24) into the constraint equation (the first of (6.7), we solve for $\dot{\alpha}_{in}$ to get

$$\dot{\alpha}^2_{in} = \frac{m^2}{12}\left[\frac{c-1}{c^2} + \frac{\phi^2_{in}}{M_p^2} + \sqrt{\frac{25(c-1)^2}{9c^4} + \frac{2(1+3c)}{3c^2}\,\frac{\phi^2_{in}}{M_p^2} + \frac{\phi^4_{in}}{M_p^4}}\right] \tag{6.25}$$

We show in Figs. 6.1, 6.2 the numerical evolution of the system. Note that the slow-

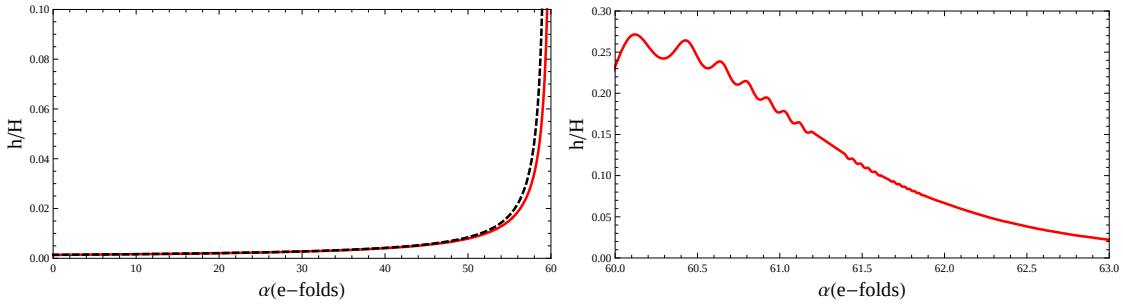

Figure 6.1: The left panel shows the evolution of anisotropy during inflation and the right panel after inflation (during when the scalar field is oscillating). $H \equiv \dot{\alpha}$ and $h \equiv \dot{\sigma}$. The black dashed curve represents the approximate slow-roll solution during inflation and the straight red curves the numerical solution.

roll and the numerical solutions are in good agreement with each other. The anisotropy in the single field model is increasing towards the end of inflation and decreases after inflation (as can be seen in the right panel of Fig. 6.1) during when the scalar field has an effective equation of state of matter. In this section, we are interested in cases where the anisotropic expansion takes place at the onset of inflation (for example as

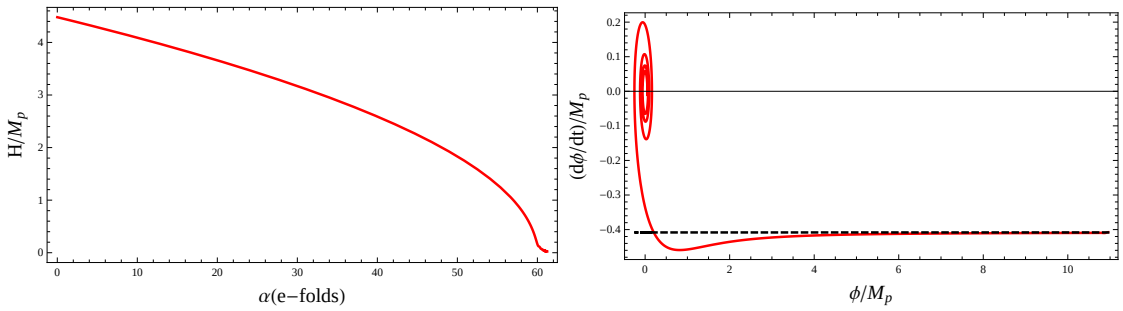

Figure 6.2: The left panel shows the evolution of the average Hubble rate ($H \equiv \dot{\alpha}$) and the right panel is the phase plot of the scalar field. Again, the black dashed lines are the slow-roll solutions. Time is measured in units of m.

in [38, 39, 40, 41] and [11]). The main reason is because we only want the largest observable scales to be modified from the perturbations that left the horizon during the anisotropic initial stage. This in turn might have some relevance to the alignment of the lowest multipoles. In the current case, all observable scales are modified (indeed smaller scales are modified even more since the anisotropy increases towards the end of inflation). Therefore, we introduce extra scalar fields as in the starting action (6.1). We discuss the background evolution for the simplest possibility of a two-field modification of the original proposal of [12] in the next subsection.

6.1.2 Two Scalar Field Inflationary Background

In this section we discuss the simplest multi-field case of the action (6.1) with $a = 1$. In this model, the extra scalar field ϕ_1 is not coupled to the vector field, and it is only relevant for the overall isotropic expansion of the universe. For the rest of the paper we will assume that $V(\phi) = m^2\,\phi^2/2$ and $V_1(\phi_1) = m_1^2\,\phi_1^2/2$. The ratio of the masses $\mu \equiv m_1/m$ is chosen to be smaller than 1. This choice leads to a two stage inflationary expansion. The first stage is driven mainly by ϕ, and due to its coupling with the vector field, this stage is anisotropic and it proceeds in a similar fashion as in the previous subsection. At the end of the first stage, the field ϕ_1 takes over the expansion, while the field ϕ starts oscillating. Since the expansion of the universe still proceeds, the Hubble friction will drive the field ϕ to zero and consequently, the coupling $f(\phi)$ approaches unity. Therefore, from (6.6), we clearly see that the effect of the vector

field quickly diminishes. Thus, after the first stage, the universe quickly isotropizes and inflation proceeds isotropically until the field ϕ_1 starts oscillating.

As we have done in the previous section, we first study the solutions to the background evolution equations, which are given in this case as

$$\begin{aligned}
3\dot{\alpha}^2 - 3\dot{\sigma}^2 &= \frac{1}{M_p^2}\left[\frac{1}{2}\,\dot{\phi}^2 + \frac{1}{2}\,\dot{\phi}_1^2 + \frac{1}{2}\,m^2\,\phi^2 + \frac{1}{2}\,\mu^2\,m^2\,\phi_1^2\right] + \frac{\tilde{p}_A^2}{2M_p^2\,f^2(\phi)} \\
2\ddot{\alpha} + 3\dot{\alpha}^2 + 3\dot{\sigma}^2 &= \frac{1}{M_p^2}\left[-\frac{1}{2}\,\dot{\phi}^2 - \frac{1}{2}\,\dot{\phi}_1^2 + \frac{1}{2}\,m^2\,\phi^2 + \frac{1}{2}\,\mu^2\,m^2\,\phi_1^2\right] - \frac{\tilde{p}_A^2}{6M_p^2\,f^2(\phi)} \\
\ddot{\sigma} + 3\dot{\alpha}\,\dot{\sigma} &= \frac{\tilde{p}_A^2}{3M_p^2\,f^2(\phi)} \\
\ddot{\phi} + 3\dot{\alpha}\,\dot{\phi} + m^2\,\phi - \frac{\tilde{p}_A^2}{f^3(\phi)}\,f'(\phi) &= 0 \\
\ddot{\phi}_1 + 3\dot{\alpha}\,\dot{\phi}_1 + m^2\,\mu^2\,\phi_1^2 &= 0
\end{aligned} \tag{6.26}$$

where $f(\phi) = e^{c\,\phi^2/2M_p^2}$ as before. We can obtain slow-roll solutions similar to (6.21), in the first stage which proceeds anisotropically. Equations (6.18) are now modified to become

$$\dot{\alpha}^2 \approx \frac{m^2}{6M_p^2}\,\left(\phi^2 + \mu^2\,\phi_1^2\right) \quad , \quad 3\,\dot{\alpha}\,\dot{\phi} \approx -m^2\,\phi + \frac{c\,\tilde{p}_A^2}{M_p^2}\,\phi\,e^{-c\,\phi^2/M_p^2} \quad , \quad 3\,\dot{\alpha}\,\dot{\phi}_1 \approx -m^2\,\mu^2\,\phi_1 \tag{6.27}$$

Initially, the field ϕ drives the expansion, so $\phi^2 \gg \mu^2\,\phi_1^2$, and the slow roll solutions for the first stage is simply given similar to (6.21) as

$$\begin{aligned}
e^{c\,\phi^2/M_p^2} &\approx \frac{c^2\,\tilde{p}_A^2}{m^2\,M_p^2\,(c-1)} \quad \rightarrow \quad \dot{\phi} \approx -\sqrt{\frac{2}{3}}\,\frac{m\,M_p}{c} \\
\dot{\phi}_1 &\approx -\sqrt{\frac{2}{3}}\,\frac{m\,M_p\,\mu^2}{\phi}\,\phi_1
\end{aligned} \tag{6.28}$$

and the anisotropy is given precisely as in equation (6.23). After this first stage ends, the isotropic expansion of the universe is driven by ϕ_1 and this second stage is described by the following slow-roll solution

$$\dot{\phi}_1 \approx -\sqrt{\frac{2}{3}}\,m\,M_p\,\mu \tag{6.29}$$

We also integrate the system (6.26) numerically and the results are shown in Figs 6.3-6.4. As we have done in the previous section, we use the slow-roll solutions and the constraint equation (the first of (6.26)) to determine the initial conditions $\dot{\phi}_{in}$, $\dot{\phi}_{1in}$, $\dot{\sigma}_{in}$, $\dot{\alpha}_{in}$ [1]

. The initial conditions for the scale factors are set as $\alpha_{in} = 0$ and σ_{in} chosen to satisfy $\sigma(t_{end}) = 0$ at the end of inflation. We have chosen $\phi_{in} = 5M_p$, $\phi_{1in} = 14M_p$ and $\mu = 1/10$, which gives around 60 e-folds of inflation, with the first 10 e-folds being anisotropic.

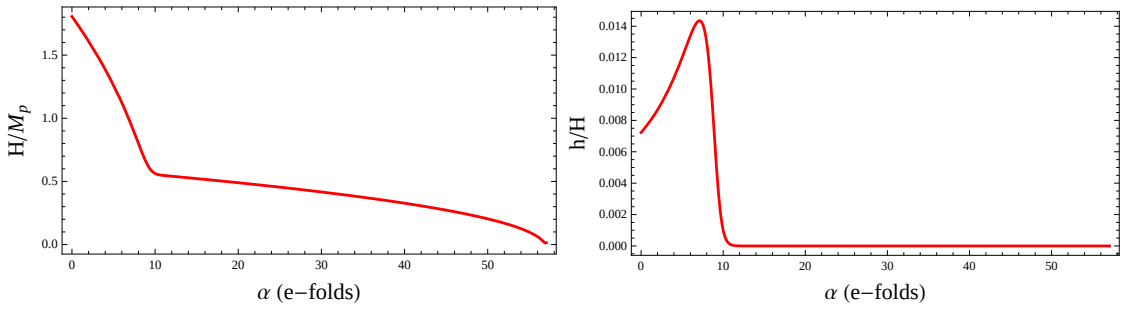

Figure 6.3: The left panel shows the evolution of the average Hubble expansion. The right panel shows the evolution of anisotropy, where $H \equiv \dot{\alpha}$ and $h \equiv \dot{\sigma}$.

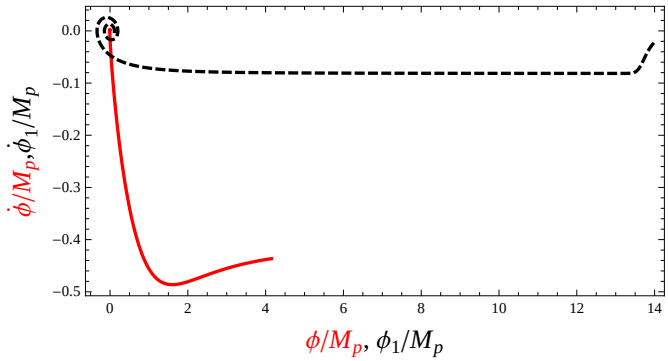

Figure 6.4: The phase portrait for the two scalar fields. The straight red line represents ϕ and the dashed black line represents ϕ_1. Time is measured in units of m.

In this type of background, when the anisotropic expansion takes place at the onset of inflation, we expect that only the largest scale perturbations are improved and at small scales standard results are recovered.

[1] In order to find the approximate slow-roll solutions, one has to ignore the effect of the second field ϕ_1 initially. Although this approximation is fairly accurate, we let the numerical evolution to run for a few e-folds until the real attractor solution is reached.

6.2 Perturbations

We study the perturbations of the background, using the formalism described in subsection 4.3.1, with the exception that we prefer to fix the freedom of coordinate gauge invariance, rather than using gauge invariant combinations for brevity. We again use the the decomposition given in equations (4.31). Furthermore, for simplicity, we use the left over $2d$ isotropy of the background to fix the comoving momentum to be aligned in the $x-y$ plane, without loss of generality. Namely, we set $k_{T3}=0$ and $k_T=k_{T2}$ in what follows. Therefore, in Fourier space, the generic $2d$ decomposition can be written as (before fixing the gauge)

$$\begin{aligned}
\delta g_{\mu\nu}(k) &= \begin{pmatrix} -2\,\Psi & -i\,a\,k_L\,\chi & -i\,b\,k_T\,B & b\,B_3 \\ & -2\,a^2\,\Psi & -a\,b\,k_L\,k_T\,\tilde{B} & -i\,a\,b\,k_L\,\tilde{B}_3 \\ & & b^2\,\left(-2\,\Sigma+2k_T^2\,E\right) & i\,b^2\,k_T\,E_3 \\ & & & -2\,b^2\,\Sigma \end{pmatrix} \\
\delta A_\mu(k) &= (\alpha_0,\,\alpha_1,\,-i\,k_T\,\alpha,\,\alpha_3)
\end{aligned} \tag{6.30}$$

Notice that, for the $2d$ vector modes, fixing $k_T=k_{T2}$ resulted in $B_2=\tilde{B}_2=E_2=\alpha_2=0$. Under the infinitesimal coordinate transformation $x^\mu\to x^\mu+\epsilon^\mu$, the metric perturbations transform as

$$\delta g_{\mu\nu}\to\delta g_{\mu\nu}-g^{(0)}_{\mu\nu,\sigma}\,\epsilon^\sigma-g^{(0)}_{\mu\sigma}\,\epsilon^\sigma_{,\nu}-g^{(0)}_{\sigma\nu}\,\epsilon^\sigma_{,\mu} \tag{6.31}$$

where we have decomposed

$$\epsilon^\mu(k)=\left(\xi^0,\,-i\,k_L\,\xi^1,\,-i\,k_T\,\xi,\,\xi^3\right) \tag{6.32}$$

We choose to fix the coordinate gauge freedom by setting $\tilde{B}=\Sigma=E=E_3=0$, namely we solve for the infinitesimal transformation to satisfy

$$\xi^0=-\frac{1}{H_b}\,\Sigma\quad,\quad\xi=-E\quad,\quad\xi^1=\frac{b}{a}\left(\tilde{B}+\frac{b}{a}\,E\right)\quad,\quad\xi^3=-E_3 \tag{6.33}$$

Since the action is invariant under the $U(1)$ gauge transformation, we can exploit this symmetry to eliminate one of the vector field perturbations. Namely, using the invariance $\delta A_\mu\to\delta A_\mu+\partial_\mu\,\lambda$, we set $\alpha=0$ in (4.31). This choice completely fixes the $U(1)$ gauge freedom. In summary, the complete system of perturbations, after fixing the

coordinate and $U(1)$ gauge freedoms, contain three $2d$ vector modes $\{\tilde{B}_3,\, \alpha_3,\, B_3\}$ and six $2d$ scalar modes $\{\Phi,\, \chi,\, B,\, \Psi,\, \alpha_0,\, \alpha_1\}$. We will also have additional scalar modes coming from the fluctuations of the scalar field(s) $\delta\phi_a$. As we have discussed previously, the modes $\{B_3,\, \Phi,\, \chi,\, B,\, \alpha_0\}$ are nondynamicel modes and can be integrated out.

It is also useful to find the connection between the perturbations defined with respect to the $2d$ decomposition and the perturbations defined with respect to standard isotropic decomposition studied in section 2.4. This is useful for discussing the phenomenological consequences. After the universe isotropizes, perturbations evolve in the standard way, what is different is that their solutions are nonstandard. However, it is useful to give results in terms of the modes which are commonlu used in FRW studies. For definiteness, we find the transformation between our choice of the gauge given in equation (6.33) and the standard longitudinal gauge. The perturbations in the $2d$ decomposition are related to the perturbations of the longitudinal gauge as (details!!!)

$$\begin{aligned}
\tilde{B}_3 &= \frac{i}{k\, k_L}\left(\frac{k_T^2 + b/a\, k_L^2}{k_T}\right) h_\times \\
\Psi &= \left(1 - \frac{H_a}{H_b}\right)\psi - \left\{\frac{H_a}{2H_b} + \frac{1}{k^2}\left[\frac{1}{2}\, k_T^2 + \frac{b^3}{a^3}\, k_L^2\left(1 + \frac{b}{a}\,\frac{2k_L^2 + k_T^2}{2k_T^2}\right)\right]\right\} h_+ \\
\delta\phi &= \delta\phi^L + \frac{\dot{\phi}}{H_b}\left(\psi + \frac{1}{2}\, h_+\right).
\end{aligned} \tag{6.34}$$

In the above equations, the terms in the left hand side are perturbations defined with respect to the $2d$ decomposition and the terms in the right hand side are perturbations in the longitudinal gauge, where $h_\times$, h_+ are the two gravitational wave polarizations, ψ is the spatial scalar perturbation and $\delta\phi^L$ is the scalar field perturbation (any generic scalar field in the model). These relations are useful in computing the power spectra of the gravitational waves and curvature perturbation.

6.2.1 General Properties of Coupled System of Perturbations

In this subsection, we discuss the general properties of the coupled system of perturbations that arise in this study. Our main discussion is based on the quadratic action for perturbations, which we need in order to determine initial conditions by canonical quantization. We compute the action for perturbations in quadratic order by inserting the decompositions (4.31), $\phi = \phi_0 + \delta\phi$ and $\phi_a = \phi_{a0} + \delta\phi_a$ into (6.1), after fixing

the $U(1)$ and coordinate gauges as described in the previous subsection. We note that the $2d$ scalar and $2d$ vector perturbations decouple in the quadratic action. We will provide explicit expressions for the scalar and vector actions in the following sections. Next we integrate out the nondynamical modes from the action, to obtain an action in terms of the dynamical modes only. More specifically, we extremize the quadratic action with respect to the nondynamical modes and obtain equations of motions for them (which are actually constraint equations). Then we solve for the nondynamical modes from their equations of motion, and insert the solutions back into the starting action. The final action we obtain depends only on the dynamical modes. The next step we perform is to find linear combinations of modes that canonically normalize the quadratic action. More specifically, the quadratic action after integrating out the non-dynamical modes is formally of the type $S \sim \int dt\, d^3k\, (\dot{\delta}_i\, K_{ij}\, \dot{\delta}_j + \dot{\delta}_i\, \Lambda_{ij}\, \delta_j - \delta_i\, \Omega^2_{ij}\, \delta_j)$, where δ_i denotes the dynamical modes. We find linear combinations $\delta_i = R_{ij}\, \delta_{cj}$ such that $\dot{\delta}_i\, K_{ij}\, \dot{\delta}_j = \frac{1}{2}\, \dot{\delta}_{ci}\, \dot{\delta}_{ci} + \dots$ where the dots denote mixed terms. The modes δ_{ci} are the canonical modes. At the moment we will study a generic action obtained after canonically normalizing the starting action, which will be relevant for both $2d$ vector and scalar modes. This action reads

$$S_{can} = \frac{1}{2} \int dt\, d^3k \left\{ \dot{\mathbf{\Phi}}^\dagger\, \dot{\mathbf{\Phi}} + \left(i\, \dot{\mathbf{\Phi}}^\dagger\, \mathbf{X}\, \mathbf{\Phi} + \text{h.c.} \right) - p^2\, \mathbf{\Phi}^\dagger\, \left(\mathbf{1} + \frac{\omega^2}{p^2} \right)\, \mathbf{\Phi} \right\} \tag{6.35}$$

where $\mathbf{\Phi}$ is a column vector made from the canonically normalized perturbations, $\mathbf{X}$ is a symmetric matrix and ω^2 is a hermitian matrix. In the above action, p is the physical momentum with $p^2 = p_L^2 + p_T^2$ where $p_L = k_L/a$ and $p_T = k_T/b$. We would like to perform a unitary transformation in the field space in order to get rid of the mixed terms $\dot{\mathbf{\Phi}}^\dagger\, X\, \mathbf{\Phi}$ and reduce the action to a canonical form that can be used to quantize the fields (and in turn obtain the initial conditions). This can be achieved by a unitary matrix $\mathbf{U}$ so that $\mathbf{\Phi} = \mathbf{U}\, \mathbf{\Psi}$ (The mixed terms can also be eliminated in the level of the Hamiltonian by canonical transformations; see for example [102].). We choose the matrix $\mathbf{U}$ to satisfy

$$\dot{\mathbf{U}} + i\, \mathbf{X}\, \mathbf{U} = 0. \tag{6.36}$$

Inserting the transformation back into (6.35) and using (6.36) (with the unitarity condition on $\mathbf{U}$), we get

$$S = \frac{1}{2} \int dt\, d^3k\, \left[\dot{\mathbf{\Psi}}^\dagger\, \dot{\mathbf{\Psi}} - \mathbf{\Psi}^\dagger\, \mathbf{U}^\dagger\, \left(p^2 + \omega^2 + \mathbf{X}^\dagger\, \mathbf{X} \right)\, \mathbf{U}\, \mathbf{\Psi} \right]. \tag{6.37}$$

We will show in the following sections that the matrix $\mathbf{X}$ is of the order of the average Hubble scale H (i.e. $\mathbf{X} = \mathrm{O}(H)$) and the matrix ω^2 is of the order of Hubble scale squared (i.e. $\omega^2 = \mathrm{O}(H^2)$). This means that in the deep UV/subhorizon regime, where $p \gg H$, these matrices will become negligible compared to p^2. Therefore, for modes that are deep inside the horizon initially, the above action reduces to a form which has diagonal mass terms

$$S = \frac{1}{2} \int dt\, d^3k \, \left[\dot{\mathbf{\Psi}}^\dagger \, \dot{\mathbf{\Psi}} - p^2 \, \mathbf{\Psi}^\dagger \, \mathbf{\Psi} + \mathrm{O}(H^2) \right] \tag{6.38}$$

In this limit when the mass terms are diagonal, the mode expansion for field $\mathbf{\Psi}$ simply reads

$$\hat{\mathbf{\Psi}}(x) = \int \frac{d^3k}{(2\pi)^{3/2}} \left[e^{i \, \overrightarrow{k} \cdot \overrightarrow{x}} \, v(t) \, \hat{a}(k) + e^{-i \, \overrightarrow{k} \cdot \overrightarrow{x}} \, v^*(t) \, \hat{a}^\dagger(k) \right] \tag{6.39}$$

The creation and annihilation operators $\hat{a}(k)$, $\hat{a}^\dagger(k)$ obey the standard bosonic commutation relations to accuracy $\mathrm{O}(H^2)$ and the mode functions $v(t)$ satisfy

$$\ddot{v} + p^2 \, v = 0. \tag{6.40}$$

The above equation can be solved using the WKB approximation in the adiabatic limit, which gives

$$v(t) = \frac{1}{\sqrt{2\omega}} \, e^{-i \int \omega \, dt'} \tag{6.41}$$

where ω is given by

$$\begin{aligned} \omega &= p - \frac{\ddot{p}}{4p^2} + \frac{3}{8} \frac{\dot{p}^2}{p^3} + \ldots \\ &= p + O(H^2) \end{aligned} \tag{6.42}$$

In the above equation, $\ldots$ represent higher order corrections which are suppressed by higher powers of H in the adiabatic solution. This is also consistent with the accuracy of the mode expansion (6.39). It is of course possible to neglect the mixed terms proportional to $\mathbf{X}$ and ω^2 from the beginning. In this way the action for the original fields $\mathbf{\Phi}$ is canonical, however we would be working with an accuracy $\mathrm{O}(H_{in}/p_{in})$ rather than $\mathrm{O}(H_{in}^2/p_{in}^2)$. This situation is more difficult in terms of the numerical computation needed, since to achieve the desired accuracy, one has to start the numerical evolution much deeper inside the horizon. Moreover, initial conditions in the standard isotropic

case are also given to an accuracy of $\mathrm{O}(H_{in}/p_{in})^2$, therefore we choose to perform the field rotation to eliminate the $\mathbf{X} \sim \mathrm{O}(H)$ terms and work with the fields $\mathbf{\Psi}$. The field rotation can be performed trivially for the case of $2d$ vector perturbations. The more accurate way of quantizing coupled fields is by diagonalizing the also the frequency squared terms, by using Bogoluibov transformations [103]. We will perform this calculation in the next chapter, for both scalar and vector modes. For the purposes of this chapter, the current approximate quantization scheme is sufficient.

The canonical quantization procedure outlined above determines the adiabatic initial conditions for the modes $\mathbf{\Psi}$. We are however interested in the values of the entries of $\mathbf{\Phi}$ evaluated at the end of inflation, which are related to the primordial power spectra. We will show in the next section that the matrix $\mathbf{X}$ along with the off-diagonal entries of ω^2 is proportional to the anisotropy, so they vanish before the end of inflation in the two field model. Therefore, it is possible to choose the transformation matrix $\mathbf{U}$ that satisfies $\mathbf{U}(t_{end}) = \mathbf{1}$, which in turn implies that $\mathbf{U}^\dagger \left(\omega^2 + \mathbf{X}^\dagger \mathbf{X}\right) \mathbf{U}$ is also diagonal at t_{end} (t_{end} is the time when inflation ends). Then we have $\mathbf{\Phi}(t_{end}) = \mathbf{\Psi}(t_{end})$ and we use the following equality to compute the two point functions for the starting modes $\mathbf{\Phi}$;

$$< \Psi_a^\dagger \Psi_b > |_{t_{end}} =< \Phi_a^\dagger \Phi_b > |_{t_{end}} \tag{6.43}$$

for the components of the fields. Therefore, instead of working with the original fields $\mathbf{\Phi}$ we work with the transformed fields $\mathbf{\Psi}$. Notice that passing to the fields $\mathbf{\Psi}$ was an important step, since the action is in its canonical form with diagonal mass terms p^2 (up to accuracy $\mathrm{O}(H^2)$) in the deep UV regime. Therefore, this field can be quantized and p represents the energy of the each particle created by $\hat{a}^\dagger(k)$. The quantization procedure also determines the mode functions v, which in turn determines initial conditions for the perturbations.

In the next subsection, we will discuss the evolution of the $2d$ vector modes, which is related to the gravitational wave polarization $h_\times$.

6.2.2 2d Vector Perturbations

We now discuss the $2d$ vector perturbations of the two field inflationary background solution discussed in the previous section. As we have argued earlier, the quadratic action for the $2d$ vector and scalar modes decouple, so we concentrate on the vector

piece here. The action for the $2d$ vector perturbations in momentum space, up to a total time derivative, is calculated as

$$\begin{aligned}
S_{2dV} &= \frac{M_p^2}{4}\int dt\, d^3k\, e^{3\alpha-2\sigma}\,\mathcal{L}_{2dV} \\
\mathcal{L}_{2dV} &= e^{2\alpha-2\sigma}\,p_L^2\left|\dot{\tilde{B}}_3\right|^2 + 2\,e^{-2\alpha}\,\frac{f^2(\phi)}{M_p^2}\,|\dot{\alpha}_3|^2 - e^{\alpha}\,p_L^2\left(\dot{\tilde{B}}_3^*\,B_3 + \text{h.c.}\right) \\
&\quad +2\,e^{-\sigma}\,\frac{\tilde{p}_A\,p_L}{M_p^2}\left(i\,\dot{\alpha}_3^*\,\tilde{B}_3 + \text{h.c.}\right) - e^{2\alpha-2\sigma}\,p_L^2\left(p_T^2 - 9\dot{\sigma}^2 - \frac{\tilde{p}_A^2}{M_p^2\,f^2(\phi)}\right)\left|\tilde{B}_3\right|^2 \\
&\quad +3\,e^{\alpha}\,\dot{\sigma}\,p_L^2\left(\tilde{B}_3^*\,B_3 + \text{h.c.}\right) - 2e^{-2\alpha}\,\frac{p^2}{M_p^2}\,f^2(\phi)\,|\alpha_3|^2 \\
&\quad +2\,e^{-\alpha+\sigma}\,\frac{\tilde{p}_A\,p_L}{M_p^2}\,(i\,\alpha_3^*\,B_3 + \text{h.c.}) + e^{2\sigma}\,p^2\,|B_3|^2
\end{aligned} \tag{6.44}$$

where we have used the physical momenta $p_L \equiv k_L/a$, $p_T = k_T/b$ and $p = \sqrt{p_L^2 + p_T^2}$. As can be seen from (6.44), the mode B_3 is nondynamical, so it can be integrated out from the action by solving its equation of motion. The solution for B_3 is obtained as

$$B_3 = e^{\alpha-2\sigma}\left[\frac{2\,i\,p_L\,\tilde{p}_A}{M_p^2\,p^2}\,e^{-2\alpha+\sigma}\,\alpha_3 + \frac{p_L^2}{p^2}\left(\dot{\tilde{B}}_3 - 3\,\dot{\sigma}\,\tilde{B}_3\right)\right] \tag{6.45}$$

We insert the solution (6.45) back into the action (6.44) and up to a total time derivative, we obtain

$$\begin{aligned}
S_{2dV} &= \frac{1}{2}\int dt\, d^3k\left\{|\dot{H}_\times|^2 + |\dot{\Delta}_-|^2 + \frac{\tilde{p}_A\,p_T}{\sqrt{2}\,M_p\,p\,f(\phi)}\left(i\,\dot{H}_\times^*\,\Delta_- + i\,H_\times\,\dot{\Delta}_-^* + \text{h.c.}\right)\right. \\
&\qquad \left. -\begin{pmatrix} H_\times^* & \Delta_-^* \end{pmatrix}\begin{pmatrix} \Omega_{11}^2 & \Omega_{12}^2 \\ \Omega_{12}^{*2} & \Omega_{22}^2 \end{pmatrix}\begin{pmatrix} H_\times \\ \Delta_- \end{pmatrix}\right\}
\end{aligned} \tag{6.46}$$

where the canonical modes $H_\times$ and Δ_- are related to the starting modes as

$$\tilde{B}_3 = \frac{\sqrt{2}\,p}{p_L\,p_T\,M_p}\,e^{-\frac{5}{2}\,\alpha+2\sigma}\,H_\times \quad , \quad \alpha_3 = \frac{e^{-\alpha/2+\sigma}}{f(\phi)}\,\Delta_- \tag{6.47}$$

and the mass terms Ω^2 are defined as

$$\begin{aligned}
\Omega_{11}^2 &\equiv p^2 - \frac{9}{4}\,\dot{\alpha}^2 + \frac{3}{4M_p^2}\left(\dot{\phi}^2 + \dot{\phi}_1^2\right) + \frac{9}{2}\left(\frac{p_L^4}{p^4} + 6\frac{p_L^2\,p_T^2}{p^4} - \frac{p_T^4}{p^4}\right)\dot{\sigma}^2 \\
&\quad + \frac{\tilde{p}_A^2}{2M_p^2\,f^2(\phi)}\left(\frac{p_L^4}{p^4} - \frac{p_T^4}{p^4}\right)
\end{aligned}$$

$$\begin{aligned}
\Omega_{12}^2 &\equiv i\,\bar{\omega}_{12}^2 = \frac{i\,\tilde{p}_A\,p_T}{\sqrt{2}\,M_p\,p\,f(\phi)}\left(\frac{4p_T^2-5p_L^2}{p^2}\,\dot{\sigma}+\dot{\alpha}-\frac{f'(\phi)}{f(\phi)}\,\dot{\phi}\right)\\
\Omega_{22}^2 &= p^2-\frac{1}{4}\,\dot{\alpha}^2+\frac{1}{4M_p^2}\left(\dot{\phi}^2+\dot{\phi}_1^2\right)-2\,\dot{\alpha}\,\dot{\sigma}+\frac{1}{2}\,\dot{\sigma}^2+\frac{\tilde{p}_A^2}{2M_p^2\,f^2(\phi)}\,\frac{5p_L^2+p_T^2}{p^2}\\
&\quad -\frac{\tilde{p}_A^2}{f^2(\phi)}\,\frac{f'(\phi)^2}{f^2(\phi)}+\left[2\,(\dot{\alpha}+\dot{\sigma})\;\dot{\phi}+V'(\phi)\right]\,\frac{f'(\phi)}{f(\phi)}-\frac{f''(\phi)}{f(\phi)}\,\dot{\phi}^2
\end{aligned}\tag{6.48}$$

The action (6.46) has regular kinetic terms, and therefore there is no ghost instability in the $2d$ vector sector, as expected. Note that the matrix $\mathbf{X}$ along with the mass matrix terms Ω^2 satisfy

$$\begin{aligned}
&\Omega_{12}^2=\mathrm{O}\left(H^2\right)\quad,\quad \Omega_{11}^2=\Omega_{22}^2=p^2+\mathrm{O}\left(H^2\right)\quad,\\
&\frac{\tilde{p}_A}{M_p\,f(\phi)}=\sqrt{6\dot{\alpha}^2-6\dot{\sigma}^2-\frac{2}{M_p^2}\,(V(\phi)+V_1(\phi_1))-\frac{1}{M_p^2}\,\left(\dot{\phi}^2+\dot{\phi}_1^2\right)}\sim\mathrm{O}(H)
\end{aligned}\tag{6.49}$$

therefore, the action (6.46) is formally of the type given in (6.35) with $\mathbf{\Phi}$ and matrix $\mathbf{X}$ given by

$$\mathbf{\Phi}\equiv\begin{pmatrix}H_\times\\ \Delta_-\end{pmatrix}\quad,\quad \mathbf{X}\equiv\begin{pmatrix}0&\lambda\\ \lambda&0\end{pmatrix}\quad,\quad \lambda\equiv\frac{\tilde{p}_A\,p_T}{\sqrt{2}\,M_p\,f(\phi)\,p}\tag{6.50}$$

We can therefore determine the transformation matrix $\mathbf{U}$, that eliminates the mixed terms $\dot{\mathbf{\Phi}}^\dagger\,\mathbf{X}\,\mathbf{\Phi}$ by solving $\dot{\mathbf{U}}+i\,\mathbf{X}\,\mathbf{U}=0$, which can be solved by diagonalizing the matrix $\mathbf{X}$. Notice that $\mathbf{R}^\dagger\,\mathbf{X}\,\mathbf{R}=D_X$ where

$$\mathbf{R}=\frac{1}{\sqrt{2}}\begin{pmatrix}1&-1\\ 1&1\end{pmatrix}\quad,\quad D_X=\begin{pmatrix}\lambda&0\\ 0&-\lambda\end{pmatrix}\tag{6.51}$$

Therefore (6.36) is solved by

$$\mathbf{U}=\mathbf{R}\,e^{-i\int^t D_X\,dt'}\,\mathbf{W}_0\tag{6.52}$$

where $\mathbf{W}_0$ is a constant unitary matrix, which does not have any physical relevance. Therefore, we choose $\mathbf{W}_0=\mathbf{R}^\dagger$, so that $\mathbf{U}=\mathbf{1}$ when $\lambda=0$ (i.e. when anisotropy vanishes). We can now determine the new mass matrix for the transformed fields $\mathbf{\Psi}$, which are given by

$$\Omega_\Psi^2=\mathbf{U}^\dagger\,\left[\Omega^2+\mathbf{X}^\dagger\,\mathbf{X}\right]\,\mathbf{U}\tag{6.53}$$

where the entries of Ω^2_Ψ are explicitly given by

$$\begin{aligned}
\Omega^2_{\Psi\,11} &= \lambda^2 + \frac{\Omega^2_{11}+\Omega^2_{22}}{2} + \frac{\Omega^2_{11}-\Omega^2_{22}}{2}\,\cos\left[2\mathcal{I}(t)\right] + \bar{\omega}^2_{12}\,\sin\left[2\mathcal{I}(t)\right] \\
\Omega^2_{\Psi\,22} &= \lambda^2 + \frac{\Omega^2_{11}+\Omega^2_{22}}{2} - \frac{\Omega^2_{11}-\Omega^2_{22}}{2}\,\cos\left[2\mathcal{I}(t)\right] - \bar{\omega}^2_{12}\,\sin\left[2\mathcal{I}(t)\right] \\
\Omega^2_{\Psi\,12} &= -\Omega^2_{\Psi\,21} = i\left\{\bar{\omega}^2_{12}\,\cos\left[2\mathcal{I}(t)\right] - \frac{\Omega^2_{11}-\Omega^2_{22}}{2}\,\sin\left[2\mathcal{I}(t)\right]\right\}
\end{aligned} \tag{6.54}$$

where

$$\mathcal{I}(t) \equiv \int_{t_k}^{t} \lambda(t')\,dt' = \begin{cases} \text{constant} & t > t_{iso} \\ \int_{t_k}^{t} \lambda(t')\,dt' & t < t_{iso} \end{cases} \tag{6.55}$$

Here, t_{iso} is the time when the universe isotropizes so $\lambda(t \geq t_{iso}) = 0$. The lower limit t_k in the integral is chosen for each comoving momentum k such that the constant value for $t > t_{iso}$ is unity [2] . This ensures that $\mathbf{U}(t_{iso}) = \mathbf{U}(t_{end}) = \mathbf{1}$ since

$$\mathbf{U} \equiv \begin{pmatrix} \cos\left[\mathcal{I}(t)\right] & -i\sin\left[\mathcal{I}(t)\right] \\ -i\sin\left[\mathcal{I}(t)\right] & \cos\left[\mathcal{I}(t)\right] \end{pmatrix} \rightarrow \mathbf{1} \quad \text{when} \quad t \geq t_{iso} \tag{6.56}$$

Finally, the fields $\mathbf{\Psi}$ satisfy the evolution equations

$$\ddot{\Psi}_a + \Omega^2_{\Psi\,ab}\,\Psi_b = 0 \tag{6.57}$$

with initial conditions on the entries of Ψ_a set by the form of the mode function $v(t)$ which are given deep inside the horizon as

$$\begin{aligned}
\Psi_{a\,in} &= \frac{1}{\sqrt{2p}} + \mathrm{O}(H^2) \\
\dot{\Psi}_{a\,in} &= \frac{1}{\sqrt{2p}}\left(-i\,p - \frac{\dot{p}}{2p}\right) + \mathrm{O}(H^2)
\end{aligned} \tag{6.58}$$

up to a nonphysical phase.

In the next section, we will numerically evaluate the evolution equations (6.57) with adiabatic initial conditions (6.58) for a range of comoving momenta, and determine the two point functions $< \Psi^\dagger_a\,\Psi_b > |_{t_{end}}$ which coincides with $< \Phi^\dagger_a\,\Phi_b > |_{t_{end}}$ as we argued

[2] It is possible to keep the lower limit in the integral arbitrary, since it has no physical relevance. However, for an arbitrary value, the mass terms for the fields $\mathbf{\Psi}$ will in general be nondiagonal at the end of inflation. In this case, one has to further rotate the fields (by a constant matrix) to obtain the physical modes. We perform this step from the beginning by choosing t_k corrrectly, so that $\mathbf{U} = 1$ at the end of inflation.

before. Finally, using (6.47) and (6.34) we deduce the power spectrum (which is related to the calculated two point functions) for the gravitational wave polarization $h_\times$. We will provide the study of the $2d$ scalar perturbations in Appendix D and leave the study of the power spectrum for the scalar modes in the next chapter for a model with single scalar field.

6.3 Power Spectrum

This section is devoted to the study of the power spectrum of the gravitational wave polarization $h_\times$. We will use the results of the previous sections to compute the evolution of the fields Ψ using their equations of motion given in (6.57) with the elements of the mass matrices given in (6.54). We perform the integration for a range of co-moving momenta k_L and k_T, which we parameterize as

$$k_L = \xi\, k \quad , \quad k_T = \sqrt{1-\xi^2}\, k \quad , \quad k \equiv \sqrt{k_L^2 + k_T^2} \quad , \quad 0 \leq \xi \leq 1. \tag{6.59}$$

Therefore, ξ is the cosine of the angle between the comoving momentum and the longitudinal component k_L. For each comoving mometa labelled by the two numbers $\{k, \xi\}$, initial conditions are given in equation (6.58). The initial time t_{in} is chosen to be the moment when

$$\frac{k}{a(t_{in})} = 50\, H(t_{in}) \quad \text{or} \quad k = 50\, \dot{\alpha}(t_{in})\, e^{\alpha(t_{in})} \tag{6.60}$$

so that the physical momentum p is sufficiently larger than the Hubble scale and the adiabatic initial conditions (6.58) are accurate. Since the mass matrix Ω^2_Ψ depends on the background quantities, we integrate the equations (6.57) together with the background equations (6.26) with initial conditions and parameters m_1, m_2 set as explained in subsection (6.1.2). Using (6.34) and (6.47) we can relate the gravitational wave polarization $h_\times$ to the canonical field $H_\times$ at the end of inflation (when $\sigma = \dot{\sigma} = 0$, so $a = b$)

$$h_\times = \frac{\sqrt{2}}{i\, M_p}\, e^{-\frac{3}{2}\alpha}\, H_\times. \tag{6.61}$$

We define the power spectrum for the gravitational wave mode $h_\times$ as

$$P_\times(\vec{k}) \equiv \left(k^3\, |h_\times|^2\right)|_{t=t_{end}} \tag{6.62}$$

At the end of inflation, the fields Ψ is identical to the starting fields Φ, so the power spectrum of the gravitational wave mode $h_\times$is obtained by evaluating the correlation function $< \Psi_1^* \, \Psi_1 >=< \Phi_1^* \, \Phi_1 >$ and using (6.61) which gives

$$P_\times(\overrightarrow{k}) = \frac{2k^3}{M_p^2} \, e^{-3\,\alpha(t_{end})} \, |\Psi_1(t_{end})|^2. \tag{6.63}$$

In Figures 6.5,6.6 we show the power spectrum obtained from the numerical integration of the background and perturbation equations. In Fig 6.5 , parts of the power spectrum is shown for fixed values of $\xi = 0,\, 0.5,\, 1$ and $10^{-1}\, k_{iso} \leq k \leq 10^{3/2}\, k_{iso}$. We have define k_{iso} to be the value of the comoving momentum, when $k = a(t_{iso})\, H(t_{iso}) = \dot{\alpha}(t_{iso})\, e^{\alpha(t_{iso})}$ where t_{iso} is the time of isotropization (we define it to be the time when $h/H = 10^{-3}$ numerically). In Fig. 6.6, we show contour plot of the full spectrum $P_\times(\overrightarrow{k})$.

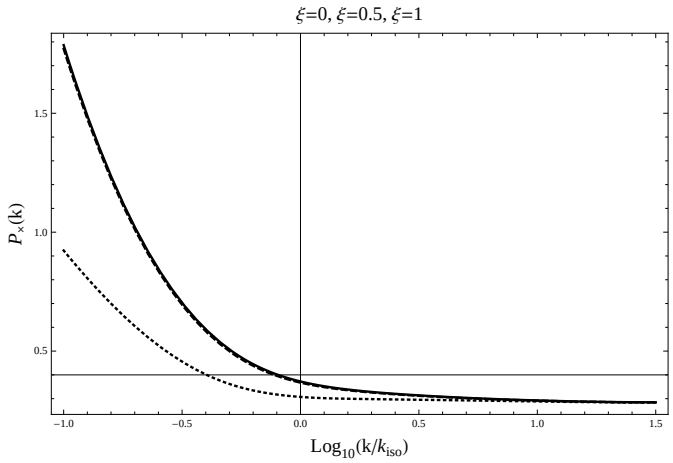

Figure 6.5: Parts of the power spectrum for $h_\times$ are shown for $\xi = 0$ (straight line), $\xi = 0.5$ (dashed line) and $\xi = 1$(dotted line).

At large scales for $k > k_{iso}$, there is more power and the spectrum has angular dependence. This in turn could be related to the CMB anomalies. Note that the spectrum reduces to the standard nearly scale invariant form when $k > k_{iso}$. Indeed, we have checked that for $k > k_{iso}$, the power spectrum reduces to

$$P_\times(k > k_{iso}) = A_T \, k^{n_T} \quad , \quad n_T \equiv -2\,\epsilon = -\frac{\dot{\phi}_1^2}{\dot{\alpha}^2 \, M_p^2} \tag{6.64}$$

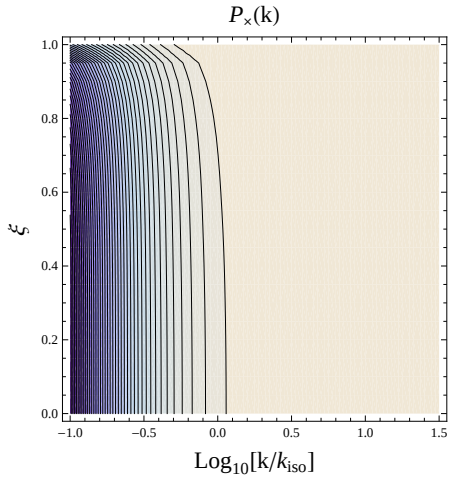

Figure 6.6: The contour plot of the full power spectrum $P_\times(k)$.

where ϵ is the standard slow-roll parameter for the field ϕ_1. Indeed, the the spectrum can be written as

$$P_\times(\overrightarrow{k}) = \begin{cases} a_T \left(\frac{k}{k_{iso}}\right)^{f(\xi,k)} & k \lesssim k_{iso} \\ a_T \left(\frac{k}{k_{iso}}\right)^{n_T} & k \gtrsim k_{iso} \end{cases} . \tag{6.65}$$

The form of the function $f(\xi, k)$ is unknown, but it is possible to consider a generic expansion of the form

$$\begin{aligned} &\mathrm{Log}_{10} P_\times = \mathrm{Log}_{10} a_T + (c_1 + d_1\,\xi^{n_1})\; x + (c_2 + d_2\,\xi^{n_2})\; x^2 + (c_3 + d_3\,\xi^{n_3})\; x^3 + \ldots \\ &x \equiv \mathrm{Log}_{10}\left(\frac{k}{k_{iso}}\right) \end{aligned} \tag{6.66}$$

We fix the unknown parameters $\mathrm{Log}_{10} a_T$ (which coincides with the $\mathrm{Log}_{10} a_T$ of the spectrum for $k < k_{iso}$) and c_1, c_2, c_3 by fitting to the numerical spectrum when $\xi = 0$. Then, we fix the parameters d_1, d_2, d_3 by fitting to the numerical spectrum when $\xi = 1$ (using the previous values of $\mathrm{Log}_{10} a_T$ and c_1, c_2, c_3). Finally, we obtain the values of n_1, n_2, n_3 by fitting to a spectrum at an intermediate value of ξ. Increasing the number of terms in the expansion (6.66), increases the accuracy of the fit. For the spectra we have obtained above, the unknown parameters are obtained as

$$\begin{aligned} &\mathrm{Log}_{10} a_T \simeq -0.43, \;\; c_1 \simeq -0.23, \;\; c_2 \simeq 0.83, \;\; c_3 \simeq 0.38 \\ &d_1 \simeq 0.82, \;\; d_2 \simeq 1.21, \;\; d_3 \simeq 0.69 \end{aligned}$$

$$n_1 \simeq 3.94, \;\; n_2 \simeq 3.38, \;\; n_3 \simeq 3.34 \tag{6.67}$$

In Fig. 6.7, we show the fitted and numerical power spectra for $k < k_{iso}$, which are in good agreement. In Fig. 6.8, we show the numerical spectra for $k > k_{iso}$, which is of the standard nearly scale invariant form.

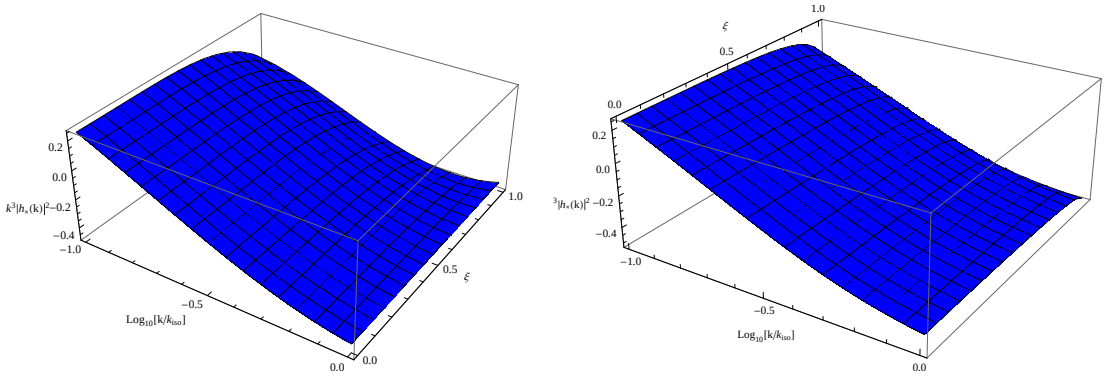

Figure 6.7: The left panel shows the fitted spectrum using (6.66) and the right panel the numerical spectrum for $k < k_{iso}$. The fitted and numerical spectra are in good agreement.

.

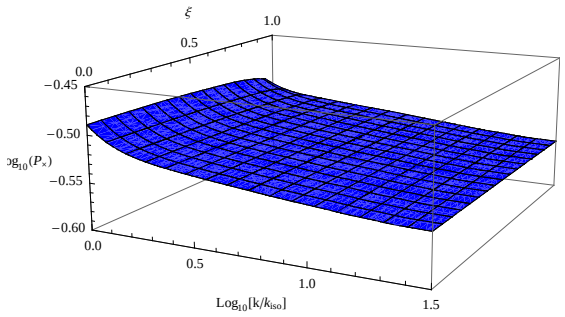

Figure 6.8: The power spectra at small scales for $k > k_{iso}$, which is of the standard nearly scale invariant form $P_\times \propto k^{n_T}$.

The power spectrum for the gravitational wave mode $h_\times$ is not of the form $P_\times = P_{\times,iso}(k) + \delta P_\times(k,\xi)$ as one would naively expect for small anisotropy for $k < k_{iso}$, with $|\delta P_\times| \ll |P_{\times,iso}|$. This is due to the two-field nature of inflation. For instance, if

the vector field was absent, we would have expected a change in the spectral index at the moment when the second field ϕ_1 takes over, since it has a different mass. This is similar to what we see in the above figures. We will show in the next chapter that a model with a single scalar field can be made to satisfy the condition $|\delta P_\times| \ll |P_{\times,\,\mathrm{iso}}|$. In this case however, all the multipoles are affected from the ansisotropic expansion, unlike the current model where only the lowest multipoles are modified.

6.4 Linearized Stability

In this section we expilictly demonstrate that the model we discuss is stable. As noted before, we have considered all possible degrees of freedom of the system, including the gravitational and vector field perturbations using a 2d decomposition. In total, we have 6 dynamical degrees of freedom. 2 of them come from the 2d vector sector and correspond to the gravity wave mode ($H_\times$) and one transverse polarization of the vector field (Δ_-). We have studied the power spectrum of the 2d vector sector in the previous section, which by itself have proven that the perturbations remain finite and this sector is stable. The rest of the 4 dynamical modes come from the 2d scalar sector and corresspond to the two Mukhanov-Sasaki variables (V, V_1), the gravity wave mode (H_+) and the one transverse polarization of the vector field (Δ_+). These modes comprise the full spectrum of the system. Note that the actions for both sectors have positive definite kinetic terms as can be seen from equations (6.46) and (D.2), which proves that there are no ghosts present in the linearized spectrum. Moreover, note that the mass squared terms for both sectors reduce to $p^2\,\mathbf{1} + O(H^2)$ in the deep UV limit, as can be seen from equations (6.48) and (D.4), therefore there are no tachyonic modes in the full spectrum either. In order to back these results, we also provide the numerical evolution of the perturbations in both sectors and demonstrate that they remain finite both in the sub-horizon and super-horizon regimes.

The numerical evolutions are initiated, starting from the subhorizon regime when $k/a(t_{in}) = 100H(t_{in})$ for each co-moving momenta. We have performed all the numerical calculations for a range of co-moving momenta k, but for providing a convenient example, we show here the results for $\xi = 0.5$ and $k = k_{iso}$ (which are defined in the previous section). The results shown here agree with the numerical results obtained for

different values of ξ and k. We have numerically solved the equations of motion for the canonical modes $H_\times$ and Δ_- resulting from the action (6.46) and for V_1, V_2, H_+ and Δ_+ resulting from the action (D.2), where initial conditions for each canonical mode is given as $\delta_{\rm can} = 1/\sqrt{2p}$ and $\dot{\delta}_{\rm can} = -i\,p\,\delta_{can}$ [3] .

We first discuss the numerical evolution of $2d$ vector modes both in the sub-horizon and super-horizon regimes. The results of the numerical analysis are shown in Fig. 6.9. In obtaining the figures, we have plotted the ratio of power at any time to initial power defined by

$$\frac{P_\times(t)}{P_\times(t_{in})} = \frac{k^3\,e^{-3\alpha(t)}\,|H_\times(t)|^2}{k^3\,e^{-3\alpha(t_{in})}\,|H_\times(t_{in})|^2} \quad , \quad \frac{P_{\Delta_-}(t)}{P_{\Delta_-}(t_{in})} = \frac{k^3\,e^{-3\alpha(t)}\,|\Delta_-(t)|^2/f^2(\phi(t))}{k^3\,e^{-3\alpha(t_{in})}\,|\Delta_-(t_{in})|^2/f^2(\phi(t_{in}))} \tag{6.68}$$

Note that the quantitity $P_\times$ is related to the power of gravity waves and P_{Δ_-} is related 2d vector mode contribution to the invariant norm $\delta A^2 = g^{\mu\nu}\,\delta A_\mu\,\delta A_\nu$ (which we treat as a measure of vector field power, see for example [56]) when the universe isotropizes, as can be seen from equations (6.47) and (D.7).

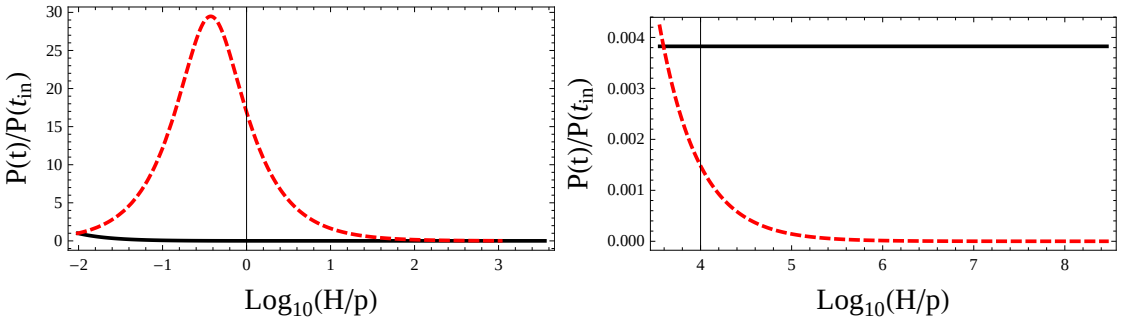

Figure 6.9: The left panel shows the evolution of normalized $2d$ vector mode power corressponding to the gravity wave mode $H_\times$ and the vector field polarization Δ_- in the sub-horizon regime for $k = k_{iso}$ and $\xi = 0.5$. The right panel shows the consequent evolution in the super-horizon regime. In the plots, dahed red lines represent the normalized power for the vector mode and the black curve represent the normalized power for the gravity wave mode.

.

Moreover, as can be seen from Fig. 6.9, the power of the vector field mode vanishes

[3] These initial conditions are $O(H)$ accurate, unlike the $O(H^2)$ accuracy we have used for obtaining the power spectrum in the previous section. Since we are not after high accuracy calculations for the purposes of this section, these initial conditions are sufficient to provide the proof of the stability of the linearized equations for perturbations.

in the super-horizon regime but the power for the gravity wave mode stays constant, as expected from the standard case. This is due to the fact that the vector field is relevant only in the sub-horizon regime when the universe was anisotropic. The numerical evolution for different co-moving momenta also produces the same results. Therefore, we have explicitly shown that the 2d vector perturbations remain stable at all scales.

Now we discuss the numerical evolution of the pertutbations in the 2d scalar sector. The results of the numerical anaylsis are shown in Figs. 6.10- 6.11, where we have again plotted the normalized power in the sub-horizon and super-horizon regimes which are defined as

$$\frac{P_+(t)}{P_+(t_{in})} = \frac{k^3\, e^{-3\alpha(t)}\, |H_+(t)|^2}{k^3\, e^{-3\alpha(t_{in})}\, |H_+(t_{in})|^2} \quad , \quad \frac{P_{\mathcal{R}}(t)}{P_{\mathcal{R}}(t_{in})} = \frac{k^3\, e^{-3\alpha(t)}\, |\mathcal{R}(t)|^2}{k^3\, e^{-3\alpha(t_{in})}\, |\mathcal{R}(t_{in})|^2}$$
$$\frac{P_{\mathcal{S}}(t)}{P_{\mathcal{S}}(t_{in})} = \frac{k^3\, e^{-3\alpha(t)}\, |\mathcal{S}(t)|^2}{k^3\, e^{-3\alpha(t_{in})}\, |\mathcal{S}(t_{in})|^2} \quad , \quad \frac{P_{\Delta_+}(t)}{P_{\Delta_+}(t_{in})} = \frac{k^3\, e^{-3\,\alpha(t)}\, \frac{p^2}{p_T^2\, f^2(\phi(t))}\, |\Delta_+(t)|^2}{k^3\, e^{-3\,\alpha(t_{in})}\, \frac{p^2}{p_T^2\, f^2(\phi(t_{in}))}\, |\Delta_+(t_{in})|^2} \tag{6.69}$$

where $\mathcal{R}$ is the adiabatic curvature perturbation and $\mathcal{S}$ is the isocurvature perturbation whcih are defined as (see reference [104] for the detailed discussion of these definitions)

$$\mathcal{R} \equiv \frac{\dot{\alpha}}{\dot{\sigma}}\, V_\sigma \quad , \quad \mathcal{S} \equiv \frac{\dot{\alpha}}{\dot{\sigma}}\, V_s \quad , \quad \dot{\sigma} \equiv \sqrt{\dot{\phi}^2 + \dot{\phi}_1^2}$$
$$V_\sigma \equiv \frac{\dot{\phi}}{\sqrt{\dot{\phi}^2 + \dot{\phi}_1^2}}\, V + \frac{\dot{\phi}_1}{\sqrt{\dot{\phi}^2 + \dot{\phi}_1^2}}\, V_1 \quad , \quad V_s \equiv \frac{\dot{\phi}}{\sqrt{\dot{\phi}^2 + \dot{\phi}_1^2}}\, V_1 - \frac{\dot{\phi}_1}{\sqrt{\dot{\phi}^2 + \dot{\phi}_1^2}}\, V \tag{6.70}$$

The modes V and V_1 are the canonical modes defined in equation (D.6) and reduce to the standard Mukhanov-Sasaki variables in the isotropic limit. Note that P_{Δ_+} is related 2d scalar mode contribution to the invariant norm $\delta A^2 = g^{\mu\nu}\, \delta A_\mu\, \delta A_\nu$ when the universe isotropizes, as can be seen from equations (D.6).

Note that the power of the vector field mode and the isocurvature mode vanishes in the super-horizon regime but the power for the gravity wave mode and the adiabatic curvature perturbation stay constant as can be seen from Figs. 6.10- 6.11. This is an expected result since the scalar field ϕ and the vector field is relevant only in the subhorizon regime when the universe was anisotropic. Therefore, in the superhorizon regime, our results reduce to that of single field isotropic inflation, which produces only adiabatic curvature perturbations. The numerical evolution for different co-moving

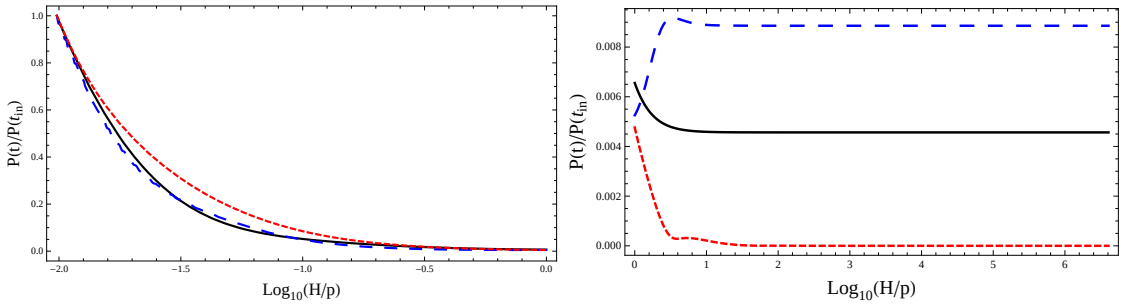

Figure 6.10: The left panel shows the evolution of normalized $2d$ scalar mode powers corressponding to the gravity wave mode (H_+), the adiabatic curvature perturbation ($\mathcal{R}$), and the isocurvature perturbation $\mathcal{S}$ in the sub-horizon regime for $k = k_{iso}$ and $\xi = 0.5$. The right panel shows the consequent evolution in the super-horizon regime. In the plots, the blue dashed curve represents normalized power for the adiabatic curvature perturbation ($\mathcal{R}$), the red dashed curve represents the normalized power for the entropy perturbation $\mathcal{S}$ and the black curve represents the normalized power for the gravity wave mode H_+.

.

momenta also produces the same results. Therefore, we have explicitly shown that the 2d scalar perturbations also remain stable at all scales, unlike other vector field driven models discussed in references [46, 8] where perurbations diverge close to horizon crossing as proven in references [52, 53, 54]. This analysis explicitly proves that the model under discussion is stable.

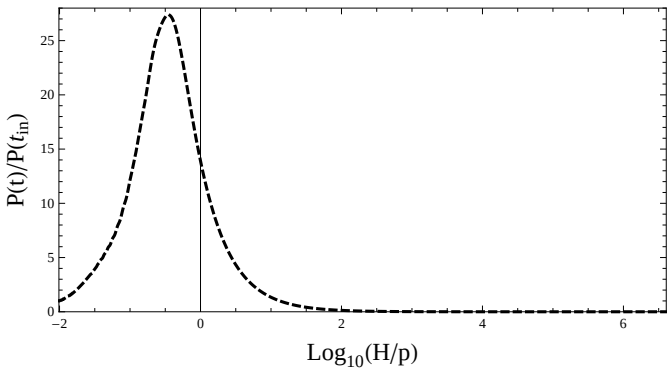

Figure 6.11: The evolution of the normalized power for the vector perturbation Δ_+ for $k = k_{iso}$ and $\xi = 0.5$.

Chapter 7

General Two Point Correlators from Anisotropic Inflation

In this chapter we revisit the model where the vector field is kinetically coupled to a scalar field, which we have discussed in the previous chapter. We will study only the case with a single scalar field, therefore inflationary expansion will preoceed anisotropically, and the universe will isotropize after inflation is over. As discussed previously, when inflation takes places anisotropically, all the scales are modified, unlike the case of the two field model of previous chapter, where only the largest scales are modified. We study the complete perturbations of the anisotropic background solution and compute two point compute two point correlation functions between physical modes of the system, and express them in terms of power spectra with angular dependence. We parameterize the anisotropic scalar-scalar power spectrum as in the case of the ACW model given as

$$P(\vec{k}) = P(k)\ \left(1 + g_*(k)\,(\hat{k}\cdot\hat{n})^2\right) \tag{7.1}$$

and we compute the parameter g_*. We also compute the tensor-tensor (as done for the two-field model of the previous chapter) and tensor-scalar correlators, and discuss possible phenomenological signatures. Our discussion follows the lines of [58].

The background evolution of the single field model is discussed in subsection (6.1.1). Equation (6.23) shows that the anisotropy is proportional to $c-1$ and the FRW limit is reached when $c \to 1$. We will assume that $c-1$ is small, so that the amount of anisotropy is within the phenomenological limits.

We now dicuss the perturbations around the anisotropic solution described in subsection (6.1.1) and study the relevant two point correlation functions.

7.1 Perturbations and Power Spectra

We decompose the perturbations as given in equations (4.31) making use of the left over $2d$ isotropy. We work in the Fourier space, where perturbations in momentum space are defined as in equation (4.16). The reality of each perturbation requires that $\delta^\dagger(\vec{k}) = \delta(-\vec{k})$. Instead of fixing the comoving momentum to be aligned along the $x-y$ plane as done in equations (6.30), we keep all the components of the comoving momenta (although final results do not depend on this choice) for generality. In this case, it is convenient to write explicitly the single degree of freedom encoded in the $2d$ vector modes. In momentum space, we define

$$B_i \equiv i\,\epsilon_{ij}\,k_{Tj}\,B_v \;\;,\;\; \tilde{B}_i \equiv i\,\epsilon_{ij}\,k_{Tj}\,\tilde{B}_v \;\;,\;\; E_i \equiv i\,\epsilon_{ij}\,k_{Tj}\,E_v \;\;,\;\; \alpha_i \equiv i\,\epsilon_{ij}\,k_{Tj}\,\alpha_j \tag{7.2}$$

where ϵ_{ij} is antisymmetric and $\epsilon_{12} = 1$. As done in section (6.2), we fix the coordinate and $U(1)$ gauge freedoms by setting $\tilde{B} = \Sigma = E = E_i = \alpha = 0$. We have previously discussed that the modes Φ, χ, B, B_i and α_0 are nondynamical, and they can be integrated out from the quadratic action of perturbations. Moreover, as discussed in the previous chapter, the quadratic action and linearized Einstein equations of the $2d$ vector and $2d$ scalar modes decouple. Then, total action describing the complete system can be written as

$$S = S_{2\mathrm{dS}}\left[\Psi,\,\delta\phi,\,\alpha_1\right] + S_{2\mathrm{dV}}\left[\tilde{B}_i,\,\alpha_i\right] \tag{7.3}$$

The fields entering in the above action are not canonically normalized. The canonically normalized fields are obtained through the redefinitions

$$\begin{aligned}
\delta\phi &\equiv e^{-3\alpha/2}\left[V_+ - \frac{\dot{\phi}}{\sqrt{2}\,M_p\,(\dot{\alpha}+\dot{\sigma})}\,H_+\right] \\
\Psi &\equiv e^{-3\alpha/2}\,\frac{2p^2\,\dot{\alpha} + \left(2p_L^2 - p_T^2\right)\,\dot{\sigma}}{\sqrt{2}\,M_p\,p_T^2\,(\dot{\alpha}+\dot{\sigma})}\,H_+ \\
\alpha_1 &\equiv e^{-\alpha/2-2\sigma}\left[\frac{p}{f(\phi)\,p_T}\,\Delta_+ - \frac{\tilde{p}_A}{\sqrt{2}\,M_p\,f^2(\phi)\,(\dot{\alpha}+\dot{\sigma})}\,H_+\right]
\end{aligned} \tag{7.4}$$

in the $2dS$ sector, and

$$\begin{aligned} \tilde{B}_i &\equiv -\sqrt{2}\,\epsilon_{ij}\,k_{Tj}\,e^{-3\alpha/2}\,\frac{e^{6\alpha\,k_L^2+k_T^2}}{M_p\,k_L\,k_T^2}\,H_\times \\ \alpha_i &\equiv i\,\epsilon_{ij}\,\frac{k_{Tj}}{k_T}\,\frac{e^{\sigma-\alpha/2}}{f(\phi)}\,\Delta_- \end{aligned} \tag{7.5}$$

in the $2dS$ sector. In terms of the canonical fields, the $2dS$ and $2dV$ actions in (7.3) have the following form (in momentum space)

$$S_{2\mathrm{dS},\,2\mathrm{dV}} = \frac{1}{2}\int d^3k\,dt\,\left[\dot{Y}^\dagger_{s,v}\,\dot{Y}_{s,v} + \dot{Y}^\dagger_{s,v}\,K_{s,v}\,Y_{s,v} - Y^\dagger_{s,v}\,K_{s,v}\,\dot{Y}_{s,v} - Y^\dagger_{s,v}\,\Omega^2_{s,v}\,Y_{s,v}\right] \tag{7.6}$$

where

$$Y_s \equiv \begin{pmatrix} V_+ \\ H_+ \\ \Delta_+ \end{pmatrix} \quad , \quad Y_v \equiv \begin{pmatrix} H_\times \\ \Delta_- \end{pmatrix} \tag{7.7}$$

The matrices $K_{s,v}$ are real and anti-symmetric [1] and $\Omega^2_{s,v}$ are real and symmetric. The explicit forms of the matrices $K_{s,v}$ and $\Omega^2_{s,v}$ are given in Appendix E.

We need to quantize the actions given in (7.6) in order to provide initial condition for the canonical modes (7.7) and the expressions for the two point correlators. The matrices appearing in (7.6) are unchanged under the parity transformation $\vec{k} \to -\vec{k}$ (as can be seen from the explicit expressions in Appendix E). We also have $Y_i^\dagger(\vec{k}) = Y_i(-\vec{k})$ from the reality of the fields entering in the actions (7.6).

In order to remove the mixed terms proportional to $K_{s,v}$ in the actions (7.6), as we have done previously in section 6.2.1, we perform the field rotation

$$\psi_{s,v} \equiv \mathbf{R}\,\mathbf{Y}_{s,v} \tag{7.8}$$

where $\mathbf{R}$ is an orthogonal matrix (so that $\dot{\mathbf{Y}}^\dagger\,\dot{\mathbf{Y}} = \dot{\psi}^\dagger\,\dot{\psi}$), satisfying

$$\dot{\mathbf{R}} = \mathbf{R}\,\mathbf{K} \quad , \quad \mathbf{R}_{\mathrm{late}} = \mathbf{1} \tag{7.9}$$

where the second condition states that $\mathbf{R}$ should reduce to the identity matrix at late times. The first condition can be also written as $\mathbf{K} = \mathbf{R}^T\,\dot{\mathbf{R}}$; we also note that $\mathbf{R}(-\vec{k}) =$

[1] Compare this form of the action with the one given in equation (6.35) where we have defined the canonical modes for the vector field without the imaginary factor i, which makes the kinetic mixing matrix symmetric. These differences in the definitions have no effect on the final result, and is done for the convenience of the relevant problem.

$\mathbf{R}(\vec{k})$, since this property is also satisfied by $\mathbf{K}$. As a consequence, each of the fields entering in the array ψ satisfies $\psi_i^\dagger(\vec{k}) = \psi_i(-\vec{k})$. In terms of the fields ψ, the action (7.6) becomes

$$S_{\rm 2dS,\,2dV} = \frac{1}{2}\int dt\, d^3k\, \left[\dot{\psi}^\dagger\,\dot{\psi} - \psi^\dagger\,\tilde{\Omega}^2\,\psi\right] \quad , \quad \tilde{\Omega}^2 \equiv \mathbf{R}\,\left(\Omega^2 + \mathbf{K}^T\,\mathbf{K}\right)\,\mathbf{R}^T \tag{7.10}$$

where we note that $\tilde{\Omega}^2$ is real, symmetric and invariant under $\vec{k} \to -\vec{k}$. In order the quantize coupled fields, one has to first find the "normal modes" by diagonalizing the time dependent frequency matrix $\tilde{\Omega}^2$. We do so by following the formalism given in reference [103]. We first introduce the matric $\mathbf{C}$ satisfying

$$\mathbf{C}^T\,\tilde{\Omega}^2\,\mathbf{C} = {\rm diag}\,\left(\omega_1^2, \ldots, \omega_N^2\right) \quad , \quad {\rm C_{end}} = 1 \tag{7.11}$$

where the second condition follows from the fact that, in the late time isotropic limit $\tilde{\Omega}^2 = \Omega^2$ is already diagonal. We note that $\mathcal{C}$ is orthogonal, and unchanged under $\vec{k} \to -\vec{k}$. We then define [103]

$$\begin{aligned} \psi_i(\vec{k}) &= C_{ij}\,\left[h_{jl}(\vec{k})\,\hat{a}_l(\vec{k}) + h^*_{jl}(\vec{k})\,\hat{a}^\dagger_l(-\vec{k})\right] \\ \pi_i(\vec{k}) = \dot{\psi}_i(\vec{k}) &= C_{ij}\,\left[\tilde{h}_{jl}(\vec{k})\,\hat{a}_l(\vec{k}) + \tilde{h}^*_{jl}(\vec{k})\,\hat{a}^\dagger_l(-\vec{k})\right] \end{aligned} \tag{7.12}$$

where $\hat{a}$ and $\hat{a}^\dagger$ are annihilation and creation operators respectively and they satisfy

$$\left[\hat{a}_i(\vec{k}),\,\hat{a}^\dagger_j(\vec{k'})\right] = \delta(\vec{k} - \vec{k'})\,\delta_{ij} \tag{7.13}$$

From the equations of motion following from (7.10), and the fact that $\pi_i = \dot{\psi}_i$, we find that the coefficients h_{ij} and $\tilde{h}_{ij}$, obey the equations (in matrix form)

$$\dot{\mathbf{h}} = \tilde{\mathbf{h}} - \mathbf{\Gamma}\,\mathbf{h} \;\;,\;\; \dot{\tilde{\mathbf{h}}} = -\mathbf{\Gamma}\,\tilde{\mathbf{h}} - \omega^2\,\mathbf{h} \;\;,\;\; \mathbf{\Gamma} \equiv \mathbf{C}^T\,\dot{\mathbf{C}} \tag{7.14}$$

From the parity of the matrices $\mathbf{C}$ and ω, and from the initial conditions (which we determine below, see equation (7.22), we see that h_{ij} and $\tilde{h}_{ij}$ are unchanged under $\vec{k} \to -\vec{k}$. [2]

We further define

$$\mathbf{h} = \frac{1}{2\omega}\,(\alpha + \beta) \quad , \quad \tilde{\mathbf{h}} = \frac{-i\,\omega}{\sqrt{2\omega}}\,(\alpha - \beta) \tag{7.15}$$

[2] This is why we wrote $h^*_{ij}(\vec{k})$ and $\tilde{h}^*_{ij}(\vec{k})$, rather than $h^*_{ij}(-\vec{k})$ and $\tilde{h}^*_{ij}(-\vec{k})$, in the decompositions (7.12)

It has been shown in [103] that the normal ordered hamiltonian for the fields ψ_i can be cast in the form

$$\hat{H} = \int d^3k\, \omega_i\, \hat{b}_i^\dagger(\vec{k})\, \hat{b}(\vec{k}) \tag{7.16}$$

where $\hat{b}_i$ and $\hat{b}_i^\dagger$ are the transformed annihilation and creation operators, related to those defined in (7.12) by (notice that the matrices α and β are unchanged under $\vec{k} \to -\vec{k}$)

$$\begin{pmatrix} \hat{\mathbf{b}}(t,\, \vec{k}) \\ \hat{\mathbf{b}}(t, -\vec{k}) \end{pmatrix} \equiv \begin{pmatrix} \alpha & \beta^* \\ \beta & \alpha^* \end{pmatrix}_{t,\,\vec{k}} \begin{pmatrix} \hat{\mathbf{a}}(\vec{k}) \\ \hat{\mathbf{a}}^\dagger(-\vec{k}) \end{pmatrix} \tag{7.17}$$

We see that the hamiltonian is diagonal in the $\hat{b}_i$, $\hat{b}_i^\dagger$ basis, so that these operators annihilate and create quanta of the (time-dependent) physical eigenstates of the system. The matrices α and β generalize to a system of N coupled fields the Bogoluibov coefficients that are needed for the quantization of a field with the time dependent frequency. As shown in [103], the canonical quantization of the ψ_i fields imposes the conditions

$$\alpha\, \alpha^\dagger - \beta^*\, \beta^T = \mathbb{1} \;\;,\;\; \alpha\, \beta^\dagger - \beta^*\, \alpha^T = 0 \tag{7.18}$$

Moreover, from the evolution equations (7.14), and the definitions (7.15), one finds that α and β obey the evolution equations [103]

$$\begin{aligned} \dot{\alpha} &= -i\, \omega\, \alpha + \frac{\dot{\omega}}{2\omega}\, \beta - I\, \alpha - J\, \beta \\ \dot{\beta} &= i\, \omega\, \beta + \frac{\dot{\omega}}{2\omega}\, \alpha - I\, \beta - J\, \alpha \end{aligned} \tag{7.19}$$

where

$$I = \frac{1}{2}\left(\sqrt{\omega}\, \Gamma\, \frac{1}{\sqrt{\omega}} + \frac{1}{\sqrt{\omega}}\, \Gamma\, \sqrt{\omega}\right) \;\;,\;\; J = \frac{1}{2}\left(\sqrt{\omega}\, \Gamma\, \frac{1}{\sqrt{\omega}} - \frac{1}{\sqrt{\omega}}\, \Gamma\, \sqrt{\omega}\right) \tag{7.20}$$

An inspection of the initial matrices $\mathbf{K}$ and Ω^2 shows that, at early times (when the mode is deeply inside the horizon) $\Omega^2 = p^2\, \mathbb{1} + \mathrm{O}(H)$ and $\mathbf{K} = \mathrm{O}(\sqrt{c-1}\, H)$ (in these expression we assume that the anisotropy is small). As a consequence,

$$\omega_i^2 \simeq p^2 + \mathrm{O}(H^2) \;\;,\;\; \Gamma,\, I,\, J,\, \frac{\dot{\omega}}{\omega} = \mathrm{O}(H) \tag{7.21}$$

in the early time regime. Therefore, we can disregard all but the first term in both of the right hand sides of (7.19). This leads to the usual adiabatic solutions [3]

$$\alpha_{\mathrm{early}} = e^{-i \int^t dt'\, \omega} \;\;,\;\; \beta_{\mathrm{early}} = 0 \tag{7.22}$$

[3] Notice that α_{early} is diagonal; the allowed initial conditions are actually more general than (7.21),

7.1.1 Two point correlation functions

By combining the various redefinitions given in the above Section, we can write the canonically normalized fields in real space as

$$Y_i\left(t,\,\mathbf{x}\right)=\int\frac{d^3k}{\left(2\pi\right)^{3/2}}\,\mathrm{e}^{i\mathbf{k}\cdot\mathbf{x}}\,\left[\Upsilon_{ij}\left(t,\,\mathbf{k}\right)\,\hat{a}_j\left(\mathbf{k}\right)+\Upsilon^*_{ij}\left(t,\,\mathbf{k}\right)\,\hat{a}^\dagger_j\left(-\mathbf{k}\right)\right] \tag{7.23}$$

where

$$\Upsilon_{ij}\left(\mathbf{k}\right)\equiv\left(R^T\,C\,h\right)_{ij} \tag{7.24}$$

(notice that h and Υ coincide at late times).

The (statistically averaged) two point correlation function can be expressed as the quantum expectation value

$$\mathcal{C}_{ij}\left(\mathbf{x},\,\mathbf{y}\right)\equiv\frac{1}{2}\langle Y_i\left(t,\,\mathbf{x}\right)\,Y_j\left(t,\,\mathbf{y}\right)+Y_j\left(t,\,\mathbf{y}\right)\,Y_i\left(t,\,\mathbf{x}\right)\rangle \tag{7.25}$$

where the symmetrization is required since the statistical average is a classical operation, independent of the ordering chosen (when computing any correlation with real data, $\mathcal{C}_{ij}\left(\mathbf{x},\,\mathbf{y}\right)=\mathcal{C}_{ji}\left(\mathbf{y},\,\mathbf{x}\right)$).

We insert (7.23) into (7.25). The resulting expression can be then simplified using the commutation relations (7.13) and the fact that the vacuum state is annihilated by $\hat{a}_i$ at all times (since the quantization of the previous Subsection is performed in the Heisenberg picture). After some algebra, we find

$$\mathcal{C}_{ij}\left(\mathbf{x},\,\mathbf{y}\right)=\int\frac{d^3k}{\left(2\pi\right)^3}\,\mathrm{e}^{i\mathbf{k}\cdot\left(\mathbf{x}-\mathbf{y}\right)}\,\mathrm{Re}\,\left[\left(\Upsilon\,\Upsilon^\dagger\right)_{ij}\right] \tag{7.26}$$

We now define the power spectra associated with these correlators. All of them are of the type

$$\mathcal{C}_{\mathcal{F}}=\int\frac{d^3k}{\left(2\pi\right)^3}\,\mathrm{e}^{i\mathbf{k}\cdot\left(\mathbf{x}-\mathbf{y}\right)}\mathcal{F}\left(\mathbf{k}\right) \tag{7.27}$$

---

since one can multiply each diagonal entry of α_{early} by a constant, and arbitrary phase factor $e^{i\gamma_i}$. This amounts in changing the matrices α and β given here by a matrix multiplication from the right, $\alpha\rightarrow\alpha\,P$, $\beta\rightarrow\beta\,P$, where $P\equiv\mathrm{diag}\left(e^{i\gamma_1},\ldots,e^{i\gamma_N}\right)$. The equations of motion (7.19) are unchanged by this multiplication. The same is true of the matrices h and $\tilde{h}$. Since h enters in the observable two point correlation function through the combination $h\,h^\dagger$, see equation...., the matrix P drops from the observable result. This confirms that the arbitrary phases contained in P are unphysical and can be set to any value. We use this freedom to set all the phases to zero at the initial time of our numerical simulations.

where the function $\mathcal{F}$ is real and it depends only on the absolute values of the components of $\mathbf{k}$ along the anisotropic $x-$direction (which we denoted by $|k_L|$), and on the $y-z$ plane (denoted by $k_T = \sqrt{k_{T2}^2 + k_{T3}^2}$). Thanks to this property (which follows from the symmetry of the background under rotations in the $y-z$ plane, and under parity), for any two points $\mathbf{x}$ and $\mathbf{y}$, we can always choose the y and z axes of the system such that the third component of $\mathbf{x}-\mathbf{y}$ vanishes (without changing $\mathcal{F}$). We therefore set

$$\mathbf{r} \equiv \mathbf{x} - \mathbf{y} \equiv (r_L,\, r_T,\, 0) \tag{7.28}$$

and $\mathbf{k} = k\left(\xi,\, \sqrt{1-\xi^2}\,\cos\phi_k,\, \sqrt{1-\xi^2}\,\sin\phi_k\right)$ in the integral (7.27), where ξ is the cosine of the angle between the $x-$axis and $\mathbf{k}$. The function $\mathcal{F}$ does not depend on ϕ_k and is even in ξ. The integral over ϕ_k then gives

$$\mathcal{C}_{\mathcal{F}} = \int \frac{dk}{k} \int_0^1 d\xi\, \cos\left(k\,\xi\, r_L\right) J_0\left(k\,\sqrt{1-\xi^2}\, r_T\right)\, P_{\mathcal{F}} \tag{7.29}$$

where J is the Bessel function of the first kind, and where we have introduced the power spectrum

$$P_{\mathcal{F}} \equiv \frac{k^3}{2\pi^2}\,\mathcal{F}\,(k,\,\xi) \tag{7.30}$$

In the case at hand, the power spectra depend both on the magnitude of the momentum of the modes, and on the angle between the momentum and the anisotropic direction.

On anisotropic backgrounds, the power spectrum is isotropic, and equation (7.29) reduces to the standard expression

$$\mathcal{C}_{\mathcal{F}} = \int \frac{dk}{k}\,\frac{\sin\left(k\,r\right)}{k\,r}\,\mathcal{P}_{\mathcal{F}} \qquad \text{isotropy} \tag{7.31}$$

7.1.2 Evolution of the perturbations and initial conditions

The equations of motion for the dynamical perturbations follow from (7.6). We expressed the action in momentum space, by Fourier transforming the starting modes as in (4.16), and by introducing the canonically normalized fields in (7.4) and (7.5). The equations of motion for the coefficient of the Fourier transforms of the canonical fields are

$$\ddot{Y}_s + 2\,K_s\,\dot{Y}_s + \left(\Omega_s^2 + \dot{K}_s\right) Y_s = 0 \quad , \quad \ddot{Y}_v + 2\,K_v\,\dot{Y}_v + \left(\Omega_v^2 + \dot{K}_v\right) Y_v = 0 \tag{7.32}$$

where the matrices $K_{s,v}$ and $\Omega_{s,v}^2$ are given in Appendix E.

We stress that these equations are a closed subset of the linearized Einstein equations for the perturbations. Specifically, all the perturbations of the model can be divided in dynamical and nondynamical ones. The nondynamical ones enter in the Einstein equations without time derivatives. One can solve the Einstein equations for these perturbations, and express the latter in terms of the dynamical ones. One then insert these expressions into the remaining Einstein equations. The resulting expressions coincide with equations (7.32). [4]

We need to specify what the coefficients $Y_{s,i}$ and $Y_{v,i}$ exactly are. The standard way to compute the generation of perturbations during inflation is a semiclassical computation, in which the perturbations are quantum fields on a classical background, as done in chapter 2. In most systems, the canonical perturbations are decoupled from each other, and can be quantized separately. This is not the case for the system we are studying, and the quantization had to be done accordingly. In the previous section, we introduced an array of annihilation/creation operators, and we saw that the Fourier coefficients of (4.16) are actually linear combinations of these operators, cf. equations (7.23):

$$Y_i\left(t,\,\mathbf{k}\right)=\Upsilon_{ij}\left(t,\,\mathbf{k}\right)\,\hat{a}_j\left(\mathbf{k}\right)+\Upsilon^*_{ij}\left(t,\,\mathbf{k}\right)\,\hat{a}^\dagger_j\left(-\mathbf{k}\right) \tag{7.33}$$

Inserting this decomposition into (7.32), we find

$$\left[\ddot{\Upsilon}_{ij}+2K_{il}\dot{\Upsilon}_{lj}+\left(\Omega^2+\dot{K}\right)_{il}\,\Upsilon_{lj}\right]a_j+\left[\ddot{\Upsilon}^*_{ij}+2K_{il}\dot{\Upsilon}^*_{lj}+\left(\Omega^2+\dot{K}\right)_{il}\,\Upsilon^*_{lj}\right]a^\dagger_j=0 \tag{7.34}$$

both in the 2d scalar and 2d vector sector. The linear combinations multiplying different annihilation and creation operators need to cancel separately; therefore

$$\ddot{\Upsilon}_{ij}+2K_{il}\dot{\Upsilon}_{lj}+\left(\Omega^2+\dot{K}\right)_{il}\,\Upsilon_{lj}=0 \tag{7.35}$$

These equations also guarantee that the linear combinations multiplying the annihilation operators vanish, since the matrices K and Ω^2 are real.

Having determined the evolution equations obeyed by Υ_{ij}, we now turn to the determination of their initial condition. We find

$$\Upsilon=R^T\,C\,h\quad,\quad\dot{\Upsilon}=-K\,R^T\,C\,h+R^T\,C\,\tilde{h} \tag{7.36}$$

[4] The explicit proof of this is given in section 6.2 of the previous section.

The first expression is simply the definition (7.24). The second expression is obtained by differentiating the first one, and by using the first and third of (7.14), as well as $K = -\dot{R}^T R$.

The initial values of $R^T C$ and ω are obtained by the diagonalization of $\Omega^2 + K^T K$ at the initial time. Indeed $R^T C$ is defined as the matrix that diagonalizes $\Omega^2 + K^T K$, while ω^2 is the diagonal matrix formed by the eigenvalues of $\Omega^2 + K^T K$, see equations (7.10) and (7.11). The initial values of h and $\tilde{h}$ follow instead from equations. (7.15), and from the initial conditions for α and β according to the adiabatic vacuum prescription, equation (7.22) $\alpha_{\rm in} = \mathbb{1}$, $\beta_{\rm in} = 0$.

7.1.3 Power spectra after isotropization

As shown in Appendix F the universe becomes isotropic after inflation, the canonical perturbations that we have introduced become the standard scalar and tensor modes of FRW cosmology. More precisely, we find that, in this regime,

$$\mathcal{R} = \frac{H}{a^{3/2}\,\dot{\phi}}\,V_+ \quad , \quad h_+ = -\frac{\sqrt{2}}{a^{3/2}\,M_p}\,H_+ \quad , \quad h_\times = \frac{i\,\sqrt{2}}{a^{3/2}\,M_p}\,H_\times \tag{7.37}$$

where $\mathcal{R}$ is the standard (scalar) comoving curvature perturbation, and h_+ and $h_\times$ are the two standard gravity wave polarizations.

We also shown in Appendix F that, in the isotropic regime, our formalism reproduces the standard evolution equations for these modes. These equations are decoupled, so that the modes evolve independently from each other (at the linearized level). However, the two 2d scalar modes V_+ and H_+ are coupled to each other, and to the mode Δ_+ during inflation, when the background is anisotropic. The mode $H_\times$ is always decoupled from these three modes, but it is coupled to the mode $\Delta_\times$ during inflation. The coupling modifies the diagonal correlation functions $\langle V_+^2\rangle$, $\langle H_+^2\rangle$, $\langle \Delta_+^2\rangle$, $\langle H_\times^2\rangle$, $\langle \Delta_\times^2\rangle$ with respect to the standard inflationary results, and it introduces the nondiagonal correlations $\langle V_+\,H_+\rangle$, $\langle V_+\,\Delta_+\rangle$, $\langle H_+\Delta_+\rangle$, $\langle H_\times\Delta_\times\rangle$, which are absent in standard inflation.

As the universe isotropizes, the two modes Δ_+ and $\Delta_\times$ become the two transverse polarizations of the vector field. These modes rapidly decrease after inflation (when the evolution of the vector becomes standard). Therefore, all correlators involving these modes become negligible at late times, and we disregard them in the remainder of this

work. The remaining correlators can be written as in equation (7.29), in terms of the power spectra

$$\begin{aligned} P_{\mathcal{R}\mathcal{R}} &= \frac{1}{2\pi^2}\,\frac{H^2}{\dot\phi^2}\,p^3\,\left(\Upsilon_s\,\Upsilon_s^\dagger\right)_{11} \\ P_{\mathcal{R}h_+} &= -\frac{1}{\sqrt{2}\pi^2}\,\frac{H}{\dot\phi\,M_p}\,p^3\,\mathrm{Re}\left[\left(\Upsilon_s\,\Upsilon_s^\dagger\right)_{12}\right] \\ P_{h_+h_+} &= \frac{1}{\pi^2\,M_p^2}\,p^3\,\left(\Upsilon_s\,\Upsilon_s^\dagger\right)_{22} \\ P_{h_\times h_\times} &= \frac{1}{\pi^2\,M_p^2}\,p^3\,\left(\Upsilon_v\,\Upsilon_v^\dagger\right)_{11} \end{aligned} \tag{7.38}$$

To evaluate the power spectra, we impose the initial conditions on Υ as discussed at the end of the previous Subsection. We then evolve Υ through their equations of motion (7.35). We remark that the resulting power spectra are dimensionless, and are written in terms of only physical quantities (namely, they are insensitive to the normalization of the scale factors; this is because only physical quantities appear in the initial conditions and the evolution equations for Υ).

Our results are shown in Figures 7.1, 7.2, and 7.3. Figure 7.1 shows the evolution of the power for the specific value of $c-1=10^{-5}$ in the kinetic function $f(\phi)$, and for a specific mode: we denote by k_* the magnitude of the momentum of a mode which barely exits the horizon at the end of inflation; we choose a mode with momentum $k=10^{-20}\,k*$, and we choose the cosine of the angle between the momentum and the privileged direction to be $\xi=1/2$ (such values have no particular meaning, and are just chosen for illustrative purposes; different values of k and ξ lead to the same qualitative behavior); this mode is initially deeply inside the horizon, and it leaves the horizon about 50 e-folds before the end of inflation. [5] The power in the scalar-scalar and tensor-tensor correlations behaves analogously to the isotropic case. The power in the scalar-tensor cross correlation is instead very small initially, and slightly increases during and immediately after inflation. The power becomes constant (at the value seen in the latest time shown in the Figure) as the universe isotropizes after inflation.

In Figure 7.2 we show the power spectra for the specific value of $c-1=10^{-5}$ in the kinetic function $f(\phi)$. The smallest momentum shown corresponds to modes that

[5] Since this choice of $c\simeq 1$ corresponds to a very small anisotropy, we define the horizon, and the number of e-folds, only through the evolution of the "average" scale factor e^α, as in FRW cosmology.

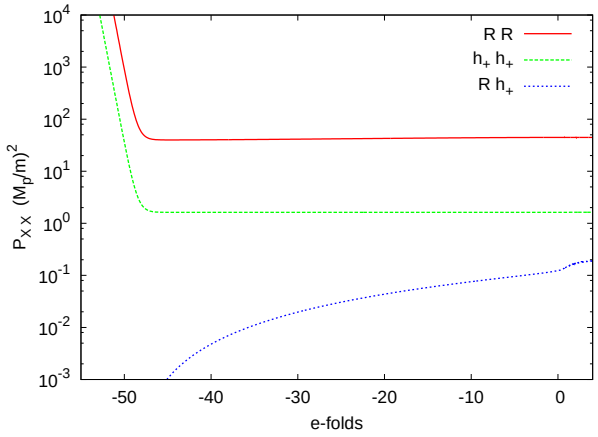

Figure 7.1: Time evolution for the power of a specific mode, on a nearly isotropic background ($c - 1 = 10^{-5}$). The number of e-folds α is used as a "time" variable, and it is normalized to 0 at the end of inflation. The mode shown leaves the horizon about 50 e-folds before the end of inflation. See the main text for details.

exited the horizon about 60 e-folds before the end of inflation. For the scalar-scalar and tensor-tensor case, the standard result is also shown for comparison. The scalar-scalar power spectrum (bottom left panel) is slightly greater than in the isotropic case; this can be compensated by decreasing the scalar field mass (for this reason, the ratio m/M_p has been kept as a free parameter in the Figure). The angular dependence of $P_{\mathcal{R}\mathcal{R}}$ is of $\mathrm{O}\left(10^{-1}\right)$ at the largest scales, while it slowly decreases at greater scales. The tensor-tensor power spectra (bottom panels) are closer to the standard result, and they exhibit a much milder angular dependence (we found g_* for the scalar spectra is suppressed with respect to g_* in the tensor spectrum by approximately the ratio between the power of the tensor and the scalar spectra). Moreover, the results for the two polarizations are nearly identical. The scalar-tensor cross correlation (upper right panel) shows a stronger angular dependence, but it is smaller than the other two spectra.

In Figure 7.3 we show the angular dependence g_* (defined in equation (7.1)) for the scalar-scalar power spectrum, for different values of c in $f(\phi)$. We remark that all values of c provide a negative g_* (in Figure 7.3 we actually show $|g_*| = -g_*$ in logarithmic scale). The value of g_* shown in the plots is obtained by comparing, for each value of $k = |\mathbf{k}|$, the power at $\xi = 0.1$ and at $\xi = 0.9$. We have however verified that the ACW parametrization (7.1) is very accurate, in the sense that, once g_* and

$P(k)$ are obtained from the results at $\xi = 0.1$ and $\xi = 0.9$, also other values of ξ are fitted very well by (7.1).

The significance of the results summarized in these Figures is discussed in the next concluding Section.

7.2 Discussion

In this section we compute the precise phenomenological signatures for the model of [12]. This model admits an anisotropic inflationary background evolution, supported by the combined presence of a scalar and a vector field. This solution is (mathematically) continuously connected to an isotropic solution, in the limit in which the energy density associated to the vector is sent to zero. Moreover, the model is free of the ghost instabilities that plague other models with vector fields during inflation, due to the U(1) invariance of its action under a shift of the vector. Therefore, it offers a complete, and stable counterexample to Wald's no hair theorem on the isotropization of Bianchi spaces [10].

We studied the simplest realization of the idea of [12], in which a single vector is present, and the potential of the scalar is taken to be that of massive chaotic inflation. We found that the scalar-scalar correlation function exhibits an angular dependence which is however of the wrong sign to account for the breaking of rotational invariance seen in the data: the model gives a negative value for g_*, while the analysis of [48] indicates that $g_* = 0.29 \pm 0.031$ in the WMAP W-band. We also found that the amount of anisotropy in the spectrum (the order of magnitude of $|g_*|$) is not of the same order of magnitude as the amount of anisotropy in the expansion (the order of magnitude of $\Delta H/H \sim \dot{\sigma}/\dot{\alpha}$, where H is the average expansion rate, and ΔH the difference between the expansion rate in the different coordinates). A $|g_*| = \mathrm{O}\left(10^{-1}\right)$ is obtained when the anisotropy in the expansion is of $\mathrm{O}\left(10^{-7} - 10^{-6}\right)$ during inflation. It is also worth noting that the anisotropy in the tensor-tensor spectrum is much milder than that in the scalar-scalar spectrum (we find that the suppression is approximately proportional to the ratio between the two power spectra).

A distinctive feature of the model (and, of anisotropic spaces in general) is a non-vanishing scalar-tensor correlation, which, if sufficiently high, may be detected through

temperature-B mode correlation in the CMB. A naive estimate actually suggests that the scalar-tensor correlation could be higher than the tensor-tensor one. Indeed the amplitude of a tensor mode is approximately multiplied by $2\sqrt{\epsilon}$ with respect to that of a scalar mode, where $\epsilon \equiv -\dot{H}/H^2$ is a slow roll parameter. [6] The tensor-tensor correlator is suppressed by one more power of this factor than the tensor-scalar correlator. However, the scalar-tensor correlator vanishes for an isotropic space, and hence must be suppressed by some factor related to the asymmetry. If one naively assumes that this factor is $|g_*|$, one would get the prediction that $P_{\mathcal{R}h}/P_{hh} \simeq |g_*|/(2\sqrt{\epsilon})$. One would then get $P_{\mathcal{R}h}/P_{hh} \simeq 6\,|g_*|$ for chaotic inflation, and a greater value for other inflationary models, characterized by a smaller value of ϵ. Our explicit results show that this estimate is reasonable, but not exact. For the case of $c - 1 = 10^{-5}$ shown in Figure 7.2 (giving $g_* \simeq -0.23$), the estimate gives $P_{\mathcal{R}h}/P_{hh} \simeq 1.4$, while the actual spectra give $P_{\mathcal{R}h}/P_{hh} \simeq 0.05 - 0.25$, depending on the orientation of the mode (the value of ξ).

To conclude, while the simplest realization of [12] cannot explain the breaking of rotational invariance seen in the data, and, most likely, it does not give rise to an interesting scalar-tensor correlation, this model is, to our knowledge, the first complete and stable model of anisotropic inflation for which the phenomenological predictions strictly follow from the action (and not from arbitrary initial conditions), and have been computed. As the observed breaking of rotational invariance awaits for a confirmation, or a refutation, from Planck, our work provides the tools for studying different models, to see whether they can reproduce the WMAP feature, and perhaps lead to new predictions.

[6] Since we are considering a small anisotropy, we can use the FRW computation in this estimate; then, comparing the two equations in (F.9) we see that $|V_+| \simeq |H_{+,\times}|$. This gives $|h_{+,\times}/\mathcal{R}| \simeq \sqrt{2}\dot{\phi}/(M_p\,H) \simeq 2\epsilon$.

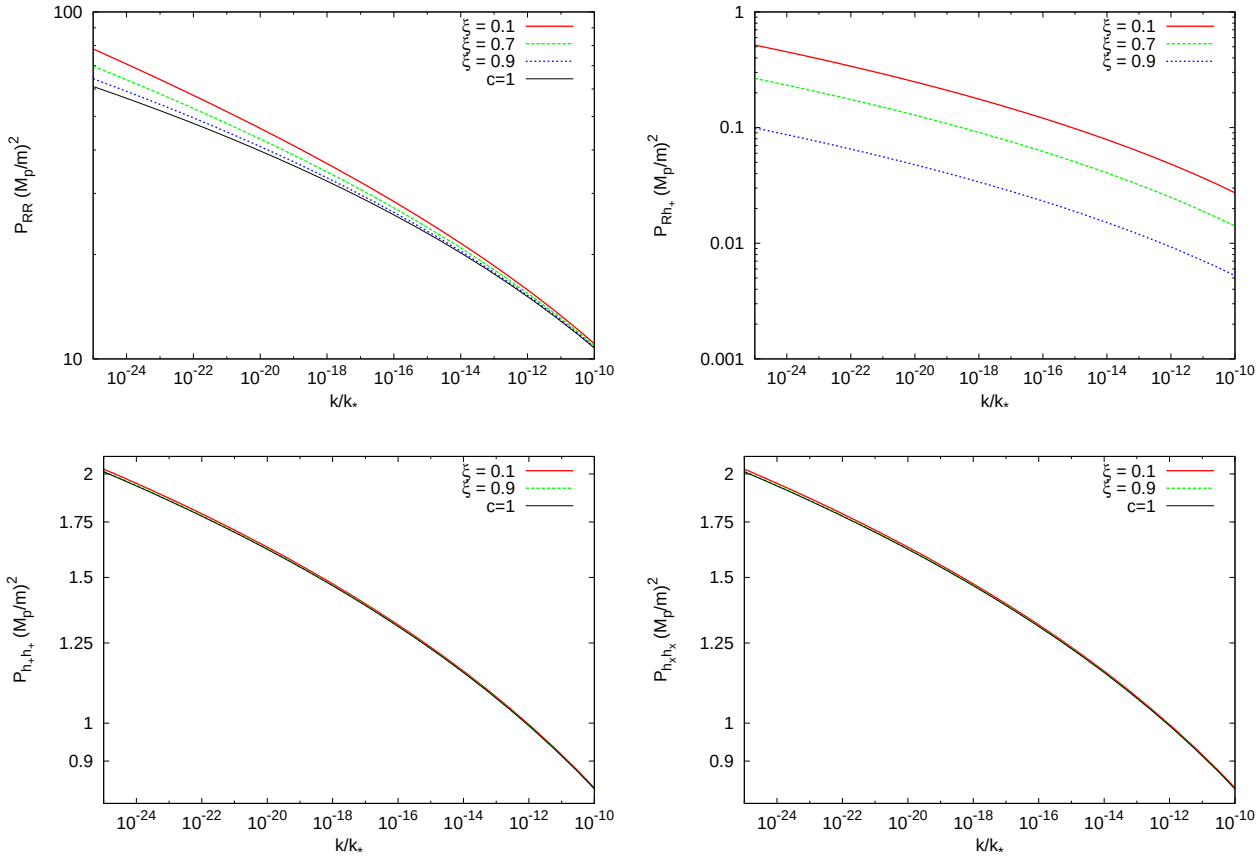

Figure 7.2: Scalar-scalar, scalar-tensor, and tensor-tensor power spectra for a nearly isotropic background ($c - 1 = 10^{-5}$). Notice that the scale on the y axis is different for the different panels. For the scalar-scalar, and the tensor-tensor spectra, we also show the standard result for comparison (in the present model, the isotropic limit is reached for $c = 1$).

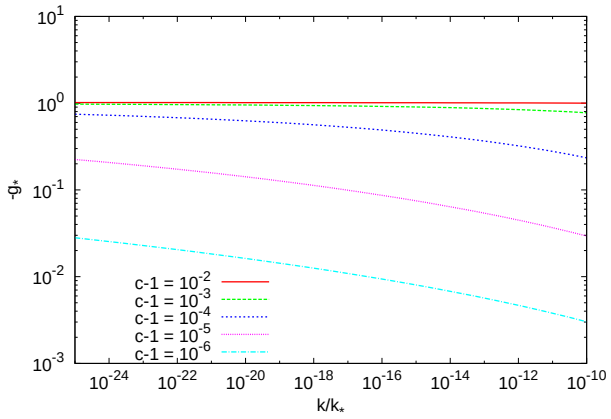

Figure 7.3: Angular dependence (expressed through the ACW g_* factor) of the scalar-scalar power spectrum for different choices of c.

Chapter 8

Conclusions

Inflation is one of the most important parts of modern cosmology. Inflationary predictions have been successfully tested by CMB experiments, and it is legitimate to claim that there is at least indirect evidence for inflation. Still, much of the physics of inflation is unknown. For instance, the energy scale at which inflation took place (thus the underlying particle physics mechanism) is unknown. There is a vast number of inflationary models based on some of the most compelling particle physics models, including supersymmetric and string theory inspired models. However, with upcoming experiments, and a possible detection of gravity waves, we would be able to measure this unknown energy scale [4]. Thus, CMB experiments would be able to probe into very high energy scales and inflationary predictions for different particle physics models would possibly be tested in the near future. Simple models of inflation assume that it is driven by scalar fields. However, it is possible that inflation could have been driven by higher spin fields. This is legitimate, given the fact that the precise mechanism of inflation is unknown. Moreover, higher spin fields, like vector fields, appear in many particle physics models and they would provide unique predictions. In this thesis, we studied the physics of vector fields during inflation.

We first discussed the motivations of inflation, including the horizon, flatness and unwanted relic problems. We have shown that these problems are related to an unnatural choice of initial conditions, and inflation removes these problems by providing an accelerated expansion in the early universe. We then discussed how inflation can be realized in a concrete model, and studied the case of inflation driven by a single scalar

field. We first studied the background evolution of the scalar field and then considered its perturbations, which are coupled to metric perturbations. We have developed the quantum theory of these perturbations, which provided us with the initial conditions of them. We then obtained the power spectra of the resulting density perturbations and gravity waves.

After studying the generation of perturbations and the formalism of their study, we have discussed how the CMB anisotropies are produced. Since the main purpose of this thesis is not the full study of CMB anisotropies, we have limited our discussion to only large scale anisotropies, which can be performed analytically, as an illustration. We then provided a comparison of inflationary predictions with the results of the CMB experiments. Then, we have discussed some of the unexplained features in the CMB data which seem to be anomalous in the standard inflationary picture. We briefly summarized the studies in the literature, including the attempts to explain them by a cosmological effect. These unexplained features in part motivated the study of vector fields during inflation.

As the first example of vector field driven model of inflation, we have discussed the ACW model [46], which leads to the alignment of multipoles in the CMB. In this model the vector field has a vev along one of the spatial directions and its norm is fixed through a lagrange multiplier term. This model has attracted particular attention since it provides a controllable background anisotropy and predicts a simple anisotropic spectrum. Moreover, there has been claims that it fits to the CMB data at a considerable level. We have studied the complete system of perturbations of this model and showed that it is plagued by ghost instabilities. Moreover, the perturbations diverge close to horizon crossing, indicating the the background solution is also unstable.

As a second example, we have discussed vector field models where there is a coupling with the curvature scalar in the mass squared term. We discussed two possible applications of this coupling, vector inflation and vector curvaton. In both cases, the coupling to curvature is used to resemble the vector field to a scalar field, through the breakage of conformal invariance of the vector field. This leads to a slow roll inflationary background solution for the vector inflation case and a nearly scale invariant spectrum of perturbations for the vector curvaton case. We have proven that both models are plagued by ghost instabilities. Moreover, we have shown that the solutions

to the equations of motion for the perturbations also diverge, indicating an instability of the background solution.

Finally, we have discussed vector fields that are coupled kinetically to a scalar field. In these types of models, the background solution is anisotropic when the vector field has a nonzero vev. We have shown that these models are stable and we have studied the spectrum of perturbations. We have computed tensor-tensor, tensor-scalar and scalar-scalar correlators in this model. We have argued that a detection of temperature-E mode polarization correlation would result in this model, so that it can be tested with CMB upcoming polarization experiments.

References

[1] A. H. Guth, Phys. Rev. D **23**, 347 (1981).

[2] E. Komatsu *et al.*, arXiv:1001.4538 [astro-ph.CO].

[3] E. L. Wright *et al.*, Astrophys. J. **396**, L13 (1992).

[4] D. Baumann *et al.* [CMBPol Study Team Collaboration], AIP Conf. Proc. **1141**, 10 (2009) [arXiv:0811.3919 [astro-ph]].

[5] V. F. Mukhanov, H. A. Feldman and R. H. Brandenberger, Phys. Rept. **215**, 203 (1992).

M. Sasaki, Prog. Theor. Phys. **76**, 1036 (1986).

[6] E. Komatsu *et al.*, arXiv:1001.4538 [astro-ph.CO].

[7] C. Armendariz-Picon and P. B. Greene, Gen. Rel. Grav. **35**, 1637 (2003) [arXiv:hep-th/0301129]; B. Saha, Phys. Rev. D **74**, 124030 (2006); C. G. Boehmer and D. F. Mota, Phys. Lett. B **663**, 168 (2008) [arXiv:0710.2003 [astro-ph]]; C. G. Boehmer, Phys. Rev. D **77**, 123535 (2008) [arXiv:0804.0616 [astro-ph]]; D. Gredat and S. Shankaranarayanan, arXiv:0807.3336 [astro-ph]. T. Watanabe, arXiv:0902.1392 [astro-ph.CO]; G. de Berredo-Peixoto and E. A. de Freitas, arXiv:0902.4025 [gr-qc];

[8] A. Golovnev, V. Mukhanov and V. Vanchurin, JCAP **0806**, 009 (2008) [arXiv:0802.2068 [astro-ph]].

[9] C. Germani and A. Kehagias, JCAP **0903**, 028 (2009) [arXiv:0902.3667 [astro-ph.CO]]; T. Kobayashi and S. Yokoyama, JCAP **0905**, 004 (2009) [arXiv:0903.2769

[astro-ph.CO]]; T. S. Koivisto and N. J. Nunes, arXiv:0907.3883 [astro-ph.CO]; C. Germani and A. Kehagias, arXiv:0908.0001 [astro-ph.CO]; T. S. K. Nunes, arXiv:0908.0920 [astro-ph.CO].

[10] R. W. Wald, Phys. Rev. D **28**, 2118 (1983).

[11] S. Kanno, M. Kimura, J. Soda and S. Yokoyama, JCAP **0808**, 034 (2008) [arXiv:0806.2422 [hep-ph]].

[12] M. a. Watanabe, S. Kanno and J. Soda, Phys. Rev. Lett. **102**, 191302 (2009) [arXiv:0902.2833 [hep-th]];

[13] K. Dimopoulos and M. Karciauskas, JHEP **0807**, 119 (2008) [arXiv:0803.3041 [hep-th]]; K. Dimopoulos, M. Karciauskas, D. H. Lyth and Y. Rodriguez, JCAP **0905**, 013 (2009) [arXiv:0809.1055 [astro-ph]].

[14] C. L. Bennett *et al.*, Astrophys. J. **464**, L1 (1996) [arXiv:astro-ph/9601067].

[15] D. N. Spergel *et al.* [WMAP Collaboration], Astrophys. J. Suppl. **148**, 175 (2003) [arXiv:astro-ph/0302209].

[16] A. de Oliveira-Costa, M. Tegmark, M. Zaldarriaga and A. Hamilton, Phys. Rev. D **69**, 063516 (2004) [arXiv:astro-ph/0307282].

[17] G. Efstathiou, Mon. Not. Roy. Astron. Soc. **348**, 885 (2004) [arXiv:astro-ph/0310207].

[18] C. Copi, D. Huterer, D. Schwarz and G. Starkman, Phys. Rev. D **75**, 023507 (2007) [arXiv:astro-ph/0605135].

[19] K. Land and J. Magueijo, Mon. Not. Roy. Astron. Soc. **357**, 994 (2005) [arXiv:astro-ph/0405519].

[20] K. Land and J. Magueijo, Phys. Rev. D **72**, 101302 (2005) [arXiv:astro-ph/0507289].

[21] T. R. Jaffe, A. J. Banday, H. K. Eriksen, K. M. Gorski and F. K. Hansen, Astrophys. J. **629**, L1 (2005) [arXiv:astro-ph/0503213].

[22] M. Tegmark, A. de Oliveira-Costa and A. Hamilton, Phys. Rev. D **68**, 123523 (2003) [arXiv:astro-ph/0302496].

[23] D. J. Schwarz, G. D. Starkman, D. Huterer and C. J. Copi, Phys. Rev. Lett. **93**, 221301 (2004) [arXiv:astro-ph/0403353].

[24] C. J. Copi, D. Huterer, D. J. Schwarz and G. D. Starkman, Mon. Not. Roy. Astron. Soc. **399**, 295 (2009) [arXiv:0808.3767 [astro-ph]].

[25] F. K. Hansen, A. J. Banday, K. M. Gorski, H. K. Eriksen and P. B. Lilje, Astrophys. J. **704**, 1448 (2009) [arXiv:0812.3795 [astro-ph]].

[26] F. K. Hansen, P. Cabella, D. Marinucci and N. Vittorio, Astrophys. J. **607**, L67 (2004) [arXiv:astro-ph/0402396].

[27] F. K. Hansen, A. J. Banday and K. M. Gorski, Mon. Not. Roy. Astron. Soc. **354**, 641 (2004) [arXiv:astro-ph/0404206].

[28] D. Hanson and A. Lewis, Phys. Rev. D **80**, 063004 (2009) [arXiv:0908.0963 [astro-ph.CO]].

[29] J. Hoftuft, H. K. Eriksen, A. J. Banday, K. M. Gorski, F. K. Hansen and P. B. Lilje, Astrophys. J. **699**, 985 (2009) [arXiv:0903.1229 [astro-ph.CO]].

[30] H. K. Eriksen, F. K. Hansen, A. J. Banday, K. M. Gorski and P. B. Lilje, Astrophys. J. **605**, 14 (2004) [Erratum-ibid. **609**, 1198 (2004)] [arXiv:astro-ph/0307507].

[31] H. K. Eriksen, A. J. Banday, K. M. Gorski, F. K. Hansen and P. B. Lilje, Astrophys. J. **660**, L81 (2007) [arXiv:astro-ph/0701089].

[32] P. Vielva, E. Martinez-Gonzalez, R. B. Barreiro, J. L. Sanz and L. Cayon, Astrophys. J. **609**, 22 (2004) [arXiv:astro-ph/0310273].

[33] P. Mukherjee and Y. Wang, Astrophys. J. **613**, 51 (2004) [arXiv:astro-ph/0402602].

[34] M. Cruz, M. Tucci, E. Martinez-Gonzalez and P. Vielva, Mon. Not. Roy. Astron. Soc. **369**, 57 (2006) [arXiv:astro-ph/0601427].

[35] M. Cruz, L. Cayon, E. Martinez-Gonzalez, P. Vielva and J. Jin, Astrophys. J. **655**, 11 (2007) [arXiv:astro-ph/0603859].

[36] M. Cruz, N. Turok, P. Vielva, E. Martinez-Gonzalez and M. Hobson, Science **318**, 1612 (2007) [arXiv:0710.5737 [astro-ph]].

[37] M. Bridges, J. D. McEwen, M. Cruz, M. P. Hobson, A. N. Lasenby, P. Vielva and E. Martinez-Gonzalez, arXiv:0712.1789 [astro-ph].

[38] A. E. Gumrukcuoglu, C. R. Contaldi and M. Peloso, arXiv:astro-ph/0608405.

[39] A. E. Gumrukcuoglu, C. R. Contaldi and M. Peloso, JCAP **0711**, 005 (2007) [arXiv:0707.4179 [astro-ph]].

[40] T. S. Pereira, C. Pitrou and J. P. Uzan, JCAP **0709**, 006 (2007) [arXiv:0707.0736 [astro-ph]].

[41] C. Pitrou, T. S. Pereira and J. P. Uzan, JCAP **0804**, 004 (2008) [arXiv:0801.3596 [astro-ph]].

[42] A. E. Gumrukcuoglu, L. Kofman and M. Peloso, Phys. Rev. D **78**, 103525 (2008) [arXiv:0807.1335 [astro-ph]].

[43] J. D. Barrow and S. Hervik, Phys. Rev. D **74**, 124017 (2006) [arXiv:gr-qc/0610013]. J. D. Barrow and S. Hervik, Phys. Rev. D **73**, 023007 (2006) [arXiv:gr-qc/0511127].

[44] N. Kaloper, Phys. Rev. D **44**, 2380 (1991). E. Di Grezia, G. Esposito, A. Funel, G. Mangano and G. Miele, Phys. Rev. D **68**, 105012 (2003) [arXiv:gr-qc/0305050].

[45] L. H. Ford, Phys. Rev. D **40**, 967 (1989).

[46] L. Ackerman, S. M. Carroll and M. B. Wise, Phys. Rev. D **75**, 083502 (2007) [Erratum-ibid. D **80**, 069901 (2009)] [arXiv:astro-ph/0701357].

[47] N. E. Groeneboom and H. K. Eriksen, Astrophys. J. **690**, 1807 (2009) [arXiv:0807.2242 [astro-ph]].

[48] N. E. Groeneboom, L. Ackerman, I. K. Wehus and H. K. Eriksen, arXiv:0911.0150 [astro-ph.CO].

[49] G. Dvali, A. Gruzinov and M. Zaldarriaga, Phys. Rev. D **69**, 023505 (2004) [arXiv:astro-ph/0303591].

L. Kofman, arXiv:astro-ph/0303614.

[50] T. R. Dulaney, M. I. Gresham and M. B. Wise, Phys. Rev. D **77**, 083510 (2008) [Erratum-ibid. D **79**, 029903 (2009)] [arXiv:0801.2950 [astro-ph]].

[51] T. R. Dulaney and M. I. Gresham, arXiv:0805.1078 [gr-qc].

[52] B. Himmetoglu, C. R. Contaldi and M. Peloso, Phys. Rev. Lett. **102**, 111301 (2009) [arXiv:0809.2779 [astro-ph]].

[53] B. Himmetoglu, C. R. Contaldi and M. Peloso, Phys. Rev. D **79**, 063517 (2009) [arXiv:0812.1231 [astro-ph]].

[54] B. Himmetoglu, C. R. Contaldi and M. Peloso, Phys. Rev. D **80**, 123530 (2009) [arXiv:0909.3524 [astro-ph.CO]].

[55] M. S. Turner and L. M. Widrow, Phys. Rev. D **37**, 2743 (1988).

[56] V. Demozzi, V. Mukhanov and H. Rubinstein, arXiv:0907.1030 [astro-ph.CO].

[57] B. Himmetoglu, JCAP **1003**, 023 (2010) [arXiv:0910.3235 [astro-ph.CO]].

[58] A. E. Gumrukcuoglu, B. Himmetoglu and M. Peloso, Phys. Rev. D **81**, 063528 (2010) [arXiv:1001.4088 [astro-ph.CO]].

[59] A. D. Linde, Phys. Lett. B **129**, 177 (1983).

[60] N. D. Birrell and P. C. W. Davies, *Cambridge, Uk: Univ. Pr. (1982) 340p*

[61] J. Lesgourgues, D. Polarski and A. A. Starobinsky, Nucl. Phys. B **497**, 479 (1997) [arXiv:gr-qc/9611019].

[62] A. R. Liddle and D. H. Lyth, Phys. Rept. **231**, 1 (1993) [arXiv:astro-ph/9303019].

[63] D. H. Lyth and D. Wands, Phys. Lett. B **524**, 5 (2002) [arXiv:hep-ph/0110002].

[64] R. L. Arnowitt, S. Deser and C. W. Misner, arXiv:gr-qc/0405109.

[65] H. V. Peiris *et al.* [WMAP Collaboration], Astrophys. J. Suppl. **148**, 213 (2003) [arXiv:astro-ph/0302225].

[66] R. A. Sunyaev and Y. B. Zeldovich, Ann. Rev. Astron. Astrophys. **18** (1980) 537.

[67] T. Pyne and S. M. Carroll, Phys. Rev. D **53**, 2920 (1996) [arXiv:astro-ph/9510041].

[68] V. F. Mukhanov, Int. J. Theor. Phys. **43**, 623 (2004) [arXiv:astro-ph/0303072].

[69] M. Zaldarriaga, D. N. Spergel and U. Seljak, Astrophys. J. **488**, 1 (1997) [arXiv:astro-ph/9702157].

[70] S. Dodelson, *Amsterdam, Netherlands: Academic Pr. (2003) 440 p*

[71] M. Kowalski *et al.* [Supernova Cosmology Project Collaboration], Astrophys. J. **686**, 749 (2008) [arXiv:0804.4142 [astro-ph]].

[72] W. J. Percival, S. Cole, D. J. Eisenstein, R. C. Nichol, J. A. Peacock, A. C. Pope and A. S. Szalay, Mon. Not. Roy. Astron. Soc. **381**, 1053 (2007) [arXiv:0705.3323 [astro-ph]].

[73] C. R. Contaldi, M. Peloso, L. Kofman and A. D. Linde, JCAP **0307**, 002 (2003) [arXiv:astro-ph/0303636].

[74] J. M. Cline, P. Crotty and J. Lesgourgues, JCAP **0309**, 010 (2003) [arXiv:astro-ph/0304558].

[75] Y. S. Piao, B. Feng and X. m. Zhang, Phys. Rev. D **69**, 103520 (2004) [arXiv:hep-th/0310206].

[76] B. A. Powell and W. H. Kinney, Phys. Rev. D **76**, 063512 (2007) [arXiv:astro-ph/0612006].

[77] J. F. Donoghue, K. Dutta and A. Ross, Phys. Rev. D **80**, 023526 (2009) [arXiv:astro-ph/0703455].

[78] C. L. Bennett *et al.*, arXiv:1001.4758 [astro-ph.CO].

[79] C. L. Francis and J. A. Peacock, arXiv:0909.2495 [astro-ph.CO].

[80] L. Grisa and L. Sorbo, arXiv:1002.0510 [astro-ph.CO].

[81] D. Hanson and A. Lewis, Phys. Rev. D **80**, 063004 (2009) [arXiv:0908.0963 [astro-ph.CO]].

[82] D. Hanson, A. Lewis and A. Challinor, arXiv:1003.0198 [astro-ph.CO].

[83] A. L. Erickcek, M. Kamionkowski and S. M. Carroll, Phys. Rev. D **78**, 123520 (2008) [arXiv:0806.0377 [astro-ph]].

[84] A. L. Erickcek, S. M. Carroll and M. Kamionkowski, Phys. Rev. D **78**, 083012 (2008) [arXiv:0808.1570 [astro-ph]].

[85] A. L. Erickcek, C. M. Hirata and M. Kamionkowski, Phys. Rev. D **80**, 083507 (2009) [arXiv:0907.0705 [astro-ph.CO]].

[86] R. Zhang and D. Huterer, Astropart. Phys. **33**, 69 (2010) [arXiv:0908.3988 [astro-ph.CO]].

[87] L. Rudnick, S. Brown and L. R. Williams, Astrophys. J. **671**, 40 (2007) [arXiv:0704.0908 [astro-ph]].

[88] K. M. Smith and D. Huterer, arXiv:0805.2751 [astro-ph].

[89] B. R. Granett, I. Szapudi and M. C. Neyrinck, arXiv:0911.2223 [astro-ph.CO].

[90] S. M. Carroll and E. A. Lim, Phys. Rev. D **70**, 123525 (2004) [arXiv:hep-th/0407149].

[91] C. Armendariz-Picon, JCAP **0407**, 007 (2004) [arXiv:astro-ph/0405267]. T. Koivisto and D. F. Mota, Astrophys. J. **679**, 1 (2008) [arXiv:0707.0279 [astro-ph]]. T. S. Koivisto and D. F. Mota, JCAP **0808**, 021 (2008) [arXiv:0805.4229 [astro-ph]].

[92] J. M. Cline, S. Jeon and G. D. Moore, Phys. Rev. D **70**, 043543 (2004) [arXiv:hep-ph/0311312].

[93] T. Chiba, JCAP **0808**, 004 (2008) [arXiv:0805.4660 [gr-qc]];

[94] L. Kofman, A. D. Linde and A. A. Starobinsky, Phys. Rev. D **56**, 3258 (1997) [arXiv:hep-ph/9704452].

[95] A. Golovnev, V. Mukhanov and V. Vanchurin, JCAP **0811**, 018 (2008) [arXiv:0810.4304 [astro-ph]].

[96] A. Golovnev and V. Vanchurin, Phys. Rev. D **79**, 103524 (2009) [arXiv:0903.2977 [astro-ph.CO]].

[97] J. M. Cline, S. Jeon and G. D. Moore, Phys. Rev. D **70**, 043543 (2004) [arXiv:hep-ph/0311312].

[98] K. Bamba, S. Nojiri and S. D. Odintsov, Phys. Rev. D **77**, 123532 (2008) [arXiv:0803.3384 [hep-th]]; T. R. Dulaney and M. I. Gresham, arXiv:0805.1078 [gr-qc]. K. Bamba and S. Nojiri, arXiv:0811.0150 [hep-th]; S. M. Carroll, T. R. Dulaney, M. I. Gresham and H. Tam, Phys. Rev. D **79**, 065011 (2009) [arXiv:0812.1049 [hep-th]]; S. M. Carroll, T. R. Dulaney, M. I. Gresham and H. Tam, Phys. Rev. D **79**, 065012 (2009) [arXiv:0812.1050 [hep-th]]; S. Koh and B. Hu, arXiv:0901.0429 [hep-th]. C. Armendariz-Picon and A. Diez-Tejedor, arXiv:0904.0809 [astro-ph.CO]; K. Dimopoulos, M. Karciauskas and J. M. Wagstaff, arXiv:0907.1838 [hep-ph].

[99] S. Yokoyama and J. Soda, JCAP **0808**, 005 (2008) [arXiv:0805.4265 [astro-ph]].

[100] N. Bartolo, E. Dimastrogiovanni, S. Matarrese and A. Riotto, arXiv:0906.4944 [astro-ph.CO].

[101] T. S. Koivisto, D. F. Mota and C. Pitrou, arXiv:0903.4158 [astro-ph.CO].

[102] L. Grisa and L. Sorbo, arXiv:0905.3391 [hep-th].

[103] H. P. Nilles, M. Peloso and L. Sorbo, JHEP **0104**, 004 (2001) [arXiv:hep-th/0103202].

[104] C. Gordon, D. Wands, B. A. Bassett and R. Maartens, Phys. Rev. D **63**, 023506 (2001) [arXiv:astro-ph/0009131].

Appendix A

Explicit expressions for the study of the ACW model

We write here some explicit steps in the linearized computation of the perturbations performed in subsection 4.3.2.

The explicit form of equations (4.39) is

$$\begin{aligned}
\mathrm{Eq}_{00}: \quad & -\frac{1}{M_p}\left\{ \left(2+\mu^2\right)\, H_a\, \dot{\hat{\Psi}} + p_T^2\, \hat{\Psi} + \left(2+\mu^2\right)\, \left(3+2\,\mu^2\right)\, H_a^2\, \hat{\Phi} - 2\, \left(1+\mu^2\right)\, H_a\, \hat{\chi} \right. \\
& \qquad - \left(2+\mu^2\right)\, H_a\, \hat{B} - \mu\, H_a\, \hat{\alpha}_0 - \mu\, H_a\, \left(\dot{\hat{\alpha}}_1 - \mu\, \dot{\hat{\Psi}}\right) \\
& \qquad \left. -\mu\, H_a^2\, \left(\hat{\alpha}_1 - \mu\, \hat{\Psi}\right) \right\} = 0 \\
\mathrm{Eq}_{01}: \quad & -\frac{i\, p_L\, a}{M_p}\left\{ 2\, \left(1+\mu^2\right)\, H_a\, \hat{\Phi} + \frac{1}{2p_L^2}\, \left[p_T^2 - 4\,\mu^2\, \left(1+\mu^2\right)\, H_a^2\right]\, \hat{\chi} - \frac{\hat{B}}{2} \right. \\
& \qquad \left. -2\,\mu\, \left(1+\mu^2\right)\, \frac{H_a^2}{p_L^2}\, \hat{\alpha}_0 \right\} = 0 \\
\mathrm{Eq}_{0i}: \quad & -\frac{i\, p_{Ti}\, b}{M_p}\, \left[\dot{\hat{\Psi}} + \left(2+\mu^2\right)\, H_a\, \hat{\Phi} - \frac{\hat{\chi}}{2} + \frac{p_L^2}{2p_T^2}\, \hat{B} - \mu\, H_a\, \hat{\alpha} + \mu\, H_a\, \left(\hat{\alpha}_1 - \mu\, \hat{\Psi}\right) \right] \\
& \qquad + \frac{b}{2}\, \left[-p_L^2\, \dot{\hat{B}}_i + H_a\, p_L^2\, \left(1+\mu^2\right)\, \hat{B}_i + p^2\, \hat{B}_i - 2\, i\, \mu\, \frac{H_a}{b}\, p_L\, \hat{\alpha}_i \right] = 0 \\
\mathrm{Eq}_{11}: \quad & -\frac{\mu\, a^2}{M_p}\left\{ \ddot{\hat{\alpha}}_1 + 2\, \left(2+\mu^2\right)\, H_a\, \dot{\hat{\alpha}}_1 + p_T^2\, \hat{\alpha}_1 + \dot{\hat{\alpha}}_0 + \left(3+2\mu^2\right)\, H_a\, \hat{\alpha}_0 - p_T^2\, \hat{\alpha} \right.
\end{aligned}$$

$$
\begin{aligned}
&-\mu\, H_a\, \dot{\hat{\Psi}} - \frac{2+\mu^2}{\mu}\, H_a\, \dot{\hat{\Phi}} + \frac{1}{\mu}\, \left[p_T^2 - \left(2+\mu^2\right)\, \left(3+2\mu^2\right)\, H_a^2\right]\, \hat{\Phi} \\
&+\frac{\dot{\hat{B}}}{\mu} + \frac{3+2\mu^2}{\mu}\, H_a\, \hat{B} + \left(9+8\,\mu^2\right)\, H_a^2\, \left(\hat{\alpha}_1 - \mu\, \hat{\Psi}\right) \Bigg\} = 0
\end{aligned}
$$

$$
\begin{aligned}
\mathrm{Eq}_{1i}: \quad & \frac{a\, b\, p_{Ti}}{2\, p_L\, M_p} \Bigg[\dot{\hat{\chi}} + 3 H_a\, \hat{\chi} + \frac{p_L^2}{p_T^2}\, \left[\dot{\hat{B}} + \left(3+4\mu^2\right)\, H_a\, \hat{B}\right] - 2\,\mu\, H_a\, \left(\dot{\hat{\alpha}} + 3 H_a\, \hat{\alpha}\right) \\
&+2 p_L^2\, \hat{\Phi} - 4\,\mu^3\, H_a^2\, \hat{\alpha} - 2\,\mu\, H_a\, \hat{\alpha}_0 \Bigg] \\
&-\frac{i\, a\, b\, p_L}{2} \Bigg[\ddot{\hat{\tilde{B}}}_i + \left(1+2\,\mu^2\right)\, H_a\, \dot{\hat{\tilde{B}}}_i - \dot{\hat{B}}_i - \left(2+3\mu^2\right)\, H_a\, \hat{B}_i \\
&+ \left[p_T^2 - H_a^2\, \left(1+\mu^2\right)\, \left(2+3\mu^2\right)\right]\, \hat{\tilde{B}}_i \\
&+2\, i\, \frac{H_a\, \mu}{b\, p_L} \left(\dot{\hat{\alpha}}_i + 2\, H_a\, \left(1+\mu^2\right)\, \hat{\alpha}_i\right) \Bigg] = 0
\end{aligned}
$$

$$
\begin{aligned}
\mathrm{Eq}_{ij}: \quad & \frac{b^2}{M_p} \Bigg\{ \Bigg[\ddot{\hat{\Psi}} + \left(3+2\mu^2\right)\, H_a\, \dot{\hat{\Psi}} + p_T^2\, \hat{\Psi} + \left(2+\mu^2\right)\, H_a\, \dot{\hat{\Phi}} \\
&- \left[p^2 - H_a^2\, \left(2+\mu^2\right)\, \left(3+2\mu^2\right)\right]\, \hat{\Phi} - \dot{\hat{\chi}} - \dot{\hat{B}} - \left(3+2\,\mu^2\right)\, H_a\, \hat{B} \\
&- \left(3+\mu^2\right)\, H_a\, \hat{\chi} + \mu\, H_a\, \dot{\hat{\alpha}}_1 + \mu\, H_a\, \hat{\alpha}_0 + \mu\, H_a^2\, \left(\hat{\alpha}_1 - \mu\, \hat{\Psi}\right) \Bigg] \delta_{ij} \\
&- p_{Ti}\, p_{Tj}\, \left[\hat{\Psi} - \hat{\Phi} - \frac{1}{p_T^2}\, \left(\dot{\hat{B}} + \left(3+2\mu^2\right)\, H_a\, \hat{B}\right)\right] \Bigg\} \\
&+i\, b^2\, \left[p_{(Ti}\, \dot{\hat{B}}_{j)} + \left(2+\mu^2\right)\, H_a\, p_{(Ti}\, \hat{B}_{j)} + p_L^2\, p_{(Ti}\, \hat{\tilde{B}}_{j)}\right] = 0
\end{aligned}
$$

$$
\begin{aligned}
\mathrm{Eq}_0: \quad & -\frac{i\, p_T^2}{p_L} \Bigg\{ \dot{\hat{\alpha}} + \frac{p_L^2}{p_T^2}\, \hat{\alpha}_1 + H_a\, \hat{\alpha} + \frac{1}{p_T^2}\, \left[p^2 - 2\, \left(1+\mu^2\right)\, H_a^2\right]\, \hat{\alpha}_0 + \mu\, \frac{p_L^2}{p_T^2}\, H_a\, \hat{\Phi} \\
&-2\,\mu\, \left(1+\mu^2\right)\, \frac{H_a^2}{p_T^2}\, \hat{\chi} + \frac{p_L^2}{p_T^2}\, H_a\, \left(\hat{\alpha}_1 - \mu\, \hat{\Psi}\right) \Bigg\} = 0
\end{aligned}
$$

$$
\mathrm{Eq}_1: \quad \frac{4\left(1+\mu^2\right)\, H_a^2}{a}\, \left(\hat{\alpha}_1 - \mu\, \hat{\Psi}\right) = 0
$$

$$
\begin{aligned}
\mathrm{Eq}_i: \quad & = -\frac{p_{Ti}}{b\, p_L} \Bigg[\ddot{\hat{\alpha}} + 3\, H_a\, \dot{\hat{\alpha}} + \dot{\hat{\alpha}}_0 + \left(p_L^2 - 2\,\mu^2\, H_a^2\right)\, \hat{\alpha} - p_L^2\, \hat{\alpha}_1 \\
&+\mu\, \frac{p_L^2}{p_T^2}\, H_a\, \hat{B} + 2\, H_a\, \hat{\alpha}_0 \Bigg]
\end{aligned}
$$

$$+\frac{i\,M_p}{b}\left[p_L\,\mu\,H_a\,\left(\dot{\hat{\tilde{B}}}_i-\left(1+\mu^2\right)\,H_a\,\hat{\tilde{B}}_i-\hat{B}_i\right)\right.$$
$$\left.-\frac{i}{b}\,\left[\ddot{\hat{\alpha}}_i+H_a\,\dot{\hat{\alpha}}_i+\left(p^2-2\,H_a^2\,\left(1+\mu^2\right)\right)\,\hat{\alpha}_i\right]\right]=0 \tag{A.1}$$

where the notation on the momenta is explained after eq.(2.33), and where $x_{(i}\,y_{j)}\equiv\frac{1}{2}\,(x_i\,y_j+x_j\,y_i)$ denotes symmetrization. Notice that it has been possible to write all the above equations in terms of gauge invariant combinations. This is a nontrivial check on our algebra.

We recall that the indices $i,j=1,2$ span the symmetric $y-z$ space. Equations carrying these indices contain both 2d scalar and 2d vector modes. However, it is easy to see that each of these equations separates in two independent equations, one for the 2d scalars and one for the 2d vectors: the equations in (A.1) carrying an i index have the following structure

$$\mathrm{Eq}_{0i}=k_{Ti}\,\mathcal{S}_1+\mathcal{V}_{1i}\;,\quad \mathrm{Eq}_{1i}=k_{Ti}\,\mathcal{S}_2+\mathcal{V}_{2i}\;,\quad \mathrm{Eq}_{ij}=\delta_{ij}\,\mathcal{S}_3+k_{Ti}\,k_{Tj}\,\mathcal{S}_4+k_{(Ti}\,\mathcal{V}_{3j)}$$
$$\mathrm{Eq}_i=k_{Ti}\,\mathcal{S}_5+\mathcal{V}_{4i} \tag{A.2}$$

where the expressions $\mathcal{S}_{1,\ldots,5}$ contain the 2d scalar, and the expressions $\mathcal{V}_{1,\ldots,4}$ contain the 2d vector modes. Due to the transversality conditions of the 2d vectors,

$$k_{Ti}\,\mathcal{V}_{1i}=\ldots=k_{Ti}\,\mathcal{V}_{4i}=0\quad\Rightarrow\quad\mathcal{V}_{1i}=\ldots=\mathcal{V}_{4i}=0 \tag{A.3}$$

so that we see explicitly that the equations for the 2d scalars and the 2d vectors are indeed decoupled from each other. We have verified that the system of 2d vectors does not contain instabilities. For brevity, we disregard these modes in the following, and we concentrate only on the 2d scalars.

We note that not all the equations in the system (A.1) are independent. Indeed, the Bianchi identities can be linearized to give

$$\nabla_\mu\left[G^\mu_\nu-\frac{1}{M_p^2}\,T^\mu_\nu\right]=0\;\;\rightarrow\;\;g^{(0)\,\mu\alpha}\,\nabla^{(0)}_\mu\,\mathrm{Eq}_{\alpha\nu}=0 \tag{A.4}$$

where $\nabla^{(0)}$ denotes the covariant derivative constructed from the background metric $g_{\mu\nu}$. These can be written as explicit relations between the linearized equations (4.39)

$$\nu=0:\qquad\frac{d}{dt}\,\mathrm{Eq}_{00}+\left(3+2\mu^2\right)\,H_a\,\mathrm{Eq}_{00}+i\,\left(\frac{p_L}{a}\,\mathrm{Eq}_{01}+\frac{p_{Ti}}{b}\,\mathrm{Eq}_{0i}\right)+\frac{H_a}{a^2}\,\mathrm{Eq}_{11}$$

$$
\begin{aligned}
&\quad + \frac{\left(1+\mu^2\right)\, H_a}{b^2}\, \delta^{ij}\, \mathrm{Eq}_{ij} = 0 \\
\nu = 1: &\quad \frac{d}{dt}\, \mathrm{Eq}_{01} + \left(3+2\mu^2\right)\, H_a\, \mathrm{Eq}_{01} + i\, \left(\frac{p_L}{a}\, \mathrm{Eq}_{11} + \frac{p_{Ti}}{b}\, \mathrm{Eq}_{1i}\right) = 0 \\
\nu = i: &\quad \frac{d}{dt}\, \mathrm{Eq}_{0i} + \left(3+2\mu^2\right)\, H_a\, \mathrm{Eq}_{0i} + i\, \left(\frac{p_L}{a}\, \mathrm{Eq}_{1i} + \frac{p_{Tk}}{b}\, \mathrm{Eq}_{ki}\right) = 0
\end{aligned}
\tag{A.5}
$$

We explicitly checked that the system of equations (4.39) satisfies the above identities (which is a further nontrivial check on our algebra). Therefore, (A.5) verifies that some of the linearized equations are redundant. By inserting the decomposition (A.2) into these identities (disregarding the 2d vector parts of the equations), we see that the $i = 2, 3$ identities become equal to each other. We also see that we can use the three nontrivial identities ($\nu = 0,\, 1,\, 2$) to express $\mathcal{S}_2, ,\, \mathcal{S}_3$ and $\mathcal{S}_4$ in terms of the other equations. Therefore, the Eq_{1i} and Eq_{ij} equations in (A.1) can be obtained from the other ones, and can be disregarded (obviously, one could equivalently choose to disregard some other equations, as long as it is possible to express them in terms of the remaining ones in (A.5)).

This leads us to eqs. (4.40)-(4.46) of the main text. We solve equations (4.42) and (4.43) for $\hat{\chi}$ and $\hat{B}$. The other equations become

$$
\begin{aligned}
&\frac{1}{H_a}\left[-\frac{1}{\mu^2}\,\frac{p_T^2\, p^2}{p_L^2} + \frac{p_T^4}{2\left(1+\mu^2\right) p_L^2} + \left(2+\mu^2\right)\frac{p_L^2 + 2\, p_T^2}{p_L^2} H_a^2\right]\dot{\hat{\Psi}} + p_T^2\, \hat{\Psi} \\
&\quad + \left[-\frac{2\left(1+\mu^2\right)}{\mu^2}\, p^2 - \frac{2\, p_T^2}{\mu^2} + \left(2+\mu^2\right)^2 \frac{p_T^2}{p_L^2}\left(-\frac{p_T^2}{2\,\mu^2\left(1+\mu^2\right)} + 2\, H_a^2\, \frac{p^2}{p_T^2}\right)\right. \\
&\qquad \left. - \left(2+\mu^2\right) H_a^2\right]\hat{\Phi} + \frac{1}{\mu}\left[\frac{p_T^2\, p^2}{p_L^2} - \mu^2\, \frac{p_T^2}{p_L^2}\left(\frac{p_T^2}{2\left(1+\mu^2\right)} + 2\left(2+\mu^2\right) H_a^2\right)\right]\hat{\alpha} \\
&\quad + \left(2+\mu^2\right) H_a\, \frac{p^2}{p_L^2}\, \frac{\hat{\alpha}_0}{\mu} = 0
\end{aligned}
\tag{A.6}
$$

$$
\begin{aligned}
&\left[\mu^2 + \frac{p_T^2}{p_L^2}\, \frac{p_T^2 - 4\,\mu^2\left(1+\mu^2\right) H_a^2}{2\,\mu^2\left(1+\mu^2\right) H_a^2}\right]\ddot{\hat{\Psi}} + \left[\mu^2\left(3+2\,\mu^2\right)\right. \\
&\qquad \left. + \frac{p_T^2}{p_L^2}\left(\frac{1-2\,\mu^2}{\mu^2\left(1+\mu^2\right)}\, \frac{p_T^2}{2\, H_a^2} - 6\right)\right] H_a\, \dot{\hat{\Psi}} + \mu^2\, p_T^2\, \hat{\Psi}
\end{aligned}
$$

$$
\begin{aligned}
&+\left[2+\mu^2+\frac{p^2}{p_L^2}\left[-2\left(2+\mu^2\right)+\frac{p_T^2}{\mu^2\,H_a^2}\right]-\frac{p_T^2}{p_L^2}\,\frac{p_T^2}{2\left(1+\mu^2\right)H_a^2}\right]H_a\dot{\hat{\Phi}}\\
&+\left[\frac{1+\mu^2}{\mu^2}+\frac{\left(2+\mu^2\right)\left(1-2\,\mu^2\right)}{2\,\mu^2\left(1+\mu^2\right)}\,\frac{p_T^2}{p_L^2}-\left(2+\mu^2\right)\left(\frac{3+2\mu^2}{p_T^2}+\frac{6}{p_L^2}\right)H_a^2\right]p_T^2\,\hat{\Phi}\\
&-\frac{1}{2\,\mu\,H_a}\,\frac{p_T^2}{p_L^2}\left(\frac{p_T^2}{1+\mu^2}-4\,\mu^2\,H_a^2\right)\dot{\hat{\alpha}}+\mu\,\frac{p_T^2}{p_L^2}\left(6\,H_a^2-p_L^2-\frac{1-2\,\mu^2}{2\,\mu^2\left(1+\mu^2\right)}\,p_T^2\right)\hat{\alpha}\\
&-\left(\frac{p_T^2}{p_L^2}-\mu^2\right)\frac{\dot{\hat{\alpha}}_0}{\mu}-\left(3\,\frac{p_T^2}{p_L^2}-3\,\mu^2-2\,\mu^4\right)H_a\,\frac{\hat{\alpha}_0}{\mu}=0
\end{aligned}
\tag{A.7}
$$

$$
-\frac{1}{\mu^2}\left(1-\mu^2\,\frac{p_L^2}{p_T^2}\right)\dot{\hat{\Psi}}-\frac{2+\mu^2}{\mu}\,\frac{p^2}{p_T^2}\,H_a\,\hat{\Phi}+\dot{\hat{\alpha}}+2\,H_a\,\hat{\alpha}+\frac{p^2}{p_T^2}\,\hat{\alpha}_0=0
\tag{A.8}
$$

$$
\begin{aligned}
&\ddot{\hat{\alpha}}+3\,H_a\,\dot{\hat{\alpha}}+\left[p_L^2-\frac{p_T^2}{2\left(1+\mu^2\right)}\right]\hat{\alpha}+\dot{\hat{\alpha}}_0+H_a\,\hat{\alpha}_0\\
&\quad+\frac{1}{2\,\mu\,H_a}\left(\frac{p_T^2}{1+\mu^2}-4\,\mu^2\,H_a^2\right)\dot{\hat{\Psi}}-\mu\,p_L^2\,\hat{\Psi}\\
&\quad+\frac{1}{\mu}\left[p^2-\frac{\mu^2}{2\left(1+\mu^2\right)}\,p_T^2-2\left(2+\mu^2\right)\mu^2\,H_a^2\right]\hat{\Phi}=0
\end{aligned}
\tag{A.9}
$$

We choose not to eliminate any more modes, but to rewrite these equations as a system of differential equations for $\dot{\hat{\Psi}}$, $\ddot{\hat{\alpha}}$, $\dot{\hat{\Phi}}$ and $\hat{\alpha}_0$. The differential equations for $\hat{\alpha}_0$ and $\hat{\Phi}$ are obtained by differentiating the two equations (A.6) and (A.8). In solving the numerical system we can replace (A.6) and (A.8) with their time derivatives, provided that these two equations are imposed as initial conditions (see below). We are thus left with the system of eqs. {(A.6)$^\bullet$, (A.7), (A.8)$^\bullet$, (A.9)}, where ($^\bullet$) indicates that we take the time derivative of the equation. This system can be recast in the form (4.48), in terms of the coefficients

$$
\begin{aligned}
\kappa_{22} &= -\frac{1}{\mu}\left(\frac{p_T^2}{p_L^2}-\mu^2\right)\\
\kappa_{23} &= \mu^2+\frac{p_T^2}{p_L^2}\,\frac{p_T^2-4\,\mu^2\left(1+\mu^2\right)H_a^2}{2\,\mu^2\left(1+\mu^2\right)H_a^2}\\
\kappa_{24} &= \left[2+\mu^2+\frac{p^2}{p_L^2}\left[-2\left(2+\mu^2\right)+\frac{p_T^2}{\mu^2\,H_a^2}\right]-\frac{p_T^2}{p_L^2}\,\frac{p_T^2}{2\left(1+\mu^2\right)H_a^2}\right]H_a\\
\kappa_{32} &= \frac{p^2}{p_T^2}
\end{aligned}
$$

$$
\begin{aligned}
\kappa_{33} &= -\frac{1}{\mu}\left(1-\mu^2\,\frac{p_L^2}{p_T^2}\right)\\
\kappa_{34} &= -\frac{2+\mu^2}{\mu^2}\,\frac{p^2}{p_T^2}\,H_a\\
\kappa_{42} &= \frac{2+\mu^2}{\mu^2}\,\frac{p^2}{p_L^2}\,H_a\\
\kappa_{43} &= \frac{p_T^2}{p_L^2}\,\frac{1}{H_a}\left[-\frac{p^2}{\mu^2}+\frac{p_T^2}{2\,(1+\mu^2)}+\left(2+\mu^2\right)\,\frac{p_L^2+2\,p_T^2}{p_T^2}\,H_a^2\right]\\
\kappa_{44} &= -\frac{2\left(1+\mu^2\right)}{\mu^2}\,p^2-\frac{2\,p_T^2}{\mu^2}+\left(2+\mu^2\right)^2\,\frac{p_T^2}{p_L^2}\left(-\frac{p_T^2}{2\,\mu^2\,(1+\mu^2)}+2\,H_a^2\,\frac{p^2}{p_T^2}\right)\\
&\qquad -\left(2+\mu^2\right)H_a^2
\end{aligned}
\tag{A.10}
$$

and

$$
\begin{aligned}
f_1 &= -3\,H_a\,\dot{\hat{\alpha}}-\left[p_L^2-\frac{p_T^2}{2\,(1+\mu^2)}\right]\hat{\alpha}-H_a\,\hat{\alpha}_0\\
&\quad -\frac{1}{2\,\mu\,H_a}\left(\frac{p_T^2}{1+\mu^2}-4\,\mu^2\,H_a^2\right)\dot{\hat{\Psi}}+\mu\,p_L^2\,\hat{\Psi}\\
&\quad -\frac{1}{\mu}\left[p^2-\frac{\mu^2}{2\,(1+\mu^2)}\,p_T^2-2\left(2+\mu^2\right)\mu^2\,H_a^2\right]\hat{\Phi}\\
f_2 &= -\left[\mu^2\left(3+2\,\mu^2\right)+\frac{p_T^2}{p_L^2}\left(\frac{1-2\,\mu^2}{\mu^2\,(1+\mu^2)}\,\frac{p_T^2}{2\,H_a^2}-6\right)\right]H_a\dot{\hat{\Psi}}-\mu^2\,p_T^2\,\hat{\Psi}\\
&\quad -\left[\frac{1+\mu^2}{\mu^2}+\frac{\left(2+\mu^2\right)\left(1-2\,\mu^2\right)}{2\,\mu^2\,(1+\mu^2)}\,\frac{p_T^2}{p_L^2}-\left(2+\mu^2\right)\,\left(\frac{3+2\mu^2}{p_T^2}+\frac{6}{p_L^2}\right)\,H_a^2\right]p_T^2\,\hat{\Phi}\\
&\quad +\frac{1}{2\,\mu\,H_a}\,\frac{p_T^2}{p_L^2}\left(\frac{p_T^2}{1+\mu^2}-4\,\mu^2\,H_a^2\right)\dot{\hat{\alpha}}-\mu\,\frac{p_T^2}{p_L^2}\left(6\,H_a^2-p_L^2-\frac{1-2\,\mu^2}{2\,\mu^2\,(1+\mu^2)}\,p_T^2\right)\hat{\alpha}\\
&\quad +\left(3\,\frac{p_T^2}{p_L^2}-3\,\mu^2-2\,\mu^4\right)H_a\,\frac{\hat{\alpha}_0}{\mu}\\
f_3 &= -2\,H_a\,\dot{\hat{\alpha}}-2\,\mu^2\,H_a\,\frac{p_L^2}{p_T^2}\,\hat{\alpha}_0-2\,\mu^3\,H_a\,\frac{p_L^2}{p_T^2}\,\dot{\hat{\Psi}}+2\left(2+\mu^2\right)\mu\,H_a^2\,\frac{p_L^2}{p_T^2}\,\hat{\Phi}\\
f_4 &= -\frac{1}{\mu}\,\frac{p_T^2}{p_L^2}\left[p^2-\mu^2\left(\frac{p_T^2}{2\,(1+\mu^2)}+2\left(2+\mu^2\right)H_a^2\right)\right]\dot{\hat{\alpha}}\\
&\quad -\frac{p_T^2}{p_L^2}\left[3\,p^2-\frac{\mu^2\,p_T^2}{1+\mu^2}+\frac{2\,p^2}{\mu^2}-4\left(2+\mu^2\right)\mu^2\,H_a^2\right]\dot{\hat{\Psi}}\\
&\quad +2\left(2+\mu^2\right)\mu\,H_a^2\,\frac{p_T^2}{p_L^2}\,\hat{\alpha}_0
\end{aligned}
$$

$$
\begin{aligned}
&+\frac{H_a\,p_T^2}{p_L^2}\left[\frac{2}{\mu}\,\left(1+\mu^2\right)p^2+\frac{\mu}{1+\mu^2}\,p_T^2-4\left(2+\mu^2\right)\mu^3\,H_a^2\right]\hat{\alpha}+2\left(1+\mu^2\right)H_a\,p_T^2\,\hat{\Psi}\\
&-\frac{p_T^2}{p_L^2}\,\frac{H_a\left(1+\mu^2\right)}{\mu^2}\\
&\qquad\times\left\{\frac{1}{p_T^2}\left[2\,p_L^2+\left(2+\mu^2\right)p_T^2\right]^2-\frac{\mu^4\left(2+\mu^2\right)^2}{\left(1+\mu^2\right)^2}\left[p_T^2+4\left(1+\mu^2\right)H_a^2\right]\right\}\hat{\Phi}
\end{aligned}
\tag{A.11}
$$

As we already mentioned, we need to impose Eqs. (A.6) and (A.8) as initial condition (this allowed us to replace these two equations with their time derivatives). By imposing them, we obtain the initial conditions for the nondynamical modes in terms of the dynamical ones:

$$
\begin{aligned}
\hat{\alpha}_{0,in} &= \frac{1}{p^2\,\mathcal{D}_{in}}\left\{-\left[4\left(1+\mu^2\right)p_L^2+\left(2+\mu^2\right)^2p_T^2\left(\frac{p_T^2}{1+\mu^2}-4\,\mu^2\,H_a^2\right)\right.\right.\\
&\qquad\left.+2\left(2+\mu^2\right)p_L^2\left(2\,p_T^2-\left(3+2\,\mu^2\right)\mu^2\,H_a^2\right)\right]\left(\dot{\hat{\alpha}}+H_a\,\hat{\alpha}\right)\\
&\qquad-\mu\,p_L^2\left[2\,p^2-\frac{\mu^2}{1+\mu^2}\,p_T^2+2\left(2+\mu^2\right)H_a^2\right]\\
&\qquad\qquad\times\left[\mu\,H_a\,\hat{\alpha}+\left(1+\mu^2\right)\left(2\,\frac{p^2}{p_T^2}-1\right)\dot{\hat{\Psi}}\right]\\
&\qquad+2\,\mu\left(2+\mu^2\right)H_a\,p_L^2\,p^2\left[\frac{2\,H_a\left(2+\mu^2\right)\left(1+\mu^2\right)}{p_T^2}\,\dot{\hat{\Psi}}+\hat{\Psi}\right]\Bigg\}_{in}\\
\hat{\Phi}_{in} &= \frac{1}{\mathcal{D}_{in}}\left\{\left[2\,p^2-\frac{\mu^2}{1+\mu^2}\,p_T^2-2\,H_a^2\left(2+\mu^2\right)\left(1+2\,\mu^2\right)\right]\left(-\frac{\dot{\hat{\Psi}}}{H_a}+\mu\,\hat{\alpha}\right)\right.\\
&\qquad\left.+2\,\mu^2\,p_L^2\,\hat{\Psi}-2\,\mu\left(2+\mu^2\right)H_a\left(\dot{\hat{\alpha}}+H_a\,\hat{\alpha}\right)\right\}_{in}\\
\mathcal{D} &\equiv \frac{1+\mu^2}{p_T^2}\left\{\left(2\,p^2-\frac{\mu^2}{1+\mu^2}\,p_T^2\right)^2-2\,H_a^2\left(2+\mu^2\right)\left[2\left(1+\mu^2\right)p^2+\frac{\mu^2}{1+\mu^2}\,p_T^2\right]\right\}
\end{aligned}
\tag{A.12}
$$

The initial conditions for $\hat{\Psi}$, $\dot{\hat{\Psi}}$, $\hat{\alpha}$, $\dot{\hat{\alpha}}$ are obtained from the early time expansion of the action (4.54). Namely, we need to expand at early times the three matrices K, X, Ω^2

entering in this action. [1] We find

$$S_{\rm 2dS} = \frac{1}{2}\int d^3k\,dt\left\{|\dot{H}_+|^2 - p^2\,|H_+|^2 + |\dot{\Delta}_+|^2 - p^2\,|\Delta_+|^2 \right. \\ \left. + \frac{\mu\,H_a}{\sqrt{2}}\,\frac{p_T}{p}\,\left(\dot{H}_+^*\,\Delta_+ - \dot{\Delta}_+\,H_+^* + \text{h.c.}\right)\right\} \tag{A.13}$$

where

$$\hat{\Psi} \equiv \frac{1}{\sqrt{a}\,b}\,\frac{2p^2+\mu^2\,\left(p^2+p_L^2\right)}{\sqrt{2}\,\left(1+\mu^2\right)\,p_T^2}\,H_+ \quad , \quad \hat{\alpha} \equiv \frac{1}{\sqrt{a}\,b}\,\left[-\frac{p}{p_T}\,\Delta_+ + \frac{\mu\,\left(p^2+p_L^2\right)}{\sqrt{2}\,p_T^2}\,H_+\right] \tag{A.14}$$

The next to leading order corrections to (A.13) and (A.14) are of $\mathrm{O}\left(H_a^2/p^2\right)$ (either p_L or p_T). Not surprisingly, the early time frequency is controlled by the momentum term (which is a common result in the theory of cosmological perturbations on a inflationary background). What is nontrivial is the relation (A.14) between the canonical variables and the original modes, which, as we shall now see, is needed in order to set the initial conditions for the latter.

Since the early time frequency varies adiabatically as

$$\omega^2 \approx p^2 \quad , \quad \frac{\dot{\omega}}{\omega^2} \approx -\frac{p^2+\mu^2\,p_T^2}{p^2}\,\frac{H_a}{p} \ll 1 \tag{A.15}$$

we can set the adiabatic initial conditions for the canonical variables

$$H_{+,in} = \Delta_{+,in} = \frac{1}{\sqrt{2p}} \ , \ \dot{H}_{+,in} = -i\,p\,H_{+,in} \ , \ \dot{\Delta}_{+,in} = -i\,p\,\Delta_{+,in} \tag{A.16}$$

which are $\mathrm{O}\left(H_a/p\right)$ accurate. Using (A.14) we then obtain the initial conditions for the original modes as

$$\begin{aligned} \hat{\Psi}_{in} &= \frac{1}{\sqrt{a}\,b}\,\frac{2p^2+\left(p^2+p_L^2\right)\,\mu^2}{2\,\sqrt{p}\,p_T^2\,\left(1+\mu^2\right)}\,\left[1+\mathrm{O}\left(\frac{H_a^2}{p^2}\right)\right] \ , \ \dot{\hat{\Psi}}_{in} = -i\,p\,\hat{\Psi}_{in}\,\left[1+\mathrm{O}\left(\frac{H_a}{p}\right)\right] \\ \hat{\alpha}_{in} &= -\frac{1}{\sqrt{a}\,b}\,\frac{\sqrt{2}\,p\,p_T - \left(p^2+p_L^2\right)\,\mu}{2\,\sqrt{p}\,p_T^2}\,\left[1+\mathrm{O}\left(\frac{H_a^2}{p^2}\right)\right] \ , \ \dot{\hat{\alpha}}_{in} = -i\,p\,\hat{\alpha}_{in}\,\left[1+\mathrm{O}\left(\frac{H_a}{p}\right)\right] \end{aligned} \tag{A.17}$$

[1] The only time dependent quantities entering in these expressions are the scale factors. Some care needs to be taken in the expansion, since $H_b > H_a$, so that $p_T \gg p_L$ in the asymptotic past. The expansion (A.13) is valid as long as $H_b < 2\,H_a$. If this is not the case, a term proportional to p_L^2 becomes smaller than a term proportional to p_T at asymptotically early times, and the expansion in powers of (H/p) that we have performed (where p is either of p_L or p_T) becomes invalid. The condition $H_b < 2\,H_a$ is not particularly stringent, since such a large anisotropic is certainly incompatible with the observations.

The initial conditions for the nondynamical modes are then obtained by inserting these expressions into (A.12). These are the initial conditions for the numerical evolution discussed in the main text, which leads to the solutions given in Figure 4.2.

Appendix B

Details of computations of subsection 5.5.1

This appendix contains the details of the stability analysis of the model of subsection 5.5.1. The explicit forms of the linearized equations (5.55) are

$$
\begin{aligned}
\mathrm{Eq}_{00}: \quad & -\frac{2}{M_p}\Bigg\{ \left[\left(1-\frac{1}{3}B_1^2\right) H + \left(1+\frac{1}{6}B_1^2\right) h + \frac{1}{6}B_1\,\dot{B}_1\right] \dot{\hat{\Psi}} \\
& + \frac{1}{2}\left[p_T^2 + \left(m^2 - \frac{p_T^2+2p_L^2}{6} + 5h^2 - 4h\,H\right) B_1^2 - 4h\,H\,B_1\,\dot{B}_1 + \dot{B}_1^2\right] \hat{\Psi} \\
& + \left[3H^2 - \left(3+\frac{5}{2}B_1^2\right) h^2 - \frac{1}{2}\dot{B}_1^2 + 2\left(B_1\,H + \dot{B}_1\right) B_1\,h\right] \hat{\Phi} \\
& - \left[\left(1+\frac{1}{6}B_1^2\right)(H+h) + \frac{1}{6}B_1\,\dot{B}_1\right] \hat{\chi} \\
& - \left[\left(1+\frac{1}{6}B_1^2\right)\left(H-\frac{1}{2}h\right) + \frac{1}{6}B_1\,\dot{B}_1\right] \hat{B} \\
& - \left[\left(\frac{1}{2}H - h\right) B_1 + \frac{1}{2}\dot{B}_1\right] \hat{\alpha}_0 \\
& - \left(\frac{1}{2}\dot{B}_1 - B_1\,h\right) \dot{\alpha}_1 \\
& + \left[\frac{1}{2}\left(\frac{1}{3}p^2 - m^2 - 5h^2 + 4h\,H\right) B_1 + h\,\dot{B}_1\right] \hat{\alpha}_1 \Bigg\} = 0 \\
\mathrm{Eq}_{01}: \quad & -2\,\frac{ip_L\,a}{M_p}\left\{\frac{1}{6}\left(\dot{\alpha}_1 - B_1\,\dot{\hat{\Psi}}\right) B_1 + \frac{B_1}{6}\left(B_1\,H - 2B_1\,h - 2\dot{B}_1\right) \hat{\Psi}\right.
\end{aligned}
$$

$$
\begin{aligned}
&+\frac{1}{6}\left(-B_1\,H+2h\,B_1+\dot{B}_1\right)\,\hat{\alpha}_1+\left(1+\frac{1}{6}B_1^2\right)\,\left(H+h+\frac{B_1\,\dot{B}_1}{6+B_1^2}\right)\,\hat{\Phi}\\
&+\left(\frac{p_T^2}{4p_L^2}+\frac{p_T^2}{24p_L^2}B_1^2-\frac{1}{3}\mathcal{D}_{\chi\chi}\right)\,\hat{\chi}-\frac{6+B_1^2}{24}\hat{B}-\frac{B_1}{3}\mathcal{D}_{\alpha_0\alpha_0}\,\hat{\alpha}_0\Bigg\}=0
\end{aligned}
$$

$$
\begin{aligned}
\mathrm{Eq}_{0i}:\quad &-2\,\frac{i\,p_{Ti}\,b}{M_p}\Bigg\{\frac{1}{2}\left(1-\frac{B_1^2}{6}\right)\,\dot{\hat{\Psi}}+\frac{1}{6}B_1\,\dot{\hat{\alpha}}_1+\left[\frac{B_1}{6}\left(HB_1-2\dot{B}_1\right)-\left(\frac{3}{2}+\frac{B_1^2}{12}\right)h\right]\,\hat{\Psi}\\
&+\left[\left(\frac{1}{3}H-\frac{7}{6}h\right)\,B_1+\frac{2}{3}\dot{B}_1\right]\,\hat{\alpha}_1+\left[\left(h-\frac{1}{2}H\right)B_1-\frac{1}{2}\dot{B}_1\right]\,\hat{\alpha}\\
&+\left[-\left(\frac{1}{2}+\frac{B_1^2}{12}\right)h+\left(1+\frac{1}{6}B_1^2\right)H+\frac{1}{6}B_1\,\dot{B}_1\right]\hat{\Phi}-\frac{1}{4}\left(1+\frac{B_1^2}{6}\right)\,\hat{\chi}\\
&+\frac{p_L^2}{4p_T^2}\,\left(1+\frac{1}{6}B_1^2\right)\,\hat{B}\Bigg\}=0
\end{aligned}
$$

$$
\begin{aligned}
\mathrm{Eq}_{11}:\quad &\frac{2a^2}{3M_p}\Bigg\{\frac{1}{2}B_1\,\left(\ddot{\hat{\alpha}}_1-2B_1\,\ddot{\hat{\Psi}}\right)-\left(3H\,B_1+2\dot{B}_1\right)B_1\,\dot{\hat{\Psi}}\\
&+\frac{1}{2}\left(-HB_1+8h\,B_1-\dot{B}_1\right)\,\dot{\hat{\alpha}}_1+\left(\mathcal{M}_{\Psi\Psi}-p_T^2\,B_1^2\right)\,\hat{\Psi}\\
&+\left(\mathcal{M}_{\Psi\alpha_1}+\frac{p_T^2}{2}B_1\right)\,\hat{\alpha}_1+\left[\left(3+\frac{1}{2}B_1^2\right)h+\left(3-B_1^2\right)H+\frac{1}{2}B_1\dot{B}_1\right]\,\dot{\hat{\Phi}}\\
&+\Bigg[\left(-\frac{9}{4}\,m^2+\frac{p_T^2+2p_L^2}{4}-\frac{15}{4}\,h^2+3\,h\,H\right)\,B_1^2+3\,h\,B_1\,\dot{B}_1\\
&\qquad-3\,\left(\frac{p_T^2}{2}\,-\frac{V_0}{2M_p^2}+\frac{3}{2}\,h^2-\frac{3}{2}\,H^2+\frac{1}{4}\,\dot{B}_1^2\right)\Bigg]\,\hat{\Phi}\\
&-\left(\frac{3}{2}-\frac{1}{4}\,B_1^2\right)\,\dot{\hat{B}}+\frac{1}{2}\,B_1^2\,\dot{\hat{\chi}}+(2H-h)\,B_1^2\,\hat{\chi}\\
&-\left[\left(\frac{9}{2}+\frac{1}{4}\,B_1^2\right)\,h+\left(\frac{9}{2}-\frac{5}{4}\,B_1^2\right)\,H+\frac{1}{2}\,B_1\,\dot{B}_1\right]\,\hat{B}\\
&\qquad+\frac{3}{2}\,\left(2h\,B_1-H\,B_1-\dot{B}_1\right)\,\hat{\alpha}_0\Bigg\}=0
\end{aligned}
$$

$$
\begin{aligned}
\mathrm{Eq}_{1i}:\quad &\frac{a\,b\,p_L\,p_{Ti}}{3M_p}\Bigg\{\frac{3}{p_L^2}\,\left[(2h-H)\,B_1-\dot{B}_1\right]\,\dot{\hat{\alpha}}_1+\mathcal{M}_{\Psi\alpha}\,\hat{\alpha}+\frac{6+B_1^2}{4p_T^2}\,\dot{\hat{B}}\\
&+\frac{6+B_1^2}{4p_T^2}\,\left(3H+6h+2\frac{B_1\,\dot{B}_1}{6+B_1^2}\right)\,\hat{B}+\frac{6+B_1^2}{4p_L^2}\,\dot{\hat{\chi}}
\end{aligned}
$$

$$
\begin{aligned}
&+\frac{6+B_1^2}{4p_L^2}\left(3H-6h+2\frac{B_1\,\dot{B}_1}{6+B_1^2}\right)\,\hat{\chi}+B_1^2\,\hat{\Psi}+\frac{1}{2}\left(6+B_1^2\right)\,\hat{\Phi}-B_1\,\hat{\alpha}_1\\
&-\frac{3}{p_L^2}\left[(H-2h)\;B_1+\dot{B}_1\right]\,\hat{\alpha}_0\Bigg\}=0
\end{aligned}
$$

$$
\begin{aligned}
\mathrm{Eq}_{ij}:\quad &\frac{b^2}{6M_p}\Bigg\{\Bigg[\left(6-B_1^2\right)\,\ddot{\hat{\Psi}}+\left[\left(18-B_1^2\right)H-\left(18+B_1^2\right)h-6B_1\,\dot{B}_1\right]\,\dot{\hat{\Psi}}\\
&+\left[\mathcal{M}_{\Sigma\Psi}+\left(6-B_1^2\right)\,p_T^2-2B_1^2\,p_L^2\right]\,\hat{\Psi}+2B_1\,\ddot{\hat{\alpha}}\\
&+2\left[(5H-7h)\,B_1+5\dot{B}_1\right]\,\dot{\hat{\alpha}}_1-\left(\mathcal{M}_{\Sigma\alpha_1}-2p^2\,B_1\right)\,\hat{\alpha}_1\\
&+\left(6+B_1^2\right)\,\left(2H-h+2\frac{B_1\,\dot{B}_1}{6+B_1^2}\right)\,\dot{\hat{\Phi}}\\
&-\Big[\left(p^2+30h^2-24h\,H\right)\,B_1^2-24h\,B_1\,\dot{B}_1\\
&\qquad+6\left(p^2+6(h^2-H^2)+\dot{B}_1^2\right)\,\Big]\,\hat{\Phi}\\
&-\left(6+B_1^2\right)\,\dot{\hat{\chi}}-\left(6+B_1^2\right)\,\left(3H-3h+2\frac{B_1\,\dot{B}_1}{6+B_1^2}\right)\,\hat{\chi}\\
&+6\left[(H-2h)\;B_1+\dot{B}_1\right]\,\hat{\alpha}_0\\
&-\left(6+B_1^2\right)\left(\dot{\hat{B}}^2+\left(3H+2\frac{B_1\dot{B}_1}{6+B_1^2}\right)\,\hat{B}\right)\Bigg]\,\delta_{ij}\\
&+p_{Ti}\,p_{Tj}\left[\frac{6+B_1^2}{p_T^2}\,\left(\dot{\hat{B}}+\left(3H+2\frac{B_1\,\dot{B}_1}{6+B_1^2}\right)\,\hat{B}\right)-\left(6-B_1^2\right)\,\hat{\Psi}\right.\\
&\qquad\left.+\left(6+B_1^2\right)\,\hat{\Phi}-2B_1\,\hat{\alpha}_1\right]\Bigg\}=0
\end{aligned}
$$

$$
\begin{aligned}
\mathrm{Eq}_0:\quad &i\,p_L\Bigg\{\dot{\hat{\alpha}}_1+\left(2\,h\,B_1-H\,B_1-\dot{B}_1\right)\,\hat{\Psi}+(H-2h)\,\hat{\alpha}_1+\frac{p_T^2}{p_L^2}\,\dot{\hat{\alpha}}+\frac{p_T^2}{p_L^2}\,(H-2h)\,\hat{\alpha}\\
&+\left(H\,B_1-2h\,B_1+\dot{B}_1\right)\,\hat{\Phi}-\frac{2}{3B_1}\,\mathcal{D}_{\chi\chi}\,\hat{\chi}\\
&+\left(1+\frac{p_T^2}{p_L^2}-\frac{2}{3}\,\mathcal{D}_{\alpha_0\alpha_0}\right)\,\hat{\alpha}_0\Bigg\}=0
\end{aligned}
$$

$$
\begin{aligned}
\mathrm{Eq}_1:\quad &\frac{1}{a}\Bigg\{\ddot{\hat{\alpha}}_1-\frac{1}{3}\,B_1\,\ddot{\hat{\Psi}}+3H\,\dot{\hat{\alpha}}_1+\left(\frac{8}{3}\,B_1\,h-\frac{7}{3}\,B_1\,H-\dot{B}_1\right)\,\dot{\hat{\Psi}}+\left(\mathcal{M}_{\alpha_1\alpha_1}+p_T^2\right)\,\hat{\alpha}_1\\
&-\frac{B_1}{3}\,p_T^2\,\hat{\Psi}+\left(\dot{B}_1-2\,B_1\,h\right)\,\dot{\hat{\Phi}}+\frac{B_1}{3}\,\left(\dot{\hat{B}}+\dot{\hat{\chi}}\right)+\dot{\hat{\alpha}}_0+\frac{B_1}{3}\,\left(p^2-6m^2\right)\,\hat{\Phi}
\end{aligned}
$$

$$
\begin{aligned}
&+\frac{1}{3}\left(7\,B_1\,h+B_1\,H-3\dot{B}_1\right)\,\hat{B}+\frac{2}{3}\,(2H-h)\,B_1\,\hat{\chi}-p_T^2\,\hat{\alpha}\\
&+2\,(h+H)\,\hat{\alpha}_0\Bigg\}=0\\
\mathrm{Eq}_i:\qquad &\frac{p_{Ti}}{p_L\,b}\Bigg\{\ddot{\hat{\alpha}}+3\,(H-2h)\,\dot{\hat{\alpha}}+\left(\mathcal{M}_{\alpha\alpha}+p_L^2\right)\,\hat{\alpha}-p_L^2\,\hat{\alpha}_1\\
&+\frac{p_L^2}{p_T^2}\left(B_1\,H-2\,B_1\,h+\dot{B}_1\right)\,\hat{B}+\dot{\hat{\alpha}}_0+(2H-4h)\,\hat{\alpha}_0\Bigg\}=0
\end{aligned}
$$

where the index i on the equations spans over the $i=2,3$ isotropic spatial directions, and where the momenta are defined as $p_L=k_L/a$, $p_T=k_T/b$ and $p^2=p_L^2+p_T^2$.

Only the 2d scalar perturbations are included in this computation. More in general, if we include both the 2d scalar and 2d vector modes, the perturbed equations carrying i or j indices split in two separate parts, one for the 2d scalar, and one for the 2d vector modes. Although we have not written the 2d vector parts of the above equations, we have explicitly checked that they are decoupled from the 2d scalar parts. The 2d vector parts are not related to the instability we have demonstrated in the main text; therefore we do not discuss them here. Another property to be noted in the system (B.1) is that not all the equations are independent. Using the perturbed Bianchi identities, it is possible to obtain eqs. Eq_{ij}, Eq_{1i} from the remaining ones in (B.1). This remaining equations are the set of linearized equations (5.56) that we have chosen to solve in the main text. [1]

For brevity, we have grouped some of the extended terms that depend on the background quantities, which appear both in the action and in the linearized equations. We have denoted them with calligraphic letters $\mathcal{D}$, $\mathcal{M}$. These terms are

$$
\begin{aligned}
\mathcal{D}_{\Psi\Psi}\;=\;&\frac{1}{18+3B_1^2+2B_1^4}\Bigg[\left(\frac{3}{2}\,m^2+\frac{195}{8}\,h^2-\frac{39}{2}\,h\,H\right)\,B_1^6\\
&+18\left(3m^2-6H^2-\frac{51}{4}\,h^2+15h\,H\right)\,B_1^2-\frac{39}{2}\,h\,\dot{B}_1\,B_1^5\\
&+\frac{9}{2}\,(6h-7H)\,\dot{B}_1\,B_1^3+27\,(8h-3H)\,B_1\,\dot{B}_1
\end{aligned}
$$

[1] One could have chosen a different but equivalent subset of independent equations. Our choice is related to the fact that the linearized equations of motion obtained by extremizing the quadratic action (5.63) precisely gives the set of equations (5.56).

$$
\begin{aligned}
& +27\left(3H^2-3h^2-\frac{5}{2}\,\dot{B}_1^2\right) \\
& +3\left(6m^2+\frac{51}{4}\,h^2-\frac{51}{4}\,H^2+\frac{13}{8}\,\dot{B}_1^2\right)B_1^4\Bigg]
\end{aligned}
$$

$$
\begin{aligned}
\mathcal{D}_{\Psi\alpha_1} &= \frac{-1}{18+3B_1^2+2B_1^4}\Bigg[\left(\frac{45}{4}\,h^2-9h\,H\right)B_1^5+27\,(2h-H)\,\dot{B}_1 \\
&\quad +3\,(H-5h)\,\dot{B}_1\,B_1^4-\frac{9}{2}\,(6h+H)\,\dot{B}_1\,B_1^2 \\
&\quad +9\left(3m^2-6h^2+12\,h\,H-9H^2+\frac{3}{2}\,\dot{B}_1^2\right)B_1 \\
&\quad +3\left(\frac{3}{2}\,m^2+\frac{39}{2}\,h^2-12h\,H-\frac{9}{2}\,H^2+\frac{7}{4}\,\dot{B}_1^2\right)B_1^3\Bigg]
\end{aligned}
$$

$$
\begin{aligned}
\mathcal{D}_{\alpha\alpha} &= \frac{3p_T^2}{p_L^2\,\left(18+3B_1^2+2B_1^4\right)}\Bigg[\left(\frac{15}{4}\,h^2-3h\,H\right)B_1^4-12\,h\,B_1\,\dot{B}_1 \\
&\quad +(2H-7h)\,\dot{B}_1\,B_1^3 \\
&\quad +9\left(m^2-2h^2+4h\,H-3H^2+\frac{1}{2}\,\dot{B}_1^2\right) \\
&\quad +\left(\frac{3}{2}\,m^2+\frac{39}{2}\,h^2-12\,h\,H-\frac{9}{2}\,H^2+\frac{7}{4}\,\dot{B}_1^2\right)B_1^2\Bigg]
\end{aligned}
$$

$$
\mathcal{D}_{\alpha_1\alpha_1} = \frac{p_L^2}{p_T^2}\,\mathcal{D}_{\alpha\alpha}
$$

$$
\begin{aligned}
\mathcal{D}_{\chi\chi} &= \frac{-1}{p_L^2\,\left(18+3B_1^2+2B_1^4\right)}\Bigg[\left(\frac{93}{4}\,h^2-21\,h\,H+3H^2\right)B_1^6-36\,h\,\dot{B}_1\,B_1^3 \\
&\quad +3\,(2H-7h)\,\dot{B}_1\,B_1^5 \\
&\quad +9\left(3m^2+6h^2-6H^2+\frac{3}{2}\,\dot{B}_1^2\right)B_1^2 \\
&\quad +3\left(\frac{3}{2}\,m^2+\frac{51}{2}\,h^2-18\,h\,H-3H^2+\frac{7}{4}\,\dot{B}_1^2\right)B_1^4\Bigg]
\end{aligned}
$$

$$
\mathcal{D}_{\alpha_0\alpha_0} = \frac{1}{B_1^2}\,\mathcal{D}_{\chi\chi}
$$

$$
\mathcal{D}_{\chi\alpha_0} = \frac{1}{B_1}\,\mathcal{D}_{\chi\chi} \tag{B.2}
$$

and

$$
\begin{aligned}
\mathcal{M}_{\Psi\Psi} &= \frac{3}{18+3B_1^2+2B_1^4}\Bigg[\left(m^2+5h^2-4h\,H\right)\,B_1^6-4h\,B_1^5\,\dot{B}_1 \\
&\quad -2\,(4H-19h)\,B_1^3\,\dot{B}_1+24\,(H-2h)\,B_1\,\dot{B}_1+3\dot{B}_1^2 \\
&\quad +\left(\frac{11}{2}m^2-\frac{91}{2}h^2+46h\,H-12H^2+\dot{B}_1^2\right)\,B_1^4 \\
&\quad -\left(3m^2+21h^2+12h\,H-36H^2+\frac{23}{2}\dot{B}_1^2\right)\,B_1^2\Bigg] \\
\mathcal{M}_{\Psi\alpha_1} &= \frac{1}{18+3B_1^2+2B_1^4}\Bigg[-\left(2m^2+5h^2-4h\,H\right)\,B_1^5-36\,(H-2h)\,\dot{B}_1 \\
&\quad +4\,(H-h)\,B_1^4\,\dot{B}_1+6\,(3H-16h)\,B_1^2\,\dot{B}_2 \\
&\quad -9\left(m^2-13h^2+12h\,H-2H^2-\frac{1}{9}\dot{B}_1^2\right)\,B_1^3 \\
&\quad +18\left(m^2+h^2+4h\,H-6H^2+\frac{5}{3}\dot{B}_1^2\right)\,B_1\Bigg] \\
\mathcal{M}_{\Psi\alpha} &= \frac{3}{2p_L^2\,\left(18+3B_1^2+2B_1^4\right)}\Bigg[-3\,(4H-5h)\,h\,B_1^5+4\,(H-5h)\,B_1^4\,\dot{B}_1 \\
&\quad -36\,(H-2h)\,\dot{B}_1-6\,(6h+H)\,B_1^2\,\dot{B}_1 \\
&\quad +36\left(m^2-2h^2+4h\,H-3H^2+\frac{1}{2}\dot{B}_1^2\right)\,B_1 \\
&\quad +6\left(m^2+13h^2-8h\,H-3H^2+\frac{7}{6}\dot{B}_1^2\right)\,B_1^3\Bigg] \\
\mathcal{M}_{\alpha_1\alpha_1} &= \frac{2}{18+3B_1^2+2B_1^4}\Bigg[\left(m^2+10h^2-8h\,H\right)\,B_1^4-8h\,B_1^3\,\dot{B}_1 \\
&\quad -6\,(2H-5h)\,B_1\,\dot{B}_1+9\left(m^2-5h^2+4h\,H-\frac{2}{3}\dot{B}_1^2\right) \\
&\quad +3\left(\frac{5}{2}m^2-\frac{13}{2}h^2+10h\,H-6H^2+\dot{B}_1^2\right)\,B_1^2\Bigg] \\
\mathcal{M}_{\alpha\alpha} &= \frac{2}{18+3B_1^2+2B_1^4}\Bigg[\left(m^2+22h^2-14h\,H\right)\,B_1^4-8h\,B_1^3\,\dot{B}_1 \\
&\quad -6\,(2H-5h)\,B_1\,\dot{B}_1+9\left(m^2+7h^2-2h\,H-\frac{2}{3}\dot{B}_1^2\right)
\end{aligned}
$$

$$
\begin{aligned}
& +3\left(\frac{5}{2}m^2-\frac{1}{2}h^2+7h\,H-6H^2+\dot{B}_1^2\right)\,B_1^2\Bigg] \\
\mathcal{M}_{\Sigma\Psi} &= \frac{12}{18+3B_1^2+2B_1^4}\Bigg[\left(m^2+5h^2-4h\,H\right)\,B_1^6-4h\,B_1^5\,\dot{B}_1+2\,(7h-4H)\,B_1^3\,\dot{B}_1 \\
& +6\,(7h-2H)\,B_1\,\dot{B}_1-15\dot{B}_1^2 \\
& +\left(15m^2-57h^2+60h\,H-18H^2-\frac{5}{2}\,\dot{B}_1^2\right)\,B_1^2 \\
& +\left(\frac{11}{2}m^2-\frac{1}{2}h^2+10\,h\,H-12H^2+\dot{B}_1^2\right)\,B_1^4\Bigg] \\
\mathcal{M}_{\Sigma\alpha_1} &= \frac{4}{18+3B_1^2+2B_1^4}\Bigg[2\left(m^2+\frac{5}{2}h^2-2h\,H\right)\,B_1^5+\frac{3}{2}\,(h-6H)\,B_1^2\,\dot{B}_1 \\
& +9\,(7h-2H)\,\dot{B}_1+(2H-11h)\,B_1^4\,\dot{B}_1 \\
& +36\left(m^2-\frac{7}{2}h^2+4h\,H-\frac{3}{2}H^2+\frac{1}{6}\dot{B}_1^2\right)\,B_1 \\
& +9\left(m^2+2h^2-2H^2+\frac{5}{9}\,\dot{B}_1^2\right)\,B_1^3\Bigg] \qquad \text{(B.3)}
\end{aligned}
$$

As we have discussed in the main text, we proceed by solving the second of (5.56) for the mode $\hat{\chi}$, and inserting the solution back into the rest of the equations. Next, we differentiate equations Eq_{00}, Eq_{0i}, Eq_0 (with the solution for $\hat{\chi}$ given in (5.57) inserted in them) in order to obtain first order differential equations for the modes $\hat{\Phi}$, $\hat{B}$, $\hat{\alpha}_0$. Combined with Eq_{11}, Eq_1, Eq_i (again with the solution (5.57) inserted in them), these equations form the set of equations to be solved numerically, summarized in matrix form in (5.59). Here we give the detailed expressions of the terms appearing in this system of equations.

We first define the following useful combinations of background dependent terms which frequently appear in the linearized system:

$$
\begin{aligned}
\mathcal{D} &= \left(6+B_1^2\right)\,p_T^2-8p_L^2\,\mathcal{D}_{\chi\chi} \\
\mathcal{H} &= H+h+\frac{B_1\,\dot{B}_1}{6+B_1^2} \qquad \text{(B.4)}
\end{aligned}
$$

where $\mathcal{D}_{\chi\chi}$ is defined in (D.5). The time derivative of $\mathcal{D}$ and $\mathcal{H}$ are also useful, which is explicitly given by

$$
\dot{\mathcal{D}} = -2\,p_T^2\,\left(6+B_1^2\right)\,(H+h)+16\,p_L^2\,(H-2h)\,\mathcal{D}_{\chi\chi}+2\,p_T^2\,B_1\,\dot{B}_1-8\,p_L^2\,\dot{\mathcal{D}}_{\chi\chi}
$$

$$\dot{\mathcal{H}} = -2\,\frac{B_1\,\dot{B}_1}{6+B_1^2}\,\mathcal{H} + \dot{H} + \dot{h} + 2\,(H+h)\,\frac{B_1\,\dot{B}_1}{6+B_1^2} + \frac{\dot{B}_1^2 + B_1\,\ddot{B}_1}{6+B_1^2} \tag{B.5}$$

where $\ddot{B}_1$, $\dot{H}$, $\dot{h}$ are obtained from (5.51):

$$\begin{aligned}
\dot{H} &= \frac{2}{18+3B_1^2+2B_1^4}\left[\left(m^2 - \frac{35}{4}h^2 + 7h\,H - 3H^2\right)\,B_1^4 + 12h\,B_1\,\dot{B}_1\right. \\
&\qquad + (7h-2H)\,B_1^3\,\dot{B}_1 - \frac{9}{2}\,\left(6h^2+\dot{B}_1^2\right) \\
&\qquad \left. -\frac{3}{2}\,\left(18h^2 - 12h\,H + \frac{7}{6}\dot{B}_1^2\right)B_1^2\right] \\
\dot{h} &= \frac{1}{18+3B_1^2+2B_1^4}\left[3\,(2H-5h)\,h\,B_1^4 + 8h\,B_1^3\,\dot{B}_1 + 6\,(2H-5h)\,B_1\,\dot{B}_1\right. \\
&\qquad +6\left(\dot{B}_1^2 - 9h\,H\right) \\
&\qquad \left. -6\left(m^2 - 2h^2 + \frac{11}{2}h\,H - 3H^2 + \frac{1}{2}\dot{B}_1^2\right)\,B_1^2\right] \\
\ddot{B}_1 &= \frac{1}{18+3B_1^2+2B_1^4}\left[-2\left(m^2+10h^2-8h\,H\right)\,B_1^5 + 2\,(8h-3H)\,B_1^4\,\dot{B}_1\right. \\
&\qquad -54H\,\dot{B}_1 + 15\,(H-4h)\,B_1^2\,\dot{B}_1 \\
&\qquad -18\left(m^2 - 5h^2 + 4h\,H - \frac{2}{3}\dot{B}_1^2\right)\,B_1 \\
&\qquad \left. -15\left(m^2 - \frac{13}{5}h^2 + 4h\,H - \frac{12}{5}H^2 + \frac{2}{5}\dot{B}_1^2\right)\,B_1^3\right]
\end{aligned} \tag{B.6}$$

We also need the explicit expressions for $\dot{\mathcal{D}}_{\chi\chi}$ and $\dot{\mathcal{D}}_{\alpha_0\alpha_0}$:

$$\begin{aligned}
\dot{\mathcal{D}}_{\chi\chi} &= 2\left[H - 2h - \frac{3+4B_1^2}{18+3B_1^2+2B_1^4}\,B_1\,\dot{B}_1\right]\,\mathcal{D}_{\chi\chi} \\
&\quad -\frac{9}{p_L^2\,\left(18+3B_1^2+2B_1^4\right)}\left[2\left(\frac{31}{4}h^2 - 7h\,H + H^2\right)\,B_1^5\,\dot{B}_1 - 12h\,B_1^2\,\dot{B}_1^2\right. \\
&\qquad +\frac{5}{3}\,(2H-7h)\,B_1^4\,\dot{B}_1^2 \\
&\qquad +6\left(m^2 + 2h^2 - 2H^2 + \frac{1}{2}\dot{B}_1^2\right)\,B_1\,\dot{B}_1 \\
&\qquad \left. +4\left(\frac{m^2}{2} + \frac{17}{2}h^2 - 6h\,H - H^2 + \frac{7}{12}\dot{B}_1^2\right)\,B_1^3\,\dot{B}_1\right.
\end{aligned}$$

$$
\begin{aligned}
&-4\dot{h}\,B_1^3\,\dot{B}_1 + \left(\frac{2}{3}\dot{H} - \frac{7}{3}\dot{h}\right)\,B_1^5\,\dot{B}_1 \\
&+6\left(m^2 + 2h^2 - 2H^2 + \frac{1}{2}\dot{B}_1^2\right)\,B_1\,\dot{B}_1 \\
&+\left(\frac{31}{6}h\,\dot{h} - \frac{7}{3}\,\left(H\,\dot{h} + h\,\dot{H}\right) + \frac{2}{3}H\,\dot{H}\right)\,B_1^6 \\
&-4h\,B_1^3\,\ddot{B}_1 + \left(\frac{2}{3}H - \frac{7}{3}h\right)\,B_1^5\,\ddot{B}_1 \\
&+\left(12\left(h\,\dot{h} - H\,\dot{H}\right) + 3\dot{B}_1\,\ddot{B}_1\right)\,B_1^2 \\
&+\left(17h\,\dot{h} - 6\left(H\,\dot{h} + h\,\dot{H}\right) - 2H\,\dot{H} + \frac{7}{6}\,\dot{B}_1\,\ddot{B}_1\right)\,B_1^4\Bigg]
\end{aligned}
$$

$$
\dot{\mathcal{D}}_{\alpha_0\alpha_0} \;=\; \frac{1}{B_1^2}\,\left(\dot{\mathcal{D}}_{\chi\chi} - 2\frac{\dot{B}_1}{B_1}\,\mathcal{D}_{\chi\chi}\right) \tag{B.7}
$$

Now we give the explicit form of the matrix $\mathcal{M}_\kappa$ used in (5.59):

$$
\begin{aligned}
\kappa_{11} &= -B_1^2 + \frac{2p_L^2\,B_1^4}{\mathcal{D}} \\
\kappa_{12} &= \frac{B_1}{2} - \frac{2p_L^2\,B_1^3}{\mathcal{D}} \\
\kappa_{14} &= \left(3 + \frac{B_1^2}{2}\right)\,h + \left(3 - B_1^2\right)\,H + \frac{1}{2}\,B_1\,\dot{B}_1 - \frac{2p_L^2\,B_1^2\,\left(6 + B_1^2\right)}{\mathcal{D}}\,\mathcal{H} \\
\kappa_{15} &= -\frac{3}{2} + \frac{B_1^2}{4} + \frac{p_L^2\,B_1^2\,\left(6 + B_1^2\right)}{2\mathcal{D}} \\
\kappa_{16} &= \frac{4p_L^2\,B_1^3\,\mathcal{D}_{\alpha_0\alpha_0}}{\mathcal{D}}
\end{aligned}
$$

$$
\begin{aligned}
\kappa_{21} &= -\frac{B_1}{3} + \frac{4p_L^2\,B_1^3}{3\mathcal{D}} \\
\kappa_{22} &= 1 - \frac{4p_L^2\,B_1^2}{3\mathcal{D}} \\
\kappa_{24} &= -2\,B_1\,h + \dot{B}_1 - \frac{4p_L^2\,B_1\,\left(6 + B_1^2\right)}{3\mathcal{D}}\,\mathcal{H} \\
\kappa_{25} &= \frac{1}{3}\,B_1\,\left(1 + \frac{p_L^2\,\left(6 + B_1^2\right)}{\mathcal{D}}\right) \\
\kappa_{26} &= 1 + \frac{8p_L^2\,B_1^2\,\mathcal{D}_{\alpha_0\alpha_0}}{3\mathcal{D}}
\end{aligned}
$$

$$\kappa_{41} = \left(1 + \frac{B_1^2}{6}\right) h + \left(1 - \frac{B_1^2}{3}\right) H + \frac{1}{6} B_1 \dot{B}_1 - \frac{2p_L^2 B_1^2 \left(6 + B_1^2\right)}{3\mathcal{D}} \mathcal{H}$$

$$\kappa_{42} = B_1 h - \frac{\dot{B}_1}{2} + \frac{2p_L^2 B_1 \left(6 + B_1^2\right)}{3\mathcal{D}} \mathcal{H}$$

$$\kappa_{44} = 3H^2 - \left(3 + \frac{5}{2} B_1^2\right) h^2 - \frac{1}{2} \dot{B}_1^2 + 2 B_1 \left(B_1 H + \dot{B}_1\right) h + \frac{2p_L^2 \left(6 + B_1^2\right)^2}{3\mathcal{D}} \mathcal{H}^2$$

$$\kappa_{45} = -\frac{1}{2} \left[\left(1 + \frac{B_1^2}{6}\right) (2H - h) + \frac{1}{3} B_1 \dot{B}_1 + \frac{p_L^2 \left(6 + B_1^2\right)^2}{3\mathcal{D}} \mathcal{H}\right]$$

$$\kappa_{46} = B_1 \left(h - \frac{H}{2}\right) - \frac{\dot{B}_1}{2} - \frac{4p_L^2 B_1 \left(6 + B_1^2\right)}{3\mathcal{D}} \mathcal{H} \mathcal{D}_{\alpha_0 \alpha_0}$$

$$\kappa_{51} = \frac{1}{2} \left(1 - \frac{1}{6} B_1^2\right) - \frac{p_L^2 B_1^2 \left(6 + B_1^2\right)}{6\mathcal{D}}$$

$$\kappa_{52} = \frac{1}{6} \left(1 + \frac{p_L^2 \left(6 + B_1^2\right)}{\mathcal{D}}\right) B_1$$

$$\kappa_{54} = \frac{1}{12} \left(6 + B_1^2\right) (2H - h) + \frac{1}{6} B_1 \dot{B}_1 + \frac{p_L^2 \left(6 + B_1^2\right)^2}{6\mathcal{D}} \mathcal{H}$$

$$\kappa_{55} = -\frac{p_L^4 \left(6 + B_1^2\right)}{3p_T^2 \mathcal{D}} \mathcal{D}_{\chi\chi}$$

$$\kappa_{56} = -\frac{p_L^2 B_1 \left(6 + B_1^2\right)}{3\,\mathcal{D}} \mathcal{D}_{\alpha_0 \alpha_0}$$

$$\kappa_{61} = -\frac{8p_L^2 B_1}{3\mathcal{D}} \mathcal{D}_{\chi\chi}$$

$$\kappa_{62} = 1 + \frac{8p_L^2}{3\mathcal{D}} \mathcal{D}_{\chi\chi}$$

$$\kappa_{63} = \frac{p_T^2}{p_L^2}$$

$$\kappa_{64} = B_1 (H - 2h) + \dot{B}_1 + \frac{8p_L^2 \left(6 + B_1^2\right)}{3B_1 \mathcal{D}} \mathcal{H} \mathcal{D}_{\chi\chi}$$

$$\kappa_{65} = -\frac{2p_L^2 \left(6 + B_1^2\right)}{3B_1 \mathcal{D}} \mathcal{D}_{\chi\chi}$$

$$\kappa_{66} = 1 + \frac{p_T^2}{p_L^2} - \frac{2p_T^2 \left(6 + B_1^2\right)}{3\mathcal{D}} \mathcal{D}_{\alpha_0 \alpha_0} \tag{B.8}$$

Finally, we explicitly write down the right hand side of (5.59) involving the functions f_i

where $i = 1 \ldots 6$. Each f_i is a linear combination of the variables

$$F_i \equiv \{\dot{\hat{\Psi}},\, \dot{\hat{\alpha}}_1,\, \dot{\hat{\alpha}},\, \hat{\Psi},\, \hat{\alpha}_1,\, \hat{\alpha},\, \hat{\Phi},\, \hat{B},\, \hat{\alpha}_0\} \tag{B.9}$$

The explicit forms of the functions $f_1, \ldots f_6$ can then be expressed as

$$f_i = \sum_j \mathcal{A}_{ij}\, F_j \tag{B.10}$$

The coefficients $\mathcal{A}_{ij}$ depend entirely on the background quantities. They are given by

$$\begin{aligned}
\mathcal{A}_{11} &= \left(2\,\dot{B}_1 + 3H\,B_1\right)\, B_1 - \frac{2p_L^2\, B_1^4}{\mathcal{D}}\, \left(H + 4h + 4\frac{\dot{B}_1}{B_1} - \frac{\dot{\mathcal{D}}}{\mathcal{D}}\right) \\
\mathcal{A}_{12} &= \left(\frac{H}{2} - 4h\right)\, B_1 + \frac{\dot{B}_1}{2} + \frac{2p_L^2\, B_1^3}{\mathcal{D}}\, \left(H + 4h + 2\frac{\dot{B}_1}{B_1} - \frac{\dot{\mathcal{D}}}{\mathcal{D}}\right) \\
\mathcal{A}_{13} &= 0 \\
\mathcal{A}_{14} &= p_T^2 B_1^2 - \mathcal{M}_{\Psi\Psi} \\
&\quad + \frac{4p_L^2\, B_1^4}{\mathcal{D}}\, \left[\frac{1}{2}\, \left(\dot{H} - 2\dot{h}\right) + \left(H + h - \frac{\dot{\mathcal{D}}}{2\mathcal{D}}\right)\, \left(H - 2h - 2\frac{\dot{B}_1}{B_1}\right)\right. \\
&\qquad \left. - \frac{\dot{B}_1^2}{B_1^2} - \frac{\ddot{B}_1}{B_1} + (H - 2h)\, \frac{\dot{B}_1}{B_1}\right] \\
\mathcal{A}_{15} &= -\frac{p_T^2}{2}\, B_1 - \mathcal{M}_{\Psi\alpha_1} - \frac{2p_L^2\, B_1^3}{\mathcal{D}}\, \left[\dot{H} - 2\dot{h} + 2\, \left(H + h - \frac{\dot{\mathcal{D}}}{2\mathcal{D}}\right)\, \left(H - 2h - \frac{\dot{B}_1}{B_1}\right)\right. \\
&\qquad \left. + (H - 2h)\, \frac{\dot{B}_1}{B_1} - \frac{\ddot{B}_1}{B_1}\right] \\
\mathcal{A}_{16} &= 0 \\
\mathcal{A}_{17} &= \frac{3}{2}\, \left(p_T^2 - \frac{V_0}{M_p^2} + 3h^2 - 3H^2 + \frac{\dot{B}_1^2}{2}\right) \\
&\quad + \frac{1}{4}\, \left(9m^2 - 2p_L^2 - p_T^2 + 15h^2 - 12h\,H\right) B_1^2 \\
&\quad - 3h\, B_1\, \dot{B}_1 + \frac{2p_L^2\, B_1^2\, \left(6 + B_1^2\right)}{\mathcal{D}}\, \left[\dot{\mathcal{H}} + 2\frac{B_1\, \dot{B}_1}{6 + B_1^2}\, \mathcal{H} + 2\left(H + h - \frac{\dot{\mathcal{D}}}{2\mathcal{D}}\right)\, \mathcal{H}\right] \\
\mathcal{A}_{18} &= \frac{9}{2}\, \left(1 + \frac{B_1^2}{18}\right)\, h + \frac{9}{2}\, \left(1 - \frac{5B_1^2}{18}\right)\, H + \frac{1}{2}\, B_1\, \dot{B}_1 \\
&\quad - p_L^2\, \left(6 + B_1^2\right)\, \left(\mathcal{H} - \frac{\dot{\mathcal{D}}}{2\mathcal{D}}\right)\, \frac{B_1^2}{\mathcal{D}}
\end{aligned}$$

$$\mathcal{A}_{19} = \frac{3B_1}{2}\left(H - 2h + \frac{\dot{B}_1}{B_1}\right) - \frac{4p_L^2\,B_1^3}{\mathcal{D}}\,\mathcal{D}_{\alpha_0\alpha_0}\left[2H + 2h + \frac{\dot{B}_1}{B_1} + \frac{\dot{\mathcal{D}}_{\alpha_0\alpha_0}}{\mathcal{D}_{\alpha_0\alpha_0}} - \frac{\dot{\mathcal{D}}}{\mathcal{D}}\right]$$

$$\mathcal{A}_{21} = \frac{1}{3}\,(7H - 8h)\,B_1 + \dot{B}_1 - \frac{4p_L^2}{3}\left(H + 4h + 4\frac{\dot{B}_1}{B_1} - \frac{\dot{\mathcal{D}}}{\mathcal{D}}\right)\frac{B_1^3}{\mathcal{D}}$$

$$\mathcal{A}_{22} = -3H + \frac{4p_L^2}{3}\left(H + 4h + 2\frac{\dot{B}_1}{B_1} - \frac{\dot{\mathcal{D}}}{\mathcal{D}}\right)\frac{B_1^2}{\mathcal{D}}$$

$$\mathcal{A}_{23} = 0$$

$$\mathcal{A}_{24} = \frac{p_T^2 B_1}{3} - \frac{8p_L^2\,B_1^3}{3\mathcal{D}}\left[\left(2H + 2h - \frac{\dot{\mathcal{D}}}{\mathcal{D}}\right)\left(h - \frac{H}{2} + \frac{\dot{B}_1}{B_1}\right) + \dot{h} - \frac{\dot{H}}{2} - (H - 2h)\,\frac{\dot{B}_1}{B_1} + \frac{\dot{B}_1^2}{B_1^2} + \frac{\ddot{B}_1}{B_1}\right]$$

$$\mathcal{A}_{25} = -p_T^2 - \mathcal{M}_{\alpha_1\alpha_1} - \frac{4p_L^2\,B_1^2}{3\mathcal{D}}\left[\left(2H + 2h - \frac{\dot{\mathcal{D}}}{\mathcal{D}}\right)\left(H - 2h - \frac{\dot{B}_1}{B_1}\right) + \dot{H} - 2\dot{h} + (H - 2h)\,\frac{\dot{B}_1}{B_1} - \frac{\ddot{B}_1}{B_1}\right]$$

$$\mathcal{A}_{26} = p_T^2$$

$$\mathcal{A}_{27} = \left(2m^2 - \frac{p^2}{3}\right)B_1 + \frac{4p_L^2\,B_1\,\left(6 + B_1^2\right)}{3\,\mathcal{D}}\left[2\left(H + h - \frac{\dot{\mathcal{D}}}{2\mathcal{D}} + \frac{B_1\,\dot{B}_1}{6 + B_1^2}\right)\mathcal{H} + \dot{\mathcal{H}}\right]$$

$$\mathcal{A}_{28} = -\left(\frac{H}{3} + \frac{7h}{3}\right)B_1 + \dot{B}_1 - \frac{2\,p_L^2\,B_1\,\left(6 + B_1^2\right)}{3\,\mathcal{D}}\left(\mathcal{H} - \frac{\dot{\mathcal{D}}}{2\mathcal{D}}\right)$$

$$\mathcal{A}_{29} = -2(H + h) - \frac{16\,p_L^2\,B_1^2\,\mathcal{D}_{\alpha_0\alpha_0}}{3\,\mathcal{D}}\left[H + h - \frac{\dot{\mathcal{D}}}{2\mathcal{D}} + \frac{\dot{B}_1}{2B_1} + \frac{\dot{\mathcal{D}}_{\alpha_0\alpha_0}}{2\mathcal{D}_{\alpha_0\alpha_0}}\right]$$

$$\mathcal{A}_{31} = \mathcal{A}_{32} = \mathcal{A}_{34} = \mathcal{A}_{37} = 0$$

$$\mathcal{A}_{33} = -3\,(H - 2h)$$

$$\mathcal{A}_{35} = p_L^2$$

$$\mathcal{A}_{36} = -p_L^2 - \mathcal{M}_{\alpha\alpha}$$

$$\mathcal{A}_{38} = -\frac{p_L^2}{p_T^2}\left((H - 2h)\,B_1 + \dot{B}_1\right)$$

$$\mathcal{A}_{39} = -2\,(H - 2h)$$

$$\mathcal{A}_{41} = \left(\frac{2}{3}H - \frac{1}{3}h\right)B_1\,\dot{B}_1 - \frac{2}{3}\dot{B}_1^2 - \frac{1}{6}B_1\,\ddot{B}_1 - \frac{p_T^2}{2}$$

$$
\begin{aligned}
&- \left(m^2 - \frac{2p_L^2 + p_T^2}{6} + 5h^2 - 4h\,H \right) \frac{B_1^2}{2} \\
&+ 2h\,B_1\,\dot{B}_1 - \left(1 + \frac{B_1^2}{6} \right) \dot{h} - \left(1 - \frac{B_1^2}{3} \right) \dot{H} \\
&+ \frac{2p_L^2\,B_1^2\,\left(6 + B_1^2\right)}{3\mathcal{D}} \left[\left(-3H + 6h + 4\frac{\dot{B}_1}{B_1} - \frac{\dot{\mathcal{D}}}{\mathcal{D}} + 2\,\frac{B_1\,\dot{B}_1}{6 + B_1^2} \right) \mathcal{H} + \dot{\mathcal{H}} \right] \\
\mathcal{A}_{42} = &\frac{1}{2} \left(m^2 - \frac{p^2}{3} + 5h^2 - 4h\,H - 2\dot{h} \right) B_1 - 2h\,\dot{B}_1 + \frac{1}{2}\,\ddot{B}_1 \\
&- \frac{2p_L^2\,B_1\,\left(6 + B_1^2\right)}{3\mathcal{D}} \left[\left(-3H + 6h + 2\frac{\dot{B}_1}{B_1} - \frac{\dot{\mathcal{D}}}{\mathcal{D}} + 2\,\frac{B_1\,\dot{B}_1}{6 + B_1^2} \right) \mathcal{H} + \dot{\mathcal{H}} \right] \\
\mathcal{A}_{43} = &\,0 \\
\mathcal{A}_{44} = &\,(H + h)\,p_T^2 - \left[\frac{2p_L^2 + p_T^2}{6} H - \frac{4p_L^2 - p_T^2}{6} h - 2\left(\dot{H}h + H\dot{h} \right) + 5h\dot{h} \right] B_1^2 \\
&- \left[m^2 - \frac{2p_L^2 + p_T^2}{6} - 4Hh - 2\dot{h} + 5h^2 \right] B_1 \dot{B}_1 \\
&- \dot{B}_1\,\ddot{B}_1 + 2\left(\dot{B}_1^2 + B_1\,\ddot{B}_1 \right) h \\
&+ \frac{2p_L^2\,B_1^2\left(6 + B_1^2\right)}{3\mathcal{D}} \left(2h - H + 2\frac{\dot{B}_1}{B_1} \right) \\
&\quad \times \left[\left(4h - 2H - \frac{\dot{\mathcal{D}}}{\mathcal{D}} + 2\,\frac{B_1\,\dot{B}_1}{6 + B_1^2} \right) \mathcal{H} + \dot{\mathcal{H}} \right] \\
&+ \frac{2p_L^2\,B_1^2\left(6 + B_1^2\right)}{3\mathcal{D}}\,\mathcal{H} \left[2\dot{h} - \dot{H} + 2\frac{\dot{B}_1^2}{B_1^2} + 2\left(2h - H \right) \frac{\dot{B}_1}{B_1} + 2\frac{\ddot{B}_1}{B_1} \right] \\
\mathcal{A}_{45} = &-h\,\ddot{B}_1 + \left[\frac{1}{2} \left(m^2 - \frac{p^2}{3} \right) + \frac{5}{2}\,h^2 - 2h\,H - \dot{h} \right] \dot{B}_1 \\
&+ \left[\left(\frac{p^2}{3} - 2\,\dot{h} \right) H + \left(\frac{-2p_L^2 + p_T^2}{3} + 5\dot{h} - 2\dot{H} \right) h \right] B_1 \\
&+ \frac{2p_L^2\,B_1\left(6 + B_1^2\right)}{3\mathcal{D}} \left(2h - H + \frac{\dot{B}_1}{B_1} \right) \\
&\quad \times \left[\left(2H - 4h + \frac{\dot{\mathcal{D}}}{\mathcal{D}} - 2\,\frac{B_1\,\dot{B}_1}{6 + B_1^2} \right) \mathcal{H} - \dot{\mathcal{H}} \right] \\
&- \frac{2p_L^2\,B_1\left(6 + B_1^2\right)}{3\mathcal{D}}\,\mathcal{H} \left[2\dot{h} - \dot{H} + \left(2h - H \right) \frac{\dot{B}_1}{B_1} + \frac{\ddot{B}_1}{B_1} \right] \\
\mathcal{A}_{46} = &\,0
\end{aligned}
$$

$$
\begin{aligned}
\mathcal{A}_{47} = & -6H\,\dot{H} + \dot{B}_1\,\ddot{B}_1 - 2h\,\left(2H\,B_1\,\dot{B}_1 + B_1^2\,\dot{H} + \dot{B}_1^2 + B_1\,\ddot{B}_1\right) \\
& -2\,B_1\,\left(B_1\,H + \dot{B}_1\right)\,\dot{h} + \left(6 + 5B_1^2\right)\,h\,\dot{h} + 5\,B_1\,\dot{B}_1\,h^2 \\
& + \frac{4p_L^2\,\left(6+B_1^2\right)^2}{3\mathcal{D}}\,\mathcal{H}\,\left[\left(H - 2h + \frac{\dot{\mathcal{D}}}{2\mathcal{D}} - 2\,\frac{B_1\,\dot{B}_1}{6+B_1^2}\right)\,\mathcal{H} - \dot{\mathcal{H}}\right] \\
\mathcal{A}_{48} = & \frac{1}{6}\,\left[(2H-h)\,B_1\,\dot{B}_1 + \dot{B}_1^2 + B_1\,\ddot{B}_1\right] - \frac{1}{12}\,\left(6+B_1^2\right)\,\left(\dot{h} - 2\,\dot{H}\right) \\
& -\frac{p_L^2\,\left(6+B_1^2\right)^2}{3\mathcal{D}}\,(H-2h)\,\mathcal{H} + \frac{p_L^2\,\left(6+B_1^2\right)^2}{6\mathcal{D}}\,\left[\left(4\,\frac{B_1\,\dot{B}_1}{6+B_1^2} - \frac{\dot{\mathcal{D}}}{\mathcal{D}}\right)\,\mathcal{H} + \dot{\mathcal{H}}\right] \\
\mathcal{A}_{49} = & \frac{1}{2}\,\ddot{B}_1 + \frac{1}{2}\,(H-2h)\,\dot{B}_1 + \frac{1}{2}\,\left(\dot{H} - 2\dot{h}\right)\,B_1 \\
& -\frac{8p_L^2\,B_1\,\left(6+B_1^2\right)}{3\mathcal{D}}\,\mathcal{D}_{\alpha_0\alpha_0}\,\left[\mathcal{H}\,\left(H - 2h + \frac{\dot{\mathcal{D}}}{2\mathcal{D}} - \frac{\dot{B}_1}{2B_1} - \frac{\dot{\mathcal{D}}_{\alpha_0\alpha_0}}{2\mathcal{D}_{\alpha_0\alpha_0}}\right)\right. \\
& \left. -\frac{1}{2}\,\dot{\mathcal{H}} - \frac{B_1\,\dot{B}_1}{6+B_1^2}\,\mathcal{H}\right]
\end{aligned}
$$

$$
\begin{aligned}
\mathcal{A}_{51} &= -\frac{1}{6}\,B_1\,\left(B_1\,H - 3\,\dot{B}_1\right) + \frac{1}{2}\,\left(3 + \frac{B_1^2}{6}\right)\,h \\
&\quad + \frac{p_L^2\,B_1^2\,\left(6+B_1^2\right)}{3\mathcal{D}}\,\left[3h - \frac{3}{2}\,H + \frac{B_1\,\dot{B}_1}{6+B_1^2} + 2\,\frac{\dot{B}_1}{B_1} - \frac{\dot{\mathcal{D}}}{2\mathcal{D}}\right] \\
\mathcal{A}_{52} &= -\frac{B_1}{6}\,(2H - 7h) - \frac{5}{6}\,\dot{B}_1 + \frac{p_L^2\,B_1\,\left(6+B_1^2\right)}{3\mathcal{D}}\,\left[\frac{3}{2}\,H - 3h - \frac{B_1\,\dot{B}_1}{6+B_1^2} - \frac{\dot{B}_1}{B_1} + \frac{\dot{\mathcal{D}}}{2\mathcal{D}}\right] \\
\mathcal{A}_{53} &= B_1\,\left(\frac{H}{2} - h\right) + \frac{\dot{B}_1}{2} \\
\mathcal{A}_{54} &= \frac{1}{6}\,h\,B_1\,\dot{B}_1 - \frac{1}{6}\,\left(B_1\,H - 2\,\dot{B}_1\right)\,\dot{B}_1 - \frac{1}{6}\,B_1\,\left(H\,\dot{B}_1 + B_1\,\dot{H} - 2\,\ddot{B}_1\right) \\
&\quad + \frac{1}{2}\,\left(3 + \frac{1}{6}\,B_1^2\right)\,\dot{h} + \frac{p_L^2\,B_1^2\,\left(6+B_1^2\right)}{3\mathcal{D}}\,\left(2h - H + 2\frac{\dot{B}_1}{B_1}\right) \\
&\quad\quad \times \left(2h - H + \frac{B_1\,\dot{B}_1}{6+B_1^2} - \frac{\dot{\mathcal{D}}}{2\mathcal{D}}\right) \\
&\quad + \frac{p_L^2\,B_1^2\,\left(6+B_1^2\right)}{6\mathcal{D}}\,\left[2\dot{h} - \dot{H} + 2\,(2h-H)\,\frac{\dot{B}_1}{B_1} + 2\,\frac{\dot{B}_1^2}{B_1^2} + 2\,\frac{\ddot{B}_1}{B_1}\right] \\
\mathcal{A}_{55} &= \frac{1}{6}\,(7h - 2H)\,\dot{B}_1 + \frac{1}{6}\,\left(7\dot{h} - 2\dot{H}\right)\,B_1 - \frac{2}{3}\,\ddot{B}_1
\end{aligned}
$$

$$
\begin{aligned}
& -\frac{p_L^2\, B_1\, \left(6+B_1^2\right)}{3\mathcal{D}}\, \left(2h - H + \frac{B_1\, \dot{B}_1}{6+B_1^2} - \frac{\dot{\mathcal{D}}}{2\mathcal{D}}\right)\, \left(2h - H + \frac{\dot{B}_1}{B_1}\right) \\
& -\frac{p_L^2\, B_1\, \left(6+B_1^2\right)}{6\mathcal{D}}\, \left[2\dot{h} - \dot{H} + (2h-H)\, \frac{\dot{B}_1}{B_1} + \frac{\ddot{B}_1}{B_1}\right]
\end{aligned}
$$

$$
\mathcal{A}_{56} = \left(\frac{\dot{H}}{2} - \dot{h}\right)\, B_1 + \left(\frac{H}{2} - h\right)\, \dot{B}_1 + \frac{\ddot{B}_1}{2}
$$

$$
\begin{aligned}
\mathcal{A}_{57} = {} & \frac{1}{6}\left[B_1\,(h-2H) - \dot{B}_1\right]\dot{B}_1 - \frac{1}{6}B_1\ddot{B}_1 + \frac{1}{12}\left(6+B_1^2\right)\left(\dot{h} - 2\dot{H}\right) \\
& + \frac{p_L^2\left(6+B_1^2\right)^2}{3\mathcal{D}}\, \left[H - 2h - 2\frac{B_1\,\dot{B}_1}{6+B_1^2} + \frac{\dot{\mathcal{D}}}{2\mathcal{D}} - \frac{\dot{\mathcal{H}}}{2\mathcal{H}}\right]\mathcal{H}
\end{aligned}
$$

$$
\begin{aligned}
\mathcal{A}_{58} = {} & \frac{p_L^4\, \left(6+B_1^2\right)\, \mathcal{D}_{\chi\chi}}{3p_T^2\,\mathcal{D}^2}\, \Bigg[12h\, \left(\mathcal{D} + 4p_L^2\,\mathcal{D}_{\chi\chi}\right) - 16p_L^2\, \frac{B_1\,\dot{B}_1}{6+B_1^2}\,\mathcal{D}_{\chi\chi} \\
& + \left(6+B_1^2\right)\, p_T^2\, \frac{\dot{\mathcal{D}}_{\chi\chi}}{\mathcal{D}_{\chi\chi}}\Bigg]
\end{aligned}
$$

$$
\begin{aligned}
\mathcal{A}_{59} = {} & \frac{p_L^2\, B_1\, \mathcal{D}_{\alpha_0\alpha_0}}{3\mathcal{D}^2}\, \Bigg[p_T^2\, B_1^3\, \dot{B}_1 + 12\left(3p_T^2 - 4p_L^2\,\mathcal{D}_{\chi\chi}\right)\, \frac{\dot{B}_1}{B_1} \\
& + 12\left(p_T^2 - 2p_L^2\,\mathcal{D}_{\chi\chi}\right)\, B_1\,\dot{B}_1 + p_T^2\, \left(6h + \frac{\dot{\mathcal{D}}_{\alpha_0\alpha_0}}{\mathcal{D}_{\alpha_0\alpha_0}}\right)\, B_1^4 \\
& + 12\left(18p_T^2\, h + 4p_L^2\,\dot{\mathcal{D}}_{\chi\chi} + \left(3p_T^2 - 4p_L^2\,\mathcal{D}_{\chi\chi}\right)\, \frac{\dot{\mathcal{D}}_{\alpha_0\alpha_0}}{\mathcal{D}_{\alpha_0\alpha_0}}\right) \\
& + 4\left(18p_T^2\, h + 2p_L^2\,\dot{\mathcal{D}}_{\chi\chi} + \left(3p_T^2 - 2p_L^2\,\mathcal{D}_{\chi\chi}\right)\, \frac{\dot{\mathcal{D}}_{\alpha_0\alpha_0}}{\mathcal{D}_{\alpha_0\alpha_0}}\right) B_1^2\Bigg]
\end{aligned}
$$

$$
\begin{aligned}
\mathcal{A}_{61} = {} & -\frac{4p_T^4}{3\mathcal{D}^2}\, \Bigg\{\frac{3}{4}\, (2h-H)\, B_1^5 - \frac{3}{4}\,\dot{B}_1\, B_1^4 - 9\, \left(3 - 4\frac{p_L^2}{p_T^2}\,\mathcal{D}_{\chi\chi}\right)\, \dot{B}_1 \\
& - \left(9 - 10\,\frac{p_L^2}{p_T^2}\,\mathcal{D}_{\chi\chi}\right)\, B_1^2\,\dot{B}_1 + 2h\, \left(9 - 20\,\frac{p_L^2}{p_T^2}\,\mathcal{D}_{\chi\chi}\right)\, B_1^3 \\
& + \left[-9\left(3+B_1^2\right) + 14\, \left(6+B_1^2\right)\, \frac{p_L^2}{p_T^2}\,\mathcal{D}_{\chi\chi} - 64\,\frac{p_L^4}{p_T^4}\,\mathcal{D}_{\chi\chi}^2\right]\, H\, B_1 \\
& + 2\, \left[27 - 120\,\frac{p_L^2}{p_T^2}\,\mathcal{D}_{\chi\chi} + 64\,\frac{p_L^4}{p_T^4}\,\mathcal{D}_{\chi\chi}^2\right]\, h\, B_1 \\
& - 2\, \left(6+B_1^2\right)\, B_1\, \frac{p_L^2}{p_T^2}\,\dot{\mathcal{D}}_{\chi\chi}\Bigg\}
\end{aligned}
$$

$$
\begin{aligned}
\mathcal{A}_{62} &= -\frac{4p_T^4}{3B_1\,\mathcal{D}^2}\left\{\frac{3}{4}\,(H-2h)\,B_1^5+4\,\frac{p_L^2}{p_T^2}\,\left(3-4\frac{p_L^2}{p_T^2}\,\mathcal{D}_{\chi\chi}\right)\,\mathcal{D}_{\chi\chi}\,\dot{B}_1-2\frac{p_L^2}{p_T^2}\,\mathcal{D}_{\chi\chi}\,B_1^2\,\dot{B}_1\right.\\
&\qquad -2\left[9\left(3+B_1^2\right)-20\left(6+B_1^2\right)\frac{p_L^2}{p_T^2}\,\mathcal{D}_{\chi\chi}+64\frac{p_L^4}{p_T^4}\,\mathcal{D}_{\chi\chi}^2\right]h\,B_1\\
&\qquad +\left[9\left(3+B_1^2\right)-14\left(6+B_1^2\right)\frac{p_L^2}{p_T^2}\,\mathcal{D}_{\chi\chi}+64\frac{p_L^4}{p_T^4}\,\mathcal{D}_{\chi\chi}^2\right]H\,B_1\\
&\qquad \left.+2\left(6+B_1^2\right)\,\frac{p_L^2}{p_T^2}\,B_1\,\dot{\mathcal{D}}_{\chi\chi}\right\}\\
\mathcal{A}_{63} &= -\frac{p_T^2}{p_L^2}\,(H-8h)
\end{aligned}
$$

$$
\begin{aligned}
\mathcal{A}_{64} &= \ddot{B}_1+(H-2h)\,\dot{B}_1+\left(\dot{H}-2\dot{h}\right)\,B_1\\
&\qquad -\frac{16\,p_L^2\,B_1}{3\mathcal{D}}\,\mathcal{D}_{\chi\chi}\,\left(2h-H+2\,\frac{\dot{B}_1}{B_1}\right)\,\left(H-2h+\frac{\dot{B}_1}{2B_1}-\frac{\dot{\mathcal{D}}_{\chi\chi}}{2\mathcal{D}_{\chi\chi}}+\frac{\dot{\mathcal{D}}}{2\mathcal{D}}\right)\\
&\qquad +\frac{8p_L^2\,B_1}{3\mathcal{D}}\,\mathcal{D}_{\chi\chi}\,\left(2\frac{\dot{B}_1^2}{B_1^2}+2\dot{h}-\dot{H}+2\,(2h-H)\,\frac{\dot{B}_1}{B_1}+2\frac{\ddot{B}_1}{B_1}\right)\\
\mathcal{A}_{65} &= 2\dot{h}-\dot{H}+\frac{16\,p_L^2}{3\mathcal{D}}\,\mathcal{D}_{\chi\chi}\,\left(2h-H+\frac{\dot{B}_1}{B_1}\right)\,\left(H-2h+\frac{\dot{B}_1}{2B_1}-\frac{\dot{\mathcal{D}}_{\chi\chi}}{2\mathcal{D}_{\chi\chi}}+\frac{\dot{\mathcal{D}}}{2\mathcal{D}}\right)\\
&\qquad -\frac{8p_L^2}{3\mathcal{D}}\,\mathcal{D}_{\chi\chi}\,\left(2\dot{h}-\dot{H}+(2h-H)\,\frac{\dot{B}_1}{B_1}+\frac{\ddot{B}_1}{B_1}\right)\\
\mathcal{A}_{66} &= -\frac{p_T^2}{p_L^2}\,\left(\dot{H}-2\dot{h}-6h\,H+12h^2\right)\\
\mathcal{A}_{67} &= -\ddot{B}_1+(2h-H)\,\dot{B}_1+\left(2\dot{h}-\dot{H}\right)\,B_1\\
&\qquad +\frac{16p_L^2\,\left(6+B_1^2\right)}{3B_1\,\mathcal{D}}\,\mathcal{D}_{\chi\chi}\,\mathcal{H}\,\left[H-2h-\frac{B_1\,\dot{B}_1}{6+B_1^2}+\frac{\dot{B}_1}{2B}-\frac{\dot{\mathcal{D}}_{\chi\chi}}{2\mathcal{D}_{\chi\chi}}+\frac{\dot{\mathcal{D}}}{2\mathcal{D}}-\frac{\dot{\mathcal{H}}}{2\mathcal{H}}\right]\\
\mathcal{A}_{68} &= -\frac{2p_L^2\,p_T^2}{3B_1^2\,\mathcal{D}^2}\,\mathcal{D}_{\chi\chi}\,\left\{\,\left[B_1^4+4\,\left(3+2\frac{p_L^2}{p_T^2}\,\mathcal{D}_{\chi\chi}\right)\,B_1^2+12\,\left(3-4\frac{p_L^2}{p_T^2}\,\mathcal{D}_{\chi\chi}\right)\right]\,\dot{B}_1\right.\\
&\qquad \left.-B_1\,\left(6+B_1^2\right)^2\,\left(6h+\frac{\dot{\mathcal{D}}}{\mathcal{D}}\right)\,\right\}\\
\mathcal{A}_{69} &= \frac{2p_T^6}{3p_L^2\,\mathcal{D}^2}\,\left\{3\,\left[3B_1^4+36\,\left(3+B_1^2\right)-16\frac{p_L^2}{p_T^2}\,\left(6+B_1^2\right)\,\mathcal{D}_{\chi\chi}\,\left(3-\frac{p_L^2}{p_T^2}\,\mathcal{D}_{\alpha_0\alpha_0}\right)\right.\right.
\end{aligned}
$$

$$
\begin{aligned}
&\quad +192\frac{p_L^4}{p_T^4}\,\mathcal{D}_{\chi\chi}^2\Bigg]\,h \\
&+\frac{p_L^2}{p_T^2}\,\mathcal{D}_{\alpha_0\alpha_0}\Bigg[-16\frac{p_L^2}{p_T^2}\,\mathcal{D}_{\chi\chi}\,B_1\,\dot{B}_1+\left(8\frac{p_L^2}{p_T^2}\,\mathcal{D}_{\chi\chi}+B_1^2\right)\,\frac{\dot{\mathcal{D}}_{\alpha_0\alpha_0}}{\mathcal{D}_{\alpha_0\alpha_0}}\,B_1^2 \\
&+4\left(3+B_1^2\right)\,\left(3-4\frac{p_L^2}{p_T^2}\,\mathcal{D}_{\chi\chi}\right)\,\frac{\dot{\mathcal{D}}_{\alpha_0\alpha_0}}{\mathcal{D}_{\alpha_0\alpha_0}} \\
&+8\left(6+B_1^2\right)\,\frac{p_L^2}{p_T^2}\,\dot{\mathcal{D}}_{\chi\chi}\Bigg]\Bigg\}
\end{aligned}
\tag{B.11}
$$

Thus, we have the full form of the equation (5.59), which we integrate numerically.

Appendix C

Early time canonical action and initial conditions

We discuss here how we set the initial conditions for the perturbations entering in the linearized system (5.59). As in the standard case [5] and chapter 2, the initial conditions follow from the quantization of the quadratic action for the dynamical modes. As we show in Section 5.3, the quadratic action - formally written in equation (4.54) - is obtained by integrating the nondynamical fields out of the quadratic action for the perturbations - formally written in equation (4.52).

The quadratic action of the 2d scalar perturbations of the model (5.48) is given in eq. (5.63). The corresponding action for the dynamical modes is extremely lengthy, and we do not explicitly write it here. Fortunately, to set the initial conditions for the perturbations we only need the leading terms in an early time expansion of this action. We are interested in the phenomenologically relevant case of moderate anisotropy ($B_1 \ll 1$), for which $H_a \simeq H_b$ are nearly constant. Therefore, the two scale factors a and b grow nearly exponentially with time, and p/H (where p is either the longitudinal or the transverse component, and H is either H_a or H_b) is exponentially large in the asymptotic past. Therefore, the early time expansion of the action coincides with the sub-horizon $p/H \gg 1$ expansion, exactly as in the standard case.

Specifically, we first compute the exact matrices K, X, Ω^2 that form the action for the dynamical modes (cf. equation (4.55)), and then expand them for $p/H \gg 1$. Since

the resulting expressions are still quite involved, we further expand them for $B_1 \ll 1$. This procedure is legitimate provided that

$$\frac{H}{p} \ll B_1 \ll 1 \tag{C.1}$$

which, as we remarked, is always true in the case of small anisotropy, and for sufficiently early times. At leading order, we obtain the expression

$$S_{\rm can} \simeq \frac{1}{2}\int d^3k\, dt\, \left\{|\dot{H}_+|^2 - p^2\,|H_+|^2 + |\dot{\Delta}_+|^2 - p^2\,|\Delta_+|^2 + |\dot{\Delta}_-|^2 - p^2\,|\dot{\Delta}_-|^2\right\} \tag{C.2}$$

where the modes H_+, Δ_+, and Δ_- are related to the original perturbations by

$$\begin{aligned}
\hat{\Psi} &= \frac{1}{\sqrt{a\,b^2}}\left\{\left(\frac{\sqrt{2}\,p^2}{p_T^2} - \frac{3H_0^4\,\left(p_L^2+10p_T^2\right) - m^2\,p_T^2\,\left(6H_0^2-m^2\right)}{18\sqrt{2}\,H_0^4\,p_T^2}\,B_1^2\right)\,H_+\right.\\
&\qquad \left. -\left(1-\frac{m^2}{3H_0^2}\right)\,\frac{p}{p_T}\,B_1\,\Delta_+ + \frac{3H_0^2\,\left(4p_L^4+7p_L^2\,p_T^2+p_T^4\right) - m^2\,p_T^2\,p^2}{6\sqrt{6}\,H_0^2\,p_T^4}\,B_1^2\,\Delta_-\right\}\\
\hat{\alpha} &= \frac{1}{\sqrt{a\,b^2}}\left\{\left(\frac{p}{2p_T}\right.\right.\\
&\qquad \left.\left. -\frac{3H_0^4\,\left(p_L^2-5p_T^2\right)\,\left(p_L^2+3p_T^2\right) + 4H_0^2\,m^2\,p_T^2\,\left(p_L^2+7p_T^2\right) - 4m^4\,p_T^4}{144H_0^4\,p_T^3\,p}\,B_1^2\right)\,\Delta_+\right.\\
&\qquad \left. +\left(\frac{\sqrt{6}}{B_1} - \frac{p_T^2-3p_L^2}{8\sqrt{6}\,p_T^2}\,B_1\right)\,\Delta_-\right\}\\
\hat{\alpha}_1 &= \frac{1}{\sqrt{a\,b^2}}\left\{-\frac{p}{\sqrt{2}\,p_T}\,\Delta_+ + \left(\frac{\sqrt{6}}{B_1} - \frac{3H_0^2\,\left(p_L^2-3p_T^2\right)+8m^2\,p_T^2}{24\sqrt{6}\,H_0^2\,p_T^2}\,B_1\right)\,\Delta_-\right\}
\end{aligned} \tag{C.3}$$

The modes H_+, Δ_+, and Δ_- are the canonical variables of the system (they are the analogous of the Mukhanov-Sasaki [5] variable v in the standard case of scalar field isotropic inflation). As in the standard case, their early times frequency is given by the momentum p, up to $\mathrm{O}\,(H/p)$ subdominant corrections. Since the momentum changes adiabatically at early times ($\dot{p}/p^2 = \mathrm{O}\,(H/p)$), we can set the initial conditions for the canonical modes according to the adiabatic vacuum prescription, precisely as done in the standard case [5]:

$$H_{+,\,in} = \Delta_{+,\,in} = \Delta_{-\,in} = \frac{1}{\sqrt{2p}} \quad , \quad \dot{H}_{+,\,in} = \dot{\Delta}_{+,\,in} = \dot{\Delta}_{-\,in} = -i\,\sqrt{\frac{p}{2}} \tag{C.4}$$

which are $\mathrm{O}\,(H/p)$ accurate. From eqs. (C.3) and (C.4) we thus obtain the initial conditions for $\{\hat{\Psi},\, \hat{\alpha},\, \hat{\alpha}_1\}$ and their time derivatives. Finally, the first, third, and fourth of eqs. (5.56) provide the initial conditions for the nondynamical modes $\hat{\Phi},\, \hat{\chi},$ and $\hat{\alpha}_0$. In this way, we have the initial conditions for all the modes of the system (5.59).

Appendix D

Details of calculations for $2d$ scalar perturbations

In this appendix, we study the $2d$ scalar perturbations. As we have done for the case of the $2d$ vector perturbations, we insert the metric and vector field decompositions (4.31) and $\phi = \phi_0(t) + \delta\phi$, $\phi_1 = \phi_{1\,0}(t) + \delta\phi_1$ into the action (6.1) (with $a = 1$), after fixing the $U(1)$ and general coordinate invariance as described previously. The quadratic action in momentum space up to a total time derivative is given by

$$
\begin{aligned}
S_{2dS} &= \frac{1}{2}\int dt\, d^3k\, e^{3\alpha}\, \mathcal{L}_{2dS} \\
\mathcal{L}_{2dS} &= |\delta\dot{\phi}|^2 + |\delta\dot{\phi}_1|^2 + e^{-2\alpha+4\sigma}\, f^2(\phi)\, |\dot{\alpha}_1|^2 - \dot{\phi}\, \left(\delta\dot{\phi}^*\, \Psi + \text{h.c.}\right) - \dot{\phi}\, \left(\delta\dot{\phi}^*\, \Phi + \text{h.c.}\right) \\
&\quad -\dot{\phi}_1\, \left(\delta\dot{\phi}_1^*\, \Psi + \text{h.c.}\right) - \dot{\phi}_1\, \left(\delta\dot{\phi}_1^*\, \Phi + \text{h.c.}\right) - 2M_p^2\, (\dot{\alpha} + \dot{\sigma})\, \left(\dot{\Psi}^*\, \Phi + \text{h.c.}\right) \\
&\quad + \frac{2e^{-\alpha+2\sigma}\, \tilde{p}_A\, f'(\phi)}{f(\phi)}\, (\dot{\alpha}_1^*\, \delta\phi + \text{h.c.}) + e^{-\alpha+2\sigma}\, \tilde{p}_A\, (\dot{\alpha}_1^*\, \Psi + \text{h.c.}) \\
&\quad - e^{-\alpha+2\sigma}\, \tilde{p}_A\, (\dot{\alpha}_1^*\, \Phi + \text{h.c.}) + e^{-\alpha+2\sigma}\, p_L\, f^2(\phi)\, (i\, \dot{\alpha}_1^*\, \alpha_0 + \text{h.c.}) \\
&\quad - \left[p^2 + V''(\phi) - \tilde{p}_A^2\, \left(\frac{f'(\phi)^2}{f(\phi)^4} + \frac{f''(\phi)}{f(\phi)^3}\right)\right]\, |\delta\phi|^2 - \left(p^2 + V_1''(\phi_1)\right)\, |\delta\phi_1|^2 \\
&\quad + \left[\tilde{p}_A^2\, \frac{f'(\phi)}{f^3(\phi)} + V'(\phi)\right]\, (\delta\phi^*\, \Psi + \text{h.c.}) - \left[\tilde{p}_A^2\, \frac{f'(\phi)}{f^3(\phi)} + V'(\phi)\right]\, (\delta\phi^*\, \Phi + \text{h.c.}) \\
&\quad + V_1'(\phi_1)\, (\delta\phi_1^*\, \Psi + \text{h.c.}) - V_1'(\phi_1)\, (\delta\phi_1^*\, \Phi + \text{h.c.}) \\
&\quad - e^{\alpha-2\sigma}\, p_L^2\, \dot{\phi}\, (\delta\phi^*\, \chi + \text{h.c.}) - e^{\alpha+\sigma}\, p_T^2\, \dot{\phi}\, (\delta\phi^*\, B + \text{h.c.}) \\
&\quad - e^{\alpha-2\sigma}\, p_L^2\, \dot{\phi}_1\, (\delta\phi_1^*\, \chi + \text{h.c.}) - e^{\alpha+\sigma}\, p_T^2\, \dot{\phi}_1\, (\delta\phi_1^*\, B + \text{h.c.})
\end{aligned}
$$

$$
\begin{aligned}
&+\frac{2\,\tilde{p}_A\,p_L\,f'(\phi)}{f(\phi)}\;(i\,\delta\phi^*\,\alpha_0+\text{h.c.})+\frac{\tilde{p}_A^2}{f(\phi)^2}\,|\Psi|^2\\
&-M_p^2\,\left(p_T^2+\frac{\tilde{p}_A^2}{M_p^2\,f^2(\phi)}\right)\;(\Psi^*\,\Phi+\text{h.c.})-3e^{\alpha+\sigma}\,M_p^2\,p_T^2\,\dot{\sigma}\;(\Psi^*\,B+\text{h.c.})\\
&+\tilde{p}_A\,p_L\;(i\,\Psi^*\,\alpha_0+\text{h.c.})-e^{-2\alpha+4\sigma}\,p_T^2\,f^2(\phi)\,|\alpha_1|^2-e^{3\sigma}\,\tilde{p}_A\,p_T^2\;(\alpha_1^*\,B+\text{h.c.})\\
&+M_p^2\,\left[\frac{\tilde{p}_A^2}{M_p^2\,f(\phi)^2}+\frac{\dot{\phi}^2}{M_p^2}+\frac{\dot{\phi}_1^2}{M_p^2}+6(\dot{\sigma}^2-\dot{\alpha}^2)\right]\;|\Phi|^2\\
&+2e^{\alpha-2\sigma}\,M_p^2\,p_L^2\;(\dot{\alpha}+\dot{\sigma})\;(\Phi^*\,\chi+\text{h.c.})+e^{\alpha+\sigma}\,M_p^2\,p_T^2\;(2\dot{\alpha}-\dot{\sigma})\;(\Phi^*\,B+\text{h.c.})\\
&-\tilde{p}_A\,p_L\;(i\,\Phi^*\,\alpha_0+\text{h.c.})+\frac{1}{2}\,e^{2\alpha-4\sigma}\,M_p^2\,p_L^2\,p_T^2\,|\chi|^2\\
&-\frac{1}{2}\,e^{2\alpha-\sigma}\,M_p^2\,p_L^2\,p_T^2\;(\chi^*\,B+\text{h.c.})+\frac{1}{2}\,e^{2\alpha+2\sigma}\,M_p^2\,p_L^2\,p_T^2\,|B|^2+p^2\,f^2(\phi)\,|\alpha_0|^2
\end{aligned}
\tag{D.1}
$$

We can see from the above action that the modes $\{\Phi,\,\chi,\,B,\,\alpha_0\}$ are nondynamical, and can be integrated out. More precisely, we extremize the action (D.1) with respect to the nondynamical modes to obtain constraint equations, which we solve for the values of the nondynamical modes. We insert the solutions back into the action (D.1) to obtain an action purely in terms of the dynamical modes $\{\delta\phi,\,\delta\phi_1,\,\Psi,\,\alpha_1\}$ up to a total time derivative. This action reads

$$
\begin{aligned}
S_{2dS} \;=\; \frac{1}{2}\int dt\,d^3k\,\Bigg\{&|\dot{V}|^2+|\dot{V}_1|^2+|\dot{H}_+|^2+|\dot{\Delta}_+|^2+\mathcal{F}\,\left(i\,\dot{V}^*\,\Delta_+ + i\,V\,\dot{\Delta}_+^*+\text{h.c.}\right)\\
&+\mathcal{G}\,\left(i\,\dot{H}_+^*\,\Delta_+ + i\,H_+\,\dot{\Delta}_+^*+\text{h.c.}\right)\\
&-\left(V^*\,V_1^*\,H_+^*\,\Delta_+^*\right)\,\Omega^2\,\begin{pmatrix} V\\ V_1\\ H_+\\ \Delta_+\end{pmatrix}\Bigg\}
\end{aligned}
\tag{D.2}
$$

where $\mathcal{F}$ and $\mathcal{G}$ are given by

$$
\mathcal{F}=-\frac{\tilde{p}_A\,f'(\phi)}{f(\phi)^2}\,\frac{p_T}{p}\quad,\quad \mathcal{G}=-\frac{\tilde{p}_A}{\sqrt{2}\,M_p\,f(\phi)}\,\frac{p_T}{p}
\tag{D.3}
$$

with $f(\phi_1)=\text{Exp}\left[\frac{4}{M_p^2}\int\frac{V_1(\phi_1)}{V_1'(\phi_1)}\,d\phi_1\right]$. Notice that the action (D.2) has regular kinetic terms, therefore the $2d$ scalar sector is free from ghost instabilities as in the case of $2d$

vector modes. The elements of the hermitian matrix Ω^2 are given as

$$
\begin{aligned}
\Omega^2_{11} &= p^2 - \frac{9}{4}\,\dot\alpha^2 + \frac{15\,\dot\phi^2}{4M_p^2} + \frac{3\,\dot\phi_1^2}{4M_p^2} + \frac{9}{2}\,\dot\sigma^2 + \frac{2\,\dot\phi_1\,V'(\phi)}{M_p^2\,\dot\alpha} + V''(\phi) - 2\,\frac{p^4}{\mathcal{D}^2}\,\frac{\dot\phi^4}{M_p^4} - 2\,\frac{p^4}{\mathcal{D}^2}\,\frac{\dot\phi^2\,\dot\phi_1^2}{M_p^4} \\
&\quad + \frac{2\,\left(p_T^2 - 2p_L^2\right)\,V'(\phi)}{\mathcal{D}}\,\frac{\dot\phi}{M_p^2\,\dot\alpha}\,\dot\sigma \\
&\quad - 3\,\left(4\,\frac{\left(2p_L^2 - p_T^2\right)\,p^2}{\mathcal{D}^2}\,\dot\alpha + \frac{8p_L^4 - 8p_L^2\,p_T^2 + 5p_T^4}{\mathcal{D}^2}\,\dot\sigma\right)\,\frac{\dot\phi^2}{M_p^2}\,\dot\sigma \\
&\quad + \frac{\tilde p_A^2}{2M_p^2\,f(\phi)^2}\,\Big[1 + \frac{2M_p^2\,\left(3p_L^2 - p_T^2\right)\,f'(\phi)^2}{p^2\,f(\phi)^2} - 4\,\frac{p_T^2\,p^2}{\mathcal{D}^2}\,\frac{\dot\phi^2}{M_p^2} \\
&\qquad\qquad - 8\,\frac{p_L^2}{\mathcal{D}}\,\frac{f'(\phi)}{f(\phi)}\,\dot\phi - 2M_p^2\,\frac{f''(\phi)}{f(\phi)}\Big]
\end{aligned}
$$

$$
\begin{aligned}
\Omega^2_{12} &= 2\,\dot\sigma\,\frac{\left(2p_L^2 - p_T^2\right)\,p^2}{\mathcal{D}^2}\,\left[\frac{\dot\phi_1\,V'(\phi)}{M_p^2} + \frac{\dot\phi\,V_1'(\phi_1)}{M_p^2} - 6\,\frac{p_L^4 - p_L^2\,p_T^2 + p_T^4}{\left(2p_L^2 - p_T^2\right)\,p^2}\,\frac{\dot\phi\,\dot\phi_1}{M_p^2}\,\dot\sigma\right] \\
&\quad - 2\,\frac{p^4}{\mathcal{D}^2}\,\left[\frac{\dot\phi^3\,\dot\phi_1}{M_p^4} - 2\,\frac{\dot\phi_1\,V'(\phi)}{M_p^2}\,\dot\alpha + \frac{\dot\phi}{M_p}\,\left(\frac{\dot\phi_1^3}{M_p^3} - 2\,\frac{V_1'(\phi_1)}{M_p}\,\dot\alpha - 6\,\frac{\dot\phi_1}{M_p}\,\dot\alpha^2\right)\right] \\
&\quad - \frac{2\,\tilde p_A^2}{M_p^2\,f(\phi)^2}\,\frac{\dot\phi\,\dot\phi_1}{M_p^2}\,\frac{p_T^2\,p^2}{\mathcal{D}^2} - \frac{2\,\tilde p_A^2}{M_p^2\,f(\phi)^2}\,\frac{f'(\phi)}{f(\phi)}\,\dot\phi_1\,\frac{p_L^2}{\mathcal{D}}
\end{aligned}
$$

$$
\begin{aligned}
\Omega^2_{13} &= -\frac{3\,\sqrt{2}\,p_T^2\,p^2\,\dot\sigma}{\mathcal{D}^2}\,\left[\frac{\dot\phi^3}{M_p^3} + \frac{\dot\phi\,\dot\phi_1^2}{M_p^3} - 6\,\frac{\dot\phi}{M_p}\,\left(\dot\alpha + \dot\sigma\right)\,\left(\dot\alpha + \frac{p_L^2 - p_T^2}{p^2}\,\dot\sigma\right)\right. \\
&\qquad\qquad \left. - \frac{V'(\phi)}{M_p}\,\left(2\dot\alpha + \frac{2p_L^2 - p_T^2}{p^2}\,\dot\sigma\right)\right] \\
&\quad - \frac{\sqrt{2}\,\tilde p_A^2\,p_T^2}{M_p^2\,f(\phi)^2\,\mathcal{D}^2}\,\left[3p_T^2\,\frac{\dot\phi}{M_p}\,\dot\sigma + M_p\,\frac{f'(\phi)}{f(\phi)}\,\left(4\,p^2\,\dot\alpha^2 + 2\,\left(7p_L^2 - 2p_T^2\right)\,\dot\alpha\,\dot\sigma\right.\right. \\
&\qquad\qquad \left.\left. + \frac{\left(2p_L^2 - p_T^2\right)\,\left(5p_L^2 - p_T^2\right)}{p^2}\,\dot\sigma^2\right)\right]
\end{aligned}
$$

$$
\begin{aligned}
\Omega^2_{14} &= \frac{i\,\tilde p_A\,p_T}{p\,f(\phi)}\,\left\{ - \frac{2\,\tilde p_A^2\,p^2}{M_p^2\,f(\phi)^2\,\mathcal{D}^2}\,\left[\frac{\dot\phi}{M_p^2}\,p_T^2 + \frac{f'(\phi)}{f(\phi)}\,p_L^2\,\left(2\dot\alpha + \frac{2p_L^2 - p_T^2}{p^2}\,\dot\sigma\right)\right]\right. \\
&\quad - 2\,\frac{p^4}{\mathcal{D}^2\,M_p}\,\left[\frac{\dot\phi^3}{M_p^3} + \frac{\dot\phi\,\dot\phi_1^2}{M_p^3} - 6\,\frac{\dot\phi}{M_p}\,\left(\dot\alpha + \dot\sigma\right)\,\left(\dot\alpha + \frac{p_L^2 - p_T^2}{p^2}\,\dot\sigma\right)\right] \\
&\quad \left. + 2\,\frac{p^4}{\mathcal{D}^2\,M_p}\,\frac{V'(\phi)}{M_p}\,\left(2\,\dot\alpha + \frac{2p_L^2 - p_T^2}{p^2}\,\dot\sigma\right) - \frac{f'(\phi)}{f(\phi)}\,\left(\dot\alpha + \frac{7p_L^2 - 2p_T^2}{p^2}\,\dot\sigma\right) + \dot\phi\,\frac{f''(\phi)}{f(\phi)}\right\}
\end{aligned}
$$

$$
\begin{aligned}
\Omega_{22}^2 &= p^2 - \frac{9}{4}\,\dot\alpha^2 + \frac{3\,\dot\phi^2}{4M_p^2} + \frac{15\,\dot\phi_1^2}{4M_p^2} + \frac{9}{2}\,\dot\sigma^2 + \frac{2\,\dot\phi_1\,V_1'(\phi_1)}{M_p^2\,\dot\alpha} + V_1''(\phi_1) - 2\,\frac{p^4}{\mathcal{D}^2}\,\frac{\dot\phi_1^4}{M_p^4} \\
&\quad -2\,\frac{p^4}{\mathcal{D}^2}\,\frac{\dot\phi^2\,\dot\phi_1^2}{M_p^4} + \frac{2\,\left(p_T^2 - 2p_L^2\right)\,V_1'(\phi_1)}{\mathcal{D}}\,\frac{\dot\phi_1}{M_p^2\,\dot\alpha}\,\dot\sigma \\
&\quad -3\,\left[4\,\frac{\left(2p_L^2 - p_T^2\right)\,p^2}{\mathcal{D}^2}\,\dot\alpha + \frac{8p_L^4 - 8\,p_L^2\,p_T^2 + 5p_T^4}{\mathcal{D}^2}\,\dot\sigma\right]\,\frac{\dot\phi_1^2}{M_p^2}\,\dot\sigma \\
&\quad +\frac{\tilde p_A^2}{2M_p^2\,f(\phi)^2}\,\left(1 - 4\,\frac{p_T^2\,p^2}{\mathcal{D}^2}\,\frac{\dot\phi_1^2}{M_p^2}\right)
\end{aligned}
$$

$$
\begin{aligned}
\Omega_{23}^2 &= -\frac{3\,\sqrt{2}\,p_T^2\,p^2\,\dot\sigma}{\mathcal{D}^2}\,\left[\frac{\dot\phi_1^3}{M_p^3} + \frac{\dot\phi^2\,\dot\phi_1}{M_p^3} - 6\,\frac{\dot\phi_1}{M_p}\,\left(\dot\alpha + \dot\sigma\right)\,\left(\dot\alpha + \frac{p_L^2 - p_T^2}{p^2}\,\dot\sigma\right)\right. \\
&\qquad \left. -\frac{V_1'(\phi_1)}{M_p}\,\left(2\,\dot\alpha + \frac{2p_L^2 - p_T^2}{p^2}\,\dot\sigma\right) + \frac{\tilde p_A^2}{M_p^2\,f(\phi)^2}\,\frac{\dot\phi_1}{M_p}\,\frac{p_T^2}{p^2}\right]
\end{aligned}
$$

$$
\begin{aligned}
\Omega_{24}^2 &= -\frac{2\,i\,\tilde p_A}{M_p\,f(\phi)}\,p_T\,p\,\left[\frac{p^2}{\mathcal{D}^2}\,\frac{\dot\phi_1^3}{M_p^3} - \frac{V_1'(\phi_1)}{\mathcal{D}\,M_p} + \frac{\tilde p_A^2}{M_p^2\,f(\phi)^2}\,\frac{\dot\phi_1}{M_p}\,\frac{p_T^2}{\mathcal{D}^2}\right. \\
&\qquad \left. +\frac{\dot\phi_1}{M_p}\,\left(\frac{p^2}{\mathcal{D}^2}\,\frac{\dot\phi^2}{M_p^2} - 6\,\left(\dot\alpha + \dot\sigma\right)\,\frac{p^2\,\dot\alpha + \left(p_L^2 - p_T^2\right)\,\dot\sigma}{\mathcal{D}^2}\right)\right]
\end{aligned}
$$

$$
\begin{aligned}
\Omega_{33}^2 &= p^2 - \frac{1}{4}\,\dot\alpha^2 + \frac{3\,\left(\dot\phi^2 + \dot\phi_1^2\right)}{4M_p^2} - 8\,\frac{p^4}{\mathcal{D}^2}\,\dot\alpha^4 - \frac{9p_T^4\,\dot\sigma^2}{\mathcal{D}^2}\,\frac{\dot\phi^2 + \dot\phi_1^2}{M_p^2} - 8\,\frac{\left(2p_L^2 - p_T^2\right)\,p^2}{\mathcal{D}^2}\,\dot\alpha^3\,\dot\sigma \\
&\quad +2\,\frac{5p_L^2 + 58\,p_L^2\,p_T^2 + 35\,p_T^4}{\mathcal{D}^2}\,\dot\alpha^2\,\dot\sigma^2 + 18\,\frac{2p_L^4 + 9\,p_L^2\,p_T^2 - p_T^4}{\mathcal{D}^2}\,\dot\alpha\,\dot\sigma^3 \\
&\quad +\frac{9}{2}\,\frac{4p_L^4 + 12\,p_L^2\,p_T^2 - 11p_T^4}{\mathcal{D}^2}\,\dot\sigma^4 + \frac{\tilde p_A^2}{2M_p^2\,f(\phi)^2}\,\frac{p_L^2 - p_T^2}{p^2} - \frac{9\,\tilde p_A^2}{M_p^2\,f(\phi)^2}\,\frac{p_T^6}{p^2\,\mathcal{D}^2}\,\dot\sigma^2
\end{aligned}
$$

$$
\begin{aligned}
\Omega_{34}^2 &= \frac{i\,\tilde p_A\,p_T}{\sqrt{2}\,M_p\,p\,f(\phi)}\,\left\{-\frac{6\tilde p_A^2}{M_p^2\,f(\phi)^2}\,\frac{p_T^4}{\mathcal{D}^2}\,\dot\sigma + \frac{f'(\phi)}{f(\phi)}\,\dot\phi - 4\,\frac{p^4}{\mathcal{D}^2}\,\dot\alpha^3\right. \\
&\qquad -6\,\frac{p_T^2\,p^2}{\mathcal{D}^2}\,\left(\frac{\dot\phi^2 + \dot\phi_1^2}{M_p^2} - 2\,\frac{p_L^2 + 4p_T^2}{p_T^2}\,\dot\alpha^2\right)\,\dot\sigma \\
&\qquad +9\,\frac{4p_L^2 + 16\,p_L^2\,p_T^2 - p_T^4}{\mathcal{D}^2}\,\dot\alpha\,\dot\sigma^2 \\
&\qquad \left. +\frac{20p_L^6 + 96p_L^4\,p_T^2 - 39p_L^2\,p_T^4 - 34p_T^6}{p^2\,\mathcal{D}^2}\,\dot\sigma^3\right\}
\end{aligned}
$$

$$\begin{aligned}\Omega_{44}^2 &= p^2 + \frac{\dot\phi^2 + \dot\phi_1^2}{4M_p^2} - \frac{1}{4}\,\dot\alpha^2 - \frac{p_L^2 - 2p_T^2}{2p^2}\left(4\,\dot\alpha - \frac{p_L^4 + 50p_L^2\,p_T^2 - 5p_T^4}{p^2\,\left(p_L^2 - 2p_T^2\right)}\,\dot\sigma\right)\,\dot\sigma \\ &+ \left[V'(\phi) + 2\,\dot\phi\,\dot\alpha + 2\,\frac{p_L^2 - 2p_T^2}{p^2}\,\dot\phi\,\dot\sigma\right]\,\frac{f'(\phi)}{f(\phi)} - \dot\phi^2\,\frac{f''(\phi)}{f(\phi)} \\ &- \frac{\tilde p_A^2\,p^2\,p_T^2}{2M_p^2\,f(\phi)^2\,\mathcal{D}^2}\left[\frac{4\,\tilde p_A^2}{M_p^2\,f(\phi)^2}\,\frac{p_T^2}{p^2} + \frac{2M_p^2\,\mathcal{D}^2}{p^2\,p_T^2}\,\frac{f'(\phi)^2}{f(\phi)^2} + \frac{4\,\left(\dot\phi^2 + \dot\phi_1^2\right)}{M_p^2} - 20\,\frac{p^2}{p_T^2}\,\dot\alpha^2\right. \\ &\left. - 4\,\frac{10p_L^4 + 17\,p_L^2\,p_T^2 + p_T^4}{p^2\,p_T^2}\,\dot\alpha\,\dot\sigma - \frac{\left(2p_L^2 + 5p_T^2\right)\,\left(10p_L^4 - p_L^2\,p_T^2 - 5p_T^4\right)}{p^4\,p_T^2}\,\dot\sigma^2\right] \qquad \text{(D.4)}\end{aligned}$$

where we have defined

$$\mathcal{D} \equiv 2p^2\,\dot\alpha + \left(2p_L^2 - p_T^2\right)\,\dot\sigma \qquad \text{(D.5)}$$

The canonically normalized modes $\{V_1,\, V_2,\, H_+,\, \Delta_+\}$ are related to the starting dynamical modes as

$$\begin{aligned}V &= e^{3\alpha/2}\,\left[\delta\phi + \frac{p_T^2\,\dot\phi}{\mathcal{D}}\,\Psi\right] \\ V_1 &= e^{3\alpha/2}\,\left[\delta\phi_1 + \frac{p_T^2\,\dot\phi_1}{\mathcal{D}}\,\Psi\right] \\ H_+ &= e^{3\alpha/2}\,\frac{\sqrt{2}\,M_p\,p_T^2\,\left(\dot\alpha + \dot\sigma\right)}{\mathcal{D}}\,\Psi \\ \Delta_+ &= e^{3\alpha/2}\,\frac{p_T}{i\,p}\,\left[\frac{\tilde p_A}{f(\phi)}\,\frac{p_T^2}{\mathcal{D}}\,\Psi + e^{-\alpha+2\sigma}\,f(\phi)\,\alpha_1\right] \qquad \text{(D.6)}\end{aligned}$$

When the universe becomes isotropic at the end of the first stage, we have $\dot\sigma = 0$ (we also rescaled the initial scale factors such that $\sigma = 0$ when the universe isotropizes). The canonical modes in the isotropic limit is related to the perturbations defined in the longitudinal gauge as

$$\begin{aligned}h_+ = -\frac{\sqrt{2}}{M_p}\,e^{-3\alpha/2}\,H_+ \;\;,\;\; V = v = e^{3\alpha/2}\,\left(\delta\phi^{(L)} + \frac{\dot\phi}{\dot\alpha}\,\Psi\right) \\ V_1 = v_1 = e^{3\alpha/2}\,\left(\delta\phi_1^{(L)} + \frac{\dot\phi_1}{\dot\alpha}\,\Psi\right) \qquad \text{(D.7)}\end{aligned}$$

where v, v_1 are the standard Mukhanov-Sasaki variables [5] (defined with respect to the action in the cosmic time). All the above quantities are gauge invariant. These relations

is useful when computing the curvature ($\mathcal{R}$) and h_+ gravitational wave polarization spectrum.

Note that the final action (D.2) is of the generic form (6.35), with the corresponding matrix $\mathbf{X}$ given by

$$\mathbf{X} = \begin{pmatrix} 0 & 0 & \mathcal{F} \\ 0 & 0 & \mathcal{G} \\ \mathcal{F} & \mathcal{G} & 0 \end{pmatrix} \tag{D.8}$$

In this case, the solution of the equation $\dot{\mathbf{U}} + i\,\mathbf{X}\,\mathbf{U} = 0$ is more challenging, since the matrix that diagonalizes $\mathbf{X}$ is given by

$$\mathbf{R} = \frac{1}{\sqrt{\mathcal{F}^2+\mathcal{G}^2}} \begin{pmatrix} \mathcal{G} & \mathcal{F}/\sqrt{2} & -\mathcal{F}/\sqrt{2} \\ -\mathcal{F} & \mathcal{G}/\sqrt{2} & -\mathcal{G}/\sqrt{2} \\ 0 & \sqrt{\mathcal{F}^2+\mathcal{G}^2}/\sqrt{2} & \sqrt{\mathcal{F}^2+\mathcal{G}^2}/\sqrt{2} \end{pmatrix}$$

$$D_X = \begin{pmatrix} 0 & 0 & 0 \\ 0 & \sqrt{\mathcal{F}^2+\mathcal{G}^2} & 0 \\ 0 & 0 & -\sqrt{\mathcal{F}^2+\mathcal{G}^2} \end{pmatrix} \tag{D.9}$$

which is not a constant matrix, unlike the case for the $2d$ vector modes.

Appendix E

Detailes of calculations for chapter 7

We provide here the explicit expressions for the matrices entering in the action and the evolution equations of the canonical modes, equations (7.6) and (7.32).

For the 2d scalar modes we have

$$K_s = \begin{pmatrix} 0 & 0 & K_{13,s} \\ 0 & 0 & K_{23,s} \\ -K_{13,s} & -K_{23,s} & 0 \end{pmatrix} \quad , \quad \Omega_s^2 = \begin{pmatrix} \Omega_{11,s}^2 & \Omega_{12,s}^2 & \Omega_{13,s}^2 \\ \Omega_{12,s}^2 & \Omega_{22,s}^2 & \Omega_{23,s}^2 \\ \Omega_{13,s}^2 & \Omega_{23,s}^2 & \Omega_{33,s}^2 \end{pmatrix} \tag{E.1}$$

where

$$K_{13,s} = -\frac{\tilde{p}_A\, p_T\, f'(\phi)}{p\, f(\phi)^2} \quad , \quad K_{23,s} = -\frac{\tilde{p}_A\, p_T}{\sqrt{2}\, M_p\, p\, f(\phi)}$$

$$\begin{aligned} \Omega_{11,s}^2 \;=\; & p^2 - \frac{9}{4}\,\dot{\alpha}^2 + \frac{15\,\dot{\phi}^2}{4M_p^2} + \frac{9}{2}\,\dot{\sigma}^2 + \frac{2\,\dot{\phi}\,V'(\phi)}{M_p^2\,\dot{\alpha}} + V''(\phi) - 2\,\frac{p^4}{\mathcal{D}^2}\,\frac{\dot{\phi}^4}{M_p^4} \\ & + \frac{2\,\left(p_T^2 - 2p_L^2\right)\,V'(\phi)}{\mathcal{D}}\,\frac{\dot{\phi}}{M_p^2\,\dot{\alpha}}\,\dot{\sigma} \\ & - 3\,\left(4\,\frac{\left(2p_L^2 - p_T^2\right)\,p^2}{\mathcal{D}^2}\,\dot{\alpha} + \frac{8p_L^4 - 8p_L^2\,p_T^2 + 5p_T^4}{\mathcal{D}^2}\,\dot{\sigma}\right)\,\frac{\dot{\phi}^2}{M_p^2}\,\dot{\sigma} \\ & + \frac{\tilde{p}_A^2}{2M_p^2\,f(\phi)^2}\,\Big[1 + \frac{2M_p^2\,\left(3p_L^2 - p_T^2\right)\,f'(\phi)^2}{p^2\,f(\phi)^2} - 4\,\frac{p_T^2\,p^2}{\mathcal{D}^2}\,\frac{\dot{\phi}^2}{M_p^2} \end{aligned}$$

$$-8\,\frac{p_L^2}{\mathcal{D}}\,\frac{f'(\phi)}{f(\phi)}\,\dot\phi - 2M_p^2\,\frac{f''(\phi)}{f(\phi)}\Big]$$

$$\begin{aligned}
\Omega^2_{12,s} &= -\frac{3\sqrt{2}\,p_T^2\,p^2\,\dot\sigma}{\mathcal{D}^2}\left[\frac{\dot\phi^3}{M_p^3} - 6\,\frac{\dot\phi}{M_p}\,(\dot\alpha+\dot\sigma)\,\left(\dot\alpha + \frac{p_L^2-p_T^2}{p^2}\,\dot\sigma\right)\right.\\
&\qquad\left. -\frac{V'(\phi)}{M_p}\,\left(2\dot\alpha + \frac{2p_L^2-p_T^2}{p^2}\,\dot\sigma\right)\right]\\
&\quad -\frac{\sqrt{2}\,\tilde p_A^2\,p_T^2}{M_p^2\,f(\phi)^2\,\mathcal{D}^2}\left[3p_T^2\,\frac{\dot\phi}{M_p}\,\dot\sigma + M_p\,\frac{f'(\phi)}{f(\phi)}\left(4\,p^2\,\dot\alpha^2 + 2\,\left(7p_L^2-2p_T^2\right)\,\dot\alpha\,\dot\sigma\right.\right.\\
&\qquad\left.\left. +\frac{\left(2p_L^2-p_T^2\right)\,\left(5p_L^2-p_T^2\right)}{p^2}\,\dot\sigma^2\right)\right]
\end{aligned}$$

$$\begin{aligned}
\Omega^2_{13,s} &= \frac{\tilde p_A\,p_T}{p\,f(\phi)}\left\{-\frac{2\,\tilde p_A^2\,p^2}{M_p^2\,f(\phi)^2\,\mathcal{D}^2}\,\left[\frac{\dot\phi}{M_p^2}\,p_T^2 + \frac{f'(\phi)}{f(\phi)}\,p_L^2\,\left(2\dot\alpha + \frac{2p_L^2-p_T^2}{p^2}\,\dot\sigma\right)\right]\right.\\
&\quad -2\,\frac{p^4}{\mathcal{D}^2\,M_p}\,\left[\frac{\dot\phi^3}{M_p^3} - 6\,\frac{\dot\phi}{M_p}\,(\dot\alpha+\dot\sigma)\,\left(\dot\alpha + \frac{p_L^2-p_T^2}{p^2}\,\dot\sigma\right)\right]\\
&\quad \left.+2\,\frac{p^4}{\mathcal{D}^2\,M_p}\,\frac{V'(\phi)}{M_p}\,\left(2\,\dot\alpha + \frac{2p_L^2-p_T^2}{p^2}\,\dot\sigma\right) - \frac{f'(\phi)}{f(\phi)}\,\left(\dot\alpha + \frac{7p_L^2-2p_T^2}{p^2}\,\dot\sigma\right) + \dot\phi\,\frac{f''(\phi)}{f(\phi)}\right\}
\end{aligned}$$

$$\begin{aligned}
\Omega^2_{22,s} &= p^2 - \frac{1}{4}\,\dot\alpha^2 + \frac{3\,\dot\phi^2}{4M_p^2} - 8\,\frac{p^4}{\mathcal{D}^2}\,\dot\alpha^4 - \frac{9p_T^4\,\dot\sigma^2}{\mathcal{D}^2}\,\frac{\dot\phi^2}{M_p^2} - 8\,\frac{\left(2p_L^2-p_T^2\right)\,p^2}{\mathcal{D}^2}\,\dot\alpha^3\,\dot\sigma\\
&\quad +2\,\frac{5p_L^4+58\,p_L^2\,p_T^2+35\,p_T^4}{\mathcal{D}^2}\,\dot\alpha^2\,\dot\sigma^2 + 18\,\frac{2p_L^4+9\,p_L^2\,p_T^2-p_T^4}{\mathcal{D}^2}\,\dot\alpha\,\dot\sigma^3\\
&\quad +\frac{9}{2}\,\frac{4p_L^4+12\,p_L^2\,p_T^2-11p_T^4}{\mathcal{D}^2}\,\dot\sigma^4 + \frac{\tilde p_A^2}{2M_p^2\,f(\phi)^2}\,\frac{p_L^2-p_T^2}{p^2} - \frac{9\,\tilde p_A^2}{M_p^2\,f(\phi)^2}\,\frac{p_T^6}{p^2\,\mathcal{D}^2}\,\dot\sigma^2
\end{aligned}$$

$$\begin{aligned}
\Omega^2_{23,s} &= \frac{\tilde p_A\,p_T}{\sqrt{2}\,M_p\,p\,f(\phi)}\left\{-\frac{6\tilde p_A^2}{M_p^2\,f(\phi)^2}\,\frac{p_T^4}{\mathcal{D}^2}\,\dot\sigma + \frac{f'(\phi)}{f(\phi)}\,\dot\phi - 4\,\frac{p^4}{\mathcal{D}^2}\,\dot\alpha^3\right.\\
&\qquad -6\,\frac{p_T^2\,p^2}{\mathcal{D}^2}\,\left(\frac{\dot\phi^2}{M_p^2} - 2\,\frac{p_L^2+4p_T^2}{p_T^2}\,\dot\alpha^2\right)\,\dot\sigma\\
&\qquad +9\,\frac{4p_L^4+16\,p_L^2\,p_T^2-p_T^4}{\mathcal{D}^2}\,\dot\alpha\,\dot\sigma^2\\
&\qquad \left.+\frac{20p_L^6+96p_L^4\,p_T^2-39p_L^2\,p_T^4-34p_T^6}{p^2\,\mathcal{D}^2}\,\dot\sigma^3\right\}
\end{aligned}$$

$$\begin{aligned}\Omega^2_{33,s} &= p^2+\frac{\dot\phi^2}{4M_p^2}-\frac{1}{4}\,\dot\alpha^2-\frac{p_L^2-2p_T^2}{2p^2}\left(4\,\dot\alpha-\frac{p_L^4+50p_L^2\,p_T^2-5p_T^4}{p^2\,\left(p_L^2-2p_T^2\right)}\,\dot\sigma\right)\dot\sigma\\ &+\left[V'(\phi)+2\,\dot\phi\,\dot\alpha+2\,\frac{p_L^2-2p_T^2}{p^2}\,\dot\phi\,\dot\sigma\right]\frac{f'(\phi)}{f(\phi)}-\dot\phi^2\,\frac{f''(\phi)}{f(\phi)}\\ &-\frac{\tilde p_A^2\,p^2\,p_T^2}{2M_p^2\,f(\phi)^2\,\mathcal{D}^2}\left[\frac{4\,\tilde p_A^2}{M_p^2\,f(\phi)^2}\,\frac{p_T^2}{p^2}+\frac{2M_p^2\,\mathcal{D}^2}{p^2\,p_T^2}\,\frac{f'(\phi)^2}{f(\phi)^2}+\frac{4\,\dot\phi^2}{M_p^2}-20\,\frac{p^2}{p_T^2}\,\dot\alpha^2\right.\\ &\left.-4\,\frac{10p_L^4+17\,p_L^2\,p_T^2+p_T^4}{p^2\,p_T^2}\,\dot\alpha\,\dot\sigma-\frac{\left(2p_L^2+5p_T^2\right)\,\left(10p_L^4-p_L^2\,p_T^2-5p_T^4\right)}{p^4\,p_T^2}\,\dot\sigma^2\right]\end{aligned} \tag{E.2}$$

and where we have defined

$$\mathcal{D}\equiv 2p^2\,\dot\alpha+\left(2p_L^2-p_T^2\right)\,\dot\sigma \tag{E.3}$$

For the 2d vector modes we have instead

$$K_v=\begin{pmatrix}0 & K_{12,v}\\ -K_{12,v} & 0\end{pmatrix}\quad,\quad \Omega^2_v=\begin{pmatrix}\Omega^2_{11,v} & \Omega^2_{12,v}\\ \Omega^2_{12,v} & \Omega^2_{22,v}\end{pmatrix} \tag{E.4}$$

where

$$\begin{aligned}K_{12,v}&=-\frac{\tilde p_A\,|p_T|}{\sqrt{2}\,M_p\,f\,(\phi)\;p}\\ \Omega^2_{11,v}&=p^2-\frac{9}{4}\dot\alpha^2-\dot\sigma^2\left[\frac{9}{2}-36\,\frac{p_L^2}{p^2}+27\,\frac{p_L^4}{p^4}\right]+\frac{3\dot\phi^2}{4M_p^2}-\frac{\tilde p_A^2}{2M_p^2 f\,(\phi)^2}\left[1-2\,\frac{p_L^2}{p^2}\right]\\ \Omega^2_{22,v}&=p^2-\frac{\dot\alpha^2}{4}-2\,\dot\alpha\,\dot\sigma+\frac{\dot\sigma^2}{2}+\frac{\dot\phi^2}{4\,M_p^2}+\frac{\tilde p_A^2}{2M_p^2 f\,(\phi)^2}\left[1+4\,\frac{p_L^2}{p^2}\right]\\ &+\left[V'\,(\phi)+2\,(\dot\alpha+\dot\sigma)\,\dot\phi\right]\frac{f'\,(\phi)}{f\,(\phi)}-\tilde p_A^2\,\frac{f'\,(\phi)^2}{f\,(\phi)^4}-\dot\phi^2\,\frac{f''\,(\phi)}{f\,(\phi)}\\ \Omega^2_{12,v}&=\frac{\tilde p_A\,|p_T|}{\sqrt{2}\,M_p\,f\,(\phi)\,p}\left[-\dot\alpha+\left(9\frac{p_L^2}{p^2}-4\right)\dot\sigma+\frac{\dot\phi\,f'\,(\phi)}{f\,(\phi)}\right]\end{aligned} \tag{E.5}$$

The physical momenta entering in these expressions are related to the comoving ones given in the main text by

$$p_L\equiv\frac{k_L}{a\,(t)}\quad,\quad p_T\equiv\frac{k_T}{b\,(t)}\quad,\quad p\equiv\sqrt{p_L^2+p_T^2} \tag{E.6}$$

Appendix F

Comparison with isotropic case relevant for chapter 7

In this Appendix we discuss the late time interpretation of the perturbations in the gauge chosen in the main text. This interpretation is done when the background has become isotropic, and the vev of the vector has gone to zero. In this case, the Fourier coefficients of our metric perturbations read

$$\delta g_{\mu\nu}(k) = \begin{pmatrix} -2\Phi & i\,a\,k_L\,\chi & ia\,(k_{T2}\,B + k_{T3}\,B_v) & ia\,(k_{T3}\,B - k_{T2}\,B_v) \\ & -2a^2\Psi & -a^2\,k_L\,k_{T3}\,\tilde{B}_v & a^2\,k_L\,k_{T2}\,\tilde{B}_v \\ & & 0 & 0 \\ & & & 0 \end{pmatrix} , \qquad \text{(F.1)}$$

as can be seen by imposing the gauge $\tilde{B} = \Sigma = E = E_i = \alpha = 0$ on the parametrization given by (4.31) and (7.2). We recall that (k_L, k_{T2}, k_{T3}) denotes the comoving momentum of the mode we are studying. [1] We perform a rotation to a coordinate system for which the momentum is along the third direction, $k_\mu \to \tilde{k}_\mu = R^\nu_\mu\,k_\nu =$

[1] In the main text, the suffices L and T refer to "longitudinal" or "transverse" with respect to direction x, which was the anisotropic one during inflation.

$\left(0,\, 0,\, \sqrt{k_L^2 + k_{T2}^2 + k_{T3}^2}\right)$. The explicit form of the rotation matrix is

$$R^\mu_\nu = \begin{pmatrix} 1 & 0 & 0 & 0 \\ 0 & -\frac{k_T}{k} & \frac{k_L\, k_{T2}}{k_T\, k} & \frac{k_L\, k_{T3}}{k_T\, k} \\ 0 & 0 & \frac{k_{T3}}{k_T} & -\frac{k_{T3}}{k_T} \\ 0 & \frac{k_L}{k} & \frac{k_{T2}}{k} & \frac{k_{T3}}{k} \end{pmatrix} \tag{F.2}$$

where $k_T = \sqrt{k_{T2}^2 + k_{T3}^2}$, and the metric transforms as

$$g_{\mu\nu} \to \widetilde{g}_{\mu\nu} = R^\alpha_\mu\, g_{\alpha\beta}\, R^\beta_\nu \tag{F.3}$$

Although the gauge in which equation (F.1) appears is nonstandard, we can combine the metric perturbations (F.1) into the gauge invariant expressions that are commonly used. These gauge invariant combinations are usually expressed starting from the most general metric perturbations, classified as scalar, vector, or tensor, with respect to 3d spatial rotations:

$$\delta g_{00} = -2\Phi_* \quad , \quad \delta g_{0i} = 2a\,(B_{*i} + \partial_i B_*) \quad , \quad \delta g_{ij} = a^2\left[-2\Psi_*\,\delta_{ij} + 2\,E_{*,ij} + E_{*(i,j)} + h_{*ij}\right] \tag{F.4}$$

where $i = 1, 2, 3$. The (3d) vectors B_{*i} and E_{*i} are transverse, while the tensor mode h_{*ij} is transverse and traceless. The remaining modes are scalar, and are coupled also to the perturbation of the scalar field $\delta\phi_*$. Out of these modes, we are interested in the the gauge invariant scalar combination as given in equation (2.97)

$$\mathcal{R} \equiv \Psi_* + \frac{H}{\dot{\phi}}\delta\phi_* \tag{F.5}$$

and in the two (gauge invariant) tensor mode polarizations h_+ and $h_\times$ encoded in h_{*ij} (the vector modes disappear once the universe becomes isotropic).

Expression (F.4) gives the metric perturbations before any gauge is chosen. By equating them with our expressions (F.1) we find how our modes can be decomposed into 3d scalar, vector, and tensor perturbations. We can then use the resulting expressions to write $\mathcal{R}$, h_+ and $h_\times$ in terms of our modes. To make this identification, we should spell out explicitly how the components of the 3d vector and tensor modes enter in (F.4), accounting for their transversality, and traceless properties. We do so in the $\tilde{x}^\mu$ coordinate system, for which the momentum of the mode is $\tilde{k}_\mu = \left(0,\, 0,\, \sqrt{k_L^2 + k_{T2}^2 + k_{T3}^2}\right)$.

In this system, eqs. (F.4) give

$$\widetilde{\delta} g_{\mu\nu}(k) = \begin{pmatrix} -2\Phi_* & a\,B_{*1} & a\,B_{*2} & a\,i\,k\,B_* \\ & a^2\,(-2\Psi_* + h_+) & a^2 h_\times & a^2\,i\,k\,E_{*1} \\ & & a^2\,(-2\Psi_* - h_+) & a^2\,i\,k\,E_{*2} \\ & & & a^2\left(-2\Psi_* - 2k^2 E_*\right) \end{pmatrix} \tag{F.6}$$

The entries of this metric can be now identified with those of our metric (F.1), transformed according to (F.3). We obtain

$$\mathcal{R} = \frac{k_T^2}{2\,k^2}\Psi + \frac{H}{\dot{\phi}}\delta\phi \quad , \quad h_+ = -\frac{k_T^2}{k^2}\,\Psi \quad , \quad h_\times = \frac{k_L\,k_T^2}{k}\,\tilde{B}_v \tag{F.7}$$

Finally, we rewrite our three variables Ψ, $\delta\phi$, and $\tilde{B}_v$ in terms of the canonically normalized modes introduced in (7.4) and (7.5). This leads to

$$R = \frac{H}{a^{3/2}\,\dot{\phi}}\,V_+ \quad , \quad h_+ = -\frac{\sqrt{2}}{a^{3/2}\,M_p}\,H_+ \quad , \quad h_\times = \frac{i\,\sqrt{2}}{a^{3/2}\,M_p}\,H_\times \tag{F.8}$$

As a check, we can verify that the our evolution equations reduce to the standard ones in the limit of isotropic background. Using $\tilde{p}_A = \dot{\sigma} = 0$ in the explicit expressions given in Appendix E, we find that $K_{s,v} = 0$ and $\Omega^2_{s,v}$ are diagonal in this limit. Therefore, all the canonical modes are decoupled. One can then show that, in this limit the equations (7.32) give

$$\begin{aligned} &\left(\frac{V_+}{\sqrt{a}}\right)'' + \left[k^2 - \frac{z''}{z}\right]\left(\frac{V_+}{\sqrt{a}}\right) = 0 \quad , \quad z \equiv \frac{a^2\,\dot{\phi}}{\dot{a}} \\ &\left(\frac{H_{+,\times}}{\sqrt{a}}\right)'' + \left[k^2 - \frac{a''}{a}\right]\left(\frac{H_{+,\times}}{\sqrt{a}}\right) = 0 \end{aligned} \tag{F.9}$$

where prime denotes differentiation with respect to conformal time η, related to the physical time t by $d\eta = dt/a$. From these expressions, and from eqs. (F.8) we find

$$v'' + \left(k^2 - \frac{z''}{z}\right) v = 0 \quad , \quad (a\,h_{+,\times})'' + \left(k^2 - \frac{a''}{a}\right)(a\,h_{+,\times}) = 0 \tag{F.10}$$

where $v \equiv z\,\mathcal{R}$. These equations are the standard ones (2.102) given in chapter 2, confirming that our formalism reduces to the standard one in the limit of isotropic background.